DOE-ET-53088-154 IFSR #154

SHEAR-ALFVÉN DYNAMICS OF TOROIDALLY CONFINED PLASMAS

R. D. Hazeltine and J. D. Meiss
Institute for Fusion Studies
The University of Texas
Austin, Texas 78712

August 1984

(Part A)

SHEAR-ALFVÉN DYNAMICS OF TOROIDALLY CONFINED PLASMAS

SHEAR-ALFVÉN DYNAMICS OF TOROIDALLY CONFINED PLASMAS

R. D. Hazeltine and J. D. Meiss

Institute for Fusion Studies

The University of Texas

Austin, Texas 78712

Abstract

Recent developments in the stability theory of toroidally confined plasmas are reviewed, with the intention of providing a picture comprehensible to non-specialists. The review considers a class of low-frequency, electromagnetic disturbances that seem especially pertinent to modern high-temperature confinement experiments. It is shown that such disturbances are best unified and understood through consideration of a single, exact fluid moment: the shear-Alfvén law. Appropriate versions of this law and its corresponding closure relations are derived: — essentially from first principles — and applied in a variety of mostly, but not exclusively, linear contexts. Among the specific topics considered are: flux coordinates (including Hamada coordinates), the Newcomb solubility condition, Shafranov geometry, magnetic island evolution, reduced MHD and its generalizations, drift-kinetic electron response, classical tearing, twisting, and kink instabilities, pressure-modified tearing instability (Δ-critical), collisionless and semi-collisional tearing modes, the ballooning representation in general geometry, ideal ballooning

instability, Mercier criterion, near-axis expansions, the second stability region, and resistive and kinetic ballooning modes. The fundamental importance of toroidal topology and curvature is stressed.

I. Introduction

A. Topic and Objectives

This review is addressed to plasma physicists, to students, and to other scientists who are curious about recent developments in magnetized plasma theory. Its subject is the basic physical ideas underlying a class of plasma motions of special importance to toroidal plasma confinement.

For the sake of wide accessibility, we have tried to make the review as self-contained as possible. In fact the reader is presumed to have no more than a mild acquaintance with elementary plasma theory. However, we have not attempted any detailed discussion of the relation between theory and the experimental controlled fusion program. Such discussions are available elsewhere (see, for example, [1]).

In mentioning plasma motions we of course have in mind primarily unstable motions. Yet the review is not restricted to linear instability theory. While most of our detailed results are linear, the basic concepts pertain nonlinearly and are developed in a general context. Moreover we review in some detail equilibrium theory, the derivation of nonlinear models, and certain nonlinear conclusions. What is omitted, most importantly, is any discussion of plasma turbulence: all the motions we consider are coherent.

Specialists would describe the instabilities under consideration as a variety of tearing modes, interchanges and ballooning modes. Such disturbances are believed to importantly affect the observed confinement in various experimental devices, including tokamaks, stellarators and the reversed-field pinch. They have in common the following properties: (i) they are slow, in a technical sense which

will be described; (ii) they are electromagnetic, in the sense of crucially involving perturbation of the magnetic field; (iii) they cannot, in general, be described adequately by ideal (dissipationless) models; (iv) they are critically affected by toroidicity of the confinement geometry — at least by toroidal topology, if not by both topology and the magnetic field curvature necessarily present in a torus.

The major theme of the review is that plasma motions of this class are best understood from a single, unifying point of view. Indeed, they are related so closely that a discussion of any one member (such as the "modified tearing mode") inevitably raises issues specifically pertinent to another (such as the "resistive ballooning mode"). Their unification is manifested in particular by the fact that crucial features of all can be understood in terms of a single equation. We call this equation the "shear-Alfvén law", essentially because shear-Alfvén waves are its most elementary prediction. Our premise is that any sufficiently slow, electromagnetic disturbance of a toroidal plasma is fundamentally constrained by shear-Alfvén dynamics.

The following section attempts to outline the central physics of the shear-Alfvén law and this review. Its anticipatory discussion may be opaque to non-specialists, but still perhaps useful as a survey of the issues to be studied. We remark that a much more detailed and concrete version of the following outline can be found in Chapter III; readers impatient to see the explicit shear-Alfvén law, for example, will find it there.

B. Shear-Alfvén Motions

Shear-Alfvén motions result from a competition between two types of physical circumstances, geometrical and dynamical.

The geometrical considerations pertain, first of all, to the nature of plasma confinement in a torus, which is characterized by a sequence of nested toroidal surfaces wound by helical magnetic field lines. When the average winding number, or field line pitch, is rational, the field line closes on itself after sufficiently many circuits of the surface; for irrational winding number the field line trajectory is quasi-periodic and ergodic on the surface. The prevalence of magnetic "shear" — a change in pitch from one surface to the next — then leads to a construct familiar from Hamiltonian dynamics: the singular yet dense occurrence of rational tori amongst a background of ergodic surfaces [2].

Rational surfaces become dynamically important because of a second geometrical consideration, involving scale-length separation. The point is that slow disturbances are typically stable unless their variation along the local magnetic field is much weaker than variation in other directions. Thus the important perturbations are stretched out along the field lines. The "aspect ratio" associated with such stretching provides an ordering parameter of fundamental importance, even in nonlinear theory. Its main significance is that infinite stretching — constancy along the direction of the confining field — allows no variation on a magnetic surface whatsoever, if field lines on the surface are ergodic. Thus, if they are not uniform on every toroidal surface, the slow, stretched motions will tend to be centered in some sense on rational surfaces.

The salient dynamical features of the shear-Alfvén law include plasma inertia as well as terms involving the plasma current density. Inertia appears primarily in the form of plasma vorticity — as in the vorticity equation of conventional fluid dynamics, which the shear-Alfvén law generalizes. Of course the current-density terms represent electromagnetic forces. Since the lowest magnetic energy state corresponds to the vacuum field, these terms provide electromagnetic "free energy" which is available in principle to drive various instabilities.

To get a sense of how geometrical and dynamical considerations are combined in the relevant motions, we first consider the steady-state shear-Alfvén law, neglecting inertia. The corresponding balance of electromagnetic forces plays an important role in equilibrium theory but also, in view of the relatively slow time scales of interest, applies approximately to non-equilibrium situations. The geometrical considerations become relevant at this point: one notices that the steady-state equation is in general singular on each rational surface.

In equilibrium theory the singularities are removed by imposing on the forces a certain solubility condition. Essentially one requires the coefficient of each singularity to vanish. For all but highly symmetric equilibrium geometries, the solubility condition is far from trivial to satisfy; it is rarely satisfied, even approximately, in the non-equilibrium context. Thus rational surface singularity plays a key role in all studies of shear-Alfvén evolution.

Failure to satisfy the solubility condition leads generally to local change in the magnetic field topology: magnetic islands form, similar to those arising near rational tori in Hamiltonian theory. The

width of a magnetic island effectively measures the degree to which the solubility condition has been violated. Linear theory applies when island widths are negligibly small; then the singularity is resolved by including, in a narrow toroidal annulus enclosing each relevant rational surface, the inertial terms in the shear-Alfvén law. In this way, divergence of the parallel wave length at the rational surface leads to a boundary-layer problem. It also requires enlargement of the theoretical description, since the boundary-layer structure is not determined by the shear-Alfvén law alone.

We defer until later chapters discussion of the layer structure, but a related issue, boundary-layer overlap, requires mention here. Depending on its harmonic content, a given perturbation will have singularities on several or even many rational surfaces (i.e., on each surface at which it fails to satisfy the solubility conditions). The singular surfaces corresponding to a given mode are called "mode-rational" surfaces; they are not dense, but separated from each other by some finite distance, Δ. This observation leads to an important eigenmode classification: perturbations for which Δ exceeds the width of a typical boundary layer have disjoint layers; in the contrary case layers centered on different surfaces strongly overlap.

We shall see that the degree of overlap depends mainly on plasma pressure: as the pressure increases, interesting instabilities are more likely to involve significant overlap. The reason is not any effect of pressure on layer widths, but rather the interaction between pressure gradients and toroidal curvature. Such "interchange" forces, which are explicit in the shear-Alfvén law, favor richer harmonic

content and smaller Δ, even at the expense of increased variation along the confining field.

It is not surprising that the mathematics of linear stability depends critically on boundary-layer overlap. When layers are well separated, each can be analyzed more or less independently (although they are strictly independent only in the absence of curvature). The resulting formalism resembles theories of shock-front structure in a fluid, with dissipative layer widths and asymptotic matching conditions, modified by certain details of plasma physics. The opposite, overlapping case requires a more elaborate and general treatment. In a sense, one considers the mode-rational surfaces as analogous to a crystal lattice; the linear problem is to find that combination of lattice excitations whose envelope yields an eigenmode.

The preceding remarks sketch a framework for the understanding and analysis of shear-Alfvén motions. The framework is obviously not our invention. The literature shows that a formalism based on shear-Alfvén time scales, solubility conditions, stretched perturbations, boundary layers, overlap and so on — what might be called the "low-frequency orthodoxy" — has been used widely, if not always explicitly, for many years. It is a framework of proven theoretical power, and one which we intend to codify and explain.

C. Synopsis

Chapter II established such fundamental equilibrium concepts as magnetic flux surfaces, "rotational transform" (measuring field-line pitch), and magnetic shear. It provides a self-contained treatment of the various coordinate systems used to study toroidal plasma dynamics.

Perhaps most importantly, Chapter II points out the occurrence, in an equilibrium context, of rational-surface singularity. The corresponding solubility conditions are discussed in some detail.

The derivation of the nonlinear shear-Alfvén law is presented in Chapter III, together with a broad discussion of its features. Most of the central issues of the review are at least mentioned in this chapter.

A direct attack on the exact shear-Alfvén law, with appropriate closure relations, is hopelessly complicated and not instructive. The problem is that the essential physics becomes hidden by a plethora of terms, whose relative magnitudes are often disparate but not trivially estimated. Therefore, in Chapter IV, we depart from the main line of argument in order to derive approximate, more tractable, dynamical descriptions. Thus we consider the closure relation obtained from (simplified) kinetic theory, as well as a variety of "reduced" fluid models. While derived primarily for the sake of later application, these compact descriptions have considerable intrinsic interest; in particular, the fluid models are widely used in the interpretation of tokamak experiments. The derivations are intended to clarify the physical processes represented by various terms, as well as permitting some assessment of a given model's accuracy.

We noted above that shear-Alfvén motions occur in two broad categories: those with well-separated boundary layers and those who boundary layers overlap. The non-overlapping category is the subject of Chapter V. Beginning with the simplest, "hydrogen atom", case — a fluid-model layer with negligible plasma pressure — we find the dispersion relations for a variety of tearing instabilities and other,

closely related, modes. The model is then enlarged, first to include plasma pressure and next to allow for the more complicated closure relations that become pertinent at longer mean-free-path. While the eigenmode equations are derived and discussed with care, the corresponding dispersion relations are usually obtained from heuristic arguments, emphasizing physical ideas rather than mathematical technique. Finally, Chapter V considers the nonlinear evolution of a coherent (single helicity) boundary layer.

The case of overlapping boundary layers is studied in Chapter VI. It is most easily treated using a relatively new technique, the "ballooning formalism". The requirements of large perpendicular wavenumbers and toroidal periodicity are satisfied by an eikonal representation, in which modes on neighboring rational surfaces are assumed to have nearly equal amplitudes. Beginning with a formal treatment in general toroidal geometry, we show how the ballooning representation separates the three-dimensional problem into an ordinary differential equation along the magnetic field lines, followed by a global eigenvalue condition for the perpendicular structure. The local equation can be solved in both the limits of strongly and weakly overlapping layers. The resulting flows are more or less like aneurisms on the magnetic surfaces, from which the term "ballooning" springs. Finally, the complications introduced by closure relations are discussed. While we would prefer to close this chapter, like the last, with a discussion of coherent nonlinear effects, this important problem has not yet received sufficient attention for review.

II. Local Equilibrium Theory

A. Introduction

Magnetic confinement is inconsistent with thermodynamic equilibrium. A magnetically confined plasma can at best approach mechanical equilibrium, in which the dominant fluid forces approximately balance. Sufficiently isolated plasmas are characterized by a nearly scalar pressure, P, so that force balance is expressed, in Gaussian units, by

$$\underset{\sim}{J} \times \underset{\sim}{B} = c\nabla P \tag{2.1}$$

where $\underset{\sim}{B}$, the magnetic field, satisfies

$$\nabla \cdot \underset{\sim}{B} = 0 \tag{2.2}$$

and where

$$\underset{\sim}{J} = (c/4\pi)\nabla \times \underset{\sim}{B} \tag{2.3}$$

is the current density.

Equation (2.1) neglects anisotropic contributions, $\underset{\approx}{\pi}$, to the stress tensor. Such contributions are not negligible in open systems ("magnetic mirrors") or in closed systems with externally driven anisotropy (such as may be associated with certain plasma heating schemes). Even for completely isolated plasmas, $\underset{\approx}{\pi}$ does not vanish; rather, it is smaller than P by at least one power of the ratio (typical particle Larmor radius/system scale-length). Nonetheless our

analysis, which is closely based on early work of Kruskal and Kulsrud [3], treats Eq. (2.1) as if it were exact.

"Confinement" can be taken to imply that the surfaces of constant pressure are closed, nested, and reasonably smooth. It is evident from Eq. (2.1), or

$$\underset{\sim}{B} \cdot \nabla P = 0 \tag{2.4}$$

that the field lines lie in the constant pressure surfaces, and this fact (with the assumption that B does not vanish within the confinement region) requires each surface to be a topological torus. In other words, a magnetically confined plasma is characterized by a set of nested toroidal surfaces containing the lines of force and on which the plasma pressure is constant. Because the surfaces consist of lines of force, they are called magnetic surfaces or flux surfaces.

The innermost flux surface is evidently a single toroidal line, called the magnetic axis. The other, nondegenerate, surfaces occur in one of two different types:

(i) periodic surfaces, on which each field line closes upon itself after one or more circuits of the torus;

(ii) quasi-periodic surfaces, which are covered quasi-periodically by a single field line. That is, a particle moving always parallel to $\underset{\sim}{B}$ eventually comes arbitrarily close to any chosen point on the flux surface.

An extreme example of the periodic case is the bumpy torus configuration in which, ideally, every surface is of type (i), with

closure occurring after a single toroidal circuit. In more common experimental devices, a typical flux surface is quasi-periodic.

Of course a flux surface configuration is determined both by currents flowing in external conductors and by plasma currents. The relative importance of plasma current differs in different machines. Thus stellarators possess quasi-periodic flux surfaces in the absence of plasma current (vacuum flux surfaces), while tokamaks, for example, depend crucially upon plasma current to provide ergodicity. The point is that tokamaks are axisymmetric (symmetric with respect to rotation about the major toroidal axis), and external coils in an axisymmetric device cannot by themselves produce ergodic, toroidal flux surfaces.

In addition to the periodic and quasi-periodic cases, there is a third possibility: the magnetic field lines might ergodically fill a three-dimensional region. This case is pathological, in that any ergodic volume could not support a pressure gradient. Yet arguments from the Hamiltonian theory of Kolmogorov, Arnold and Moser [2] show that small ergodic volumes are certain to occur, unless the configuration is rigorously axisymmetric. Fortunately it is possible to design asymmetric systems in such a way that the ergodic regions occupy a manageably small fraction of the total plasma volume. This issue is instructively considered by Grad [4].

In the remainder of this section we assume that any ergodic regions have negligible volume. We also exclude from detailed consideration the purely closed field line case. Thus we consider magnetic confinement systems with nested flux surfaces, almost every one of which is ergodically covered by a single magnetic field line.

It is useful to distinguish two kinds of equilibrium studies:

1. Global equilibrium theory attempts to calculate $\underset{\sim}{B}(\underset{\sim}{x})$ throughout the confining region, using Eqs. (2.1)-(2.3), appropriate boundary data, and knowledge of the pressure profile. Especially for three-dimensional (asymmetric) geometries, such calculations are rarely tractable analytically and always device-specific.

2. Local equilibrium theory, on the other hand, studies conditions in the close vicinity of a single flux surface. One considers, in particular, how quantities such as $B = |\underset{\sim}{B}|$, or some component of $\underset{\sim}{J}$, vary on a given surface. The variation of field quantities from one surface to another is conveniently parametrized, but not predicted.

We restrict our analysis to local theory. The point is that our main interest is not in equilibrium theory by itslf, but in stability; and a wide class of plasma stability issues depend critically upon conditions near a single flux surface.

B. Toroidal Coordinates

1. Flux coordinates

Smoothly varying coordinates on a toroidal surface are necessarily angle coordinates: multivalued functions of position, $\underset{\sim}{x}$, which change by fixed amounts when either the magnetic axis or the major toroidal axis is encircled. We denote these angles by ϑ and ζ; ϑ, the poloidal angle, is assumed to change by 2π on any closed path encircling the magnetic axis, and to be single-valued on all other paths. Similarly, the toroidal angle, ζ, changes by 2π only on circuits of the major axis. We assume that the functions $\vartheta(\underset{\sim}{x})$ and $\zeta(\underset{\sim}{x})$

are suitably smooth. Any ϑ and ζ having these periodicity and smoothness properties are called "good" angle variables.

A third, "radial", coordinate, F, labels each surface and is constant on it

$$\underset{\sim}{B} \cdot \nabla F = 0 \ , \tag{2.5}$$

but varies smoothly from surface to surface. We call any such function a flux-surface label; an example is the plasma pressure, P.

Notice that any two sets of good angle variables, (ϑ,ζ) and (ϑ',ζ'), are related by

$$\begin{aligned} \vartheta' &= \vartheta + g_1(F,\vartheta,\zeta) \\ \zeta' &= \zeta + g_2(F,\vartheta,\zeta) \end{aligned} \tag{2.6}$$

where the functions g_1 and g_2 must be 2π-periodic in ϑ and ζ.

Next consider the magnetic field. It is not hard to show, from Eqs. (2.1)-(2.3), that $\underset{\sim}{B}$ can always be expressed as [3]

$$\underset{\sim}{B} = \nabla F \times \nabla G \tag{2.7}$$

where $G(F,\vartheta,\zeta)$ has the form

$$G = \alpha_1(F)\vartheta - \alpha_2(F)\zeta + G_0(F,\vartheta,\zeta) \ . \tag{2.8}$$

Here α_1 and α_2 depend only on F, and the function G_0 is an arbitrary periodic function of ϑ and ζ. The form of Eq. (2.8) is determined essentially by the requirement that $\underset{\sim}{B}$ be single-valued.

We emphasize that Eqs. (2.7) and (2.8) pertain for arbitrarily chosen (good) angle variables and flux label. Various simplified representations for $\underset{\sim}{B}$ are obtained by suitably restricting the coordinates. The most important restricted coordinate set is obtained from (F,ϑ,ζ) by the replacement $\vartheta \to \vartheta_f = \vartheta + G_0/\alpha_1$, which is clearly permitted by Eq. (2.6). It is also convenient to replace F by $\chi(F)$ where $d\chi/dF = \alpha_2$. The result can be written as

$$\underset{\sim}{B} = \nabla\chi \times \nabla(q\vartheta_f - \zeta_f) \ . \tag{2.9}$$

This "flux representation" for $\underset{\sim}{B}$ differs from the general representation of Eq. (2.7) mainly in that the G_0 of Eq. (2.8) does not appear. Coordinates $(\chi,\vartheta_f,\zeta_f)$ which yield this simplification are called flux coordinates. The significance of the quantity $q(\chi)$ will be considered presently.

Equation (2.9) suggests a natural decomposition of $\underset{\sim}{B}$ into poloidal ($\underset{\sim}{B}_P$) and toroidal (B_T) components:

$$\underset{\sim}{B} = \underset{\sim}{B}_P + \underset{\sim}{B}_T \ ,$$

$$\underset{\sim}{B}_P = \nabla\zeta_f \times \nabla\chi \ , \ \underset{\sim}{B}_T = q\nabla\chi \times \nabla\vartheta_f \tag{2.10}$$

The quantities χ and $q\vartheta_f - \zeta_f$ uniquely specify an individual field line; just as χ is the flux surface label, $q\vartheta_f - \zeta_f$ is sometimes called the field line label.

Flux coordinates are evidently not unique; in particular, we have yet to specify the toroidal angle. Two particularly useful flux coordinate sets are symmetry coordinates, denoted by $(\chi,\vartheta_0,\zeta_0)$, and

Hamada coordinates, denoted by $(\chi,\vartheta_H,\zeta_H)$. The first set requires axisymmetry; one chooses ζ_0 such that $\nabla\zeta_0 \cdot \nabla\vartheta_0 = \nabla\zeta_0 \cdot \nabla\chi = 0$. Hamada coordinates, which do not depend upon symmetry, are chosen such that the inverse volume element $\nabla\chi \cdot \nabla\vartheta_H \times \nabla\zeta_H$ is a flux label. Both systems are developed in some detail below.

Not all useful coordinate systems are flux coordinates. For example, Shafranov coordinates, (r,ϑ_s,ζ_s), satisfy only Eqs. (2.7) and (2.8), rather than Eq. (2.9). This system nonetheless simplifies the study of large aspect-ratio axisymmetric confinement; see for example [5]. The reduced coordinates of Chapter IV are also not flux coordinates.

In constructing and using the various coordinate systems, we will omit identifying subscripts whenever it is clear from context which system is under consideration.

Finally, notice that most of the useful coordinate systems are not orthogonal. Thus products like $\nabla\chi \cdot \nabla\vartheta$ cannot be presumed to vanish.

2. Rotational transform

Consider the flux surface, S_F, labelled by F, and let ϑ and ζ be any good angle variables on the surface. We cut the torus by a constant-ζ surface, S_ζ, in order to create a volume, $\mathcal{V}(F)$, bounded by S_ζ and S_F, inside of which $\zeta(\underset{\sim}{x})$ is single-valued. The magnetic flux through S_ζ is called the toroidal flux and denoted by

$$\psi_T = \int_{S_\zeta} d\underset{\sim}{S} \cdot \underset{\sim}{B} \tag{2.11}$$

where $d\underset{\sim}{S}$ is the vector surface element. It should be evident that ψ_T

is independent of the choice of angle coordinates, and is in fact a well-defined flux label.

A more convenient expression for ψ_T is given by

$$2\pi\psi_T = \int d\underset{\sim}{x}\ \nabla\zeta \cdot \underset{\sim}{B} . \tag{2.12}$$

The equivalence of Eqs. (2.11) and (2.12) can be seen by applying Gauss' theorem to Eq. (2.12), which can be written as

$$2\pi\psi_T = \int d\underset{\sim}{x}\nabla \cdot (\zeta\underset{\sim}{B})$$

Notice that Gauss' theorem is applicable only because of the cut, i.e., the integrand must be single-valued. The surface of $\mathscr{V}$ consists of S_F, which clearly cannot contribute, and <u>both sides</u> of S_ζ, across which ζ changes by 2π. Thus one obtains Eq. (2.11).

Similarly, the flux through a constant-ϑ surface (ribbon) is the poloidal flux, ψ_P. It can be written as

$$2\pi\psi_P = \int d\underset{\sim}{x}\ \nabla\vartheta \cdot \underset{\sim}{B} \tag{2.13}$$

and is also a flux label.

The rotational transform is defined by

$$\iota \equiv 2\pi \frac{d\psi_P}{d\psi_T} . \tag{2.14}$$

It measures the average winding number, or field line pitch, on a flux surface. Consider the successive intersections of a single field line

with the "surface of section", S_ζ. In general, each intersection will occur at a different ϑ; the change in ϑ between successive intersections need not be constant, but the average change, after many toroidal circuits, converges to ι [3]. In other words ι equals the average change in poloidal angle when a field line is followed over a complete toroidal circuit. From Eq. (2.14) and the properties of ψ_P and ψ_T, it is clear that ι is independent of the choice of angle variables, and that it is a flux label.

Let us specialize to flux coordinates. We substitute Eq. (2.9) into Eq. (2.12) to write the toroidal flux as

$$2\pi\psi_T = \int d^3\underset{\sim}{x}\ q\nabla\chi \times \nabla\vartheta_f \cdot \nabla\zeta_f \ .$$

This expression simplifies because of the geometrical identity

$$d^3\underset{\sim}{x} = \frac{d\chi d\vartheta d\zeta}{\nabla\chi\cdot(\nabla\vartheta\times\nabla\zeta)} \tag{2.15}$$

which gives the Jacobian (volume element) for any right-handed coordinate set (χ,ϑ,ζ). Thus

$$\psi_T = (2\pi)^{-1} \oint d\vartheta_f\ d\zeta_f \int_F d\chi\ q \ .$$

Here,

$$\oint d\vartheta_f\ d\zeta_f \equiv \int_0^{2\pi} d\vartheta_f \int_0^{2\pi} d\zeta_f \tag{2.16}$$

and

$$\int_F d\chi \equiv \int_0^{\chi(F)} d\chi \ .$$

Since q is a flux label, we have

$$\psi_T = 2\pi \int_F d\chi \ q(\chi) \ . \tag{2.17}$$

We can similarly compute

$$\psi_P = 2\pi \int_F d\chi = 2\pi \ \chi(F) \ . \tag{2.18}$$

Thus the flux label χ is simply related to the poloidal flux. Furthermore, Eq. (2.17) shows that $d\psi_T/d\chi = 2\pi q$, or

$$\frac{d\psi_T}{d\psi_P} = q = \frac{2\pi}{\iota} \ . \tag{2.19}$$

The quantity q is called the safety factor. It is an alternative measure of field line pitch which will be used, instead of ι, in most of this review.

A naive measure of field line pitch is the ratio $d\vartheta/d\zeta$, where $d\vartheta$ and $d\zeta$ (not necessarily flux coordinates) are measured along the field line trajectory:

$$\frac{d\vartheta}{d\zeta} = \frac{\underset{\sim}{B}\cdot\nabla\vartheta}{\underset{\sim}{B}\cdot\nabla\zeta} \ .$$

This quantity depends upon the choice of angle variables and generally varies on a flux surface. Thus, if the cut toroidal surface is

unrolled, the field lines on it are not generally straight. Suppose, however, that flux coordinates are employed, and that the unrolled surface is deformed into a square on which the lines of constant ϑ_f and ζ_f form a Cartesian grid. On this surface, the field lines will be straight, because Eq. (2.9) yields

$$\frac{d\vartheta_f}{d\zeta_f} = \frac{\underset{\sim}{B}\cdot\nabla\vartheta_f}{\underset{\sim}{B}\cdot\nabla\zeta_f} = \frac{1}{q(\chi)} . \tag{2.20}$$

Equation (2.20) expresses the major advantage of flux coordinates, which are sometimes called "straight field-line coordinates".

Equation (2.20) also shows that the field lines on a surface with rational safety factor must be closed. Thus if $q = m/n$, a field line starting at $\underset{\sim}{x}$ will return precisely to $\underset{\sim}{x}$ after m toroidal circuits ($\Delta\vartheta = 2\pi n/m$ $\Delta\zeta = 2\pi n$). Thus these rational flux surfaces are necessarily periodic surfaces. Conversely, when q is irrational, which is the typical case, the poloidal and toroidal periods are not rationally related – the field line is quasi-periodic – and the flux surface is covered ergodically.

A relevant quantity in this context is the magnetic shear, which describes the change in field line pitch from surface to surface. It is measured by, for example, $dq/d\chi$. Systems without shear (such as the bumpy torus, in which q is everywhere infinite) need not have ergodic surfaces, but ergodicity will clearly prevail whenever shear is present.

We note finally that Eqs. (2.10), (2.18) and (2.19) allow us to express $\underset{\sim}{B} = \underset{\sim}{B}_P + \underset{\sim}{B}_T$ in terms of its fluxes:

$$\underset{\sim}{B}_P = (2\pi)^{-1} \nabla\zeta_f \times \nabla\psi_P$$

$$\underset{\sim}{B}_T = (2\pi)^{-1} \nabla\psi_T \times \nabla\vartheta_f \ . \qquad (2.21)$$

3. Magnetic differential equations

Equations of the form

$$\underset{\sim}{B} \cdot \nabla u(\underset{\sim}{x}) = S(\underset{\sim}{x}) \ , \qquad (2.22)$$

where $S(\underset{\sim}{x})$ is a prescribed source and the single-valued function $u(\underset{\sim}{x})$ is to be determined, are called magnetic differential equations. They occur frequently in both equilibrium and stability investigations. We study Eq. (2.22) using flux coordinates, suppressing the f-subscript.

First note that Eq. (2.22) can determine u only up to an additive function, $h(\underset{\sim}{x})$, which satisfies

$$\underset{\sim}{B} \cdot \nabla h(\underset{\sim}{x}) = 0 \ . \qquad (2.23)$$

On any ergodic flux surface, Eq. (2.23) requires h to be a flux label,

$$h(\underset{\sim}{x}) = h(\chi(\underset{\sim}{x})) \ ,$$

since one can follow a field line, without change in h, to a neighborhood of any point on the surface. If $h(\underset{\sim}{x})$ is assumed to be

continuous, then the existence of a dense subset of rational surfaces clearly cannot affect this conclusion.

Suppose on the other hand that the confining volume includes a shear-free region in which $q = m/n$ is rational. An acceptable solution is then any function of χ and the field line label:

$$h(\underset{\sim}{x}) = h(\chi, m\vartheta - n\zeta) \ . \tag{2.24}$$

The main point here is that dependence on the variable $n(q\vartheta - \zeta)$ is consistent with periodicity (single-valuedness) of h,

$$h(\chi, \vartheta + 2\pi, \ \zeta + 2\pi) \ = \ h(\chi, \vartheta, \zeta) \ , \tag{2.25}$$

only when q is rational.

In the context of linear stability theory, perturbations which satisfy Eq. (2.23) are called flute modes. We have observed that flute modes strictly can occur only in shear-free regions. Similarly, a perturbation $g(\underset{\sim}{x})$ which satisfies

$$\underset{\sim}{B} \cdot \nabla g(\underset{\sim}{x}) \approx 0 \ , \tag{2.26}$$

i.e., which is <u>nearly</u> constant along $\underset{\sim}{B}$, is called flute-like. For a variety of reasons, variation along $\underset{\sim}{B}$ tends to be stabilizing, so that flute-like modes are often the most dangerous. A significant issue in stability theory is the construction of functions which are single-valued yet satisfy Eq. (2.26), in the presence of shear. The modern treatment of this issue is reviewed in Chapter VI.

Next we return to Eq. (2.22). In flux coordinates,

$$\underset{\sim}{B} \cdot \nabla u = \underset{\sim}{B} \cdot \nabla\vartheta\left(\frac{\partial u}{\partial \vartheta} + q \frac{\partial u}{\partial \zeta}\right) . \tag{2.27}$$

Also, since $u(\chi,\vartheta,\zeta)$ is periodic we may write

$$u = \sum_{m,n} u_{mn}(\chi) \exp\, i(m\vartheta - n\zeta) ,$$

where

$$u_{mn}(\chi) = \oint \frac{d\vartheta d\zeta}{(2\pi)^2} u \exp\, i(n\zeta - m\vartheta) \tag{2.28}$$

is the Fourier coefficient, and we use the abbreviation of Eq. (2.16). Since q is a flux label, the u_{mn} satisfy uncoupled equations:

$$i(m-nq)u_{mn} = (S/\underset{\sim}{B}\cdot\nabla\vartheta)_{mn} . \tag{2.29}$$

Note that the decoupling depends upon our use of flux coordinates.

An important feature of Eq. (2.29) is that the left-hand side vanishes on each rational surface χ_{mn}, where

$$q(\chi_{mn}) = m/n . \tag{2.30}$$

Let us require each u_{mn} to be a continuous function of χ. Then a solubility condition for the magnetic differential equation is

$$(S/\underset{\sim}{B}\cdot\nabla\vartheta)_{mn} = 0 \quad \text{when} \quad \chi = \chi_{mn} . \tag{2.31}$$

This condition is clearly necessary; that it is also sufficient was first demonstrated by Newcomb [6]. Kruskal and Kulsrud [3] noted the necessary (but not sufficient) solubility condition,

$$(S/\underset{\sim}{B}\cdot\nabla\vartheta)_{00} = 0 \tag{2.32}$$

which must hold on every surface. More concise formulations of both conditions are considered below.

4. Flux-surface average

As in Eq. (2.12), we let $\mathscr{V}(F)$ be the volume contained within the flux surface labelled by F:

$$\mathscr{V}(F) = \int_F d\underset{\sim}{x} \ . \tag{2.33}$$

Similarly,

$$\Delta\mathscr{V} = \int_{\Delta F} d\underset{\sim}{x} \tag{2.34}$$

measures the differential volume between two neighboring surfaces, F and F + ΔF. The flux-surface average of any quantity $A(\underset{\sim}{x})$ is then defined as

$$\langle A\rangle_F = (\Delta\mathscr{V})^{-1} \int_{\Delta F} d\underset{\sim}{x}\ A \tag{2.35}$$

in the limit of vanishing ΔF. It is clear that $\langle A\rangle_F$ depends upon position only through F.

The crucial property of the flux-surface average is that it annihilates the operator $\underset{\sim}{B}\cdot\nabla$. That is,

$$\langle \underset{\sim}{B}\cdot\nabla u(\underset{\sim}{x})\rangle_F = 0 \tag{2.36}$$

for any single-valued function $u(\underset{\sim}{x})$. Equation (2.36) is an immediate consequence of $\nabla\cdot\underset{\sim}{B} = 0$ and Gauss' theorem.

It can be seen that the perpendicular distance between two neighboring flux surfaces is given by $dF/|\nabla F|$; hence the volume element is

$$d\underset{\sim}{x} = dS dF/|\nabla F| \ , \tag{2.37}$$

where dS is the surface element and F is as usual an arbitrary flux label. By choosing $F = \mathcal{V}$, we can express $\langle A\rangle_F$ in terms of a surface integral,

$$\langle A\rangle_F = \int_{S_F} \frac{dS}{|\nabla \mathcal{V}|} A \ . \tag{2.38}$$

Next let $\underset{\sim}{A}$ be an arbitrary (single-valued) vector, and consider its averaged divergence:

$$\langle \nabla\cdot\underset{\sim}{A}\rangle_F = \frac{1}{\Delta\mathcal{V}} \int_{\Delta F} d\underset{\sim}{x}\ \nabla\cdot\underset{\sim}{A}$$

$$= \frac{1}{\Delta\mathcal{V}} \int_{S_{\Delta F}} dS\ \frac{\underset{\sim}{A}\cdot\nabla\mathcal{V}}{|\nabla\mathcal{V}|}$$

Here the integration surface, $S_{\Delta F}$, consists of the two flux surfaces enclosing the volume $\Delta\mathcal{V}$. Thus, in view of Eq. (2.38),

$$\langle\nabla\cdot\underset{\sim}{A}\rangle_F = \frac{d}{d\mathcal{V}}\langle\underset{\sim}{A}\cdot\nabla\mathcal{V}\rangle_F \ . \tag{2.39}$$

A corollary is the useful relation,

$$\langle\nabla F\cdot\nabla\times\underset{\sim}{A}\rangle_F = 0$$

for any flux label F, since $\nabla F\cdot\nabla\times\underset{\sim}{A} = \nabla\cdot(\underset{\sim}{A}\times\nabla F)$.

In terms of arbitrary toroidal coordinates (F,ϑ,ζ), Eqs. (2.15) and (2.35) provide the expression

$$\langle A\rangle_F = \frac{dF}{d\mathcal{V}}\oint\frac{d\vartheta d\zeta\ A(F,\vartheta,\zeta)}{\nabla F\cdot\nabla\vartheta\times\nabla\zeta} \ . \tag{2.40}$$

By choosing A=1, we obtain a useful expression for $dF/d\mathcal{V}$:

$$\left(\frac{dF}{d\mathcal{V}}\right)^{-1} = \oint\frac{d\vartheta d\zeta}{\nabla F\cdot\nabla\vartheta\times\nabla\zeta} \ . \tag{2.41}$$

In particular, for $F = \mathcal{V}$ we have

$$\oint\frac{d\vartheta d\zeta}{\nabla\mathcal{V}\cdot\nabla\vartheta\times\nabla\zeta} = 1 \ . \tag{2.42}$$

In flux coordinates, Eq. (2.40) becomes

$$\langle A\rangle_F = \frac{d\chi}{d\mathscr{V}} \oint \frac{d\vartheta_f d\zeta_f A(\chi,\vartheta_f,\zeta_f)}{\underset{\sim}{B}\cdot\nabla\vartheta_f} \tag{2.43}$$

which is to be compared with Eq. (2.32): the latter can evidently be written as

$$\langle S\rangle_F = 0 \ . \tag{2.44}$$

Similarly, the necessary and sufficient solubility condition of Eq. (2.31) has the expression

$$\langle S \exp i(n\zeta-m\vartheta)\rangle_F = 0 \ , \text{ on } \chi_{mn} \ . \tag{2.45}$$

We next derive an alternative version of Eq. (2.45), following Newcomb [6]. We begin with the explicit form

$$(S/\underset{\sim}{B}\cdot\nabla\vartheta)_{mn} = \oint \frac{d\vartheta d\zeta}{(2\pi)^2} \frac{S}{\underset{\sim}{B}\cdot\nabla\vartheta} \exp i(n\zeta-m\vartheta)$$

$$= \frac{q}{(2\pi)^2} \oint d\vartheta \frac{d\zeta}{\underset{\sim}{B}\cdot\nabla\zeta} S \exp i(n\zeta-m\vartheta) \ ,$$

suppressing the f-subscript. Next we change integration variables, $(\vartheta,\zeta) \rightarrow (\alpha,\ell)$, where α is the field line label,

$$\alpha \equiv \zeta - q\vartheta \tag{2.46}$$

and ℓ is the arc length along $\underset{\sim}{B}$. The ℓ-integration (at fixed α) is performed first, using

$$d\zeta/\underset{\sim}{B}\cdot\nabla\zeta \;=\; d\ell/B$$

and denoting by L the total arc length along $\underset{\sim}{B}$ for one toroidal circuit. The result is

$$\left(\frac{S}{\underset{\sim}{B}\cdot\nabla\vartheta}\right)_{mn} = \oint \frac{d\alpha}{(2\pi)^2}\, I(\alpha)\exp(in\alpha)$$

where α goes from 0 to $2\pi/q$ and

$$I(\alpha) = \oint \frac{d\zeta}{\underset{\sim}{B}\cdot\nabla\zeta}\, S\left(\chi, \frac{\zeta-\alpha}{q}, \zeta\right)$$

$$= \int_0^{L(\alpha)} \frac{d\ell}{B}\, S \;. \qquad (2.47)$$

Thus, Eq. (2.45) has been reduced to the requirement that

$$\oint d\alpha\; e^{in\alpha} I(\alpha) = 0 \qquad (2.48)$$

whenever nq is an integer.

Notice that the contour in Eq. (2.47) is not in general closed, since a field line on χ_{mn} closes only after m toroidal circuits. By extending the contour (along $\underset{\sim}{B}$) until it closes we obtain the quantity

$$I_c = \oint \frac{d\ell}{B}\, S \qquad (2.49)$$

which is related to $I(\alpha)$ through

$$I_c = \sum_{p=0}^{m-1} I(\alpha+2\pi p) \ . \qquad (2.50)$$

We next show that, because of Eq. (2.48), I_c vanishes. Substituting the Fourier decomposition of I into Eq. (2.50), we find that

$$I_c = \sum_k I_k \exp(-ik\alpha/q) \sum_{p=0}^{m-1} \exp(2\pi ikp/q) \ .$$

But the sum

$$\sum_{p=0}^{m-1} \exp(2\pi ikp/q) = \sum_{p=0}^{m-1} \exp(2\pi ikpn/m)$$

vanishes, unless $kn/m = k/q$ is an integer. Since Eq. (2.48) rules out such integral contributions, we have

$$\oint \frac{d\ell}{B} S = 0 \qquad (2.51)$$

on each rational surface.

We have thus shown that Eq. (2.45) is equivalent to the "Newcomb condition", Eq. (2.51). Since the magnetic differential equation can always be written as

$$B \ \partial u/\partial \ell = S \ ,$$

the form of the Newcomb condition is not surprising.

5. Hamada coordinates

The volume element for arbitrary toroidal coordinates can be expressed in terms of the Jacobian, $\sqrt{g}$, as

$$d\underset{\sim}{x} = \sqrt{g}\ dF d\vartheta d\zeta \ .$$

In other words [recall Eq. (2.15)]

$$\sqrt{g} = (\nabla F \cdot \nabla\vartheta \times \nabla\zeta)^{-1} \ . \tag{2.52}$$

Both sides of this relation are positive since we assume (F,ϑ,ζ) to form a right-handed coordinate set.

The Jacobian for flux coordinates is evidently given by

$$\sqrt{g}_f = (\nabla\chi \cdot \nabla\vartheta_f \times \nabla\zeta_f)^{-1} = (\underset{\sim}{B} \cdot \nabla\vartheta_f)^{-1}$$

Consider the flux-surface average of $1/\sqrt{g}_f$:

$$\begin{aligned} \langle g_f^{-1/2} \rangle_F &= \langle \nabla\chi \cdot \nabla\vartheta_f \times \nabla\zeta_f \rangle_F \\ &= \oint d\vartheta_f d\zeta_f / \oint d\vartheta_f d\zeta_f \ \sqrt{g}_f \end{aligned}$$

where, according to Eq. (2.41),

$$\oint d\vartheta_f d\zeta_f \ \sqrt{g}_f = d\mathcal{V}/d\chi \ .$$

Hence

$$\langle g_f^{-1/2} \rangle_F = (2\pi)^2 \ d\chi/d\mathcal{V}$$

and a trivial change in only the radial coordinate, $\chi \to V(\chi)$, where

$$V \equiv \mathscr{V}/(2\pi)^2 \tag{2.53}$$

conveniently makes the averaged Jacobian equal unity. Recalling that flux coordinates are not unique, we are led to ask whether some choice might make the unaveraged Jacobian equal unity at each point. Such coordinates were originally found by Hamada [7]; they are denoted here by $(V, \vartheta_H, \zeta_H)$.

Because Hamada coordinates are a special case of flux coordinates, we must have

$$\underset{\sim}{B} = \nabla\chi(V) \times \nabla(q\vartheta_H - \zeta_H) \ , \tag{2.54}$$

together with the defining property

$$\nabla V \cdot \nabla\vartheta_H \times \nabla\zeta_H = 1 \ . \tag{2.55}$$

Equation (2.54) suggests that

$$\begin{aligned} \vartheta_H &= \vartheta_f + K(\vartheta_f, \zeta_f)/q \\ \zeta_H &= \zeta_f + K(\vartheta_f, \zeta_f) \ , \end{aligned} \tag{2.56}$$

which is consistent with Eq. (2.6) for any periodic function K. Substituting Eqs. (2.56) into Eq. (2.55) one obtains, after simple manipulation, a magnetic differential equation for K:

$$\underset{\sim}{B}\cdot\nabla K = q\,\frac{d\chi}{dV}\left[1-\nabla V\cdot(\nabla\vartheta_f\times\nabla\zeta_f)\right] . \tag{2.57}$$

This is soluble if it satisfies the Newcomb condition,

$$\oint \frac{d\ell}{B}\left[1 - \nabla V\cdot(\nabla\vartheta_f\times\nabla\zeta_f)\right] = 0 \tag{2.58}$$

on each rational surface. Equation (2.58) has been verified by Greene and Johnson [8]; we omit the proof [cf. Eq. (2.89) et seq.]. Notice that the simpler, necessary solubility condition, Eq. (2.44), is clearly satisfied, in view of Eq. (2.40).

One advantage of Hamada coordinates is that they simplify the form of the flux-surface average. From Eqs. (2.40), (2.53), and (2.55) we have

$$\langle A\rangle_F = \oint \frac{d\vartheta_H d\zeta_H}{(2\pi)^2} A . \tag{2.59}$$

6. Symmetry coordinates

The natural toroidal angle for axisymmetric systems is the angle, ζ_0, which measures rotation about the symmetry axis (major toroidal axis). The distance between a point, $\underset{\sim}{x}$, and the symmetry axis is the major radius of $\underset{\sim}{x}$, denoted by $R(\underset{\sim}{x})$. Notice that (R,ζ_0) comprise ordinary polar coordinates on each plane normal to the symmetry axis, whence

$$|\nabla\zeta_0| = R^{-1} . \tag{2.60}$$

Axisymmetry obviously implies

$$\nabla\chi \cdot \nabla\zeta_0 = 0 \ . \tag{2.61}$$

Further, it is possible to choose the poloidal angle, ϑ_0, such that

$$\nabla\vartheta_0 \cdot \nabla\zeta_0 = 0 \ , \tag{2.62}$$

while still retaining the flux representation,

$$\underset{\sim}{B} = \nabla\chi \times \nabla(q\vartheta_0 - \zeta_0)$$

Thus, in the sense of Eqs. (2.61) and (2.62), symmetry coordinates are partially orthogonal. (In general, $\nabla\chi \cdot \nabla\vartheta_0$ remains non-zero.)

The most important consequence of partial orthogonality is that the toroidal field,

$$\underset{\sim}{B}_T = q\nabla\chi \times \nabla\vartheta_0 \tag{2.63}$$

is parallel to $\nabla\zeta_0$:

$$\underset{\sim}{B}_T \times \nabla\zeta_0 = 0 \ . \tag{2.64}$$

A stronger version of Eq. (2.64) can be obtained as follows. Consider the line integral of $\underset{\sim}{B}$ around any circle, C, centered on the symmetry axis. By axisymmetry and Stokes' theorem,

$$2\pi B_T R = \frac{4\pi}{c} \int_A d\underset{\sim}{S} \cdot \underset{\sim}{J} \tag{2.65}$$

where the surface of integration, A, is the disc bounded by C and $\underset{\sim}{J}$ is the current density. Next consider a different circle, C′, which lies on the same flux surface as C. Because Eq. (2.1) implies current must flow on flux surfaces, $\underset{\sim}{J}\cdot\nabla\chi = 0$, the new contour cannot change the value of the right-hand side of Eq. (2.65). Thus

$$B_T R = I(\chi)$$

where I is a flux label. The form

$$B_T = I(\chi)\nabla\zeta_0 \tag{2.66}$$

is often more convenient than the flux representation, Eq. (2.63); but it should be emphasized that Eq. (2.66) pertains only in axisymmetric geometry.

Equation (2.66) also provides a useful expression for the Jacobian, $\sqrt{g_0}$, corresponding to symmetry coordinates:

$$\frac{1}{\sqrt{g}_0} = \nabla\vartheta_0 \cdot \nabla\zeta_0 \times \nabla\chi = \nabla\vartheta_0\cdot\underset{\sim}{B}$$

$$= \frac{1}{q}\,\underset{\sim}{B}\cdot\nabla\zeta_0 = I/(R^2 q)$$

in view of Eqs. (2.20) and (2.60). Since I and q are flux labels, the Jacobian varies with ϑ_0 only through R^2,

$$\sqrt{g}_0 = (q/I)R^2(\chi,\vartheta_0)\ . \tag{2.67}$$

Note finally that if f is a physical equilibrium quantity in any axisymmetric system, then one can take $f(\underset{\sim}{x}) = f(\chi,\vartheta)$, i.e., $\partial f/\partial\zeta = 0$, for <u>any</u> choice of toroidal angle ζ. However, $\nabla f \cdot \nabla\zeta$ will vanish in general only if ζ is the symmetry angle, ζ_0.

7. Tensor notation

The vector relation

$$\underset{\sim}{J}\times\underset{\sim}{B} = cdP/d\chi\ \nabla\chi \tag{2.68}$$

has its most interesting component in the direction of $\nabla\chi$. One way to isolate this component is scalar multiplication with $\nabla\vartheta \times \nabla\zeta$. In view of Eq. (2.52) and the vector identity,

$$\nabla\vartheta\times\nabla\zeta \cdot (\underset{\sim}{J}\times\underset{\sim}{B}) = (\underset{\sim}{J}\cdot\nabla\vartheta)(\underset{\sim}{B}\cdot\nabla\zeta) - (\underset{\sim}{J}\cdot\nabla\zeta)(\underset{\sim}{B}\cdot\nabla\vartheta)$$

one obtains in this way

$$\sqrt{g}\ [(\underset{\sim}{J}\cdot\nabla\vartheta)(\underset{\sim}{B}\cdot\nabla\zeta) - (\underset{\sim}{J}\cdot\nabla\zeta)(\underset{\sim}{B}\cdot\nabla\vartheta)] = cdP/d\chi\ . \tag{2.69}$$

Multiplication of Eq. (2.68) by some other cross-product, such as $\nabla\chi \times \nabla\vartheta$, yields an identity, since $\underset{\sim}{J}\cdot\nabla\chi = \underset{\sim}{B}\cdot\nabla\chi = 0$.

Of course arguments of this sort can always be used to find the relevant components of a vector equation. But a much more efficient way to obtain, and especially to write, results like Eq. (2.69) uses tensor notation. Only the most elementary features of tensor formalism will be required here [9]. Thus we introduce, for flux coordinates $(\xi^\chi,\xi^\vartheta,\xi^\zeta) \equiv (\chi,\vartheta,\zeta)$ and an arbitrary vector $\underset{\sim}{A}$, the contravariant

components $A^\mu = (A^\chi, A^\vartheta, A^\zeta)$ and covariant components $A_\mu = (A_\chi, A_\vartheta, A_\zeta)$. Readers unfamiliar with tensor formalism can consider these quantities to be defined by $A^\mu = \underset{\sim}{A}\cdot\nabla\xi^\mu$, or

$$A^\chi = \underset{\sim}{A}\cdot\nabla\chi, \quad A^\vartheta = \underset{\sim}{A}\cdot\nabla\vartheta, \quad A^\zeta = \underset{\sim}{A}\cdot\nabla\zeta \tag{2.69}$$

and

$$\begin{aligned} A_\chi &= \sqrt{g}\ \nabla\vartheta \times \nabla\zeta\cdot\underset{\sim}{A}\ , \\ A_\vartheta &= \sqrt{g}\ \nabla\zeta \times \nabla\chi\cdot\underset{\sim}{A}\ , \\ A_\zeta &= \sqrt{g}\ \nabla\chi \times \nabla\vartheta\cdot\underset{\sim}{A}\ , \end{aligned} \tag{2.70}$$

respectively. We can expand $\underset{\sim}{A}$ in terms of either component set:

$$\underset{\sim}{A} = A_\chi\nabla\chi + A_\vartheta\nabla\vartheta + A_\zeta\nabla\zeta \tag{2.71}$$

$$= \sqrt{g}\ \left(A^\chi\nabla\vartheta \times \nabla\zeta + A^\vartheta\nabla\zeta \times \nabla\chi + A^\zeta\nabla\chi \times \nabla\vartheta\right) . \tag{2.72}$$

From Eqs. (2.71) and (2.72), it is easily seen that

$$\underset{\sim}{A}\cdot\underset{\sim}{B} = A^\mu B_\mu \equiv A^\chi B_\chi + A^\vartheta B_\vartheta + A^\zeta B_\zeta$$

agrees with the usual scalar product. (A sum over repeated dummy indices is always implicit.)

The vector product,

$$\underset{\sim}{W} = \underset{\sim}{A}\times\underset{\sim}{B}$$

has contravariant components

$$W^{\mu} = g^{-1/2}\ \varepsilon_{\mu\kappa\lambda}\ A_{\kappa}\ B_{\lambda}\ , \tag{2.73}$$

and covariant components

$$W_{\mu} = g^{1/2}\ \varepsilon_{\mu\kappa\lambda}\ A^{\kappa}\ B^{\lambda}\ . \tag{2.74}$$

Here $\varepsilon_{\mu\kappa\lambda}$ is the usual antisymmetrical matrix, with non-zero components $\varepsilon_{\chi\vartheta\zeta} = \varepsilon_{\zeta\chi\vartheta} = \varepsilon_{\vartheta\zeta\chi} = 1$, $\varepsilon_{\vartheta\chi\zeta} = \varepsilon_{\zeta\vartheta\chi} = \varepsilon_{\chi\zeta\vartheta} = -1$. Thus, for example,

$$W_{\chi} = g^{1/2}(A^{\vartheta}B^{\zeta} - A^{\zeta}B^{\vartheta})\ .$$

The coordinates, ξ^{μ}, do not constitute contravariant components of any vector. However, each ξ^{μ} [e.g., $\xi^{\chi} = \chi(\underset{\sim}{x})$] can be considered as a scalar function of position.

Next we need to write three differential operators in tensor form.

The gradient of a scalar, ∇S, has a natural covariant representation:

$$(\nabla S)_{\mu} = \frac{\partial S}{\partial \xi^{\mu}}\ . \tag{2.75}$$

In particular, when S is one of the coordinates, then

$$(\nabla \xi^{\nu})_{\mu} = \delta_{\mu\nu} \tag{2.76}$$

where $\delta_{\mu\nu}$ is the Kronecher delta. Thus, for example

$$(\nabla P)_\mu = \frac{\partial P}{\partial \chi}\,\delta_{\mu\chi} \ .$$

Notice also that for any vector $\underset{\sim}{A}$,

$$\underset{\sim}{A}\cdot\nabla S = A^\mu \frac{\partial S}{\partial \xi^\mu} \tag{2.77}$$

The divergence of a vector is conveniently written in terms of its contravariant components:

$$\nabla\cdot\underset{\sim}{A} = \frac{1}{\sqrt{g}} \frac{\partial}{\partial \xi^\mu} \sqrt{g}\ A^\mu \ . \tag{2.78}$$

Finally, the curl,

$$\underset{\sim}{B} = \nabla\times\underset{\sim}{A}$$

has contravariant components given by

$$B^\mu = \frac{\varepsilon_{\mu\kappa\lambda}}{\sqrt{g}} \frac{\partial A_\lambda}{\partial \xi^\kappa} \ , \tag{2.79}$$

in terms of the covariant components of $\underset{\sim}{A}$.

As a simple application of these formulae, we consider the magnetic field. From Eqs. (2.9), (2.52) and (2.69) we find that $\underset{\sim}{B}$ has the following contravariant components:

$$B^\chi = 0 \ , \ B^\vartheta = g^{-1/2}, \ B^\zeta = qB^\vartheta \ . \tag{2.80}$$

The covariant components, e.g.,

$$B_\chi = \sqrt{g}\ \nabla\vartheta \times \nabla\zeta \cdot \underset{\sim}{B}$$

do not have such a simple representation.

In Hamada coordinates,

$$\underset{\sim}{B} = \chi'\ \nabla V \times \nabla(q\vartheta_H - \zeta_H)$$

where

$$\chi'(V) \equiv d\chi/dV\ . \tag{2.81}$$

Thus, suppressing H-subscripts, we obtain the contravariant Hamada components

$$B^V = 0,\ B^\vartheta = \chi',\ B^\zeta = q\chi'\ . \tag{2.82}$$

Notice that both B^ϑ and B^ζ (rather than only their ratio) are flux labels in the Hamada case.

C. Plasma Current

1. Significance

In this section we consider the force balance relation and Ampere's law explicitly. Plasma currents are important, firstly, because they help to determine the flux-surface configuration. Indeed, for axisymmetric systems, toroidal flux surfaces are not possible

without toroidal plasma current. Secondly, the disposition of plasma currents has striking effects on plasma stability. Thus equilibrium current along the direction of $\underset{\sim}{B}$ can destabilize certain "current-driven" modes, while current perpendicular to $\underset{\sim}{B}$ is associated with "pressure-driven" instabilities.

Subsection C.2 considers those properties of current flow which follow from Eq. (2.1) and the quasineutrality condition,

$$\nabla \cdot \underset{\sim}{J} = 0 \ , \tag{2.83}$$

an immediate consequence of Eq. (2.3). One finds that these relations always permit a simple parameterization of $\underset{\sim}{J}$ in terms of two flux labels. Equations (2.2) and (2.83) also reveal an important constraint, related to the Newcomb condition, which bears on the existence of Hamada coordinates.

Ampere's law is studied in Subsection C.3. It is found, in particular, that the sign of the poloidal current characterizes important features of toroidal equilibria. The concept of "return current" is also introduced.

The arguments of Subsections C.2 and C.3 pertain in an arbitrary toroidal geometry. The special case of axisymmetric geometry allows more explicit conclusions regarding the plasma current. These are derived in Subsection C.4.

2. Force balance

In this and the following subsection we use Hamada coordinates exclusively. Thus the force balance relation, Eq. (2.68), is written as

$$\chi'(qJ^{\vartheta}-J^{\zeta}) = cP' \tag{2.84}$$

in the notation of Eq. (2.81) [cf. Eq. (2.69)]. Certain formal consequences of Eq. (2.84) enter stability studies; we derive them here.

We first substitute Eq. (2.84) into Eq. (2.83). Since the Hamada Jacobian is unity, we can write [recall Eq. (2.78)]

$$\frac{\partial J^{\vartheta}}{\partial \vartheta} + \frac{\partial J^{\zeta}}{\partial \zeta} = 0 \ . \tag{2.85}$$

Because χ',P' and q are flux labels, Eqs. (2.84) and (2.85) imply

$$(\frac{\partial}{\partial \vartheta} + q \frac{\partial}{\partial \zeta}) J^{\vartheta} = 0 \ ,$$

which is equivalent to $\underset{\sim}{B}\cdot\nabla J^{\vartheta} = 0$ and therefore requires J^{ϑ} to be a flux label. Equation (2.84) then shows that J^{ζ} is also a flux label. Since $J^{V} = 0$, we obtain, from Eq. (2.72),

$$\underset{\sim}{J} = J^{\vartheta}(V)\nabla\zeta\times\nabla V + J^{\zeta}(V)\nabla V\times\nabla\vartheta \tag{2.86}$$

a flux representation for $\underset{\sim}{J}$ which is closely analogous to Eq. (2.9).

Two alternative versions of Eq. (2.86) are derived by eliminating either $\nabla\zeta\times\nabla V$ or $\nabla V\times\nabla\vartheta$ in favor of $\underset{\sim}{B}$, and then using Eq. (2.84). The parallel components of the resulting expressions give useful expressions for the covariant components of $\underset{\sim}{B}$:

$$(\chi'/B)J_{\parallel} = J^{\vartheta} - (cP'/B^2)B_{\zeta} \tag{2.87a}$$

$$(q\chi'/B)J_{\parallel} = J^{\zeta} + (cP'/B^2)B_{\vartheta} \ . \tag{2.87b}$$

We next return to Eq. (2.68) to consider the magnitude of the perpendicular current density, $J_{\perp} = |\underset{\sim}{J}_{\perp}|$,

$$\underset{\sim}{J}_{\perp} \equiv \underset{\sim}{J} - \underset{\sim}{B}J_{\parallel}/B \ . \tag{2.88}$$

Evidently,

$$J_{\perp} = cP' \ |\nabla V|/B$$

or

$$J_{\perp} \frac{\Delta V}{|\nabla V|} = (c/B)\Delta P$$

where ΔV is the volume of the narrow annulus between two surfaces whose pressures differ by ΔP. Notice that this region will necessarily contain closed field lines (since rational surfaces are dense) and recall that its width is $\Delta V/|\nabla V|$. Hence the total current flowing across a closed field line in the annulus can be computed from

$$\oint d\ell\, J_\perp \frac{\Delta V}{|\nabla V|} = c\Delta P \oint \frac{d\ell}{B} .$$

Since current cannot escape the annulus, this integral must be the same for each closed field line of the same pitch, i.e., it must be a flux label. Since ΔP is also a flux label, we conclude that the integral

$$I_0(V) = \oint d\ell/B \qquad (2.89)$$

is a flux label. This argument is due to Greene and Johnson [8], who also note that Eq. (2.89) implies Eq. (2.58).

The physical interpretation of $I_0(V)$ is well known. Consider a flux tube of cross-sectional area dA surrounding the closed field line. The contained magnetic flux is $d\psi = BdA$, while the volume element is $d\underset{\sim}{x} = dAd\ell$; thus $I_0(V)$ is the volume per unit flux of the flux tube.

Recall that flux surfaces can be defined, in an asymmetric system, without reference to plasma pressure (Section A). Hence, ignoring the axisymmetric case, it is possible to consider the quantity I_0 in a vacuum system, with $J_\perp = 0 = \Delta P$. Since the argument leading to Eq. (2.89) breaks down for this case, the vacuum I_0 can vary on a rational surface. Indeed, three-dimensional vacuum flux surfaces typically display such variation in I_0. In other words, the vacuum limit of an asymmetric toroidal system is singular. As Grad [4] originally emphasized, the singularity is potentially serious, especially since such systems often operate at very low pressure. This issue continues to attract considerable theoretical interest [10].

Once the perpendicular current is known, the parallel current can be obtained from Eq. (2.83), expressed as

$$\underset{\sim}{B}\cdot\nabla(J_{\parallel}/B) = -\nabla\cdot\underset{\sim}{J}_{\perp} \ , \tag{2.90}$$

which is a magnetic differential equation. To explore its solubility, we consider, in Hamada coordinates, the quantity

$$\nabla\cdot\underset{\sim}{J}_{\perp} = \frac{\partial}{\partial\vartheta} J^{\vartheta}_{\perp} + \frac{\partial}{\partial\zeta} J^{\zeta}_{\perp} \ .$$

Recalling that

$$\underset{\sim}{J}_{\perp} = cP' \ \underset{\sim}{B} \times \nabla V/B^2$$

we find

$$\nabla\cdot\underset{\sim}{J}_{\perp} = cP' \left(\frac{\partial}{\partial\vartheta}\frac{B_{\zeta}}{B^2} - \frac{\partial}{\partial\zeta}\frac{B_{\vartheta}}{B^2}\right) \ .$$

Simple manipulation, using Eq. (2.87) and (2.84), reduces this expression to

$$\nabla\cdot\underset{\sim}{J}_{\perp} = cP' \left(\frac{\partial}{\partial\vartheta} + q\frac{\partial}{\partial\zeta}\right)\frac{B_{\zeta}}{B^2} = \underset{\sim}{B}\cdot\nabla\left(\frac{cP'}{\chi' B^2} B_{\zeta}\right) \ , \tag{2.91}$$

a form which manifestly satisfies Eq. (2.51).

We conclude that the magnetic differential equation (2.90) is soluble whenever Hamada coordinates exist. Since the existence of Hamada coordinates depends upon Eq. (2.89), we see that the latter is the true solubility condition for Eq. (2.90).

3. Ampere's law

In Hamada coordinates, the three (contravariant) components of Ampere's law,

$$\nabla \times \underset{\sim}{B} = (4\pi/c)\underset{\sim}{J}$$

are given by [cf. Eq. (2.79)]

$$J^V = 0 = \frac{\partial B_\vartheta}{\partial \zeta} - \frac{\partial B_\zeta}{\partial \vartheta} , \tag{2.92}$$

$$\frac{4\pi}{c} J^\vartheta = \frac{\partial B_V}{\partial \zeta} - \frac{\partial B_\zeta}{\partial V} , \tag{2.93}$$

$$\frac{4\pi}{c} J^\zeta = \frac{\partial B_\vartheta}{\partial V} - \frac{\partial B_V}{\partial \vartheta} . \tag{2.94}$$

In combination with our previous results (together with appropriate boundary data and profile information), these equations determine the global flux surface configuration. Unfortunately, in general geometry the equations are not analytically tractable. Useful local information can nonetheless be obtained from the flux-surface averaged equations.

Recalling Eq. (2.59), we use an abbreviated notation,

$$\bar{A} \equiv \langle A \rangle_F = \oint \frac{d\vartheta d\zeta}{(2\pi)^2} A \tag{2.95}$$

to write the averages of Eqs. (2.93) and (2.94) as

$$J^\vartheta = -(c/4\pi)\bar{B}_\zeta', \quad J^\zeta = (c/4\pi)\bar{B}_\vartheta' \ .$$

Overbars are not needed on J^ϑ and J^ζ, since they are flux labels. We substitute these results into Eq. (2.84) to obtain

$$\bar{B}_\vartheta' + q\bar{B}_\zeta' = -4\pi P'/\chi' \ . \tag{2.96}$$

The right-hand side of Eq. (2.96) (which must be typically positive) measures the local degree to which plasma thermal energy is confined. Hence terms on the left-hand side are contributing to confinement only when they are positive. The first term on the left almost always contributes in this sense (i.e., $J^\zeta > 0$; recall that $\bar{B}_\vartheta$ vanishes on the magnetic axis). However, the $\bar{B}_\zeta'$ term can have either sign, depending upon experimental conditions. When it is positive (negative), the plasma is said to be diamagnetic (paramagnetic) with respect to the toroidal field. The direction of the poloidal current J^ϑ indicates which case pertains.

Ohmically heated tokamaks and stellarators typically have $J^\zeta >> J^\vartheta$, while $B_\zeta >> B_\vartheta$. Equation (2.96) shows an economic disadvantage of such schemes: the large investment in toroidal magnetic field makes a relatively small (if not negative) direct contribution to plasma pressure containment. "Current-free" stellarators (in which $J^\zeta < J^\vartheta$) and high-beta tokamaks (which are

strongly diamagnetic) are examples of confinement concepts in which this disadvantage is ameliorated.

Next we consider the radial component of Ampere's law, Eq. (2.92). It is easily combined with Eqs. (2.87) to obtain

$$\chi'\left(\frac{\partial}{\partial\vartheta} + q\,\frac{\partial}{\partial\zeta}\right)(BJ_{\|}) = \left(J^{\vartheta}\,\frac{\partial}{\partial\vartheta} + J^{\zeta}\,\frac{\partial}{\partial\zeta}\right)B^2$$

or

$$(\underset{\sim}{B}\cdot\nabla)(J_{\|}B) = (\underset{\sim}{J}\cdot\nabla)B^2 \ , \tag{2.97}$$

showing that part of the parallel current is driven by variation of the field magnitude on a flux surface. The point is that $\nabla\cdot\underset{\sim}{J}_{\perp}$, Eq. (2.91), does not vanish unless B is a flux label. Thus "return currents" along $\underset{\sim}{B}$ are required to maintain quasineutrality. The return current is automatically included in Eqs. (2.86) and (2.87).

We point out here that $B = |\underset{\sim}{B}|$ is a flux label only in very exceptional cases, and that the variation of B on a surface importantly affects both plasma plasma stability and collisional transport.

4. Axisymmetric geometry

The plasma current in axisymmetric geometry could be studied simply by neglecting ζ-derivatives in the formulae of the previous subsection, i.e., in Hamada coordinates. However, it is ultimately more efficient to use symmetry coordinates, because of their partial orthogonality ($\nabla\zeta_0\cdot\nabla\vartheta_0 = 0 = \nabla\zeta_0\cdot\nabla\chi$). The 0-subscript is hereafter suppressed.

We begin with Eq. (2.68), which takes the form

$$qJ^{\vartheta} - J^{\zeta} = cdP/d\chi \ , \tag{2.98}$$

essentially identical to the Hamada case. However, the quasineutrality condition is now much simpler:

$$\frac{\partial}{\partial\vartheta}\sqrt{g}\ J^{\vartheta} = 0 \ .$$

Thus we have

$$J^{\vartheta} = K(\chi)/\sqrt{g} \ , \tag{2.99}$$

where K is a flux label and $\sqrt{g} = \sqrt{g_0}$ is given by Eq. (2.67).

Next we write $\underset{\sim}{J}$ in vector form using Eq. (2.72):

$$\underset{\sim}{J} = \sqrt{g}(J^{\vartheta}\nabla\zeta\times\nabla\chi + J^{\zeta}\nabla\chi\times\nabla\vartheta) \ .$$

This simplifies, not only because of Eq. (2.99), but also because symmetry coordinates satisfy

$$\nabla\chi\times\nabla\vartheta = (I/q)\nabla\zeta$$

as follows from Eqs. (2.63) and (2.66). Hence we have

$$\underset{\sim}{J} = K(\chi)\nabla\zeta\times\nabla\chi + J^{\zeta}R^2\nabla\zeta \ ,$$

or, in view of Eqs. (2.67), (2.98) and (2.99),

$$\underset{\sim}{J} = K(\chi)\underset{\sim}{B} - c\,\frac{dP}{d\chi}\,R^2\nabla\zeta \qquad (2.100)$$

Equation (2.100) conveniently summarizes forces balance in an axisymmetric system.

An instructive consequence of Eq. (2.89), in the axisymmetric case, deserves mention. Suppose there is no rotational transform (as in, for example, the vacuum case), so that

$$\underset{\sim}{B} = \underset{\sim}{B}_T = I\nabla\zeta \ .$$

Then

$$I_0(V) = 2\pi R^2/I \qquad (2.101)$$

is constant on surfaces of constant R: cylinders centered on the symmetry axis. Since such non-toroidal surfaces are inconsistent with confinement, we see that axisymmetric equilibrium requires rotational transform: systems with ι=0 necessarily have asymmetrizing "bumps" in the magnetic field.

Next we consider some consequences of Ampere's law in an axisymmetric system. The radial component,

$$J^\chi = 0 = \frac{1}{\sqrt{g}}\,\frac{\partial B_\zeta}{\partial\vartheta} \ ,$$

requires B_ζ to be a flux label. Since Eq. (2.66) implies $B_\zeta = I(\chi)$, this information is not new.

The ϑ-component of Ampere's law,

$$J^{\vartheta} = -\frac{c}{4\pi\sqrt{g}}\frac{\partial B_{\zeta}}{\partial \chi} = -\frac{c}{4\pi\sqrt{g}}\frac{dI}{d\chi}$$

implies, in view of Eq. (2.99),

$$K(\chi) = -\frac{c}{4\pi}\frac{dI}{d\chi} .$$

We substitute this result into Eq. (2.100),

$$\underset{\sim}{J} = -\frac{c}{4\pi}\frac{dI}{d\chi}\underset{\sim}{B} - c\frac{dP}{d\chi}R^2\nabla\zeta \qquad (2.102)$$

and thereby compute

$$J^{\zeta} \equiv \underset{\sim}{J}\cdot\nabla\zeta = -\frac{c}{4\pi R^2} I\frac{dI}{d\chi} - c\frac{dP}{d\chi} , \qquad (2.103)$$

using Eq. (2.60).

Finally, the ζ-component of Ampere's law,

$$J^{\zeta} = \frac{c}{4\pi\sqrt{g}}\left(\frac{\partial B_{\vartheta}}{\partial \chi} - \frac{\partial B_{\chi}}{\partial \vartheta}\right)$$

is analyzed by recalling Eq. (2.70):

$$B_{\vartheta} = \sqrt{g}\ \nabla\zeta\times\nabla\chi\cdot\underset{\sim}{B} = \sqrt{g}\ \nabla\chi\cdot\nabla\chi/R^2 .$$

Similarly,

$$B_\chi = - \sqrt{g}\nabla\chi\cdot\nabla\vartheta/R^2 \ .$$

Hence

$$\frac{1}{\sqrt{g}}\left(\frac{\partial B_\vartheta}{\partial\chi} - \frac{\partial B_\chi}{\partial\vartheta}\right) = \nabla \cdot (R^{-2}\nabla\chi)$$

from Eq. (2.78). We introduce the differential operator [11]

$$\Delta^*\chi \equiv R^2\nabla \cdot (R^{-2}\nabla\chi)$$

in order to write

$$J^\zeta = \frac{c}{4\pi} R^{-2}\Delta^*\chi \ . \qquad (2.104)$$

Equations (2.103) and (2.104) combine to yield the Grad-Shafranov equation,

$$\Delta^*\chi = -I\frac{dI}{d\chi} - 4\pi R^2\frac{dP}{d\chi} \qquad (2.105)$$

[11,12] which determines the flux-surface configuration $\chi(\underset{\sim}{x})$, if the functions $I(\chi)$ and $P(\chi)$ are known. In axisymmetric systems, the global equilibrium problem discussed in Subsection A reduces to solving Eq. (2.105). Unfortunately, the Grad-Shafranov equation has no simple non-axisymmetric counterpart.

The return current (or Pfirsch-Schlüter current [13]) in an axisymmetric system is easily understood from Eq. (2.102):

$$J_{\parallel} = -\frac{c}{4\pi}\frac{dI}{d\chi}B - c\,I\,\frac{dP}{d\chi}\frac{1}{B}\,, \tag{2.106}$$

which is the axisymmetric version of Eq. (2.87). Here all the ϑ-dependence resides in $B(\chi,\vartheta)$; hence $J_{\parallel}$ can vanish uniformly on a given surface only if B is a flux label on that surface.

D. Large Aspect Ratio, Axisymmetric Geometry

The aspect ratio of a circular cross-section tokamak is R_0/a, where R_0 is the major radius of the magnetic axis and a is the minor radius (limiter radius) of the confining vessel. More generally, aspect ratio measures the ratio of cylindrical curvature to toroidal curvature, in any device. Thus at sufficiently large aspect ratio a tokamak appears nearly cylindrical with respect to curvature, while remaining toroidal in the topological sense [e.g., $f(\zeta) = f(\zeta+2\pi)$]. Large aspect ratio approximations treat toroidal curvature effects perturbatively:

$$\varepsilon \equiv a/R_0 \ll 1\,. \tag{2.107}$$

They effect such enormous simplification on a variety of problems as to be very helpful, despite the fact that experimental aspect ratios are often no larger than four.

Here we use Eq. (2.107) to solve the Grad-Shafranov equation analytically, through first order in ε, following Shafranov [5]. We begin by recalling that tokamak rotational transform is produced by an externally driven, toroidal plasma current. The force ("hoop force") of this toroidal current loop on itself will push the magnetic axis outwards in major radius. On the other hand, for large aspect ratio and moderate plasma pressure, the flux surfaces should have, like the confining vessel, nearly circular poloidal cross-section. Thus we are led to try solving Eq. (2.105) by presuming circular, non-concentric flux surfaces, which are shifted with respect to the geometric minor axis as indicated in Figure 1.

Coordinates appropriate to this geometry, called Shafranov coordinates, are defined as follows. Let (R,φ,Z) be ordinary cylindrical coordinates, with R the major radius, φ the symmetry angle, and Z the vertical distance along the symmetry axis. Also let $R_c(r)$ be a smooth function satisfying $R_c(0) = R_0$, the major radius of the magnetic axis. Then Shafranov coordinates, $(r_s,\vartheta_s,\zeta_s)$, are defined by

$$\begin{aligned} R &= R_c(r_s) + r_s \cos\vartheta_s \ , \\ \varphi &= -\zeta_s \ , \\ Z &= r_s \sin\vartheta_s \ . \end{aligned} \tag{2.108}$$

Notice that $R_c(r_s)$ is the major radius of the center of that circle whose radius is r_s; its explicit functional form is considered below. In most of the following discussion, the S-subscript is suppressed.

In terms of the unit vectors $\hat{R} = \nabla R$, $\hat{Z} = \nabla Z$ and $\hat{\varphi} = R\nabla\varphi$, we can compute

$$\nabla r = \frac{\hat{Z}\ \sin\vartheta + \hat{R}\cos\vartheta}{X} = \frac{\hat{r}}{X} , \tag{2.109}$$

$$r\nabla\vartheta = \frac{\hat{Z}(R_c' + \cos\vartheta) - \hat{R}\sin\vartheta}{X} \tag{2.110}$$

and $\hat{\zeta} = -\hat{\varphi}$, where

$$X \equiv 1 + R_c' \cos\vartheta$$

and $R_c' \equiv dR_c/dr$. Notice that

$$r\nabla\vartheta \cdot \nabla r = R_c' \sin\vartheta / X$$

is not zero: Shafranov coordinates are not orthogonal. The Jacobian is

$$\sqrt{g_s} = rRX . \tag{2.111}$$

We mentioned previously that Shafranov coordinates are not flux coordinates. However, the variable r is an approximate flux label. Specifically, for $\varepsilon << 1$, the function R_c can be chosen such that

$$\chi = \chi(r) + O(\varepsilon^2) , \tag{2.112}$$

and

$$R_c' = O(\varepsilon) \ . \tag{2.113}$$

In other words, the shifted circle equilibrium, with a rather small shift, is indeed consistent with the Grad-Shafranov equation. Before verifying this statement, we consider some of its consequences.

Since ζ_s coincides with ζ_0, the symmetry coordinate, we know that

$$\underset{\sim}{B} = I\nabla\zeta + \nabla\zeta\times\nabla\chi = I\hat{\zeta}/R + \frac{\partial\chi}{\partial r}\,\nabla\zeta\times\nabla r + O(\varepsilon^2) \ .$$

Recalling Eq. (2.10), we write

$$\underset{\sim}{B} = \underset{\sim}{B}_P + \underset{\sim}{B}_T \tag{2.114}$$

with $\underset{\sim}{B}_P = \partial\chi/\partial r\nabla\zeta\times\nabla r$ and $\underset{\sim}{B}_T = I\hat{\zeta}/R$. Neglecting $O(\varepsilon^2)$ terms, we have

$$B_P = B_{P0}(r)\left(1 + \frac{r}{R_c}\,\Lambda\,\cos\vartheta\right) \ , \tag{2.115}$$

$$B_T = B_{T0}(r)\left(1 - \frac{r}{R_c}\cos\vartheta\right) \ . \tag{2.116}$$

Here $B_{P0}(r) = R_c^{-1}\,\partial\chi/\partial r$, $B_{T0}(r) = R_0^{-1}I$, and $\Lambda(r)$ is given by

$$\Lambda(r) = -\left(1 + \frac{R_c}{r}\,R_c'\right) \ . \tag{2.117}$$

Notice, from Eq. (2.113), that $\Lambda(r) = O(1)$.

To represent the flux surface average in Shafranov coordinates, we use the general definition, Eq. (2.35), and Eq. (2.111). Neglecting $O(\varepsilon^2)$ as usual, we find that

$$\langle A \rangle = \oint \frac{d\vartheta}{2\pi} \left(1 - \frac{r}{R_c} \wedge \cos\vartheta\right) A(r,\vartheta) \tag{2.118}$$

The safety factor is also computed from its definition, Eq. (2.19). Because ϑ is not a flux coordinate, $q \neq \underset{\sim}{B}\cdot\nabla\zeta/\underset{\sim}{B}\cdot\nabla\vartheta$. In fact, $\underset{\sim}{B}\cdot\nabla\zeta/\underset{\sim}{B}\cdot\nabla\vartheta = rB_T/(RB_P)$ depends on ϑ in first ε-order and is therefore not a flux label. However, it is a simple matter to compute, from Eq. (2.12),

$$\frac{d\psi_T}{dr} = \oint \frac{d\vartheta}{R} IrX$$

whence

$$\begin{aligned} q &= (d\psi_T/dr)/(d\chi/dr) \\ &= rI/(R_0 d\chi/dr) + O(\varepsilon^2) \\ &= rB_{T0}/(R_0 B_{P0}) + O(\varepsilon^2) \ . \end{aligned} \tag{2.119}$$

Now we consider the Grad-Shafranov equation. To emphasize the ϑ-dependence arising through $R(r,\vartheta)$, we write Eq. (2.105) as

$$R^2\nabla\cdot(R^{-2}\nabla\chi) = c_1(\chi) + R^2 c_2(\chi) \tag{2.120}$$

where $c_1 = -IdI/d\chi$, $c_2 = -4\pi dP/d\chi$. We compute the divergence from Eq. (2.78),

$$\nabla\cdot(R^{-2}\nabla\chi) = \frac{1}{\sqrt{g_s}}\left\{\frac{\partial}{\partial r}\sqrt{g_s}\,R^{-2}\chi'\nabla r\cdot\nabla r\right.$$

$$\left.+\frac{\partial}{\partial\vartheta}\sqrt{g_s}\,R^{-2}\chi'\nabla r\cdot\nabla\vartheta\right) ,$$

which can be further explicated by means of Eqs. (2.109)-(2.111). A straightforward ε-expansion, exploiting Eq. (2.113), then yields, in zeroth order,

$$\frac{1}{r}\frac{\partial}{\partial r}\,r\,\frac{\partial\chi}{\partial r} = c_1 + R_0^2 c_2 .$$

We multiply this result by $\partial\chi/\partial r$ to obtain

$$\frac{d}{dr}\,r^2(B_{P0}^2 + B_{T0}^2) = 2rB_{T0}^2 - 8\pi r^2\,\frac{dP}{dr} . \qquad (2.121)$$

The first-order, $O(\varepsilon)$, terms in Eq. (2.120) are all proportional to $\cos\vartheta$; omitting the $\cos\vartheta$-factor, we have

$$\left(1 - \frac{R_c}{r}\,R_c'\right)\frac{\partial}{\partial r}\left(\frac{r}{R_c}\,\frac{\partial\chi}{\partial r}\right) - \frac{R_c}{r}\,\frac{\partial}{\partial r}\left[\frac{r}{R_c}\left(\frac{r}{R_c} + R_c'\right)\frac{\partial\chi}{\partial r}\right]$$

$$+\frac{R_c'}{r}\,\frac{\partial\chi}{\partial r} - 2r\,R_c\,c_2 = 0 ,$$

which reduces to

$$\frac{d}{dr}\left[(1+\Lambda)r^2B_{P0}^2\right] = rB_{P0}^2 - 8\pi r^2 dP/dr \ . \qquad (2.122)$$

In higher order, the ϑ-dependence of χ, corresponding to non-circularity of the flux-surfaces, would enter. Since the main purpose of Shafranov geometry is to obtain simple, albeit approximate, formulae, the higher order terms are generally ignored.

Our results, Eqs. (2.121) and (2.122), are simply the two dominant Fourier components of the Grad-Shafranov equation for large aspect ratio. Recalling that the Grad-Shafranov equations prescribes $\chi(\underset{\sim}{x})$ for given $P(\chi)$ and $I(\chi)$, we see that Eqs. (2.121) and (2.122) are to be solved for $B_{P0}(r)$ and $\Lambda(r)$, for given $P(r)$ and $B_{T0}(r)$. The point is that for $\varepsilon << 1$, $\chi(r,\vartheta)$ can be parametrized in terms of two functions which depend only on r; the first function, $B_{P0}(r)$, prescribes the magnitude of χ on each surface, while the second, $\Lambda(r)$, gives the disposition of the surfaces.

For unspecified pressure and toroidal field profiles, the solutions to Eqs. (2.121) and (2.122) can be expressed in terms of a radial (volume) average. We introduce, for any f(r),

$$\bar{f} \equiv 2r^{-2}\int_0^r dr'r'f(r') \ .$$

It can be seen that $\bar{f}$ is the normalized volume average, over all radii less than r, of f. Consider first Eq. (2.121). A radial average yields

$$B_{P0}^2(r) + B_{T0}^2(r) = \overline{B_{T0}^2}(r) - 8\pi[P(r)-\bar{P}(r)] \ . \qquad (2.123)$$

In particular, since

$$P(a) = 0 \ ,$$

we have

$$\beta_P = 1 + \frac{B_{T0}^2(a) - \overline{B_{T0}^2}(a)}{B_{P0}^2(a)} \tag{2.124}$$

where

$$\beta_P \equiv 8\pi\bar{P}(a)/B_{P0}^2(a) \ , \tag{2.125}$$

is called the poloidal beta. It conveniently parametrizes tokamak equilibria in terms of the field component, B_P, which is primarily responsible for large aspect-ratio tokamak confinement. Equation (2.125) shows that β_P exceeds unity when and only when $B_{T0}(r)$ increases, on the average, with increasing minor radius. In Subsection C, we noted that this case, diamagnetic with respect to the toroidal field, has negative poloidal current. Thus the sense of the poloidal current is determined by the sign of $\beta_P - 1$.

We can similarly integrate Eq. (2.122) to obtain

$$\frac{R_c^2}{R_0^2} = 1 - \frac{1}{2}\frac{r^2}{R_0^2}\left\{\overline{B_{P0}^{-2}}\ \overline{B_{P0}^2} + 16\pi\left(\frac{\overline{\bar{P}-P}}{B_{P0}^2}\right)\right\} \tag{2.126}$$

Here the first term inside the brackets represents the hoop force, resulting from toroidal current. The second term, related to β_P, is a

correction resulting from plasma pressure. It can be seen that Eq. (2.124) is consistent with the initial assumption, Eq. (2.113), only if this second term is O(1) or smaller: the shifted-circle geometry becomes invalid when β_P much exceeds unity.

The consistent ordering,

$$\beta_P \sim 1 \tag{2.127}$$

implies that the toroidal beta

$$\beta_T \equiv \frac{8\pi\bar{P}(a)}{B_T^2} \tag{2.128}$$

is small,

$$\beta_T \sim \varepsilon^2 \tag{2.129}$$

since, for $q \sim 1$, Eq. (2.119) yields

$$B_P/B_T \sim \varepsilon \ . \tag{2.130}$$

Thus Shafranov geometry corresponds to a low-beta equilibrium; Eq. (2.129) is often called the low-beta tokamak ordering. Low-beta equilibria are characterized, in particular, by a weak radial variation of $B_{T0}(r)$,

$$\frac{B_{T0}^2}{\overline{B_{T0}^2}} - 1 = O(\varepsilon^2) \ , \tag{2.131}$$

in view of Eq. (2.123). Thus the main spatial dependence of B_T resides in the R^{-1} factor,

$$B_T \simeq \text{const}/R \ , \tag{2.132}$$

as in Eq. (2.116).

While the Shafranov shift, $R_c - R_0$, is rather small, it is experimentally measurable and has diagnostic value. It also can have surprisingly important implications with regard to low-beta tokamak stability. More recent investigations [14] concern solution to the Grad-Shafranov equation for a high-beta tokamak ordering,

$$\beta_T \sim \varepsilon \ , \ \beta_P \sim \varepsilon^{-1} \ , \tag{2.133}$$

which is of course economically advantageous. Unfortunately the high-beta analysis is much more complicated, because the flux surfaces need no longer be approximately circular.

III. Shear-Alfvén Law

A. Significance

The shear-Alfvén law is an exact consequence of Maxwell's equations and plasma momentum conservation. It displays, in model-independent form, the essential physics of low-frequency stability and nonlinear evolution: rational-surface singularity, interchange forces, current gradients, plasma vorticity and magnetic nonlinearity. It also helpfully motivates the introduction of fundamental spatial and temporal scale-separation arguments.

Section B of the present chapter derives the exact, nonlinear shear-Alfvén law. Its salient properties are discussed in Sec. C. A formal ordering based on scale-separation is used to develop, in Sec. D, a simplified version of the shear-Alfvén law. Finally, Sec. E introduces the physical issues associated with rational-surface singularity of the shear-Alfvén law: boundary layers and magnetic islands.

It must be pointed out that the shear-Alfvén law does not by itself provide a closed description of the linear or nonlinear dynamics. All but the simplest cases require additional information, such as an Ohm's law, an energy conservation law and a parallel acceleration law, for closure. Closure relations are always approximate; each has a limited domain of validity. A variety of closure schemes are considered in Chapter IV.

B. Exact shear-Alfvén Law

1. Flute-like Perturbations

Consider an arbitrary perturbation, $u(\underset{\sim}{x},t)$, of some variable describing a toroidally confined plasma. Periodicity permits the Fourier decomposition

$$u(\chi,\vartheta,\zeta) = \sum_{m,n} u_{mn}(\chi) \exp i(m\vartheta - n\zeta),$$

where (χ,ϑ,ζ) are flux coordinates and the coefficients u_{mn} are given by Eq. (2.28). Any actual disturbance will necessarily involve more than one of the u_{mn}, because toroidal curvature couples various harmonics. [Equation (2.29), for example, is uncoupled only when S is presumed given; for a linear eigenmode, S will be proportional to u and $(S/\underset{\sim}{B}\cdot\nabla\vartheta)_{mn}$ will depend upon components other than u_{mn}.] However, the coupling is not always crucial, and many perturbations of interest are dominated by a single harmonic, or wave-vector,

$$\underset{\sim}{k} = m\nabla\vartheta - n\nabla\zeta \quad . \tag{3.1}$$

The integers m and n are called respectively the poloidal and toroidal mode numbers. The ratio m/n evidently characterizes the helicity of the chosen harmonic.

Let us denote the unperturbed magnetic field by $\underset{\sim}{B}_o$ and introduce the unit vector

$$\underset{\sim}{b}_o \equiv \underset{\sim}{B}_o/B_o \quad . \tag{3.2}$$

Then the parallel wave vector is

$$k_{\|} \equiv \underset{\sim}{b}_o \cdot \underset{\sim}{k} = (\underset{\sim}{B}_o \cdot \nabla\vartheta / B)\ (m - nq) \quad , \tag{3.3}$$

and a perpendicular wave-vector can be defined by

$$\underset{\sim}{k} = \underset{\sim}{b}_o k_{\|} + \underset{\sim}{k}_{\perp} \quad . \tag{3.4}$$

Both $k_{\|}$ and $\underset{\sim}{k}_{\perp}$ depend upon position. It shall become clear that the χ-dependence of $k_{\|}$ is of particular importance.

Flute-like perturbations, mentioned in Chapter II, are characterized by $k_{\|}$ being small,

$$k_{\|} << k_{\perp} \ , \ k_r \quad , \tag{3.5}$$

relative to both $k_{\perp}$ and the radial wavenumber scale, k_r, which is defined by the χ-component of ∇u. That these modes are most likely to be unstable can be understood (see, for example [15]) from the stabilizing effects of field-line bending: such bending invokes strong restoring forces, but is minimized by small $k_{\|}$. Other considerations, such as the stabilizing influence of parallel sound-wave propagation, make flute-like modes appear relatively dangerous in non-fluid (kinetic) regimes as well, even in the purely electrostatic case.

Notice that in large aspect-ratio geometry, with $B_P \sim (r/R)B$, $k_{\|}$ is inherently rather small,

$$k_{\|} \sim (r/qR)\ k_{\perp} \quad . \tag{3.6}$$

However, flute-like behavior usually involves much smaller $k_\parallel$, requiring the existence of "mode-rational" values of the safety factor,

$$q(\chi_{mn}) = m/n \quad . \tag{3.7}$$

When the perturbation of interest is dominated by a single helicity, $k_\parallel$ becomes a strong function of χ, vanishing at χ_{mn} and approaching some fraction of $k_\perp$ as $|\chi-\chi_{mn}|$ increases. (Over the same radial range, $k_\perp$ changes relatively little.) Thus single-helicity modes must be localized near χ_{mn} in order to preserve their flute-like character.

A mode involving many helicities can be flute-like over a much wider radial domain. In this case, the dominant helicity changes with χ, so as to approximately satisfy Eq. (3.7) and preserve $\nabla_\parallel \ll \nabla_\perp$ on each surface: the mode helicity tracks the field-line pitch.

An important consequence of the flute-like ordering is that it permits two time scales for electromagnetic disturbances to be distinguished. We introduce the Alfvén speed,

$$v_A \equiv B_o/(4\pi n_o m_i)^{1/2} \quad , \tag{3.8}$$

where n_o is the plasma (equilibrium) density and m_i is the ion mass. Recall [16] that shear-Alfvén waves have the frequency

$$\omega_{SA} \equiv k_\parallel v_A \quad , \tag{3.9}$$

while compressional Alfvén waves are described, for small plasma pressure, by

$$\omega \simeq \omega_{CA} \equiv kv_A \quad . \tag{3.10}$$

Evidently, $\omega_{SA} << \omega_{CA}$ in the flute-like case. (Of course ω_{SA} shares with $k_\parallel$ a strong radial dependence; we estimate its size by evaluation at some radius characterizing the half-width of the mode.) Furthermore, the most important toroidal instabilities have frequencies no larger than ω_{SA}: the slow time scale is of primary interest.

The significance of the two time scales is best understood from consideration of the plasma acceleration law,

$$m_i n \frac{d\underset{\sim}{V}}{dt} + \nabla\cdot\underset{\approx}{\pi} = -\nabla P + c^{-1}\, \underset{\sim}{J} \times \underset{\sim}{B} \quad . \tag{3.11}$$

Here $\underset{\sim}{V}$ is the plasma fluid velocity,

$$\frac{d}{dt} \equiv \frac{\partial}{\partial t} + \underset{\sim}{V}\cdot\nabla \quad , \tag{3.12}$$

and $\underset{\approx}{\pi}$ represents nonisotropic contributions to the plasma stress tensor. Thus $\underset{\approx}{\pi}$ includes various viscous effects, as well as anisotropy of the Chew-Goldberger-Low [17] form, $P_\parallel \neq P_\perp$. For present purposes it suffices to assume that $\nabla\cdot\underset{\approx}{\pi}$ is no larger than the first, inertial term in Eq. (3.11).

Hence plasma acceleration is measured by imbalance between the two terms on the right-hand side of Eq. (3.11). Simple estimates from Ampere's law show that the "bare" $\underset{\sim}{J}\times\underset{\sim}{B}$ force would yield acceleration on the fast scale, ω_{CA}:

$$J_\perp \sim (c/4\pi)k_\perp B \Longrightarrow (d/dt)(V/v_A) \sim \omega_{CA} \quad .$$

Evolution on slower time scales must therefore proceed through a sequence of near-equilibrium states, in which the dominant part of the $\underset{\sim}{J}\times\underset{\sim}{B}$ force is effectively shielded:

$$\underset{\sim}{J}\times\underset{\sim}{B} - c\nabla P = O(k_\parallel/k_\perp) \quad . \tag{3.13}$$

2. Derivation

A simple way to describe such slow evolution - which critically involves the error term in Eq. (3.13) - is obtained from the parallel component of the curl of Eq. (3.11). [Equivalently, one solves Eq. (3.11) for $\underset{\sim}{J}_\perp$ and combines the result with $\nabla\cdot\underset{\sim}{J} = \nabla\cdot\underset{\sim}{J}_\perp + \underset{\sim}{B}\cdot\nabla(J_\parallel/B) = 0$.]. We call the resulting equation the "shear-Alfvén law"; it is the plasma equation of motion, in which the strong part of the $\underset{\sim}{J}\times\underset{\sim}{B}$ force has been annihilated by the operation $\underset{\sim}{B}\cdot\nabla\times$.

In other words, when $\omega \leqslant \omega_{SA}$, the relevant electromagnetic driving force is to be extracted from $\underset{\sim}{B}\cdot\nabla\times(\underset{\sim}{J}\times\underset{\sim}{B})$. This quantity is conveniently expressed in terms of the magnetic field curvature,

$$\underset{\sim}{\kappa} \equiv (\underset{\sim}{b}\cdot\nabla)\underset{\sim}{b} \quad , \quad \underset{\sim}{b} \equiv \underset{\sim}{B}/B \quad , \tag{3.14}$$

which we briefly digress to consider. Since $\nabla(\underset{\sim}{b}\cdot\underset{\sim}{b}) = 0$,

$$\underset{\sim}{\kappa} = -\underset{\sim}{b} \times (\nabla \times \underset{\sim}{b})$$

$$= -B^{-1}\, \underset{\sim}{b} \times (\nabla \times \underset{\sim}{B}) - \underset{\sim}{b} \times (\nabla B^{-1} \times \underset{\sim}{B})$$

$$= \frac{4\pi}{c} \frac{\underset{\sim}{J} \times \underset{\sim}{B}}{B^2} + \frac{\nabla_\perp B}{B} \quad . \tag{3.15}$$

Hence, if the left-hand side of Eq. (3.11) is denoted for convenience by

$$\underset{\sim}{f} \equiv m_i n \frac{d\underset{\sim}{V}}{dt} + \nabla \cdot \underset{\sim}{\pi} \quad , \tag{3.16}$$

then we can write

$$\underset{\sim}{\kappa} = \frac{4\pi}{B^2} (\nabla P + \underset{\sim}{f}) + \frac{\nabla_\perp B}{B} \quad . \tag{3.17}$$

Notice that in Eqs. (3.15) and (3.17),

$$\nabla_\perp \equiv \nabla - \underset{\sim}{b}(\underset{\sim}{b} \cdot \nabla) \quad , \tag{3.18}$$

is defined in terms of the full magnetic field, rather than $\underset{\sim}{b}_o$.

Now consider $\underset{\sim}{B} \cdot \nabla \times (\underset{\sim}{J} \times \underset{\sim}{B})$. Ampere's law implies that

$$\underset{\sim}{B} \cdot \nabla \times (\underset{\sim}{J} \times \underset{\sim}{B}) = \nabla \cdot [(\underset{\sim}{J} \times \underset{\sim}{B}) \times \underset{\sim}{B}] = -\nabla \cdot (B^2 \underset{\sim}{J}_\perp) \quad ,$$

and therefore

$$\underset{\sim}{B}\cdot\nabla \times (\underset{\sim}{J}\times\underset{\sim}{B}) = B^2\underset{\sim}{B} \cdot \nabla(J_{\parallel}/B) - B^{-2}[\underset{\sim}{B} \times (\underset{\sim}{J}\times\underset{\sim}{B})] \cdot \nabla_{\perp}B^2 \quad ,$$

or, in view of Eq. (3.15),

$$\underset{\sim}{B}\cdot\nabla \times (\underset{\sim}{J}\times\underset{\sim}{B}) = B^2\underset{\sim}{B} \cdot \nabla(J_{\parallel}/B) - \frac{c}{4\pi}\,\underset{\sim}{B}\times\underset{\sim}{\kappa} \cdot \nabla_{\perp}B^2 \quad .$$

Combining this result with the left-hand side of Eq. (3.11) yields the (nonlinear) shear-Alfvén law

$$c\underset{\sim}{B} \cdot \nabla\times\underset{\sim}{f} = B^2\underset{\sim}{B} \cdot \nabla(J_{\parallel}/B) - (c/4\pi)\underset{\sim}{B}\times\underset{\sim}{\kappa} \cdot \nabla_{\perp}B^2 \quad , \tag{3.19}$$

A more convenient form is obtained by using Eq. (3.17) to eliminate $\nabla_{\perp}B^2$ from the last term on the right-hand side. Thus

$$\underset{\sim}{B} \cdot (\nabla\times\underset{\sim}{f} - 2\underset{\sim}{\kappa}\times\underset{\sim}{f}) = c^{-1}B^2\underset{\sim}{B}\cdot\nabla(J_{\parallel}/B) + 2\underset{\sim}{B}\times\underset{\sim}{\kappa}\cdot\nabla P \quad , \tag{3.20}$$

where $\underset{\sim}{f}$ is given by Eq. (3.16).

C. Interpretation

1. Neighboring Equilibria

The left-hand side of Eq. (3.20) describes plasma inertia. The curl of the acceleration, $\underset{\sim}{f}$, prominently involves the fluid vorticity, $\nabla\times\underset{\sim}{V}$; in fact the shear-Alfvén law is often referred to as a vorticity equation. Other contributions to $\nabla\times\underset{\sim}{f}$, from ∇n and $\nabla\cdot\underset{\approx}{\pi}$, involve details of the plasma response which are sensitive to collision

frequency, ν. When ν is small, these contributions should be computed from kinetic theory (see IVC).

This left-hand side can be neglected whenever the frequency, ω, and anisotropic pressure contributions are sufficiently small (that is, when $\pi << P$ and when ω is less than the local shear-Alfvén frequency, $k_{\|}(\chi)v_A$). In this case the shear-Alfvén law reduces to the relation

$$B^2(\underset{\sim}{B}\cdot\nabla)\left(\frac{J_{\|}}{B}\right) + 2c\underset{\sim}{B}\times\underset{\sim}{\kappa}\cdot\nabla P = 0 \quad . \tag{3.21}$$

These two terms will be referred to as the Newcomb terms. Equation (3.21) expresses quasineutrality, $\nabla\cdot J = 0$, for a plasma whose perpendicular current satisfies equilibrium force balance, Eq. (2.1). Considered as a nonlinear equilibrium relation, Eq. (3.21) has already been studied in Chapter II; it has the general solution given by Eq. (2.86). In the context of stability theory, Eq. (3.21) is to be linearized about some chosen equilibrium. The linearized form, a "generalized Newcomb equation", evidently pertains to the existence of neighboring equilibria.

The importance of neighboring equilibria is obvious in the case of ideal magnetohydrodynamics (MHD), in which $\underset{\sim}{\pi}=0$ and the boundary of marginal stability must have vanishing frequency (hence, $\underset{\sim}{f}=0$). Thus growing modes will exist whenever the linearized form of Eq. (3.21) has well-behaved solutions. The original Newcomb equation [18] arose in this context; it is Eq. (3.21), linearized in cylindrical geometry. Outside the domain of ideal MHD, Eq. (3.21) will remain pertinent, for

small ω and $\underset{\sim}{\pi}$, provided that the singularities associated with rational magnetic surfaces can be avoided.

The question of singularity in Eq. (3.21) is sufficiently important to deserve separate consideration, which is provided in Section E. Here we point out that Eq. (3.21) is a magnetic differential equation whose solubility condition, Eq. (2.89), is not necessarily satisfied in the perturbed state. We noted in Sec. IIC that the same issue arises even in a strict equilibrium context. Of course in the neighborhood of the rational surface inertial terms in the shear-Alfvén law become important and a boundary-layer analysis is appropriate.

2. Current-driven and Pressure-driven Modes.

Roughly speaking, the left-hand side of Eq. (3.20) describes the plasma response to driving forces contained in the right-hand side. Of the two terms on the right, the first, involving $J_{\|}$, is said to be associated with "current-driven" modes; the second, involving ∇P, is associated with "pressure-driven" modes. (In a more accurate terminology, the two types of modes would be called "parallel-current-driven" and "perpendicular-current-driven," respectively. Note also that, in general, disturbances will be affected by both terms.) Here we point out salient features of the two driving forces.

The term involving $J_{\|}$ is approximately linearized according to

$$\underset{\sim}{B}\cdot\nabla(J_{\|}/B) \simeq \delta\underset{\sim}{B}\cdot\nabla(J_{\|o}/B_o) + \underset{\sim}{B}_o\cdot\nabla(\delta J_{\|}/B_o) \quad , \tag{3.22}$$

since the perturbation in field magnitude is relatively small. (Here

$\delta f = f - f_o$ is the perturbation in any field quantity f.) Current-driven instability depends upon gradients in the equilibrium parallel current, as given by the first, "kink" term on the right-hand side of Eq. (3.22). Typical current-driven modes, such as the kink mode or tearing mode, are not in general localized or even flute-like. However, the kink mode often has small $k_\parallel$, in the sense of Eq. (3.5), and the tearing mode growth rate depends crucially upon processes occurring near the mode-rational surface.

The remaining linear term in Eq. (3.22), involving $\delta J_\parallel$, is loosely associated with bending of the magnetic field lines [15,19]. The point is that $\delta J_\parallel$ is relatively small when $\delta \underset{\sim}{B}$ and $\underset{\sim}{B}_0$ are parallel: it reflects perturbation of the direction of $\underset{\sim}{B}$. The most important feature of the line-bending term is its singularity on mode-rational surfaces. The singularity affects virtually all electromagnetic disturbances; it is discussed in Sec. E.

The second Newcomb term, involving $\underset{\sim}{\kappa}$ and ∇P, is often called the interchange term because of its role in Rayleigh-Taylor instabilities, which depend upon the interchange of fluid elements. Such pressure-driven modes are conveniently understood from the viewpoint of the MHD energy principle; a recent, instructive discussion is given by Freidberg [15]. Because interchanges are destabilized by components of $\underset{\sim}{\kappa}_o$ in the direction of ∇P_o, the case $\underset{\sim}{\kappa}_o \cdot \nabla P_o > 0$ ($\underset{\sim}{\kappa}_o \cdot \nabla P_o < 0$) is referred to as unfavorable (favorable) curvature. Since $\underset{\sim}{\kappa}_o \cdot \nabla P_o$ will usually change sign at different locations in the torus, an appropriate average of $\underset{\sim}{\kappa}_o$ is ultimately most relevant. Ballooning instability is characterized by perturbations localized in regions of unfavorable curvature (as opposed to the radial localization of a single-helicity

flute-like mode). Such instability clearly becomes more important at large plasma pressure and, in fact, often limits the maximum pressure which can be confined.

In addition to the conventional interchange and ballooning instabilities, a number of other modes, such as the tearing mode, are affected by the interchange term. A prominent example is studied in Chapter V.

Finally, we remark that both current ($J_{\|}$)-driven and pressure ($J_{\perp}$)-driven instabilities can be viewed as a mechanisms by which the magnetic field attempts to relax to its lowest free-energy state: $\nabla \times \underset{\sim}{B} = 0$ [1].

D. Flute-reduced Shear-Alfvén Law

1. Multiple Scale Reduction

While the structure of the exact shear-Alfvén law determines the types of instability, an exact linearization of this law is complicated due to the large number of terms present. It is thus useful to develop systematic approximation schemes to clarify the linear analysis and also to make a nonlinear treatment feasible.

One such technique, referred to as "reduction", uses a multiple-scale perturbation theory based on the flute-like ordering, Eq. (3.5). Since the shear-Alfvén mode decouples from the compressional mode in just this limit, it is clear that the reduction will be appropriate precisely when the shear-Alfvén law is relevant.

There are two ways in which $k_\parallel/k_\perp$ can be small. In the first case, large aspect ratio geometry leads naturally to $k_\parallel a \ll 1$ for $k_\perp a \sim 1$, as displayed in Eq. (3.6). A reduction scheme based on this ordering was developed by Strauss, and will be discussed in Chapter IV. An alternative ordering assumes $k_\parallel a \sim 1$ but $k_r a, k_\perp a \gg 1$. The corresponding "flute reduction" scheme limits consideration to modes with short radial scale and/or large Fourier mode numbers. An advantage of this ordering is that arbitrary geometries may be treated. Of course this scheme is valid only if the dominant helicity of the mode is locally close to that of the magnetic field.

The assumption of large $k_\perp$ is exploited by separating spatial dependences into two parts, fast and slow, and expressing functions as

$$f(\underset{\sim}{x},t) = f(\frac{1}{\varepsilon}\,\underset{\sim}{x},\underset{\sim}{x},t) = f(\underset{\sim}{x}_f,\underset{\sim}{x}_s,t) \quad , \tag{3.23}$$

where $\varepsilon \ll 1$ represents $k_\parallel/k_\perp$. Derivatives must now be taken with respect to both sets of variables

$$\nabla = \frac{\partial}{\partial \underset{\sim}{x}} = \frac{1}{\varepsilon}\,\nabla_f + \nabla_s \quad , \tag{3.24}$$

where $\nabla_f = \frac{\partial}{\partial \underset{\sim}{x}_f}$, etc. The choice of the fast variables $\underset{\sim}{x}_f(\underset{\sim}{x})$ is limited by the flute-like ordering to

$$(\underset{\sim}{B}_o \cdot \nabla)\ \underset{\sim}{x}_f = 0 \quad , \tag{3.25}$$

so that all variation parallel to the equilibrium field is contained in

the dependence on $\underset{\sim}{x}_s$. An equivalent form of Eq. (3.25) is obtained using the notation of Eq. (3.24)

$$\underset{\sim}{B}_o \cdot \nabla_f = 0 \quad . \tag{3.26}$$

Equation (3.25) is a magnetic differential equation whose solutions were discussed in Sec. IIB.3 in terms of flux coordinates. If the fast dependence is limited to the flux coordinate, χ, then the reduced equation applies to modes that vary rapidly near a particular rational surface. If an additional fast dependence on $\zeta - q\vartheta$ is allowed then ballooning modes can be treated. In this section, however, no explicit choice of fast coordinates is necessary and the reduced shear-Alfvén law will be valid independent of magnetic field geometry, or radial localization.

Although the space of dependent variables has been enlarged in Eq. (3.23) (from four to seven dimensions) and thus the resulting equations appear to have been complicated, an expansion in the small parameter ε will actually yield much simplified equations. To accomplish this expansion, equilibrium quantities, denoted by subscript zero, will be assumed $O(1)$ and to depend only on the slow variables. The perturbation will be assumed $O(\varepsilon)$ and to depend on both sets of variables. Explicitly we set

$$\begin{aligned}
\underset{\sim}{B} &= \underset{\sim}{B}_o(\underset{\sim}{x}_s) + \varepsilon \underset{\sim}{B}_1(\underset{\sim}{x}_f, \underset{\sim}{x}_s, t) \quad ; \\
P &= P_o(\underset{\sim}{x}_s) + \varepsilon P_1(\underset{\sim}{x}_f, \underset{\sim}{x}_s, t) \quad ; \\
n &= n_o(\underset{\sim}{x}_s) + \varepsilon n_1(\underset{\sim}{x}_f, \underset{\sim}{x}_s, t) \quad ; \\
\underset{\sim}{V} &= \varepsilon \underset{\sim}{V}_1(\underset{\sim}{x}_f, \underset{\sim}{x}_s, t) \quad ;
\end{aligned} \tag{3.27}$$

$$\underset{\sim}{\pi} = \varepsilon \underset{\sim}{\pi}_1(\underset{\sim}{x}_f, \underset{\sim}{x}_s, t) \quad .$$

The anisotropic pressure has been assumed small since the equilibrium is determined by scalar pressure. The ordering of the size of the perturbing quantities, relative to equilibrium, has been chosen so that nonlinear effects are as important as linear ones.

2. Derivation

The ordering implied by Eq. (3.27) can be substituted directly into the shear-Alfvén law to obtain the reduced version. Because the strong force has been annihilated it is only necessary to retain terms in the shear-Alfvén law to lowest order $[O(1)]$ to obtain the evolution equation. For clarity we consider the effect of the ordering on each of the terms in Eq. (3.20) separately.

A representation for the perturbed magnetic field may be obtained from the $\nabla \cdot \underset{\sim}{B} = 0$. This becomes, from Eqs. (3.24) and (3.27)

$$0 = \nabla_s \cdot \underset{\sim}{B}_o + \nabla_f \cdot \underset{\sim}{B}_1 + \varepsilon \nabla_s \cdot \underset{\sim}{B}_1 = \nabla_f \cdot \underset{\sim}{B}_1 + O(\varepsilon) \quad ,$$

and implies that $\underset{\sim}{B}_1$ can be represented in terms of two scalar fields:

$$\underset{\sim}{B}_1 = \nabla_f \psi \times \underset{\sim}{B}_o + B_{\parallel} \frac{\underset{\sim}{B}_o}{B_o^2} \quad . \tag{3.28}$$

Here $\psi(\underset{\sim}{x}_f, \underset{\sim}{x}_s, t)$ is the parallel vector potential and $B_{\parallel} = \underset{\sim}{B}_o \cdot \underset{\sim}{B}_1$. The contribution of $B_{\parallel}$ to $\nabla_f \cdot \underset{\sim}{B}_1$ is zero by virtue of Eq. (3.26).

The parallel gradient operator is expressed as

$$\underset{\sim}{B}\cdot\nabla = (\underset{\sim}{B}_o+\varepsilon\underset{\sim}{B}_1)\cdot(\frac{1}{\varepsilon}\nabla_f+\nabla_s)$$

$$= \underset{\sim}{B}_o\cdot\nabla_s + \underset{\sim}{B}_1\cdot\nabla_f + O(\varepsilon) \quad , \tag{3.29}$$

where Eq. (3.26) has been used to eliminate $\underset{\sim}{B}_o\cdot\nabla_f$. Use of Eq. (3.28) allows a compact notation for this operator:

$$\underset{\sim}{B}\cdot\nabla = \underset{\sim}{B}_o\cdot\nabla_s - [\psi, \ ] \quad , \tag{3.30}$$

where the bracket gives the nonlinear terms and is defined by

$$[\psi,\varphi] = \underset{\sim}{B}_o\cdot\nabla_f\psi\times\nabla_f\varphi \quad . \tag{3.31}$$

The current is obtained from Ampere's law which is expressed as

$$\underset{\sim}{J} = \frac{c}{4\pi}(\frac{1}{\varepsilon}\nabla_f+\nabla_s)\times(\underset{\sim}{B}_o+\varepsilon\underset{\sim}{B}_1) \quad ,$$

$$= \underset{\sim}{J}_o + \frac{c}{4\pi}\nabla_f\times\underset{\sim}{B}_1 + O(\varepsilon) \quad . \tag{3.32}$$

Note that even though the perturbing field is small, there is an O(1) correction to the equilibrium current. The representation of Eq. (3.28) easily yields an expression for the parallel current:

$$\frac{J_\parallel}{B} = \frac{\underset{\sim}{J}\cdot\underset{\sim}{B}}{B^2} = \frac{J_{\parallel o}}{B_o} - \frac{c}{4\pi}\nabla_f^2\psi + O(\varepsilon) \quad . \tag{3.33}$$

Thus, from Eq. (3.30) and (3.33), the reduced form of the first Newcomb term of Eq. (3.20) is obtained.

The expansion of the curvature term of Eq. (3.20) exhibits in general three separate linear terms as well as a host of nonlinear terms. The flute-like ordering implies that only one of these terms is important. This significant reduction follows from expanding the curvature (with $\underset{\sim}{b} = \underset{\sim}{B}/B$):

$$\underset{\sim}{\kappa} = \underset{\sim}{b}\cdot\nabla\underset{\sim}{b} = \underset{\sim}{b}_o\cdot\nabla_s\underset{\sim}{b}_o + \varepsilon(\underset{\sim}{b}_1\cdot\nabla_s\underset{\sim}{b}_o + \underset{\sim}{b}_o\cdot\nabla_s\underset{\sim}{b}_1 + \underset{\sim}{b}_1\cdot\nabla_f\underset{\sim}{b}_1) + O(\varepsilon^2) \quad ,$$

showing that there is no O(1) correction to the equilibrium curvature, $\underset{\sim}{\kappa}_o = \underset{\sim}{b}_o\cdot\nabla_s\underset{\sim}{b}_o$. An alternative expression is obtained from Eq. (3.17) which gives

$$\underset{\sim}{\kappa} = \underset{\sim}{\kappa}_o + \frac{4\pi}{B_o^2}\nabla_f(P_1+B_\parallel) + O(\varepsilon) \quad . \tag{3.34}$$

That the second term in Eq. (3.34) is zero follows from our above discussion or from the O(1) part of the equation of motion, (3.11):

$$0 = -\nabla_f(P_1+B_\parallel) \quad .$$

This is simply the expression of perturbed pressure balance implied by Eq. (3.13).

Consider next the inertial terms. The perturbed velocity is written in the general form

$$\underset{\sim}{V}_1 = \underset{\sim}{V}_\perp + V_\parallel\underset{\sim}{B}_o/B_o^2 \quad , \tag{3.35}$$

where $\underset{\sim}{V}_\perp = \underset{\sim}{b}_o \times \underset{\sim}{V}_1 \times \underset{\sim}{b}_o$, so that the convective derivative is

$$\frac{d}{dt} = \frac{\partial}{\partial t} + \underset{\sim}{V}_\perp \cdot \nabla_f + O(\varepsilon) \quad . \tag{3.36}$$

The angular acceleration is given by

$$\underset{\sim}{B} \cdot \nabla \times \left(m_i n \frac{d\underset{\sim}{V}}{dt}\right) = m_i n_o \underset{\sim}{B}_o \cdot \left(\nabla_f \times \frac{d}{dt} \underset{\sim}{V}_1\right) + O(\varepsilon) \quad . \tag{3.37}$$

Upon manipulation this term can be expressed in terms of the parallel vorticity, defined by

$$U = \underset{\sim}{B}_o \cdot \nabla_f \times \underset{\sim}{V}_1 = \underset{\sim}{B}_o \cdot \nabla_f \times \underset{\sim}{V}_\perp \quad , \tag{3.38}$$

and the divergence of the flow $\nabla_f \cdot \underset{\sim}{V}_1 = \nabla_f \cdot \underset{\sim}{V}_\perp$:

$$\underset{\sim}{B} \cdot \nabla \times \left(m_i n \frac{d\underset{\sim}{V}}{dt}\right) = m_i n_o \left[\left(\frac{\partial}{\partial t} + \underset{\sim}{V}_\perp \cdot \nabla_f\right) U + U(\nabla_f \cdot \underset{\sim}{V}_\perp)\right] \quad . \tag{3.39}$$

The remaining term is the Coriolis-like expression

$$\underset{\sim}{\kappa} \times \underset{\sim}{f} = \underset{\sim}{\kappa}_o \times (\nabla_f \cdot \underset{\approx}{\pi}_1) + O(\varepsilon) \quad , \tag{3.40}$$

which depends solely on the anisotropic pressure.

Substituting Eqs. (3.30-3.40) into Eq. (3.20) yields the reduced shear-Alfvén law

$$m_i n_o\left(\frac{d}{dt}\, U+U\nabla_\perp\cdot\underset{\sim}{V}_\perp\right) = -\frac{B_0^2}{4\pi}\left(\underset{\sim}{B}_o\cdot\nabla\nabla_\perp^2\psi - [\psi,\nabla_\perp^2\psi]\right) + 2\underset{\sim}{B}_o\times\underset{\sim}{\kappa}_o\cdot\nabla_\perp(P_1+\underset{\approx}{\pi}_1) \quad . \quad (3.41)$$

Here, since the only component of the slow dependence which enters is in the $\underset{\sim}{B}_o$ direction, we have replaced ∇_f by the perpendicular gradient, $\nabla_\perp$, and written $\underset{\sim}{B}_o\cdot\nabla_s = \underset{\sim}{B}_o\cdot\nabla_\parallel$.

3. Discussion

Regarding the shear–Alfvén driving terms, the kink term does not appear in Eq. (3.41) while the interchange term appears explicitly linearized. The kink term is unimportant in the flute-like ordering since the gradients of the equilibrium parallel current are small. Thus modes which are localized about rational surfaces or have large mode numbers are affected only by the interchange term.

The exact equilibrium curvature appears in the reduced shear–Alfvén law, but perturbed curvature components are small due to $B_o\cdot\nabla_f = 0$. In general the curvature can be written

$$\underset{\sim}{\kappa}_o = \kappa_n\nabla V + \kappa_g(\nabla\zeta - q\nabla\vartheta) \quad , \quad (3.42)$$

since Eq. (3.15) implies $\underset{\sim}{B}_o\cdot\underset{\sim}{\kappa}_o = 0$. The two components are referred to as normal and geodesic curvature, respectively. The geodesic component is called such because if the field lines happen to be geodesics on flux surfaces, $\kappa_g = 0$[20]. It is clear that for modes localized near a single rational surface the perturbed pressure gradient will be largest in the χ direction and the geodesic curvature will dominate. In general, geodesic curvature has zero average on a flux surface and is

therefore not as destabilizing as it might appear. A perturbation with high mode numbers will generally feel the effect of the normal curvature, and in the ballooning case both components are important. (See VIC).

The inertial term in Eq. (3.41) contains two nonlinearities. The convective derivative contains only the perpendicular velocity which advects the parallel vorticity. The divergence term implies that when the fluid has a perpendicular divergence, the vorticity changes to conserve angular momentum, just as the ice skater's angular velocity depends on the extension of his arms. Note that the parallel velocity appears nowhere in the reduced law.

The final nonlinear term, $[\psi,\nabla_f^2\psi]$, represents magnetic reconnection and will be discussed in the next section.

It is of interest that when the reduced law is linearized, and $\underset{\sim}{\pi}$ is neglected, only the three scalar fields (U,ψ,P_1) appear. It is these fields, and possibly one more, which typically govern the evolution of low frequency plasmas. Obtaining closed sets of equations in these fields is the subject of Chapter IV.

E. Rational Surfaces and Magnetic Reconnection

1. Boundary layer

It is useful to rewrite the exact shear-Alfvén law, Eq. (3.20), in the following schematic form:

$$\underset{\sim}{B}_o\cdot\nabla(\delta J_\parallel/B_o) = \delta N + \delta^2 N + L\cdot(\delta\underset{\sim}{f}) + \delta L\cdot(\delta\underset{\sim}{f}) \quad . \tag{3.43}$$

Here δN represents the linearized Newcomb terms, i.e., the interchange and kink terms; the operator L represents that on the left-hand side of Eq. (3.20); and the two $O(\delta^2)$-terms represent nonlinear contributions to N and $L \cdot \underset{\sim}{f}$. The main point of Eq. (3.43) is of course to isolate the singularity at $k_{\|} = 0$.

Suppose first that the nonlinear terms are neglected, and that L is relatively small (as it typically is for $\chi \neq \chi_{mn}$). The resulting lowest order equation

$$\underset{\sim}{B}_o \cdot \nabla(\delta J_{\|}/B_o) \cong \delta N \quad , \tag{3.44}$$

is simply a linear description of neighboring equilibrium. It is well-posed, provided δN satisfies the appropriate Newcomb condition on any mode-rational surfaces which may be present. Instabilities for which δN does satisfy this constraint include the ideal interchange and kink modes.

However, especially when the ideal modes are found to be stable, a complete stability investigation requires loosening the constraint. Thus we admit perturbations δN which do not satisfy Eq. (2.51). Notice that, for small δ and L, Eq. (3.44) remains approximately valid in radial regions suitably removed from the mode-rational surface. Near $\chi = \chi_{mn}$, however, it would predict divergence of the Fourier coefficient $(\delta J_{\|})_{mn}$ and is therefore inadequate.

Thus the shear-Alfvén law leads to a classical boundary-layer problem; the exterior of the boundary layer (or "current layer") is described by Eq. (3.44) while its interior description must include one or more additional terms from Eq. (3.43), in order to resolve the

singularity. Solution of the boundary-layer problem follows, in general, the classical prescription: one solves the interior and exterior equations separately, allowing enough freedom in boundary values to asymptotically match the two solutions. Examples are treated in Chapter V; anticipating that discussion, we remark that Eq. (3.44) can, with suitable approximation, be reduced to an ordinary differential equation for the χ-dependent amplitude $(\delta\underset{\sim}{B}\cdot\nabla\chi)_{mn}$. One then finds that the annulus $\chi = \chi_{mn}$ corresponds to a regular singular point of this equation.

The radial width of the boundary layer, w, depends upon ω, magnetic shear, and various dissipative effects, but it is always very small compared to the plasma minor radius: $w \ll a$. Hence, in solving the interior problem, one can evaluate most equilibrium parameters at $\chi = \chi_{mn}$, and identify $\omega_{SA} \cong k_{\|}(|\chi-\chi_{mn}| = w)v_A$. In Sec. IIA we distinguished between local equilibrium theory and global equilibrium theory. It is now clear that only the former enters solution of the interior boundary layer problem, and also that solution of the exterior problem shares with global equilibrium theory the properties of being analytically intractable and highly device-specific.

Linear resolution of the singularity evidently depends upon the inertial term, $L\cdot\delta\underset{\sim}{f}$, and therefore requires additional physical information, relating $\delta\underset{\sim}{f}$ to $\delta\underset{\sim}{B}$, for closure. A general prescription for closure is not easily written down, even schematically; closure schemes are sensitive to various plasma parameters, such as collisionality, and often complicated. The enormous variety of distinct boundary-layer modes reflects a corresponding variety of

approximate closure relations. Several examples are considered in the following chapter.

Nonlinear treatment of the singularity relies primarily on the term $\delta^2 N$, i.e., on nonlinear magnetic perturbation. The point is that nonlinear structures often evolve slowly, so that inertial effects remain small. The most striking feature of the $\delta^2 N$ term is that it is usually associated with changes in the magnetic field topology: the original toroidal flux surface is deformed, near the rational surface, into a more complicated structure involving multiple tori. Thus a Newcomb condition applied to the unperturbed rational surface is no longer relevant. One can say that the $\delta^2 N$ terms, when they change the field topology, serve to obviate the singularity rather than to resolve it.

2. Magnetic Islands

We wish to consider static perturbations of the equilibrium field studied in Chapter I,

$$\underset{\sim}{B}_o = \nabla\zeta\times\nabla\chi + q\nabla\chi\times\nabla\vartheta \quad .$$

As usual, we suppose that $\underset{\sim}{B}_o$ is characterized by a sequence of nested tori. By including a perturbation, $\delta\underset{\sim}{B} << \underset{\sim}{B}_o$, we shall find that some of these tori suffer topological change, which is generically referred to as magnetic reconnection. (The general problem of field-line flow has been treated using the modern methods of Hamiltonian dynamics by Cary and Littlejohn [21].)

To avoid confusion, one technical point should be mentioned first. Recall from Chapter II that, except in the strictly axisymmetric case, the unperturbed field will necessarily include "bad" regions, with small magnetic islands and thin ergodic volumes. While the total volume of such regions is presumed to be negligible, their existence means that $\delta\underset{\sim}{B}$ can strictly have only a quantitative, rather than qualitative effect. That is, the perturbed field differs from $\underset{\sim}{B}_o$ in that its bad regions, while perhaps occupying a small fraction of the plasma volume, are nonetheless of appreciable size.

We restrict our attention here to island structure. The dynamics of magnetic reconnection is studied in subsequent chapters.

It is convenient to express $\delta\underset{\sim}{B}$ in terms of a vector potential: $\delta\underset{\sim}{B} = \nabla\times\delta\underset{\sim}{A}$. Magnetic reconnection requires only a single component of $\delta\underset{\sim}{A}$; we choose the toroidal component for simplicity and because it often dominates in linear stability considerations: $\delta\underset{\sim}{A} = A_\zeta\nabla\zeta$. Supposing first that A_ζ contains only the helicity (m,n), we write

$$A_\zeta(\chi,\vartheta,\zeta) = -\frac{n}{m}A(\chi,n\alpha) \ ,$$

where

$$\alpha \equiv \zeta - \frac{m}{n}\vartheta \ , \tag{3.45}$$

is a helical angle and the $(-n/m)$ factor is inserted for convenience. Thus

$$\delta\underset{\sim}{B} = \nabla A_\zeta \times \nabla\zeta = \frac{n}{m}\frac{\partial A}{\partial \chi}\nabla\zeta\times\nabla\chi + \frac{\partial A}{\partial \alpha}\nabla\vartheta\times\nabla\zeta \quad .$$

Two components of the full magnetic field, $\underset{\sim}{B}_o + \delta\underset{\sim}{B}$, are relevant,

$$B^\chi = \delta\underset{\sim}{B}\cdot\nabla\chi = \frac{1}{\sqrt{g}}\frac{\partial A}{\partial \alpha} \quad ,$$

and

$$B^\alpha = \underset{\sim}{B}_o\cdot\nabla\alpha + \delta\underset{\sim}{B}\cdot\nabla\alpha = \frac{1}{\sqrt{g}}\left(q - \frac{m}{n} - \frac{\partial A}{\partial \chi}\right) \quad .$$

The trajectory of a field line in the (χ,α) plane is described by the equation

$$\frac{d\chi}{d\alpha} = \frac{B^\chi}{B^\alpha} = \frac{\partial A/\partial\alpha}{q-m/n-\partial A/\partial\chi} \quad , \tag{3.46}$$

which has the solution $\chi = \chi_*(\alpha)$, say. It is clear that when χ is far from the rational surface:

$$|q(\chi) - m/n| >> \partial A/\partial\chi \quad ;$$

the field line trajectory varies only mildly with α; in fact, Eq. (3.46) yields

$$\chi_* \cong \chi_o + A/[q(\chi_o)-m/n] \quad . \tag{3.47}$$

However, in the neighborhood of the rational surface, the perturbation is much more important. For this case we can expand χ and q about the rational surface, letting

$$\chi_* = \chi_{mn} + X(\alpha)$$
$$q(\chi_*) = m/n + q'X \ . \tag{3.48}$$

Using these approximations the first integral of Eq. (3.46) takes the simple form

$$H = \frac{q'}{2} X^2(\alpha) - A(X(\alpha),\alpha) \tag{3.49}$$

where H is the integration constant. We have written the result in this form to exhibit the analogy with the Hamiltonian mechanics of a particle with momentum X and mass $1/q'$, in a potential $-A$ (which may be momentum dependent) where time can be interpreted as $n\zeta/m$.

For illustrative purposes, suppose that

$$A(X,\alpha) = a(X)\cos n\alpha$$

There are two important cases. Consider first the case in which a(X) is approximately constant; that is

$$q'X^2 \sim a >> a'X \ ,$$

which implies

$$q'a(X) >> (a')^2 \ . \tag{3.50}$$

Neglecting the X dependence of a reduces Eq. (3.48) to the pendulum Hamiltonian. This Hamiltonian has stable fixed points at (X=0, $n\alpha = 2\pi k$; k=0,1,...,n-1) which therefore corresponds to a single helical field line with rotational transform m/n. Encircling this field line, which is effectively a new magnetic axis, are new magnetic surfaces, which form a helically twisted torus. From the definition of α it follows that on a surface of constant ϑ (or ζ) these surfaces look like a chain of n(or m) islands.

The unstable fixed points for the pendulum Hamiltonian, at [X=0, $n\alpha = (2k+1)\pi$, k=0,1,...,n-1], are the x-points at which the reconnection of field lines to create the islands occurs. Connecting the x-points is the separatrix which still encircles the original axis, as in Eq. (3.47). On the separatrix H=a, and Eq. (3.49) gives

$$X = \pm W \cos(n\alpha/2) \tag{3.51}$$

where W is evidently the island half width and is given by

$$W = 2(a/q')^{1/2} \ . \tag{3.52}$$

The new torus has its own sequence of nested surfaces, and therefore its own flux coordinates, $(\chi_I, \vartheta_I, \zeta_I)$. It is clear that these variables cannot smoothly connect, at the separatrix, to (χ, ϑ, ζ). For example, ϑ_I changes by 2π in a region over which ϑ changes by less than $2\pi/m$. In particular, the island safety factor is measured with respect

to an O-point and is therefore very different from q (see, for example, [22]). It is not hard to show that

$$\frac{1}{q_I} \simeq \frac{m}{2}\left(\frac{1}{q}\right)' W \quad , \tag{3.53}$$

on typical island surfaces; thus, for weak perturbations, $q_I >> q$. On the separatrix, q_I is always infinite, since x-points prevent separatrix field lines from encircling the island magnetic axis.

Returning now to Eq. (3.50) we see that it may be violated when the magnetic perturbation is odd about the rational surface, as in the case of electromagnetic drift waves [23]. In this case we can set $a(X) = a'X$ with a' constant and obtain the trajectory solution from Eq. (3.49). The unstable fixed points occur at $(X=0, \quad n\alpha = (2k+1)\pi/2)$ where the energy, H, is zero. Therefore, the separatrix solutions from Eq. (3.49) are

$$X(\alpha) = 0 \quad ; \quad X(\alpha) = (2a'/q')\cos n\alpha \quad .$$

The odd magnetic field case is primarily distinguished by its relatively small island half-width,

$$W = a'/q' \tag{3.54}$$

which is proportional to δB rather than $(\delta B)^{1/2}$. In this sense, topological change is significantly less serious when $\delta B^X(\chi_{mn}) = 0$. The reason for this difference can be understood by noticing the similarity between the trajectory equation, Eq. (3.46), and the magnetic

differential equation, Eq. (2.29). Observe that the solubility condition for the latter, Eq. (2.31), corresponds to $A_{mn} = 0$. Thus "strong" magnetic reconnection, with $W \sim (\delta B)^{1/2}$, is an artifact of failure to satisfy the Newcomb condition. It is a necessary artifact when S, in Eq. (2.31), includes terms proportional to δB^{χ}.

3. Islands and Linear Theory

Linear theory assumes that field perturbations such as δB are arbitrarily small, and it rules out the occurrence of terms involving $(\delta B)^{1/2}$. But we have seen that $(\delta B)^{1/2}$ necessarily enters if

$$(\delta \underset{\sim}{B} \cdot \nabla \chi)_{mn} \neq 0 \quad \text{at} \quad \chi = \chi_{mn} \quad , \tag{3.55}$$

however small the perturbation may be. Thus Eq. (3.55) is inconsistent with any strictly linear analysis.

That a linear description of reconnection is nonetheless possible can be understood as follows. Note that dependence on $(\delta B)^{1/2}$ occurs only near and within the separatrix; far outside the separatrix, Eq. (3.47) displays a simple linear perturbation of the trajectory. Furthermore $\delta \underset{\sim}{B}$ need not vary across the separatrix width; the topology change depends on Eq. (3.55) but is otherwise quite insensitive to its spatial structure. Thus it is possible for the important variation of $\delta \underset{\sim}{B}$ to occur in that region, far outside the separatrix, where linearization is valid. A linear description, ignoring the island region entirely, is clearly adequate in that case.

The linear regime for magnetic reconnection is therefore characterized by

$$w >> W \quad . \tag{3.56}$$

Here w, the width of the shear-Alfvén boundary layer, is identified with the local spatial scale for variation of δB^{χ}. Since w is independent of amplitude, Eq. (3.56) will always be satisfied for sufficiently small $\delta \underset{\sim}{B}$.

4. Rational Surface Spacing

In addition to w and W, there is a third width of basic importance: the spacing between mode-rational surfaces.

Consider a field perturbation, $A(\chi,\vartheta,\zeta)$ which lacks helical symmetry but is reasonably smooth. Then many Fourier components, A_{mn}, will contribute to A and islands will form near many rational surfaces χ_{mn}. However, the smoothness of A requires the A_{mn}, and therefore the corresponding island widths W_{mn}, to become small for large m and n. If islands smaller than a certain size (such as a charged particle Larmor radius, or the island size associated with $\underset{\sim}{B}_o$) are acknowledged to be irrelevant, then there is an effective bound on n,

$$A_{mn} = 0 \quad , \quad n > N \quad ,$$

and, for sufficiently small A, most irrational magnetic surfaces will survive destruction. (The KAM theorem [2] yields a stronger version of this statement, implying that the total volume of "bad" regions is

small whenever A is sufficiently small and sufficiently differentiable.)

Two nearest neighbor surfaces on which appreciable islands can be found correspond to χ_{mN} and

$$\chi_{m+1,N} = \chi_{mN} + \Delta\chi_{mN} \quad .$$

For a smooth q-profile, we have

$$m+1 = Nq(\chi_{m+1,N}) \simeq m + Nq'\Delta\chi_{mN} \quad .$$

Thus

$$\Delta\chi_{mN} \simeq \left[Nq'(\chi_{mN})\right]^{-1} \quad , \qquad (3.57)$$

measures, in units of χ, the rational surface spacing.

Our study of island structure considered only a single helicity perturbation. It is nonetheless locally accurate provided that

$$\Delta\chi_{mn} >> W_{mn} \quad .$$

The opposite case,

$$\Delta\chi_{mn} \lesssim W_{mn} \quad ,$$

evidently corresponds to the overlap of magnetic islands centered on neighboring rational surfaces. Trajectory equations involving multiple helicities are easily written down for the overlapping case. However,

as pointed out by Chirikov [24] and others, the multiple helicity equations are nonintegrable, and numerical solutions display a chaotic wandering of field lines which satisfies typical criteria for randomness. One says that the field lines become stochastic; the threshhold for stochasticity has been studied in numerous cases and is roughly approximated by the "Chirikov condition",

$$\Delta\chi_{mn} = 2W_{mn} \quad .$$

The significance of island overlap obviously extends beyond the domain of instability theory. In particular, overlap is responsible for the previously mentioned formation of ergodic volumes: stochastic regions display poor plasma confinement [25,26,27]. Thus, while the nonlinear growth to macroscopic width of a single island chain will clearly degrade confinement, the possibility of overlap between numerous, relatively small island chains is at least equally serious.

In the context of linear theory, the relevant comparison is between $\Delta\chi_{mn}$ and w_{mn}, the layer width of the (m,n)-Fourier mode. Notice that, even in the presence of numerous harmonics A_{mn}, a single component can locally dominate if

$$\Delta\chi_{mn} >> w_{mn} \quad . \tag{3.58}$$

In this case it is sensible to restrict attention to a single rational surface. Toroidal curvature may still couple various harmonics, but the fundamental, whose shear-Alfvén law is uniquely singular, will be readily distinguishable. Most linear theories of tearing instability are based on Eq. (3.58).

The opposite case

$$\Delta\chi_{mn} \leq w_{mn} \quad , \tag{3.59}$$

corresponds to overlapping boundary layers and often characterizes ballooning instability. The corresponding eigenmodes intrinsically involve many helicities, even locally; they typically extend over numerous rational surfaces. The linear analysis of such eigenmodes requires a distinct methodology, which is studied in Chapter VI.

The mode-number-dependence of w_{mn} is usually weak compared to that of $\Delta\chi_{mn} \sim n^{-1}$. Therefore the issue of boundary-layer overlap depends largely on n, and one can roughly associate Eqs. (3.58) and (3.59) with the cases of "small n" and "large n" respectively (recall $q \sim m/n \sim 1$).

Let us summarize. The physics of magnetic island formation depends critically upon the relative magnitudes of W, $\Delta\chi$ and w. The first two of these widths are given by Eqs. (3.52) [or Eq. (3.54)] and Eq. (3.57); the third is a local scale length for $\delta\underset{\sim}{B}$ depending upon boundary-layer dynamics which have yet to be considered concretely.

When $\Delta\chi$ is the largest of the three widths, the dynamics are locally controlled by a single helicity. This case corresponds to conventional boundary-layer modes, in linear theory ($\Delta\chi > w > W$), or to coherent evolution of a single island chain, in nonlinear theory ($\Delta\chi > W > w$).

When the largest width is W, field lines become stochastic and inadequately approximated by $\underset{\sim}{B}_o$. Linear theory is rarely useful; the relative ordering of w and $\Delta\chi$ becomes irrelevant.

Finally, when the largest width is w, one finds linear perturbations without well-defined helicity ($w > \Delta\chi > W$) or nonlinear evolution modified by local stochasticity ($w > W > \Delta\chi$; see, for example, [28]).

IV. Reduced Fluid Models

A. Introduction

Exact linearization of the shear-Alfvén law produces a multitude of terms, especially in toroidal geometry. Similarly, closure of the system can become extremely complicated unless severe approximations are made at the start. Such considerations have motivated the construction of numerous, more or less systematic, simplification schemes.

Two sorts of simplifying approximation can be distinguished. First, the plasma dynamics may be simplified by presuming each plasma species to be adequately represented by a (moving) Maxwellian distribution function. The defects of this "fluid approximation" are clear, but not always serious (see Sec. C).

In the second sort of approximation, one uses a scale length ordering (as in Sec. IID) to select dominant effects. When such geometrical simplification is applied ab initio (rather than to the linear dispersion relation, for example), the resulting dynamical system is said to be "reduced". Reduction based on large aspect ratio, for example, yields results which usually approximate those of more elaborate calculations. Moreover, the exceptional cases of qualitative disagreement are fairly well understood.

Reduced fluid theory, the main subject of this chapter, combines both types of approximation, and therefore may appear rather crude. Yet even the simplest reduced fluid models have been found to be remarkably predictive: they simulate such important tokamak phenomena as dynamic island formation, magnetic stochasticity and plasma disruption (see, for example, [29,30,31]). Numerical solution of such

models has become a crucial element in the interpretation and design of tokamak experiments. The putative reason for this success is that, while fluid-reduction may blur certain features of the linear response, it adequately represents the dominant nonlinear effects.

Here we consider reduced fluid theory as a pedagogical tool, and therefore emphasize its linear predictions. The point is that key features of less approximate linear theories usually survive, in simplified form, the reduction process. On the other hand, the reduced equations are relatively compact, transparent, and analytically tractable. In this sense, they provide a "hydrogen-atom" model for toroidal plasma electrodynamics.

In Sec. B we derive one of the simplest reduced fluid models: reduced MHD. The earliest version of reduced MHD is due to Kadomtsev and Pogutse [32]. This version was studied numerically by Rosenbluth et al. [33] and then significantly developed by Strauss [34,35]. The model assumes axisymmetry of the vacuum magnetic field, and is therefore appropriate to a large aspect-ratio tokamak.

Modifications and elaborations of reduced MHD are studied in Sec. C. These include both geometrical and, especially, kinetic refinements. We point out that certain non-MHD effects, usually computed from kinetic theory, can be obtained as well from a generalized, reduced fluid model.

B. Reduced MHD

1. Normalized Coordinates

Reduced MHD is derived from an expansion in the inverse aspect ratio:

$$\varepsilon \equiv \frac{a}{R_0} << 1$$

[recall Eq. (2.107)]. The ordering procedure is clarified by means of dimensionless field variables and coordinates, chosen to make the various powers of ε explicit. A convenient set of dimensionless coordinates (x,y,z) is defined in terms of cylindrical coordinates, (R,ζ,Z), by

$$x = \frac{R-R_0}{a} \quad ; \quad y = \frac{Z}{a} \quad ; \quad z = -\zeta \quad . \tag{4.1}$$

Thus (x,y) represent coordinates in the plane perpendicular to the vacuum toroidal field and are scaled with the minor radius, while z is scaled with R. For this section we will henceforth use a dimensionless gradient operator defined by

$$a\nabla \rightarrow \nabla \equiv \hat{x}\frac{\partial}{\partial x} + \hat{y}\frac{\partial}{\partial y} + \hat{z}\frac{\varepsilon}{1+\varepsilon x}\frac{\partial}{\partial z} \tag{4.2}$$

where the unit vectors $\hat{x} = \hat{R}$, and $\hat{z}=-\hat{\zeta}$ are position dependent, $\hat{y}=\hat{Z}$ and $1+\varepsilon x = R/R_0$. It is convenient to decompose vectors into two parts, transverse ($\perp$) and longitudinal (z) defined by

$$\underset{\sim}{A} = \underset{\sim}{A}_\perp + \hat{z}A_z$$

$$\underset{\sim}{A}_\perp \equiv \hat{x}\underset{\sim}{A}_x + \hat{y}\underset{\sim}{A}_y \tag{4.3}$$

where $\perp$ designates components perpendicular to the vacuum field, and A_x, etc., designate the ordinary components of the vector.

The subsequent calculations are simplified if the curvature terms arising from $\frac{\partial}{\partial z}\hat{x} = \hat{z}$ and $\frac{\partial}{\partial z}\hat{z} = -\hat{x}$ are made explicit. For example, the dimensionless divergence and curl are

$$\nabla\cdot\underset{\sim}{A} = \nabla_\perp\cdot\underset{\sim}{A}_\perp + \frac{\varepsilon}{1+\varepsilon x}\left(\frac{\partial A_z}{\partial z} + A_x\right) \tag{4.4}$$

$$\nabla\times\underset{\sim}{A} = -\hat{z}\times\nabla_\perp A_z + \hat{z}(\hat{z}\cdot\nabla_\perp\times\underset{\sim}{A}_\perp)$$

$$+ \frac{\varepsilon}{1+\varepsilon x}\left[-\hat{x}\frac{\partial A_y}{\partial z} + \hat{y}\left(\frac{\partial A_x}{\partial z} - A_z\right)\right] \tag{4.5}$$

where the transverse operator $\nabla_\perp$ is to be computed as if the coordinates were Cartesian, e.g.

$$\nabla_\perp\cdot\underset{\sim}{A}_\perp = \frac{\partial A_x}{\partial x} + \frac{\partial A_y}{\partial y} . \tag{4.6}$$

The fundamental time scale in MHD is set by the Alfvén speed,

$$v_A^2 \equiv B_c^2/4\pi n_c m_i ,$$

where B_c and n_c are constants, measuring respectively the vacuum magnetic field and ion density at the magnetic axis. The poloidal

dimension sets $k_\perp \sim a^{-1}$, so that the compressional Alfvén time is measured by

$$\tau_A \equiv a/v_A \ . \tag{4.7}$$

Recalling from Eq. (3.6) that

$$k_\parallel/k_\perp \sim O(\varepsilon) \tag{4.8}$$

we see that the shear Alfvén time is τ_A/ε. Hence the appropriate dimensionless time is given by

$$\tau = (\varepsilon/\tau_A)t \ . \tag{4.9}$$

The significance of reduced coordinates should be clear. Large aspect ratio has been used to distinguish the transverse (a) and longitudinal (R_0) scale lengths. The character of tokamak confining fields ($B_P/B_T \sim \varepsilon$) guarantees that their ratio, ε, will be comparable to the flute-like ordering parameter, as in Eq. (4.8). In this case, as noted in Chapter III, the shear-Alfvén time scale becomes of primary interest.

We point out that our definitions [which make $(\hat{x},\hat{y},\hat{z})$ a right-handed triplet] differ slightly from those of Strauss. The different convention affects some signs in the final equations.

2. Normalized Fields

The dimensionless fields of reduced MHD are defined in terms of the natural units B_c, v_A, and a. In this section the orderings for "high-beta" reduced MHD are displayed, leading to the conclusion that only three fields (ψ,φ,p) are required through order ε^2.

The vacuum magnetic field

$$\hat{z}B_c/(1+\varepsilon x)$$

has a controlling influence on tokamak dynamics. Reduced MHD expresses this fact by assuming that corrections to it are of relative order ε. Using B_c to normalize we write

$$\frac{\underset{\sim}{B}}{B_c} \rightarrow \underset{\sim}{B} = \frac{\hat{z}}{1+\varepsilon x} + \varepsilon\nabla\times\underset{\sim}{\mathcal{A}} \tag{4.10}$$

where $\varepsilon\,\underset{\sim}{\mathcal{A}}$ is the dimensionless vector potential given by $\underset{\sim}{A}/(B_c a)$. Following Eq. (4.3) the perturbing field is split into longitudinal and transverse parts. Letting

$$\begin{aligned} B_\parallel &= \hat{z}\cdot\nabla_\perp\times\underset{\sim}{\mathcal{A}}_\perp \\ \psi &= \mathcal{A}_z \end{aligned} \tag{4.11}$$

we can use Eq. (4.5) to expand $\underset{\sim}{B}$ as

$$\underset{\sim}{B} = \hat{z} + \varepsilon(-\hat{z}x + \hat{z}B_\parallel - \hat{z}\times\nabla_\perp\psi) + O(\varepsilon^2)\ . \tag{4.12}$$

It can be seen that $(-\psi)$ is proportional to the poloidal flux. Similarly the dimensionless current is defined by

$$\frac{4\pi}{c}\frac{a}{B_c}\underset{\sim}{J} \rightarrow \underset{\sim}{J} = \nabla\times\underset{\sim}{B} \tag{4.13}$$

where $\underset{\sim}{J} = O(\varepsilon)$ follows directly from Eq. (4.12).

Next consider the electric field, $\underset{\sim}{E}$. We introduce the dimensionless electrostatic potential by

$$\frac{c}{v_A}\frac{1}{B_c a}\Phi = \varepsilon\varphi \tag{4.14}$$

where Φ is the ordinary potential. Then Faraday's law

$$\underset{\sim}{E} = -\nabla\Phi - \frac{1}{c}\frac{\partial\underset{\sim}{A}}{\partial t}$$

leads to the definition of the dimensionless electric field

$$\frac{c}{v_A}\frac{1}{B_c}\underset{\sim}{E} \rightarrow \underset{\sim}{E} = -\varepsilon(\nabla\varphi + \varepsilon\,\partial\,\underset{\sim}{\mathcal{A}}/\partial\tau) \tag{4.15}$$

where the dimensionless gradient and shear-Alfvén time scale are used. Note that our normalizations have made the lowest order transverse field electrostatic; this is a physical artifact of the shear-Alfvén time scale.

Velocity is naturally expressed in units of v_A, and we assume it is order ε:

$$\frac{\underset{\sim}{V}}{v_A} = \varepsilon \underset{\sim}{u} \ . \tag{4.16}$$

Finally, we need a normalized measure of the plasma pressure, P. We use a high-beta ordering, as in Eq. (2.133),

$$P \sim \varepsilon B_c^2/8\pi \ ,$$

and therefore define the dimensionless pressure, p, by

$$\frac{8\pi}{B_c^2} P = \varepsilon p \ . \tag{4.17}$$

Substituting the dimensionless fields into the equation of motion, Eq. (3.11), immediately gives

$$\varepsilon^2 \frac{n}{n_c} \frac{d\underset{\sim}{u}}{d\tau} = -\frac{\varepsilon}{2} \nabla p + (\nabla \times \underset{\sim}{B}) \times \underset{\sim}{B} \tag{4.18}$$

where we set the anisotropic pressure to zero in MHD. The $\underset{\sim}{J} \times \underset{\sim}{B}$ term can be simplified by means of Eqs. (4.5) and (4.12):

$$(\nabla \times \underset{\sim}{B}) \times \underset{\sim}{B} = -\varepsilon \underset{\sim}{\nabla}_\perp B_\parallel + O(\varepsilon^2) \ . \tag{4.19}$$

Therefore, Eq. (4.18) yields

$$\varepsilon\nabla_\perp(B_\parallel+p/2) = O(\varepsilon^2) \tag{4.20}$$

expressing lowest order force balance as in Eq. (3.13).

Equation (4.20) will allow us to eliminate $B_\parallel$, the diamagnetic correction to $\underset{\sim}{B}_T$, from the closed system. Notice that $B_\parallel \sim \mathscr{A}_\perp \sim \psi$ is not negligibly small, as it would be in low-beta ($\beta_T \sim \varepsilon^2$) theory. [The present analysis parallels, in more concrete form, the general discussion of Chapter III. For example, Eq. (4.20) explicitly expresses the shielding of the "strong" $\underset{\sim}{J}\times\underset{\sim}{B}$ force and shows why this force is annihilated by $\underset{\sim}{B}\cdot\nabla\times$.]

3. Reduced Shear-Alfvén Law

The shear-Alfvén law, Eq. (3.20) can be expressed in dimensionless form using Eqs. (4.10)-(4.17). Here we again use the MHD approximation $\underset{\sim}{\pi}=0$ to obtain

$$\varepsilon^2\underset{\sim}{B}\cdot(\nabla\times - 2\underset{\sim}{\kappa}\times)\frac{n}{n_c}\frac{d\underset{\sim}{u}}{d\tau} = B^2\underset{\sim}{B}\cdot\nabla(J_\parallel/B) + \varepsilon B\cdot\underset{\sim}{\kappa}\times\nabla p \ ,$$

$$\frac{d}{d\tau} = \frac{\partial}{\partial\tau} + \underset{\sim}{u}\cdot\nabla \ . \tag{4.21}$$

The reduced law follows from expanding Eq. (4.21) in powers of ε and discarding $O(\varepsilon^3)$ terms. As we will see below, the lowest order nonvanishing contribution to each of the terms in Eq. (4.21) is $O(\varepsilon^2)$; therefore, each term needs only be calculated to lowest order. We found a similar result in the flute reduction of Sec. IID.

Consider first the "kink" term on the right-hand side. Equations (4.12) and (4.2) imply

$$\underset{\sim}{B}\cdot\nabla = \varepsilon\left(\frac{\partial}{\partial z} - \hat{z}\times\nabla_\perp\psi\cdot\nabla_\perp\right) + O(\varepsilon^2) \ . \tag{4.22}$$

That the parallel gradient is $O(\varepsilon)$ is consistent with Eq. (4.8). The parallel current, as defined by Eq. (4.13), becomes

$$\begin{aligned} J_\parallel &= \frac{1}{B}\,\underset{\sim}{B}\cdot\nabla\times\underset{\sim}{B} = \hat{z}\cdot\nabla\times\underset{\sim}{B} + O(\varepsilon^2) \ ; \\ &= -\varepsilon\nabla_\perp^2\psi + O(\varepsilon^2) \ . \end{aligned} \tag{4.23}$$

The combination of Eqs. (4.22) and (4.23) shows the kink term is $O(\varepsilon^2)$ as expected.

The interchange term involves the curvature $\underset{\sim}{\kappa}$ which, from Eq. (3.17), can be written

$$\underset{\sim}{\kappa} = \frac{\varepsilon}{2}\,\nabla_\perp(p+B^2) + O(\varepsilon^2) = \varepsilon\nabla_\perp(p/2 + B_\parallel - x) + O(\varepsilon^2)$$

where in the first equation the corrections are due to inertial terms and in the second we expand B^2 using Eq. (4.12). Combining this expression with the force balance relation, Eq. (4.20), we find

$$\underset{\sim}{\kappa} = -\varepsilon\nabla_\perp x \ . \tag{4.24}$$

Since $\underset{\sim}{\kappa} = O(\varepsilon)$ the lowest order field may be used to obtain the interchange term:

$$\varepsilon \underset{\sim}{B}\times\underset{\sim}{\kappa}\cdot\underset{\sim}{\nabla}p = -\varepsilon^2\hat{z}\times\nabla_\perp x\cdot\underset{\sim}{\nabla}_\perp p \ . \tag{4.25}$$

Treatment of the inertial terms on the left-hand side of Eq. (4.21) requires a closure relation for the velocity. Here we use the MHD ansätz,

$$\underset{\sim}{V} = c\underset{\sim}{E}\times\underset{\sim}{B}/B^2 + \hat{b}V_\parallel \ , \tag{4.26}$$

that the perpendicular velocity is given by the $\underset{\sim}{E}\times\underset{\sim}{B}$ drift (this is refined in Sec. C). In dimensionless variables [Eqs. (4.15)-(4.16)], we obtain

$$\underset{\sim}{u} = \hat{z}\times\nabla_\perp\varphi + u_\parallel\hat{z} + O(\varepsilon) \tag{4.27}$$

which shows that only the electrostatic drift enters at the required order of approximation.

A distinct simplification is to replace the factor n/n_c in Eq. (4.21) by unity. This approximation, called the Boussinesq approximation by analogy with a similar one used in the theory of convection [36], is not strictly justified by the ε-ordering; however, density gradient terms do not appear to be important in the present context, and they would yield undesirable cubic nonlinearity.

Because of Eqs. (4.24) and (4.27), the lowest order inertial term simplifies to

$$\varepsilon^2\hat{z}\cdot\nabla\times\frac{d\underset{\sim}{u}}{d\tau} = \varepsilon^2\frac{\partial}{\partial\tau}\nabla_\perp^2\varphi + \varepsilon^2\hat{z}\cdot\nabla\times(\underset{\sim}{u}\cdot\nabla\underset{\sim}{u}) \ .$$

The nonlinear term can be simplified using

$$\nabla\times(\underset{\sim}{u}\cdot\nabla\underset{\sim}{u}) = -\nabla\times[\underset{\sim}{u}\times(\nabla\times\underset{\sim}{u})]$$

and Eq. (4.5) to show that the parallel velocity does not contribute and therefore

$$\varepsilon^2\hat{z}\cdot\nabla\times\frac{d\underset{\sim}{u}}{d\tau} = \varepsilon^2[\frac{\partial}{\partial\tau} + \hat{z}\cdot\nabla_\perp\varphi\times\nabla_\perp]\nabla_\perp^2\varphi + O(\varepsilon^3) \quad . \tag{4.28}$$

Note that no assumption that $u_\parallel << u_\perp$ was made.

Equations (4.22), (4.23), (4.25) and (4.28) combine to yield the nonlinear, reduced shear-Alfvén law. The final expression is made compact by means of certain (conventional) abbreviations. The normalized longitudinal current is denoted by

$$J = \nabla_\perp^2\psi \quad ,$$

(note that $J \propto -J_\parallel$) and the vorticity by

$$U = \nabla_\perp^2\varphi \quad .$$

We also introduce, for any functions f and g, the bracket

$$[f,g] \equiv \hat{z}\cdot\nabla_\perp f\times\nabla_\perp g \quad .$$

Finally, the reduced law is written as

$$\frac{\partial}{\partial\tau} U + [\varphi,U] = - \frac{\partial J}{\partial z} + [\psi,J] - [x,p] \ . \tag{4.29}$$

4. Closure Relations

A closed system for (ψ,φ,p) evidently requires, in addition to Eq. (4.29), two other relations. In reduced MHD, the latter are obtained from a parallel Ohm's law,

$$\underset{\sim}{B}\cdot(\underset{\sim}{E}+c^{-1}\underset{\sim}{V}\times\underset{\sim}{B}) = \eta_{\|}\underset{\sim}{B}\cdot\underset{\sim}{J} \ , \tag{4.30}$$

and from the MHD energy conservation law,

$$\frac{\partial P}{\partial t} + \underset{\sim}{V}\cdot\underset{\sim}{\nabla}P = - \frac{5}{3} P\underset{\sim}{\nabla}\cdot\underset{\sim}{V} \ . \tag{4.31}$$

In Eq. (4.30), $\eta_{\|}$ represents parallel resistivity.

Reduction of Eqs. (4.30) and (4.31) closely follows the scheme of the previous subsection and need not be elaborated here. However, a few comments are in order.

In the Ohm's law, $\underset{\sim}{E}$ is provided by Eq. (4.15) and $\underset{\sim}{V}$ by Eq. (4.27). Notice that the electrostatic contribution to $E_{\|} = \underset{\sim}{B}\cdot\underset{\sim}{E}/B$ does not dominate, as it does for $\underset{\sim}{E}_{\perp}$, because of Eq. (4.2). Thus the dimensionless parallel electric field is

$$E_{\|} = -\varepsilon^2(\frac{\partial\varphi}{\partial z} - [\psi,\varphi] + \frac{\partial\psi}{\partial\tau}) + O(\varepsilon^3) \ . \tag{4.32}$$

On the right-hand side of Eq. (4.30), $\eta_{\parallel}$ is presumed to be very small, so that only the lowest order $J_{\parallel} \simeq J_z$ is retained. Thus one finds that

$$\frac{\partial \psi}{\partial \tau} + \frac{\partial \varphi}{\partial z} - [\psi, \varphi] = \eta J \ ,$$

with

$$\eta \equiv \tau_A / \varepsilon \tau_S \ . \tag{4.33}$$

Here τ_S is the resistive skin time given by

$$\tau_S = 4\pi a^2 / (c^2 \eta_{\parallel}) \ . \tag{4.34}$$

The energy conservation law in dimensionless form is

$$\varepsilon^2 \frac{\partial p}{\partial \tau} + \varepsilon^2 \underset{\sim}{u} \cdot \nabla p = \varepsilon^2 \frac{5}{3} p \nabla \cdot \underset{\sim}{u} \ .$$

Since $\nabla \cdot \underset{\sim}{u}$, from Eq. (4.27), is clearly $O(\varepsilon)$, the compressibility term on the right-hand side may be consistently neglected: reduced MHD yields an effectively incompressible plasma fluid. Pressure evolution is then determined by simple $\underset{\sim}{E} \times \underset{\sim}{B}$ convection:

$$\frac{\partial p}{\partial \tau} + [\varphi, p] = 0 \ .$$

In summary, high-beta reduced MHD is defined by the following system [35]:

$$\frac{\partial U}{\partial \tau} + [\varphi, U] = -\nabla_{\parallel} J - [x, p] \ , \tag{4.35}$$

$$\frac{\partial \psi}{\partial \tau} + \nabla_{\parallel} \varphi = \eta J \ , \tag{4.36}$$

$$\frac{\partial p}{\partial \tau} + [\varphi, p] = 0 \ , \tag{4.37}$$

with

$$U = \nabla_{\perp}^2 \varphi, \ J = \nabla_{\perp}^2 \psi \tag{4.38}$$

$$\nabla_{\parallel} = \frac{\partial}{\partial z} - [\psi, \ ] \tag{4.39}$$

and

$$[f, g] = \hat{z} \cdot \nabla_{\perp} f \times \nabla_{\perp} g = \nabla_{\perp} \cdot (g \hat{z} \times \nabla_{\perp} f) \tag{4.40}$$

Note that $\nabla_{\parallel}$ denotes the nonlinear gradient along $\underset{\sim}{B}$.

Equations (4.35)-(4.40) have been written in a form which allows straightforward transformation of the transverse coordinates, x and y. Cylindrical coordinates, (r, ϑ), defined by

$$x = r\cos\vartheta, \ y = r\sin\vartheta \ , \tag{4.41}$$

are frequently useful. We then have

$$\nabla_{\perp}^2 = \frac{1}{r} \frac{\partial}{\partial r} r \frac{\partial}{\partial r} + \frac{1}{r^2} \frac{\partial^2}{\partial \vartheta^2}$$

and

$$[f,g] = \frac{1}{r}\left(\frac{\partial f}{\partial r}\frac{\partial g}{\partial \vartheta} - \frac{\partial g}{\partial r}\frac{\partial f}{\partial \vartheta}\right) . \qquad (4.42)$$

5. Discussion

Reduced MHD is a sifted version of the full MHD system. The sifting process is severe, but emphatically self-consistent. Because of the "drop ε^3" rule, it provides a three-field model without explicit dependence on aspect ratio. Thus all terms in the final equaions are formally comparable.

The reduced equations are nearly devoid of toroidicity. For example, the Grad-Shafranov operator, Δ_*, is reduced to $\nabla_\perp^2$, as would pertain in a cylindrical tokamak. Toroidicity explicitly survives only in the interchange term,

$$[x,p] \propto \hat{z}\times\nabla_\perp R\cdot\nabla_\perp p ,$$

and this remnant is rather crude: it corresponds to the curvature of a purely toroidal ($\underset{\sim}{B}=\underset{\sim}{B}_T$) field line.

Low-beta reduced MHD assumes $\beta_T \sim \varepsilon^2$ and thus omits the interchange term, decoupling the pressure. The resulting two-field theory evidently models a cylinder, although toroidal <u>topology</u> can still be imposed through periodicity conditions.

The parallel flow speed is absent from Eqs. (4.35)-(4.39) not because $u_\parallel (\sim u_\perp)$ is presumed small, but because of scale-length separation, Eq. (4.8). In fact, $u_\parallel$ evolves without affecting ψ,φ or p

[35]. Similarly, the transverse vector potential is not presumed small: $\mathscr{A}_\perp \sim \psi$. Rather, $\mathscr{A}_\perp$ is eliminated from the final system by means of lowest order force balance (equilibration of compressional Alfvén waves) as in Eq. (3.13) or (4.20).

It is instructive to examine the reduced MHD equilibrium. Considering first Eq. (4.36), we set

$$\varphi_0 = 0$$

but retain, temporarily, $\partial/\partial\tau$. Then

$$\frac{\partial\psi_0}{\partial\tau} = \eta\nabla_\perp^2\psi_0 \ ,$$

an equation describing resistive diffusion of the poloidal field. The relevant time scale is evidently the skin time of Eq. (4.34), which is very long ($\tau_s \sim 1$ sec.) under experimental conditions of interest. In studying instability, one ignores such slow variation and neglects $\partial\psi_0/\partial\tau$.

Observe next that the reduced energy conservation law becomes empty in the equilibrium state. The reason is that equilibrium pressure is controlled by processes faster than shear-Alfvén dynamics and therefore missing from the reduced system. The relevant constraint is familiar and obtained from, for example, Eq. (4.18): $\underset{\sim}{B}_0\cdot\nabla p_0 = 0$. We use Eq. (4.22), assuming an axisymmetric equilibrium, to infer that $[p_0,\psi_0] = 0$, or

$$p_0 = p_0(\psi_0) \ , \qquad (4.43)$$

a reduced version of the general equilibrium result.

Upon substituting Eq. (4.43) into the equilibrium version of Eq. (4.35),

$$[\psi_0, J_0] - [x, p_0] = 0 \ ,$$

we obtain

$$[\psi_0, \ J_0 + x p_0'] = 0 \ , \tag{4.44}$$

where $p_0' = dp_0/d\psi_0$ and we used the identity

$$[f, g(\psi_0)] = g'[f, \psi_0]$$

for any functions $f(\underset{\sim}{x})$ and $g(\psi_0)$. Equation (4.44) implies that $J_0 + 2xp_0'$ is an arbitrary function of ψ_0 and thus yields the reduced Grad-Shafranov equation

$$\nabla_\perp^2 \psi_0 = -x p_0' + F(\psi_0) \ . \tag{4.45}$$

Since $ax = R-R_0$, this result is related to the exact version, Eq. (2.105), in an obvious way. It also shows explicitly why the normalized minor radius, r, cannot label equilibrium flux surfaces. In fact, a solution of the form $\psi_0(x,y) = \psi_0(r)$ is permitted only when p_0' is neglected, as in the low-beta case. Equations (4.43) and (4.45) are the essential results of reduced equilibrium theory.

Finally, we comment upon the integral invariants of reduced MHD. Most of these are derived from the identities

$$\int d\underset{\sim}{x} f[g,h] = \int d\underset{\sim}{x} g[h,f] = \int d\underset{\sim}{x} h[f,g] \ , \tag{4.46}$$

which follow from Eq. (4.40), provided surface contributions are neglected. Here, f,g and h are arbitrary functions and $d\underset{\sim}{x} = dxdydz$. A corollary is

$$\int d\underset{\sim}{x}[f,g] = 0 \ ,$$

which, in view of Eq. (4.35), implies vorticity conservation:

$$\frac{d}{d\tau} \int d\underset{\sim}{x} \ U = 0 \ .$$

The energy invariant is perhaps most interesting. We multiply Eq. (4.35) by φ, Eq. (4.36) by J, add the results and integrate. Because of Eq. (4.46), the result is

$$\int d\underset{\sim}{x}\{\varphi \frac{\partial U}{\partial \tau} + J \frac{\partial \psi}{\partial \tau} + x[p,\varphi]\} = \int d\underset{\sim}{x} \ \eta J^2 \ .$$

Here, $[p,\varphi]$ can be eliminated by means of Eq. (4.37), while the first two terms in brackets are simplified by partial integration. Thus we find

$$\frac{\partial}{\partial \tau} \frac{1}{2} \int d\underset{\sim}{x}\{|\nabla_\perp \varphi|^2 + |\nabla_\perp \psi|^2 - 2xp\} = -\int d\underset{\sim}{x} \ \eta J^2 \ , \tag{4.47}$$

showing that the sum of kinetic, magnetic and interchange energy changes at the rate prescribed by Ohmic dissipation.

A survey of reduced MHD invariants is provided elsewhere [37].

C. Generalizations of Reduced MHD

1. Introduction

We have already noted that reduced MHD accounts for tokamak curvature rather crudely. For example, it omits cylindrical curvature terms, resulting from the poloidal component of $\underset{\sim}{B}$. Such weaknesses result solely from the aspect ratio expansion and can be remedied by the inclusion of higher order terms [38,39]. Other physical deficiencies of the model are not related to reduction but reside in MHD itself. For example, MHD assumes the perpendicular plasma velocity to be approximated by the $\underset{\sim}{E}\times\underset{\sim}{B}$ drift velocity, as in Eq. (4.26). This assumption can be justified only if $\underset{\sim}{V}_E$ is quite large,

$$V_E \sim v_{th_i} , \tag{4.48}$$

[we use the notation $v_{th_s} \equiv (2T_s/m_s)^{1/2}$ for the thermal speed of species s]. Most observed plasma motions are considerably slower.

Such MHD simplifications as Eq. (4.26) are sometimes justified as describing the small gyroradius limit,

$$k\rho_i \ll 1 , \tag{4.49}$$

where k is the wavenumber, and

$$\rho_i = v_{th_i}/\Omega_i$$

measures a typical ion gyroradius ($\Omega_s \equiv eB/m_s c$). In fact, the actual justification for MHD is more complicated, for two reasons. First, certain critical MHD assumptions involve parallel dynamics and therefore are not related to gyration. Second, even for the perpendicular dynamics, Eq. (4.49) does not imply Eq. (4.26). One must additionally assume that the motions of interest are fast, both in the sense of Eq. (4.48) and in the sense that

$$\omega \sim \omega_{MHD} \sim (k\rho_i)\Omega \ . \tag{4.50}$$

Here ω represents a frequency of interest and ω_{MHD} can be estimated by

$$\omega_{MHD} \sim k\left(v_{th_i}^2 + v_A^2\right)^{1/2} \ .$$

Both Eqs. (4.48) and (4.50) are applicable in certain circumstances (such as tokamak disruption), but neither is appropriate for describing a wide class of observed and potentially dangerous perturbations. The latter are roughly described by Eq. (4.49), with

$$V \sim (k\rho_i)v_{th_i} \tag{4.51}$$

and

$$\omega \sim (k\rho_i)\omega_{MHD} \ . \tag{4.52}$$

The MHD simplification of <u>parallel</u> dynamics mainly concerns electron motion. It is best appreciated in terms of Eq. (4.30):

$$J_{\parallel} = \sigma_s E_{\parallel} \ . \tag{4.53}$$

Here $\sigma_s = 1/\eta_{\parallel}$ is the conductivity first calculated by Spitzer and Härm [40],

$$\sigma_s \simeq 2e^2 n/(\nu_e m_e) \ , \tag{4.54}$$

where $\nu_e \propto nT_e^{-3/2}$ is the electron collision frequency. The point is that Eq. (4.53) is derived from a mild generalization of the Chapman–Enskog procedure, neglecting time variation of the fields and, most importantly, assuming that the collisional mean free path,

$$\lambda_{mfp} \equiv v_{the}/\nu_e$$

is shorter than other scale lengths of interest. In other words, σ_s is a "D–C" conductivity, whose accuracy requires

$$\omega \ll \nu_e \tag{4.55}$$

$$k_{\parallel}\lambda_{mfp} \ll 1 \ . \tag{4.56}$$

Notice that Eqs. (4.55) and (4.56) provide two distinct measures of collisionality. Experimentally observed modes often satisfy Eq. (4.55), while contradicting Eq. (4.56) everywhere except in a small neighborhood of some rational surface: the long mean-free-path conductivity is typically more pertinent than σ_s.

A generalized conductivity, $\sigma_*(\nu,\omega,k_\parallel v_{the})$, would satisfy

$$\sigma_*(\nu,0,0) = \sigma_S \ , \tag{4.57}$$

but would also describe the electron response for larger frequency and shorter wavelengths. We shall see that σ_* can be calculated, at least approximately, and that at appreciable distances from the rational surface,

$$\sigma_* << \sigma_S \ .$$

In this "A–C" sense, even a very hot plasma can be a poor conductor – a fact which has important consequences.

A third weakness of reduced MHD is its effective incompressibility. This simplification results from reduction, rather than from MHD, but it appears potentially more serious than the purely geometrical simplifications mentioned previously. The point is that the right–hand side of Eq. (4.31), while formally small, includes terms having a special qualitative importance. For example, in linear boundary layer theory, the order of the closed differential system changes (from fourth order to sixth) when certain compressibility terms are retained.

In summary, the various dynamical simplifications of reduced MHD are physically consistent only in certain circumstances (large V, large ν, etc.) which do not always correspond to experiment. Generalizations of the model, describing a wider class of disturbances, are the subject of the present section. Specifically, we replace the reduced MHD

closure scheme by one which is more complicated but more generally credible.

It is appropriate to emphasize here that reduced MHD was constructed for the purpose of studying nonlinear phenomena. Because it does this well, as noted in Sec. A, criticism of the model's linear predictions can be misleading. Physical plasmas rarely evolve according to linear theory.

It should also be emphasized that the four-field model, a generalization of reduced MHD summarized in Subsection 4, has its own limitations. The four-field model is introduced for mainly pedagogical reasons: it displays several physical effects of current interest in conveniently simplified form. It is also representative of a number of recently constructed nonlinear fluid models which attempt to extend reduced MHD [41-44]. As experimental plasmas enter higher temperature regimes, some such extension is likely to become as valuable as reduced MHD.

2. Electron Kinetic Theory

This subsection is concerned with a kinetic description of the electron response. Our main purpose is to review some of the methods and approximations commonly used in kinetic theory. Furthermore our result, a generalized linear conductivity σ_*, provides instructive contrast with fluid model result obtained in Subsection 4. We derive here only the very simplest version of σ_*; the kinetic equation is solved essentially by a sequence of ever cruder approximations. However, we attempt to indicate the physical effects which each approximation omits.

The kinetic theory is obtained from the Boltzmann equation for the distribution function $f_s(\underset{\sim}{x},\underset{\sim}{v},t)$:

$$\frac{\partial f_s}{\partial t} + \underset{\sim}{v}\cdot\nabla f_s + \frac{q_s}{m_s}\left(\underset{\sim}{E} + \frac{1}{c}\,\underset{\sim}{v}\times\underset{\sim}{B}\right)\cdot\frac{\partial f_s}{\partial \underset{\sim}{v}} = C_s \qquad (4.58)$$

where s is the species label (i or e) and

$$C_s = \sum_{s'} C_{ss'}(f_s, f_{s'})$$

represents Coulomb collisions, due to both like ($s'=s$) and unlike ($s'\neq s$) species. We assume that $C_{ss'}$ is bilinear in its arguments. It is best represented in Fokker–Planck form, but often, as below, more crudely simplified. The electron kinetic equation can be simplified using the fact that

$$\rho_e \equiv v_{the}/\Omega_e \ ,$$

the thermal electron gyroradius, is typically small compared to both the equilibrium scale length, a, and the perturbation scale length, k^{-1}(or w). It is convenient to indicate both small ratios by the same symbol:

$$\delta_e \sim (k\rho_e,\ \rho_e/a) \ll 1 \ . \qquad (4.59)$$

Small δ_e permits a description of electron motion in which the details of Larmor gyratron are averaged out [45,46].

This contracted description, the "drift kinetic" equation, is obtained by defining a gyro-averaged distribution function $f_{gc}(\underset{\sim}{x},\mu,K,t)$, where

$$\mu = v_\perp^2/2B \tag{4.60}$$

is the magnetic moment and

$$K = v^2/2 \tag{4.61}$$

measures the kinetic energy. The third velocity coordinate is the gyrophase, φ_g, where

$$\underset{\sim}{v} = \underset{\sim}{b}v_\parallel + |v_\perp|(\underset{\sim}{e}_2\cos\varphi_g + \underset{\sim}{e}_3\sin\varphi_g) \ . \tag{4.62}$$

Here $\underset{\sim}{e}_2$ and $\underset{\sim}{e}_3$ are unit vectors chosen such that $(\underset{\sim}{b},\underset{\sim}{e}_2,\underset{\sim}{e}_3)$ forms a right-handed triplet. The gyro-averaged distribution is

$$f_{gc} = \frac{1}{2\pi}\oint d\varphi_g f \ , \tag{4.63}$$

where the integral is performed at fixed $\underset{\sim}{x}$, μ and K. Thus

$$f(\underset{\sim}{x},\mu,K,\varphi_g) = f_{gc}(\underset{\sim}{x},\mu,K) + \tilde{f}(\underset{\sim}{x},\mu,K,\varphi_g) \ , \tag{4.64}$$

where $\tilde{f}$, which is relatively small,

$$|\tilde{f}/f_{gc}| = O(\delta_e) \ ,$$

describes Larmor gyration.

The perturbation expansion of the kinetic equation proceeds by noting that

$$(e/mc)\underset{\sim}{v}\times\underset{\sim}{B}\cdot\partial f/\partial\underset{\sim}{v} \simeq \Omega\partial\tilde{f}/\partial\varphi_g \ ,$$

is the largest term in the equation for $\tilde{f}$. Equation (4.58) can be solved perturbatively for $\tilde{f}$ in terms of f_{gc}. The drift kinetic equation is then obtained by the gyrophase average of Eq. (4.58), noting that $\tilde{f}(f_{gc})$ contributes due to the phase dependence of $\underset{\sim}{v}$.

A mildly simplified version of the drift-kinetic equation is given by

$$\left(\frac{\partial}{\partial t} + \underset{\sim}{v}_{gc}\cdot\nabla\right)f_{gc} - \frac{e}{m}\,\underset{\sim}{v}_{gc}\cdot\underset{\sim}{E}\,\frac{\partial f_{gc}}{\partial K} = C \ . \tag{4.65}$$

Here

$$\underset{\sim}{v}_{gc} = \underset{\sim}{b}v_{\|} + \underset{\sim}{v}_D$$

where

$$v_{\|} = \pm\ [2(K-\mu B)]^{1/2} \tag{4.66}$$

is the parallel speed and

$$\underset{\sim}{v}_D \equiv \underset{\sim}{b}\times(e\nabla\Phi/m + \mu\nabla B + v_{\|}^2\underset{\sim}{\kappa})/\Omega \tag{4.67}$$

is the guiding center drift. We have suppressed the species subscript

while choosing the sign of the charge, $q_e = -e$ to correspond to electrons.

The form of Eq. (4.65) is easily understood. Its first two terms have an obvious interpretation, while the third term simply measures the rate of change of guiding-center kinetic energy:

$$dK/dt = -(e/m)\underset{\sim}{v}_{gc}\cdot\underset{\sim}{E} \ .$$

Furthermore, the analogous term for the magnetic moment has been neglected since μ is an adiabatic invariant: $\dot{\mu} \approx 0$.

When the small δ_s approximation is not valid, as is more typically the case for ions, a much more complicated analysis is necessary. For this case the particle position $\underset{\sim}{x}$, is expanded about the position of the guiding center, $\underset{\sim}{x}_{gc}$. The resulting theory gives the gyrokinetic equation [47]. We consider the ions in Subsection 3, employing a fluid theory to obtain finite δ_i corrections. In this section we henceforth restrict the analysis to the electrons.

Several approximations will be used in the solution of Eq. (4.65). First notice that the function $v_{\|}$, given by Eq. (4.66) can vanish on a trajectory when $\mu B_{max} \geq K$ where B_{max} represents the maximum value of B along a chosen field line. In this case the electrons are "trapped" in regions of smaller B.

Trapping effects complicate the electron response in a manner which remains incompletely understood. With a few exceptions [48,49], studies of electron trapping have been restricted to the electrostatic case, associated with trapped-particle-destabilized drift waves, which have been reviewed elsewhere [50,51]. We restrict our attention to the

far-untrapped particles ($K >> \mu B_{max}$) in a large aspect-ratio tokamak. Since $|B-B_{max}| \sim \varepsilon$ in this case, untrapped particles form the bulk of the population and $v_\parallel$ becomes an approximate spatial constant. With this approximation the variable K in f_{gc} can be replaced by $v_\parallel$: $f_{gc}(\underset{\sim}{x}, v_\parallel, \mu)$.

A second approximation relates to the drift velocity, Eq. (4.67). The magnitudes of the ∇B and curvature drift relative to the $\underset{\sim}{E}\times\underset{\sim}{B}$ drift can be obtained by using the large aspect ratio ordering. Thus with $\mu\nabla B \sim v_\parallel^2 \underset{\sim}{\kappa} \sim v_{the}^2(\varepsilon/a)$ and taking $e\Phi/T_e \sim 1$ we have

$$\frac{\mu\nabla B}{e\nabla\Phi/m} \sim \varepsilon \ .$$

Therefore, we let

$$v_D \simeq \frac{e}{m}\, \underset{\sim}{b}\times\nabla\Phi \ .$$

A final simplification of the drift kinetic equation results from replacing the full collision operator by the simple Krook model [52]:

$$C(g) = -\nu(g - n_g f_M/n) \tag{4.68}$$

where

$$n_g \equiv \int d^3v g \ ,$$

g denotes an arbitrary distribution, and f_M denotes a Maxwellian distribution with density n:

$$f_M = n/(\pi^{3/2}v_{th}^3)\exp(-mK/T) \quad . \tag{4.69}$$

The collision frequency $\nu \approx \nu_e$ is presumed to be constant. Of course, the Maxwellian term is appended to ensure particle conservation,

$$\int d^3v\ C(g) = 0 \quad .$$

Equation (4.68) is obviously rather crude. It fails to conserve energy, omits velocity-space diffusion, and so on. Such weaknesses are critical in certain applications, including trapped-particle effects (which can depend upon collisional smoothing of velocity-space boundary layers [48]) and certain temperature-gradient-driven instabilities [53]. More commonly, however, the simple Krook model yields stability predictions in qualitative accord with those obtained from more accurate, and much more complicated, collision operators.

The equilibrium solutions to the drift kinetic equation are obtained by neglecting Φ and time derivatives giving

$$v_\parallel \underset{\sim}{b}_0 \cdot \nabla f_0 = C(f_0) \tag{4.70}$$

which is solved by the Maxwellian, Eq. (4.69), providing $\underset{\sim}{b}\cdot\nabla f_M = 0$. Since

$$\nabla f_M = f_M[\nabla \ell n\ n_0 + (\frac{mK}{T} - \frac{3}{2})\nabla \ell nT] \tag{4.71}$$

we see that the equilibrium density and temperature must be flux labels:

$$n = n(\chi) \quad , \quad T = T(\chi) \ .$$

Of course, since Eq. (4.70) is valid only to $O(\delta_e)$, there are corrections to f_M of this order. These corrections are calculated in neoclassical transport theory [54], and can affect the stability of certain perturbations, but are rarely of critical importance. We ignore the corrections here.

Linearization of the drift kinetic equation about this equilibrium is accomplished by letting

$$f = f_0 + f_1 \ ,$$

$$\underset{\sim}{B} = \underset{\sim}{B}_0 + \underset{\sim}{B}_1 \ ,$$

$$\Phi = \Phi_1 \ .$$

The perturbed distribution satisfies

$$\mathscr{L}_0 \, f_1 = -\underset{\sim}{v}_1 \cdot \nabla f_0 + \frac{e}{m} \, v_\parallel \underset{\sim}{b}_0 \cdot \underset{\sim}{E}_1 \, \frac{\partial f_0}{\partial K} \tag{4.72}$$

where

$$\mathscr{L}_0 = \frac{\partial}{\partial t} + v_\parallel \underset{\sim}{b}_0 \cdot \nabla - C \tag{4.73}$$

$$\underset{\sim}{v}_1 = \underset{\sim}{b}_1 v_\parallel + \frac{e}{m} \, \underset{\sim}{b}_0 \times \nabla \Phi_1 \ , \tag{4.74}$$

It is customary to write

$$f_1 = -\frac{e}{m}\frac{\partial f_0}{\partial K}\Phi_1 + g_1 \ .$$

Using the Maxwellian equilibrium we see that this becomes

$$f_1 = f_0\, e\Phi_1/T_e + g_1 \ . \tag{4.75}$$

Here the first term can be recognized as a linearized Maxwell–Boltzmann factor, $\exp(e\Phi/T)$; it corresponds to electron equilibrium in an electrostatic field. In fact, if we neglect $\underset{\sim}{A}_1$ in Eq. (4.72), and assume

$$\frac{\partial}{\partial t} \ll v_\parallel \underset{\sim}{b}\cdot\nabla \ , \tag{4.76}$$

then $f_1 = f_0\, e\Phi_1/T$ becomes an approximate solution. Equation (4.76) allows electrons to sample the parallel structure of the perturbed potential before the latter changes appreciably. Thus the Maxwell–Boltzmann term is said to describe "adiabatic" electrons, and Eq. (4.76) is referred to as the adiabatic limit. Here we note that, aside from omitting electromagnetic terms, Eq. (4.76) will clearly break down in the vicinity of a mode–rational surface. Substituting the decomposition of Eq. (4.75) into the linearized drift kinetic equation (4.72) gives

$$\mathscr{L}_0 g_1 = Q$$

$$Q = -\frac{e}{T} f_0 \frac{\partial}{\partial t}\left(\Phi_1 - \frac{v_\parallel}{c}\,\underset{\sim}{b}_0\cdot\underset{\sim}{A}_1\right) - \underset{\sim}{v}_1\cdot\nabla f_0 \tag{4.77}$$

where we have used $\underset{\sim}{b}_0 \cdot \nabla f_0 = 0$ and $C(\mathcal{P}_1 f_0) = 0$.

Consider first the inversion of the operator $\mathscr{L}_0$. For constant $v_\parallel$, it is permissible to write

$$g_1 = \exp(i\omega t + im\vartheta - i\ell\zeta)\hat{g}(\chi,\mu,K) \tag{4.78}$$

in terms of flux coordinates (χ,ϑ,ζ). [Note that such a Fourier representation would not be valid in the trapped region, where only a limited range of ϑ is accessible]. Then, from Eqs. (4.73) and (4.78), we easily find that

$$\mathscr{L}_0 g_1 = [-i(\omega - k_\parallel v_\parallel) - C]\hat{g} \tag{4.79}$$

where

$$k_\parallel \equiv (m - \ell q)/(\sqrt{g}B)$$

and the eikonal factor is suppressed.

Equation (4.79) displays the competition between oscillation (or growth), parallel streaming, and collisions which was discussed in Subsection 1. Furthermore, the familiar resonance, $\omega = k_\parallel v_\parallel$, associated with parallel Landau damping is explicit. As we will see below, the most important aspect of $\mathscr{L}_0$ is neither the detailed form of the collision operator nor the possibility of Landau resonance. What matters, rather, is the radial variation of $\mathscr{L}_0$ associated with the rational flux surfaces.

Inversion of the operator $\mathscr{L}_0$ has become trivial. From Eq. (4.68) and (4.79) we obtain

$$g_1 = i \frac{(Q+\nu n_g f_M/n)}{\omega - k_\parallel v_\parallel + i\nu} \tag{4.80}$$

We integrate to eliminate n_g, noting that

$$\int \frac{d^3v \; f_M}{\omega - k_\parallel v_\parallel + i\nu} = - \frac{n}{|k_\parallel| v_{th}} Z(z) \; . \tag{4.81}$$

Here

$$z = (\omega + i\nu)/(|k_\parallel| v_{th}) \tag{4.82}$$

and Z is the plasma dispersion function [55]. For

$$\mathrm{Im}(z) > 0 \; , \tag{4.83}$$

we have

$$Z(z) = \pi^{-1/2} \int_{-\infty}^{\infty} \frac{dt \; e^{-t^2}}{t - z} \; . \tag{4.84}$$

Recall that Z(z) is defined for $\mathrm{Im}(z) < 0$ by analytic continuation of Eq. (4.84). The absolute value appearing in Eqs. (4.81) and (4.82) is occasioned by Eq. (4.83). Thus we find

$$\left[1 + \frac{i\nu}{|k_\parallel| v_{th}} Z(z)\right] n_g = i \int \frac{d^3v\ Q}{\omega - k_\parallel v_\parallel + i\nu} \ . \tag{4.85}$$

Our immediate objective is to compute the electron parallel flow

$$nV_{\parallel e} = \int d^3v\ v_\parallel f = \int d^3v\ v_\parallel g_1$$

which, from Eq. (4.75), resides entirely in the function g_1. Equation (4.80) allows this moment to be evaluated directly, but a more efficient procedure uses the velocity integral of Eq. (4.72): the particle conservation law,

$$-ik_\parallel\ nV_{\parallel e} = i\omega n_g + \int d^3v\ Q \ . \tag{4.86}$$

Thus the desired flow is determined by Eq. (4.85) alone.

Turning our attention to the source term, Q, we note that since $\nabla f_0 = \nabla\chi\ \partial f_0/\partial\chi$, only the parallel component of the vector potential, which we write as $A_1 = \underset{\sim}{b}_0 \cdot \underset{\sim}{A}_1$, is required. The eikonal form allows us to express the source term, Eq. (4.77), as

$$\hat{Q} = i(e/T) f_M (\omega - \omega_*) \left[\hat{\Phi}_1 - (v_\parallel/c)\hat{A}_1\right] \ , \tag{4.87}$$

where

$$\omega_* = \Omega^{-1} \frac{(\partial f_0/\partial\chi)}{(\partial f_0/\partial K)} \left(\frac{\ell B_\vartheta + mB_\zeta}{\sqrt{g}B}\right) \tag{4.88}$$

is the so-called drift frequency. The form of Eq. (4.88) depends upon

neglecting the ∇B and curvature drifts. Notice that B_ϑ and B_ζ are covariant components of $\underset{\sim}{B}$. It is easy to see from Eq. (2.80) that

$$B_\vartheta + qB_\zeta = \sqrt{g}\, B^2$$

for any flux coordinates. Hence we find that

$$\omega_* = -\frac{\ell T c}{e}\frac{\partial \ell n f_0}{\partial \chi}\left[1 - \frac{B_T^2}{B^2}\left(1 - \frac{m}{\ell q}\right)\right] \tag{4.89}$$

with $B_T^2 = B_\zeta B^\zeta$.

It is clear from Eq. (4.87) that the dispersion relations for a variety of perturbations will involve ω_* and its ion counterpart in a prominent way. In fact,

$$\mathrm{Re}(\omega) \sim \omega_* \sim k_\perp \rho_e v_{the}/a \tag{4.90}$$

is appropriate for many modes of interest. The occurrence of ω_* is sometimes ascribed to diamagnetic rotation,

$$(nV_D)_s \equiv (m_s \Omega_s)^{-1}\, \underset{\sim}{b}\times\nabla P_s \ ,$$

where s is a species label. The point is that for

$$\nabla T = 0 \ ,$$

one finds

$$\omega_{*s} = \underset{\sim}{k}_{\perp} \cdot \underset{\sim}{V}_{Ds} \tag{4.91}$$

so that $(\omega-\omega_*)$-factors appear to reflect a simple Doppler shift. Here we emphasize that Eq. (4.91) holds only in the isothermal case. In the presence of temperature gradients, Eq. (4.71) shows that ω_* depends upon particle energy. Even its Maxwellian average fails to satisfy Eq. (4.91), because

$$\int d^3v \; f_M \left(\frac{mK}{T} - \frac{3}{2}\right) = 0 \; .$$

Thus, while ω_*-terms often correspond to mode-rotation, they do not in general reflect bulk plasma motion. Because of the change in sign of $\partial f_M/\partial\chi$ occurring at $K = 3T_s/2m_s$, temperature gradients can modify the electron response in subtle but important ways [53,56-58]. We avoid these complications by now assuming

$$dT/d\chi = 0 \; .$$

Constant ω_* makes evaluation of the integrals in Eqs. (4.85) and (4.86) especially straightforward. One finds, after simple manipulation, that

$$V_{\parallel e} = \frac{ieE_\parallel}{T} \frac{(\omega-\omega_*)}{k_\parallel^2} \frac{1+zZ(z)}{1 + \dfrac{i\nu}{|k_\parallel| v_{the}} Z(z)} \; , \tag{4.92}$$

where

$$E_{\parallel} = i\left(\frac{\omega}{c} A_1 - k_{\parallel}\Phi_1\right) \tag{4.93}$$

is the parallel electric field perturbation and circumflexes are suppressed.

A noteworthy feature of Eq. (4.92) is that the parallel flow depends upon A_1 and Φ_1 only through $E_{\parallel}$. This circumstance, which is unsurprising on physical grounds, survives both the inclusion of temperature gradients and the use of more realistic collision operators [53,58]. However, it does depend on our neglect of non-Maxwellian corrections to f_0.

The most important feature of Eq. (4.91) is the strong radial dependence of the electron response, resulting from the $k_{\parallel}$ dependence of z, Eq. (4.82). Near the rational surface, that is for

$$k_{\parallel} v_{the} \ll \omega, \nu \tag{4.94}$$

we have $z \gg 1$ and it is easily seen that

$$\frac{1+zZ}{1 + \frac{i\nu}{|k_{\parallel}| v_{the}} Z} \rightarrow -\frac{1}{2} \frac{(k_{\parallel} v_{the})^2}{\omega(\omega+i\nu)} \quad , \quad z \gg 1 \ . \tag{4.95}$$

Hence the parallel velocity becomes

$$V_{\parallel e} \simeq -i \frac{eE_{\parallel}}{m_e} \frac{\omega-\omega_*}{\omega(\omega+i\nu)} \ . \tag{4.96}$$

On the other hand, when $k_\parallel$ is large so that the inequality is reversed, one finds that

$$\frac{1+zZ}{1+i\nu Z/(|k_\parallel| v_{the})} = 1 + O(k_\parallel^{-1}) \ , \tag{4.97}$$

whence

$$V_{\parallel e} \cong \frac{ieE_\parallel}{T_e} \frac{(\omega-\omega_*)}{k_\parallel^2} \tag{4.98}$$

which is relatively small.

The parallel current density is given by

$$J_\parallel = en(V_{\parallel i}-V_{\parallel e}) \ , \tag{4.99}$$

and therefore requires the ion as well as the electron velocity. For sufficiently small $k\rho_i$, $nV_{\parallel i}$ is given by the obvious modification of Eq. (4.92): $e \to -e$, $v_{the} \to v_{thi}$, etc.. In particular, the argument of the z-function becomes

$$z_i \equiv \frac{\omega+i\nu_i}{|k_\parallel| v_{thi}} \ ,$$

where ν_i is the ion collision frequency. Because

$$\nu_i \sim (m_e/m_i)^{1/2} \nu_e \ ,$$

it is frequently omitted. In any case, we see that (for $T_i \sim T_e$),

$$z_i \sim (m_i/m_e)^{1/2} z$$

and therefore $z_i \gg 1$ unless z is very small. It follows that $V_{\parallel i}$ is typically approximated by the large $-z_i$ limit, as in Eq. (4.96):

$$V_{\parallel i} \simeq i \frac{eE_\parallel}{m_i} \frac{(\omega-\omega_{*i})}{\omega^2} \ll V_{\parallel e} \ . \tag{4.100}$$

The inequality (4.100) simply expresses the relatively large ion inertia. It is often used to neglect $V_{\parallel i}$ in Eq. (4.99), and we do so below. Notice, however, that for sufficiently large $k_\parallel$, the response becomes independent of mass, as in Eq. (4.98). Therefore perturbations with sufficient radial width, such as electrostatic drift waves [50], as well as certain nearly collisionless tearing instabilities [59] can be strongly affected by $V_{\parallel i}$.

Equations (4.92), (4.99) and (4.100) may be combined to form a generalized Ohm's law, Eq. (4.53), where

$$\sigma_* = -i \frac{ne^2}{T} \frac{(\omega-\omega_*)}{k_\parallel^2} \frac{1+zZ(z)}{1+i\nu Z(z)/(|k_\parallel| v_{the})} \ . \tag{4.101}$$

While the generalized conductivity depends upon radial position through such slowly-varying quantities as ω_*, T and ν, its strongest and most important radial dependence occurs through $k_\parallel^{-2}$ and $z \propto |k_\parallel|^{-1}$. In fact, z varies markedly over distances shorter than the rational

surface spacing, which is much smaller than the equilibrium scale length. To see this, we use Eqs. (2.66), (2.67) and (4.79) to estimate

$$k_{\parallel} \sim (\sqrt{g}B)^{-1} \sim (qR)^{-1} .$$

If we assume that $\omega \sim \omega_*$, then Eq. (4.90) yields

$$\frac{\omega}{k_{\parallel} v_{the}} \sim \frac{qR}{a} (k_{\perp}\rho_e) .$$

The right-hand side of this equation is typically very small ($k_{\perp}\rho_e \sim m\times 10^{-4}$ in conventional devices, and m-values larger than about 10^2 are rarely of interest). Furthermore, while the collision frequency often exceeds ω, for many important modes it does so only moderately. Thus we conclude that, typically, the variable z ranges from infinity at the rational surface to a value $z \ll 1$ at distances comparable to the surface spacing. In studying boundary-layer modes, it is therefore appropriate to evaluate all slowly varying quantities at the mode-rational surface. The main result is to simplify Eq. (4.89), which becomes

$$\omega_* \cong - \frac{\ell T_c}{e} \frac{\partial \ell n f_0}{\partial \chi}$$

for $q \approx m/\ell$.

The strong radial variation is usually simplified by assuming that $k_{\parallel}(\chi) = k_{\parallel}(\chi_{m\ell}+x)$ [cf. Eq. (3.48)] is approximately linear in x near $\chi_{m\ell}$:

$$k_{\parallel} = k_{\parallel}' \, x \ , \tag{4.102}$$

with $k_{\parallel}' = \text{const.}$. This assumption requires q to be locally linear, and will break down when the rational surface nearly coincides with an extremum of q,

$$\partial q/\partial \chi \Big|_{\chi_{m\ell}} \simeq 0 \ . \tag{4.103}$$

Equation (4.103) pertains in the presence of a locally peaked current density ("skin current") as usually characterizes the initial phase of an Ohmically heated tokamak discharge. Boundary layer modes associates with skin currents have been studied [60] but will not be reviewed here. With Eq. (4.102) we have

$$z = (\omega + i\nu)/(|k_{\parallel}' x| v_{the}) \ , \tag{4.104}$$

and σ_* is evidently an even function of x:

$$\sigma_*(-x) = \sigma_*(x) \ .$$

This property significantly simplifies boundary-layer analysis.

Notice that $x = \chi - \chi_{m\ell}$ is defined to have units of magnetic flux, and the prime in Eq. (4.104) stands for $\partial/\partial\chi$. However, we could just as well interpret the prime as an ordinary radial derivative, $\partial/\partial r$, in which case x has units of length. Hereafter, we consider x to be a length, for convenience.

The distance

$$x_e \equiv |\omega|/(|k_\parallel'|v_{the}) \tag{4.105}$$

corresponds to parallel Landau resonance of a thermal electron (unless ν is much larger than ω, x_e defines the scale length for variation of σ_*). When $|x| << x_e$, $z >> 1$ and Eq. (4.95) becomes valid: well inside the electron Landau resonance,

$$\sigma_* \cong \sigma_{*o} \equiv \frac{e^2 n}{m_e \nu} \frac{\omega - \omega_*}{\omega(1 - i\omega/\nu)} \ . \tag{4.106}$$

In the special case defined by

$$\omega_* << |\omega| << \nu \ , \tag{4.107}$$

Equation (4.106) becomes

$$\sigma_{*o} \cong \frac{e^2 n}{m_e \nu} \tag{4.108}$$

which should be compared with Eq. (4.54). Aside from an ill-defined numerical factor (associated with our use of a Krook model), we see that σ_* reproduces the Spitzer result in this limit: we have confirmed Eq. (4.57). Notice that it was necessary to assume both large collisionality, in the sense of Eqs. (4.55)-(4.56), and high-frequency, in the sense of Eq. (4.50).

Equation (4.90) shows that x_e is very short,

$$x_e \sim \frac{k_\perp}{k_\parallel'} \frac{\rho_e}{a} \ll a \ . \tag{4.109}$$

The ratio, $k_\perp/k_\parallel'$, is often called the shear length and denoted by

$$L_s \equiv |k_\perp/k_\parallel'| \simeq \frac{qR}{r} \frac{q}{q'} \ . \tag{4.110}$$

It is usually larger than a, but by little more than an order of magnitude, so that the ordering (4.109) is strongly satisfied. The "classical" region, $|x| < x_e$, is very narrow indeed.

For $|x| \gg x_e$, the size of z is evidently determined by ν in Eq. (4.104). The collisional term

$$\frac{i\nu}{|k_\parallel' x| v_{the}} = \frac{i}{|k_\parallel \lambda_{mfp}|}$$

measures collisionality in the spatial sense of Eq. (4.56). Recalling that observed modes are rarely so narrow (or so collisional) as to satisfy Eq. (4.56) over the full boundary-layer width, we expect the region in which $|z| \ll 1$ to be important. The corresponding limit of σ_* is denoted by $\sigma_{*\infty}$ and provided by Eq. (4.97),

$$\sigma_{*\infty} = -\frac{ie^2 n}{T_e} \frac{(\omega-\omega_*)}{k_\parallel^2} \ . \tag{4.111}$$

Hence, σ_* becomes small, $O(x^{-2})$, for large x. The ratio

$$\sigma_{*\infty}/\sigma_{*o} = -2\omega(\omega+i\nu)/(k_{\parallel}v_{the})^2 \qquad (4.112)$$

characterizes the gross spatial variation of σ_*. Its relevance to boundary-layer mode stability is made explicit in Chapter V.

These conclusions are somewhat modified when the ion contribution to σ_* is included. We have already noted that the parallel ion flow is negligible for small $|k_{\parallel}|$, so that Eq. (4.106) is not changed. Considering large $|k_{\parallel}|$, however, one finds that Eq. (4.111) describes σ_* only in the range

$$x_e << |x| << x_i \ ,$$

where

$$x_i = \omega/(|k_{\parallel}'|v_{thi}) \ ,$$
$$\sim (m_i/m_e)^{1/2}\, x_e \qquad (4.113)$$

corresponds to ion response. When $|x| > x_i$, the ion response is approximated by Eq. (4.98), with the obvious change in subscripts. However, for certain applications it is also necessary to retain finite gyroradius corrections to $V_{\parallel i}$. The point can be seen from Eq. (4.35): $V_{\parallel}J_{\parallel}$ contains terms involving perpendicular inertia (acceleration), which are omitted from Eq. (4.98) because they enter kinetic theory, through the "polarization drift", in higher δ-order [61]. The small mass ratio makes inertia irrelevant for electrons, and relevant to the <u>parallel</u> ion response only when $V_{\parallel i} \sim V_{\parallel e}$, i.e., only when $|x| > x_i$.

The ultimate effect of self-consistently including ion inertia is to replace Eq. (4.111) by

$$\sigma_{*\infty} \simeq \frac{i}{4\pi} \frac{m_e}{m_i} \frac{\omega_{pe}^2}{\omega} , \quad |x| > x_i \tag{4.114}$$

where

$$\omega_{pe} = (4\pi n e^2/m_e)^{1/2}$$

is the plasma frequency. Thus σ_* finally asymptotes to a constant value,

$$\sigma_{*\infty}/\sigma_{*0} = O(m_e/m_i) .$$

Equation (4.114) is implicit, if not always fully accounted for, in kinetic treatments which consider the $|x| > x_i$ region (see, for example, [56]). It is derived from fluid theory in the following subsection.

That σ_* becomes very small at sufficiently large $|x|$ could have been anticipated from Eq. (4.72); the important x-dependence of g resides in $\mathscr{L}_0^{-1}$. The main point is that, for large $|k_\parallel|$, the electron response is predominantly adiabatic. Electrons equilibrate with the perturbed potential, as in Eq. (4.75), with little net parallel flow.

It should be emphasized that the function $\sigma_*(x)$ of Eq. (4.101) has a much richer structure than is suggested by such ratios as Eq. (4.112). In particular, the asymptotics omit the effects of Landau damping, occurring in the radial neighborhood of x_e, which Eq. (4.101)

includes. The point is that Eq. (4.101), despite all its approximations, is a true kinetic result: it includes physics which no analysis of fluid (moment) equations could reproduce. (Closure schemes for moment equations require truncation, and effects of microscopic resonance, $\omega = k_{\parallel} v_{\parallel}$, do not survive truncation.) This property of σ_* makes it a useful standard for comparison with the generalized conductivity computed in the following subsection. The latter uses fluid equations exclusively.

3. Derivation of the four-field model

We derive here a nonlinear fluid model which generalizes reduced MHD, by including physics relevant to regimes of lower collisionality and slower evolution [62]. Our objective is to partially remedy the weaknesses of reduced MHD which were summarized in Subsections 1 and 2. In spirit and derivation, the new model is very similar to reduced MHD. It differs mainly in requiring four (instead of three) field variables: ψ, φ, p_e, and v. Here ψ and φ are the usual potentials, defined by Eqs. (4.11) and (4.14), while p_e and v are given by

$$p_e \equiv \frac{8\pi}{\varepsilon B_c^2} \left(P_e - P_{ec}\right) \tag{4.115}$$

$$v \equiv V_{\parallel i}/(\varepsilon v_A) \tag{4.116}$$

where $P_e = nT_e$ denotes the electron pressure,

$$P_{ec} = n_c T_{ec}$$

is a constant and $V_{\parallel i}$ is the bulk ion flow speed in the direction of $\underset{\sim}{B}$. (The other symbols were defined in Sec. B.) Since the equations of motion involve only ∇P, the constant term in Eq. (4.115) has no direct dynamical significance; it is introduced to allow a certain freedom with regard to ordering, as shall become clear presently.

Besides the additional field, the four-field model involves two new, constant parameters:

$$\beta_e \equiv \frac{8\pi P_{ec}}{B_c^2}$$

and

$$\delta \equiv (2\Omega_c \tau_A)^{-1} \tag{4.117}$$

where

$$\Omega_c \equiv eB_c/(m_i c) \ .$$

The notation in Eq. (4.117) requires some comment. The symbol δ is intentionally reminiscent of the gyroradius parameter, δ_e, of Subsection 2. In fact, terms involving δ will enter the four-field equations as finite gyroradius terms in a conventional sense. However, δ, which is independent of both temperature and magnetic field, clearly does not measure $k\rho \sim k_\perp v_{thi}/\Omega$. In fact, from the definition we find

$$\delta = \frac{1}{2} \frac{c}{\omega_{pi} a}$$

where $\omega_{pi} = (4\pi n_e^2/m_i)^{1/2}$ is the ion plasma frequency.

Notice that, with regard to the formal ε-ordering, factors of a may be identified with $k_\perp^{-1}$ or w,

$$a\nabla \sim \nabla_\perp \sim 1$$

[recall Eq. (4.2)] even when the perturbation scale-length is somewhat shorter than that of the equilibrium. Thus, to allow for a range of perturbation scales, we assume

$$\delta \sim 1 \ . \tag{4.118}$$

With regard to the appropriate β_e-ordering, we observe from the definitions that (for $T_i \sim T_e$)

$$\delta^2\beta_e \sim \rho_i^2/a^2 \sim \rho_i^2\nabla_\perp^2$$

where ρ_i is the ion gyroradius. Hence $\delta^2\beta_e$ is O(1) for disturbances varying over a gyroradius; the corresponding ordering, $\delta \sim \beta_e \sim 1$, yields a rather complicated four-field model containing numerous finite-gyroradius corrections. (Even this model requires $\rho_i\nabla_\perp$ to be somewhat smaller than unity.) Here we are less ambitious, restricting our attention to the small gyroradius case, and therefore assuming $\delta^2\beta_e \sim \varepsilon$. In view of Eq. (4.118), this requires

$$\beta_e \sim \varepsilon \tag{4.119}$$

as in conventional reduced MHD. It is not hard to show that this

ordering, together with Eq. (4.118), is consistent with the low frequency case described by Eqs. (4.51) and (4.52), the importance of which was previously emphasized.

Derivation of the generalized model begins with exact moments of the kinetic equation, Eq. (4.58). The moment equations are truncated by an ansätz concerning the single-species pressure tensor,

$$\underset{\approx}{P}_s \equiv \int d^3v \; f_s m_s \; (\underset{\sim}{v}-\underset{\sim}{V}_s)(\underset{\sim}{v}-\underset{\sim}{V}_s) \; .$$

We assume that

$$\underset{\approx}{P}_s = \underset{\approx}{I} \; P_s + \underset{\approx}{\Pi}_{gs} + O(\varepsilon^3) \tag{4.120}$$

where $\underset{\approx}{I}$ is the unit tensor and $\underset{\approx}{\Pi}_g$ denotes the gyroviscosity tensor, whose form and significance will be considered presently.

A more general truncation would allow, in particular, for anisotropy of the Chew-Goldberger-Low form [17],

$$\underset{\approx}{P} = \underset{\sim\sim}{bb} P_{\parallel} + (\underset{\approx}{I}-\underset{\sim\sim}{bb})P_{\perp} \; .$$

Then trapped-particle effects, as well as parallel Landau resonance, could enter through $(P_{\parallel}-P_{\perp})$. On the other hand, it shall be seen that key features of the kinetic electron response, including those associated with long mean-free-path, survive our simple truncation. Furthermore it can be shown that $(P_{\parallel}-P_{\perp})$ does not enter the reduced shear-Alfvén law.

Equation (4.120) also requires both species to be magnetized, in the sense of Eq. (4.49). In fact, Π_g can be considered as the leading term in an expansion of the pressure tensor in powers of $\rho_i \nabla_\perp$. When ions are barely magnetized with respect to the perturbed fields, the pressure tensor becomes much more complicated and a strictly fluid model is rarely adequate. The gyrokinetic equation, which allows $\rho_i \nabla_\perp \sim 1$, will not be considered here.

Thus Eq. (4.120) differs from the MHD truncation only in retaining gyroviscous terms. Gyroviscosity is an artifact of Larmor gyration: when the mean velocity of guiding centers varies spatially, a momentum flux, perpendicular to the velocity gradient, is induced [63]. This nondissipative flux is independent of collision frequency and measured by

$$\Pi_{gs} \sim \frac{P_s}{\Omega_s} \nabla V_s$$

[see Eq. (4.131), below]. In the MHD case, $V_E >> V_D$, gyroviscosity can be consistently neglected. For slower motions, including those described by Eq. (4.51), gyroviscosity becomes comparable to convective inertia and yields important simplification of the equations of motion.

Our main additional simplification is to neglect temperature gradients:

$$T_s = T_{sc} \ . \tag{4.121}$$

This assumption could be relaxed, without fundamental change in the reduction argument, by increasing the number of field variables and

equations. A reduced fluid theory which emphasizes ∇T_e (with $T_i = 0$) has been constructed [43]. We adopt Eq. (4.121) because the isothermal case has sufficient interest and importance.

Now consider the exact equation of motion,

$$m_s n \frac{d_s \underset{\sim}{V}_s}{dt} + \nabla \cdot \underset{\approx}{P}_s - q_s n(\underset{\sim}{E} + c^{-1} \underset{\sim}{V}_s \times \underset{\sim}{B}) = \underset{\sim}{F}_s \qquad (4.122)$$

i.e., the $m\underset{\sim}{v}$-moment of Eq. (4.58), in which we use the abbreviation,

$$\frac{d_s}{dt} = \frac{\partial}{\partial t} + \underset{\sim}{V}_s \cdot \nabla \ .$$

The quantity F represents the rate of change of collisional momentum exchange ("friction force"),

$$\underset{\sim}{F}_s \equiv \int d^2v \ m_s \underset{\sim}{v} C_s$$

and satisfies $\sum_s \underset{\sim}{F}_s = 0$ or

$$\underset{\sim}{F}_i = -\underset{\sim}{F}_e$$

in the standard case of a single-ion species. It is consistent with Eqs. (4.120) and (4.121) to assume

$$\underset{\sim}{F}_e = en\eta_s \underset{\sim}{J} \qquad (4.123)$$

where $\eta_s = \sigma_s^{-1}$ is the resistivity, which is presumed small,

$$\eta_s = o(\varepsilon) \ .$$

The distinction between $\eta_\perp$ and $\eta_\parallel$ is ignored for simplicity.

The species sum of Eq. (4.122) is given by

$$\underset{\sim}{f} + \nabla P = c^{-1} \underset{\sim}{J} \times \underset{\sim}{B} \tag{4.124}$$

where, in the notation of Chapter III,

$$\underset{\sim}{f} = m_i n \frac{d_i \underset{\sim}{V}_i}{dt} + \underset{\sim}{\nabla} \cdot \underset{\approx}{\Pi}_{gi} + O(m_e/m_i) \ . \tag{4.125}$$

It is clear that the lowest order velocity, $V_i \sim \varepsilon v_A$, contributes $O(\varepsilon^2)$ to $\underset{\sim}{f}$; this lowest order form is sufficient because $O(\varepsilon^3)$ will be neglected. We will find presently that only the lowest order expression for $\underset{\approx}{\Pi}_g$ is needed, for the same reason. However, $\underset{\sim}{V}_i$ is no longer approximated by Eq. (4.26); to compute $\underset{\sim}{V}_i$, we write

$$\underset{\sim}{V}_i = \underset{\sim}{b} V_{\parallel i} + \underset{\sim}{V}_{\perp i}$$

and solve Eq. (4.122) for $V_{\perp i}$. Neglecting $O(\varepsilon^2)$ terms from $\underset{\sim}{f}_i$, $\underset{\sim}{F}_i$ and toroidicity, we obtain the familiar result

$$\underset{\sim}{V}_{\perp i} = \underset{\sim}{V}_E + \underset{\sim}{V}_D + O(\varepsilon^2)$$

where

$$\underset{\sim}{V}_E = (c/B_c) \ \hat{z} \times \nabla \Phi$$

$$\underset{\sim}{V}_D = (T_i/m_i\Omega_c)\hat{z}\times\nabla \ln n \ . \tag{4.126}$$

Alternatively,

$$\underset{\sim}{V}_{\perp i} = \hat{z}\times\nabla\varphi_* \tag{4.127}$$

where

$$\varphi_* = \varepsilon v_A\left(\varphi + \delta\,\frac{\beta_e}{\varepsilon}\,\frac{T_i}{T_e}\,\ln n\right)$$

is a flow potential. Notice that

$$\nabla\cdot\underset{\sim}{V}_i = O(\varepsilon^2)$$

as in reduced MHD.

Returning to Eq. (4.125), and suppressing error terms, we may write

$$\underset{\sim}{f} = m_i n\,\frac{d_i\underset{\sim}{V}_E}{dt} + m_i n\,\frac{d_i\underset{\sim}{V}_\parallel}{dt} + \underset{\sim}{g} \ , \tag{4.128}$$

with

$$\underset{\sim}{g} = m_i n\,\frac{d_i V_D}{dt} + \nabla\cdot\underset{\approx}{\Pi}_{gi} \ .$$

This form for $\underset{\sim}{f}$ is motivated by the following important identity:

$$\underset{\sim}{g}_i = -\nabla\left[(P_i/2\Omega_i)\underset{\sim}{b}\cdot\underset{\sim}{\nabla}\times\underset{\sim}{V}_{\perp i}\right] - \underset{\sim}{b}mn(\underset{\sim}{V}_D\cdot\underset{\sim}{\nabla})V_{\parallel i} + O(\varepsilon^3) \ . \qquad (4.129)$$

Before verifying Eq. (4.129), we comment on its significance. The gradient term in $\underset{\sim}{g}$ evidently provides a small correction to the pressure,

$$P_i \to P_i\left[1 + \frac{\underset{\sim}{b}\cdot\nabla\times\underset{\sim}{V}_{\perp i}}{2\Omega_i}\right] = P_i\left[1 + O(\varepsilon)\right]$$

because $V_{\perp i} = O(\varepsilon)$. It easily follows that lowest order force balance, Eq. (4.20), is unaffected by $\underset{\sim}{g}$. Moreover, since

$$\underset{\sim}{b} = \hat{z} + O(\varepsilon)$$

it's clear that $\underset{\sim}{b}\cdot\underset{\sim}{\nabla}\times\underset{\sim}{g} \sim O(\varepsilon^3)$, and thus that $\underset{\sim}{g}$ cannot contribute, directly or indirectly, to the shear-Alfvén law. Finally, regarding the parallel ion dynamics, we observe that

$$\underset{\sim}{b}\cdot\underset{\sim}{f} = m_i n\left(\frac{\partial V_{\parallel i}}{\partial t} + \underset{\sim}{V}_E\cdot\nabla\ V_{\parallel i}\right) + O(\varepsilon^3)$$

i.e., that $\underset{\sim}{b}\cdot\underset{\sim}{g}$ cancels the diamagnetic contribution to $d_i V_{\parallel i}/dt$.

Thus gyrovoscosity serves to simplify the nonlinear equations of motion, by cancelling various acceleration terms. The importance of such "gyroviscous cancellation" was noted by Stringer [64], Hinton and Horton [65], and others [66]. The cancellation survives in the presence of temperature gradients [67], and obviously is still important when higher-order corrections are included. However,

although the corrections due to magnetic curvature are demonstrably of higher order, they are not easily written down. The problem is that $\underset{\approx}{\Pi}_g$ itself has been computed only for the case of a uniform magnetic field. It is the formal ε-expansion which justifies application of such slab-geometry results in the toroidal case.

To verify Eq. (4.129), we first consider

$$m_i n \frac{d_i \underset{\sim}{V}_D}{dt} = \frac{P_i}{\Omega_i} \left(\frac{\partial}{\partial t} + \underset{\sim}{V}_i \cdot \nabla\right)(\hat{z} \times \nabla \ell n\ n)$$

where the right-hand side needs to be evaluated only in lowest order. The particle conservation law, together with Eq. (4.126), shows that

$$m_i n \frac{d_i \underset{\sim}{V}_D}{dt} = \frac{P_i}{\Omega_i} \left[\underset{\sim}{V}_{\perp i} \cdot \nabla (\hat{z} \times \ell n\ n) - (\hat{z} \times \nabla)(\underset{\sim}{V}_{\perp i} \cdot \nabla) \ell n\ n\right] .$$

Recalling that $\nabla \propto \nabla_\perp$ in lowest order, one easily verifies the commutation rule

$$(\underset{\sim}{V}_{\perp i} \cdot \nabla)(\hat{z} \times \nabla f) - (\hat{z} \times \nabla)(\underset{\sim}{V}_{\perp i} \cdot \nabla f) = (\nabla f \cdot \nabla) \nabla \varphi_* - \nabla f (\nabla_\perp^2 \varphi_*)$$

for any function f. Thus

$$m_i n \frac{d_i \underset{\sim}{V}_D}{dt} = \frac{P_i}{\Omega_i} \left[(\nabla \ell n\ n \cdot \nabla) \nabla \varphi_* - (\nabla \ell n\ n) \nabla^2 \varphi_*\right] . \qquad (4.130)$$

Regarding the gyroviscosity tensor, we use the formulae of Braginskii [68] (cf. also [69]), which may be expressed as

$$\underset{\approx}{\Pi}_{gi} = \frac{P_i}{4\Omega_i}\left[(\hat{z}\times\nabla)\underset{\sim}{V}_{\perp i} + \nabla(\hat{z}\times\underset{\sim}{V}_{\perp i}) + \text{transpose}\right]$$

$$+ \frac{P_i}{\Omega_i}\left[\hat{z}(\hat{z}\times\nabla V_{\parallel i}) + \text{transpose}\right] \qquad (4.131)$$

provided $\nabla_\parallel \sim \frac{\partial}{\partial z} \sim \varepsilon\nabla_\perp$ terms are neglected. To clarify the tensor character of the right-hand side, we mention that

$$\left[(\hat{z}\times\nabla)\underset{\sim}{V}_\perp\right]_{\alpha\beta} = (\hat{z}\times\nabla)_\alpha V_{\perp\beta} ,$$

$$\left[\nabla(\hat{z}\times\underset{\sim}{V}_\perp)\right]_{\alpha\beta} = \nabla_\alpha(\hat{z}\times\underset{\sim}{V}_\perp)_\beta ,$$

etc.. We simplify Eq. (4.131) by means of the easily verified tensor identity

$$(\hat{z}\times\nabla)\underset{\sim}{V}_\perp - \left[\nabla(\hat{z}\times\underset{\sim}{V}_\perp)\right]^t = \underset{\approx}{I}\hat{z}\cdot\nabla\times\underset{\sim}{V}_\perp \qquad (4.132)$$

where the transpose is indicated by a t. Since $\hat{z}\times\underset{\sim}{V}_{\perp i} = -\nabla\varphi_*$,

$$\nabla(\hat{z}\times\underset{\sim}{V}_{\perp i}) = -\nabla\nabla\varphi_*$$

and the second term on the left-hand side of Eq. (4.132) is symmetric. Furthermore, the right-hand side is simply $\underset{\approx}{I}\nabla^2\varphi_*$. Combining these results, we find that

$$\underset{\approx}{\Pi}_{gi} = \frac{P_i}{2\Omega_i} \left\{ \underset{\approx}{I}\nabla^2\varphi_* - 2\nabla\nabla\varphi_* + 2\left[\hat{z}(\hat{z}\times\nabla V_{\parallel i}) + (\hat{z}\times\nabla V_{\parallel i})\hat{z}\right]\right\}$$

and therefore that

$$\nabla\cdot\underset{\approx}{\Pi}_{gi} = \frac{P_i}{\Omega} \left[\frac{-1}{2}\nabla(\nabla^2\varphi_*) + \frac{1}{2}(\nabla \ell n\ n)\nabla^2\varphi_* - (\nabla \ell n\ n\cdot\nabla)\nabla\varphi_*\right.$$

$$\left. + \hat{z}\ \hat{z}\cdot\nabla V_{\parallel i}\times\nabla \ell n\ n\right] + O(\varepsilon^3) \ . \qquad (4.133)$$

Finally, we combine Eqs. (4.130) and (4.133) to compute $\underset{\approx}{g}$. With the neglect of $O(\varepsilon^3)$, the result confirms Eq. (4.129).

Our derivation of the gyroviscous cancellation accounts for the full effects of density variation. However, to avoid cubic nonlinearity, along with other complications, in the final equations we must employ the Boussinesq approximation. This is accomplished, formally, by noting that the density can be written as

$$n/n_c = 1 + \varepsilon p_e/\beta_e$$

and treating β_e as $O(1)$ in this special context. Then

$$\nabla \ell n\ n = (\varepsilon/\beta_e)\nabla p_e + O(\varepsilon^2) \ .$$

We may also note here that p, the pressure varible of Sec. B, satisfies $\nabla p = (1+T_i/T_e)\nabla p_e$. Therefore Eq. (4.20) implies

$$\nabla_\perp B_\parallel = -\frac{1}{2}(1 + T_i/T_e)\nabla_\perp p_e \ . \qquad (4.134)$$

With these remarks, it is a simple matter to write down reduced equations for the evolution of v and φ. First, we take the parallel component of Eq. (4.124), using Eq. (4.129), and neglecting $O(\varepsilon^3)$. The result, in terms of normalized variables, is

$$\partial v/\partial\tau + [\varphi,v] + \frac{1}{2}\left(1 + \frac{T_i}{T_e}\right)\nabla_\parallel p_e = 0 \ . \tag{4.135}$$

The shear-Alfvén law for φ is obtained by the method of Sec. B, with one change in notation ($p \to p_e$) and one additional term, describing diamagnetic convection of $\underset{\sim}{v}_E$. Thus Eq. (4.29) is replaced by

$$\frac{\partial U}{\partial\tau} + [\varphi,U] + \hat{z}\cdot\nabla\times[\underset{\sim}{u}_D\cdot\nabla_\perp\underset{\sim}{u}_E] = -\nabla_\parallel J - (1 + T_i/T_e)[x,p_e] + O(\varepsilon^2) \ .$$

The diamagnetic term can be written through $O(\varepsilon^2)$

$$\delta\hat{z}\cdot\nabla\times[(\hat{z}\times\nabla_\perp p_e)\cdot\nabla_\perp\underset{\sim}{u}_E] = \frac{\delta}{2}\left\{[p_e,\nabla_\perp^2\varphi] + [\varphi,\nabla_\perp^2 p_e] + \nabla_\perp^2[p_e,\varphi]\right\}$$

Thus we obtain the shear-Alfvén law

$$\frac{\partial U}{\partial\tau} + [\varphi,U] + \nabla_\parallel J + \left(1 + \frac{T_i}{T_e}\right)[x,p_e]$$

$$= -\frac{\delta}{2}\frac{T_i}{T_e}\left\{[p_e,U] + [\varphi,\nabla_\perp^2 p_e] + \nabla_\perp^2[p_e,\varphi]\right\} \ . \tag{4.136}$$

We consider next the generalized Ohm's law, i.e., the parallel acceleration law for electrons. First recall that the parallel current is related to $J = \nabla_\perp^2 \psi$ by

$$J_\parallel = -\frac{\varepsilon c B_c}{4\pi a} J + O(\varepsilon^2) \ .$$

Hence, in view of Eq. (4.116), we have

$$V_{\parallel e} = \varepsilon v_A (v + 2\delta J) + O(\varepsilon^2) \ . \qquad (4.137)$$

Electron inertia is simplified by gyroviscosity in precisely the same manner as the ion case. Thus, neglecting $O(\varepsilon^2)$, electron parallel dynamics are described by [69]

$$m_e n \left(\frac{\partial}{\partial t} + \underset{\sim}{V}_E \cdot \nabla\right) V_{\parallel e} = -enE_\parallel - \underset{\sim}{b} \cdot \nabla p_e + en\eta J_\parallel$$

and straightforward normalization, using Eq. (4.137), yields

$$\left(\frac{\partial}{\partial \tau} + \underset{\sim}{u}_E \cdot \nabla\right)(v + 2\delta J) = \frac{1}{2\delta} \frac{m_i}{m_e} \left[\nabla_\parallel \varphi + \frac{\partial \psi}{\partial \tau} - \delta \nabla_\parallel p_e - \eta \nabla_\perp^2 \psi\right] .$$

Here, because of Eq. (4.135), the terms involving v yield only an $O(m_e/m_i)$ correction to $\nabla_\parallel p_e$:

$$\nabla_\parallel p_e \to \left[1 - \frac{m_e}{m_i}\left(1 + \frac{T_i}{T_e}\right)\right] \nabla_\parallel p_e \ .$$

We neglect this correction to write the reduced Ohm's law as

$$\frac{\partial \psi}{\partial \tau} + \nabla_{\parallel}\varphi = \eta J + \delta \nabla_{\parallel} p_e + 4\delta^2 \frac{m_e}{m_i}\left(\frac{\partial J}{\partial \tau} + [\varphi, J]\right) . \qquad (4.138)$$

The $O(m_e/m_i)$ electron inertia terms are retained because of their qualitative importance in the collisionless limit.

Equations (4.135), (4.136), and (4.138) provide three equations for our four fields. The fourth equation is derived from particle conservation, as in Sec. B. Of course, when ε-terms are strictly neglected, the result is Eq. (4.37), describing incompressible convection of the normalized pressure. We noted in Subsection 1 that compressibility has a special significance in certain contexts, and therefore wish to include its effects in the fourth equation, without attempting to include all $O(\varepsilon^3)$ terms. To this end, we apply the same device as was used in justifying the Boussinesq approximation: treating β_e as $O(1)$. Equivalently, the compressible, reduced conservation law results from neglecting $O(\varepsilon^3)$, but retaining $O(\beta_e \varepsilon^2)$.

The reduced equation is most simply derived from electron particle conservation:

$$\frac{\partial n}{\partial t} + \nabla \cdot (n \underset{\sim}{V}_e) = 0 .$$

Normalization according to Eq. (4.115) quickly yields

$$\frac{\partial p_e}{\partial \tau} + [\varphi, p_e] = - \frac{\beta_e}{\varepsilon} \nabla \cdot \underset{\sim}{u}_e \tag{4.139}$$

showing that only the lowest order, $O(\varepsilon)$, contribution to $\nabla \cdot \underset{\sim}{u}_e$ is needed. The parallel contribution is easily written down,

$$\frac{\beta_e}{\varepsilon} \nabla \cdot \underset{\sim}{b} u_{\parallel e} = \beta_e \nabla_{\parallel} (v + 2\delta J)$$

so we can restrict our attention to $\nabla \cdot \underset{\sim}{u}_{\perp e}$. From Eq. (4.122) we find, with sufficient accuracy,

$$n \underset{\sim}{V}_{\perp e} = -(c/eB) \underset{\sim}{b} \times [\nabla P_e + en \underset{\sim}{E} - \underset{\sim}{F}_e + O(m_e/m_i)]$$

or, in view of Eq. (4.123)

$$\underset{\sim}{u}_{\perp e} = (\underset{\sim}{B}/B^2) \times [\nabla \varphi + \varepsilon \frac{\partial \underset{\sim}{A}}{\partial \tau} - \delta \frac{n_c}{n} \nabla p_e] + \eta B^{-2} [\underset{\sim}{B} \times (\nabla \times \underset{\sim}{B})] \ .$$

Note that η measures $\eta_{\perp}$ in the present case. The dissipative term corresponds to resistive diffusion, as can be seen from Eqs. (4.19) and (4.134):

$$B^{-2} \underset{\sim}{B} \times (\nabla \times \underset{\sim}{B}) = - \frac{\varepsilon}{2} (1 + \frac{T_i}{T_e}) \nabla_{\perp} p_e + O(\varepsilon^2) \ .$$

Hence we have

$$\underset{\sim}{u}_{\perp e} = (\underset{\sim}{B}/B^2) \times \left[(\nabla\varphi + \frac{\partial \underset{\sim}{\mathcal{A}}}{\partial\tau}) - \delta\frac{n_c}{n}\nabla p_e\right]$$

$$- \frac{\varepsilon}{2}\eta\left(1 + \frac{T_i}{T_e}\right)\nabla_\perp p_e + O(\varepsilon^2)$$

and one easily finds that

$$\frac{\beta_e}{\varepsilon}\nabla\cdot\underset{\sim}{u}_{\perp e} = -\frac{\beta_e}{2}\eta\left(1 + \frac{T_i}{T_e}\right)\nabla_\perp^2\rho_e + C_\perp + O(\varepsilon)$$

where

$$C_\perp = \frac{\beta_e}{\varepsilon}\nabla\cdot\left[\frac{\underset{\sim}{B}}{B^2}\times\left(\nabla\varphi+\varepsilon\frac{\partial\underset{\sim}{\mathcal{A}}}{\partial\tau} - \frac{n_c}{n}\delta\nabla p_e\right)\right] . \qquad (4.140)$$

Evaluation of the right-hand side of Eq. (4.140) is straightforward, if somewhat complicated. Considering first the term involving $\underset{\sim}{\mathcal{A}}$, we find that

$$\beta_e\nabla\cdot\left(\frac{\underset{\sim}{B}}{B^2}\times\frac{\partial\underset{\sim}{\mathcal{A}}}{\partial\tau}\right) = -\beta_e\frac{\partial B_\parallel}{\partial\tau} + O(\varepsilon) ,$$

$$= \frac{\beta_e}{2}\left(1 + \frac{T_i}{T_e}\right)\frac{\partial p_e}{\partial\tau} + O(\varepsilon) .$$

in view of Eq. (4.134). Here we assumed that any spatially constant contribution to $B_\parallel$ is also temporally constant. The other terms in $C_\perp$

are computed using Eq. (4.12) for the magnitude of $\underset{\sim}{B}$ and Eq. (4.134). One finds

$$\frac{\beta_e}{\varepsilon} \nabla \cdot \left[\frac{\underset{\sim}{B}}{B^2} \times \left(\nabla\varphi - \frac{n_c}{n}\, \delta\nabla p_e\right)\right] = 2\beta_e[\varphi-\delta p_e, x] + \frac{1}{2}\left(1 + \frac{T_i}{T_e}\right)\beta_e[\varphi, p_e] + O(\varepsilon) \ .$$

Noticing that $C_\perp$ and Eq. (4.139) contain the same convective derivative of p_e, we introduce the abbreviation

$$\beta = \frac{\beta_e}{1 + \frac{1}{2}\left(1 + \frac{T_i}{T_e}\right)\beta_e} \ . \tag{4.141}$$

Then, combining results, we can write the pressure evolution law as

$$\frac{\partial p_e}{\partial \tau} + [\varphi, p_e] = \beta\left\{2[x, \varphi-\delta p_e] - \nabla_\parallel (v+2\delta J) + \frac{1}{2}\left(1 + \frac{T_i}{T_e}\right)\eta \nabla_\perp^2 p_e\right\} \ . \tag{4.142}$$

The first term on the right-hand side of Eq. (4.142) measures perpendicular compressibility, and arises because the perpendicular flow, $\underset{\sim}{V}_E + \underset{\sim}{V}_D$, has a divergence whenever B varies on a magnetic surface. We noted in Chapter II that such variation is an important consequence of toroidal curvature; in fact the perpendicular compressibility term is similar in form and significance to the interchange term in Eq. (4.136).

The parallel compressibility term involves both v and J. The contribution from v is pertinent to sound wave propagation along $\underset{\sim}{B}$, which tends to reduce pressure variation. The contribution from J is

omitted in unreduced MHD (which has $\delta=0$), but has crucial importance in some applications, one of which is studied in the following Subsection. Finally, the diffusive term in Eq. (4.142) has an obvious interpretation.

4. Four-field Model

The four-field model is defined by Eqs. (4.135), (4.136), (4.138) and (4.142). We repeat the equations here, with one minor change in notation: the quantity $(R-R_0)/a$ is denoted by

$$h \equiv (R-R_0)/a$$

instead of x, essentially because (x,y) coordinates are less useful in application than they were in deriving the model. Thus we have the shear-Alfvén law,

$$\partial U/\partial\tau + [\varphi,U] + \nabla_\parallel J + (1 + T_i/T_e)[h,p_e]$$
$$= (\delta/2)(T_i/T_e)\{[U,p_e] + [\nabla_\perp^2 p_e,\varphi] + \nabla_\perp^2[\varphi,p_e]\} \ , \qquad (4.143)$$

the generalized Ohm's law,

$$\partial\psi/\partial\tau + \nabla_\parallel\varphi - \eta J = \delta\nabla_\parallel p_e + \frac{4m_e}{m_i}\,\delta^2(\partial J/\partial\tau + [\varphi,J]) \ , \qquad (4.144)$$

the parallel acceleration law,

$$\partial v/\partial\tau + [\varphi,v] + \frac{1}{2}(1 + T_i/T_e)\nabla_\parallel p_e = 0 \ , \qquad (4.145)$$

and the energy conservation law,

$$\partial p_e/\partial\tau + [\varphi, p_e] = \beta\{2[h, \varphi - \delta p_e] - \nabla_\parallel (v + 2\delta J) + \frac{1}{2}(1 + T_i/T_e)\eta\nabla_\perp^2 p_e\} \quad . \tag{4.146}$$

Recall also that

$$J \equiv \nabla_\perp^2 \psi \quad , \quad U = \nabla_\perp^2 \varphi \quad ,$$

and that $\nabla_\parallel$ denotes the nonlinear parallel gradient,

$$\nabla_\parallel f = \partial f/\partial z - [\psi, f] \tag{4.147}$$

with

$$[f, g] = \hat{z} \cdot \underset{\sim}{\nabla}_\perp f \times \underset{\sim}{\nabla}_\perp g \quad .$$

It is apparent that reduced MHD [Eqs. (4.35)-(4.37)] is recovered from the four-field model in the limit

$$\delta \to 0 \quad , \quad \beta \to 0 \quad .$$

Finite δ allows for finite ω_*/ω; neglecting δ is equivalent to assuming the MHD orderings, Eqs. (4.48) and (4.50). Finite β, on the other hand, restores the plasma compressibility terms which are present in MHD but neglected by the conventional reduction process.

The remainder of this Subsection concerns certain elementary effects of finite δ and of parallel compressibility. The significance of perpendicular compressibility is considered in subsequent Chapters.

The four-field equilibrium is very similar to that of reduced MHD. In particular, for φ_0=0, Eqs. (4.143) and (4.145) imply

$$J_0 = \bar{J}_0(\psi_0) - h(1 + T_i/T_e) \frac{dp_{e0}}{d\psi_0} \tag{4.148}$$

which differs from Eq. (4.45) only in notation. A new feature appears regarding the equilibrium parallel flow. Equation (4.146) requires

$$-2\delta[h,p_0] + [\psi_0,v_0] + 2\delta[\psi_0,J_0] = 0 ,$$

when the very small equilibrium diffusion term in neglected. We combine this result with Eq. (4.148), assuming T_i=T_e for simplicity, and find that

$$[\psi_0,v_0] + 2\delta[h,p_0] = 0 ,$$

whence

$$v_0 = \bar{v}_0(\psi_0) + 2\delta h \frac{dp_{e0}}{d\psi_0} . \tag{4.149}$$

Thus pressure gradients demand an equilibrium parallel flow. Like the current of Eq. (4.148), v_0-$\bar{v}_0$ is a return flow, induced by the variation of B on a magnetic surface (cf. Sec. D of Chapter II). As

indicated by the δ-factor, the return flow is a finite gyroradius effect. It plays an important role in neoclassical transport theory [54]. The first term on the right-hand side of Eq. (4.149) is small in most toroidal experiments.

In linear theory, δ has two elementary consequences: it allows the ion diamagnetic frequency, ω_{i*}, to enter the shear-Alfvén law, and it provides appropriate "kinetic" effects, involving ω_{e*} as well as $k_{\|}v_{the}$, in the generalized parallel conductivity. We study these effects in cylindrical geometry, neglecting toroidal curvature (h=0) and assuming the equilibrium pressure depends only on r. Thus we use the coordinates of Eq. (4.41).

The linearization is accomplished by expressing the spatial dependence of any field variable, f, as

$$f = f_0(r) + \hat{f}(r)\exp i(m\vartheta - \ell z) \quad . \tag{4.150}$$

The eikonal factor is usually left implicit. Hence Eq. (4.147) yields

$$\nabla_{\|} f = -i\ell\hat{f} - \frac{1}{r}\frac{\partial\psi_0}{dr}\, im\hat{f} + i\,\frac{m}{r}\frac{df_0}{dr}\,\hat{\psi} \quad ,$$

in which the first two terms must correspond to $k_{\|}\hat{f} \propto (\ell - m/q)\hat{f}$. In fact, the reduced safety factor is given by

$$\frac{1}{q} = -\frac{1}{r}\frac{d\psi_0}{dr} \quad . \tag{4.151}$$

Thus, after introducing the normalized wave vectors

$$R_0 k_\parallel \to k_\parallel \equiv m/q - \ell \ . \tag{4.152}$$

and

$$a k_\perp \to k_\perp \equiv m/r \ , \tag{4.153}$$

we can write

$$\nabla_\parallel f = i k_\parallel \hat{f} + i k_\perp f_0' \hat{\psi} \ , \tag{4.154}$$

where the prime denotes a radial derivative. We similarly introduce the normalized frequency,

$$(\tau_A/\varepsilon)\omega \to \omega \ ,$$

such that $\partial f/\partial\tau$ becomes $-i\omega\hat{f}$. Hereafter the carets are suppressed.

The significance of ω_{i*} is most simply understood from the incompressible energy conservation law: Eq. (4.146) with β=0. Linearization provides the "hydrodynamic" perturbation

$$p_e = -k_\perp p_{eo}' \varphi/\omega \ , \tag{4.155}$$

which is substituted into Eq. (4.127) for the perturbed ion flow. One finds that

$$\underset{\sim}{u}_{i\perp} = \left(1 - \frac{\omega_{i*}}{\omega}\right) \hat{z}\times\nabla_\perp \varphi \ , \tag{4.156}$$

where

$$\omega_{i*} \equiv \delta \frac{T_i}{T_e} k_\perp p'_{eo}$$

is the ion diamagnetic frequency in terms of reduced variables. It is convenient to write

$$\omega_{i*} = -(T_i/T_e)\omega_{e*} \ , \tag{4.157}$$

where

$$\omega_{e*} = -\delta k_\perp p'_{eo} \ , \tag{4.158}$$

is the normalized version of the drift-frequency appearing in Eq. (4.89). Equation (4.156) shows that ω_{i*}-terms correspond to perturbed diamagnetic flows. They are omitted in MHD because, as we have noted, $\omega_{MHD} >> \omega_* \sim \delta$.

The way in which ω_{i*} actually enters the closed linear system is somewhat different: it does not depend upon incompressibility or Eq. (4.155), but does depend upon gyroviscosity. Yet the result is the same; denoting the right-hand side of Eq. (4.143) by G, we linearize to compute

$$(2/\delta)(T_e/T_i)G = -ik_\perp p'_{eo} U + ik_\perp \varphi p'''_{eo} - \nabla_\perp^2 (ik_\perp p'_{eo} \varphi) \ .$$

If perturbed amplitudes vary in radius more sharply than p_{eo}, we have

$$G \cong (\delta/2)(T_i/T_e)(-2ik_\perp p'_{eo})U = -i\omega_{i*}U \ , \tag{4.159}$$

which combines with the first term on the left-hand side of Eq. (4.143) to produce the usual shift, $-i(\omega-\omega_{i*})U$, as in Eq. (4.156). We remark that without Π_g the result would have been quite different and inconsistent with ion kinetic theory.

Next we turn our attention to the electron dynamics. The normalized, linear, parallel electric field,

$$\mathcal{E} \equiv -i\omega\psi + ik_\parallel\varphi \ , \tag{4.160}$$

should be related to the parallel current by an Ohmic relation,

$$J = \sigma_4\mathcal{E} \tag{4.161}$$

which defines the four-field conductivity, σ_4. Of course σ_4 is dimensionless; denoting its dimensional version by σ_{*4}, and recalling the normalizations of $J_\parallel \to J$ and $E_\parallel \to \mathcal{E}$, we find that

$$\sigma_4 = \frac{4\pi a^2}{c^2\tau_A}\,\sigma_{*4} \ , \tag{4.162}$$

as in Eq. (4.33).

We calculate σ_4 for the equal temperature case, assuming $\varphi_0=0$ and neglecting equilibrium current gradients; analogous simplifications were used in Subsection 2. Then Eq. (4.145) implies

$$-i\omega v + \nabla_\parallel p_e = 0 \ , \tag{4.163}$$

and substitution into Eq. (4.144) yields

$$\mathcal{E} = \left(\eta - 4i \frac{m_e}{m_i} \delta^2 \omega\right) J + i\delta\omega v \ . \tag{4.164}$$

To compute v, we use Eqs. (4.154) and (4.158) to write Eq. (4.163) as

$$i\delta\omega v = ik_{\parallel} \delta p_e - i\omega_{e*} \psi \ , \tag{4.165}$$

and combine it with the linearized energy conservation law,

$$-i\omega p_e - ik_{\perp} p_0' \varphi = -ik_{\parallel} \beta (v + 2\delta J) \ . \tag{4.166}$$

Here we have neglected resistive diffusion for simplicity. (The influence of resistive diffusion is studied in Chapter V.) One finds that

$$i\delta\omega v \left(1 - \frac{k_{\parallel}^2 \beta}{\omega^2}\right) = \frac{\omega_{e*}}{\omega} \mathcal{E} + \frac{2i\delta^2 \beta k_{\parallel}^2}{\omega} J \ . \tag{4.167}$$

Notice in particular that the φ-term in Eq. (4.166) has combined with the ψ-term in Eq. (4.165) to form $\mathcal{E}$.

Equation (4.167) is to be substituted into Eq. (4.164). It is convenient to introduce the quantity Δ_i, such that

$$\left(1 - \frac{k_{\parallel}^2 \beta}{\omega^2}\right)^{-1} \equiv 1 + \Delta_i \ . \tag{4.168}$$

Then one obtains Eq. (4.161), with

$$\sigma_4 = \frac{\omega-\omega_{e*}(1+\Delta_i)}{\eta\omega-4i(m_e/m_i)\delta^2\omega^2+2i\delta^2\beta k_\parallel^2(1+\Delta_i)} \quad . \tag{4.169}$$

In order to compare this result with its kinetic counterpart, σ_* [recall Eq. (4.101)], we first rewrite Eq. (4.169) in terms of dimensional quantities. The relevant normalizations are given by Eq. (4.162),

$$(k_\parallel v_{the})^2/(\omega\nu) \rightarrow 2\delta^2\beta_e k_\parallel^2/(\omega\eta) \quad ,$$

$$(k_\parallel v_{thi})^2/\omega^2 = \frac{m_e}{m_i}\left(\frac{k_\parallel v_{the}}{\omega}\right)^2 \rightarrow \frac{k_\parallel^2\beta_e}{\omega^2}$$

and

$$2\omega/\nu_e \rightarrow 4(m_e/m_i)\delta^2\omega/\eta \quad .$$

We also note that

$$\beta = \beta_e + O(\beta_e^2) \quad ,$$

from Eq. (4.141), and therefore ignore the distinction between β and β_e. Then Eq. (4.169) becomes

$$\sigma_{*4} = \sigma_s \left[\frac{1-(\omega_{e*}/\omega)(1+\Delta_i)}{1-2i(\omega/\nu_e)+i(k_\parallel v_e)^2(1+\Delta_i)/(\omega\nu_e)}\right] \tag{4.170}$$

with

$$1 + \Delta_i \simeq \left[1 - (x/x_i)^2\right]^{-1}$$

where x_i is defined by Eq. (4.113).

Equation (4.170) differs from the result of Subsection 2 for obvious reasons: a fluid description, without microscopic wave–particle interaction, cannot provide the Z–functions found in kinetic theory. Thus, for $|x| \sim x_e$ (or x_i), Eq. (4.170) oversimplifies the electron response. However, the more striking feature of Eq. (4.170) is that it reproduces, with good qualitative accuracy, all the asymptotic limits of the kinetic version: Eqs. (4.106), (4.111) and (4.114).

We point out that the agreement between σ_{4*} and σ_* for $k_\parallel v_{th} \to 0$ is not surprising, since truncation is essentially exact in this limit. It is the agreement for $(k_\parallel v_{th})^2 >> \omega(\omega+i\nu)$ which is noteworthy.

Equation (4.170), with $\Delta_i = 0$, was derived by Rutherford and Furth [70], who noted that σ_{4*} becomes small for large $k_\parallel$, i.e., at "large" distances from the rational surface. This circumstance was discussed in Subsection 2; its significance is considered in the following chapter.

DOE-ET-53088-154 IFSR #154

SHEAR-ALFVÉN DYNAMICS OF TOROIDALLY CONFINED PLASMAS

R. D. Hazeltine and J. D. Meiss

(Part B)

V. Radial Boundary Layer Theory

A. Introduction

Having derived tractable models for the plasma dynamics, we return our attention here to the main issue discussed at the end of Chapter III: resolution of the rational flux surface singularity. This chapter considers the case in which perturbations are dominated by a single helicity. The well-defined boundary layer characterizing the single-helicity case leads to a relatively simple, one-dimensional problem. More general perturbations, involving strongly coupled helicities and often lacking distinct radial boundary layers, are studied in Chapter VI.

Of course a one-dimensional analysis is strictly appropriate only in the case of cylindrical symmetry. However, we have seen that toroidal curvature enters the reduced equations primarily through the interchange term, which is negligible for sufficiently small pressure. Hence the low-beta case ($\beta \sim \varepsilon^2$) is effectively cylindrical and rigorously consistent with single-helicity theory. When δ is neglected it describes such current-driven modes as the classical tearing instability, twisting modes and the ideal kink. Apart from such specific applications, low-beta reduced MHD provides the simplest possible concrete example of several topics emphasized in Chapter III: neighboring equilibria, boundary-layer analysis, and closure of the shear Alfvén law. It is the main subject of Section B.

At higher pressure ($\beta \sim \varepsilon$), the interchange term must be included, and toroidal curvature, coupling different helicity components, plays a crucial role. Nonetheless, as long as $w \ll \Delta\chi$, a single helicity can continue to dominate, yielding a distinct radial boundary layer. The

corresponding linear instabilities include radially localized interchange and pressure-modified tearing modes. The main burden in analyzing high-beta disturbances is the derivation, from partial differential equations, of ordinary differential equations for amplitudes describing the dominant helicity. This decoupling analysis can be performed in two ways. The first way, which depends upon boundary-layer orderings (e.g., $k_\perp w << 1$) is reviewed in Section C of the present chapter. The second method, which is more complicated but also more general, is the subject of Chapter VI.

In Sec. D we consider the effects of finite δ, emphasizing the modified electron response. When the collisional conductivity, σ_s, is replaced by σ_*, a new scale-length enters the linear problem, allowing for qualitatively different instability mechanisms.

Nonlinear resolution of the rational surface singularity is discussed in Section E. It was pointed out in Chapter III that the crucial nonlinearity results from field-line reconnection. Thus one studies the evolution of a magnetic island whose width has become comparable to the linear layer width (W~w).

B. Low-beta Stability

1. Linearization

In this section we study the linear eigenmodes of low-beta reduced MHD. Thus the interchange term in Eq. (4.35) is neglected, and the dynamical equations become

$$\partial U/\partial \tau + [\varphi, U] = -\nabla_\parallel J \qquad (5.1)$$

$$\partial\psi/\partial\tau + \nabla_{\parallel}\varphi = \eta J \tag{5.2}$$

We noted previously that cylindrical coordinates are appropriate in this case: low-beta allows one to assume that equilibrium quantities depend only on r. Each field quantity is expressed as an eikonal, as in Eq. (4.150). After suppressing carets we obtain the linearized system,

$$-\omega\nabla_{\perp}^2\varphi + k_{\parallel}\nabla_{\perp}^2\psi + k_{\perp}J_0'\psi = 0 \tag{5.3}$$

$$-\omega\psi + k_{\parallel}\varphi = -i\eta\nabla_{\perp}^2\psi \tag{5.4}$$

where

$$\nabla_{\perp}^2 = \frac{1}{r}\frac{\partial}{\partial r}\, r\, \frac{\partial}{\partial r} - k_{\perp}^2 \ .$$

Equation (5.3) is a simplified, linearized verison of the general shear-Alfvén law discussed in Chapter III. Equation (5.4) is of course the corresponding closure relation. Thus we have a simple model for the boundary-layer theory outlined in Sec. C of Chapter III, which we very briefly review.

With the neglect of plasma inertia, Eq. (5.3) becomes an autonomous equation for ψ, or

$$\underset{\sim}{B}\cdot\nabla\chi \propto B_r = -ik_{\perp}\psi \ ,$$

describing neighboring equilibria,

$$k_{\parallel}\nabla_{\perp}^{2}\psi + k_{\perp}J_{0}'\psi = 0 \ , \tag{5.5}$$

as in Eq. (3.21). A regular singular point of Eq. (5.5) occurs at r_s, where

$$k_{\parallel}(r_s) = 0 \ ,$$

unless

$$J_{0}'(r_s) = 0 \ . \tag{5.6}$$

When Eq. (5.6) does not hold, the singularity yields two types of solutions: regular solutions, characterized by

$$\psi(r_s) = 0 \ , \tag{5.7}$$

and singular solutions, with finite $\psi(r_s)$. This and the following three subsections are devoted to the singular case. The regular solutions, corresponding to ideal kink instability, are considered in Subsection 5.

It is evident from Eq. (5.5) that a large parallel current forms near the boundary layer ("current layer") surrounding the rational surface. In the layer interior, we must include inertia to keep J finite; thus Eq. (5.4) becomes necessary for closure. Outside the current layer, however, Eq. (5.5) remains approximately valid, since $\omega \lesssim \omega_{SA} \sim k_{\parallel}(w)v_A \ll k_{\parallel}(r)v_A$, for $|r-r_s| \gg w$.

Notice that J, rather than ψ, tends to diverge at r_s. Thus the boundary-layer equations, in order to round off the current spike, must contain $\partial^2 J/\partial r^2$, and the boundary-layer equation for ψ will be at least fourth order. Equations (5.3) and (5.4) indeed yield uncoupled fourth order equations for ψ and φ; any alternative closure of lower order could not treat the singular case.

As in Chapter III, the radial width of the boundary layer is denoted by w. It evidently depends upon η and magnetic shear; the specific form will be considered presently. Notice that w is dimensionless in reduced coordinates; hence the thinness of the boundary layer is expressed by

$$w \ll 1 \ . \tag{5.8}$$

2. Layer interior

We begin our analysis by considering the layer interior. Assuming $|r-r_s| \sim w \ll r_s$, we write

$$r = r_s + x \quad , \quad x \ll r_s$$

$$k_\parallel(r) \cong k_\parallel' x \ , \tag{5.9}$$

as in Eq. (3.48). (Note that the "x" used here is a radial variable, which should not be confused with the Cartesian "x" of Sec. IVB.) We also assume that

$$(k_\perp w)^2 \ll 1 \ ,$$

corresponding to small or moderate values of the poloidal mode number m. Then we have

$$\nabla_\perp^2 = \partial^2/\partial x^2 + O(w/r_s) \ .$$

Finally we neglect the kink term, involving J_0', in Eq. (5.3). The kink term is primarily important outside the layer; its importance to layer physics will be assessed a posteriori. Thus we obtain the interior system,

$$-\omega\varphi'' + k_\parallel' \times \psi'' = 0 \tag{5.10}$$

$$-\omega\psi + k_\parallel' \times \varphi = -i\eta\psi'' \ . \tag{5.11}$$

Notice that Eq. (5.10) replaces the general shear-Alfvén law, Eq. (3.20), by an ordinary differential equation, balancing plasma inertia against line bending, without any vestige of toroidal curvature. In fact the same result could have been obtained from a slab model. However, Eq. (5.10) does not correspond to a homogeneous medium, because it contains an artifact of mode-rational surfaces: Eq. (5.9). In other words, what finally survives the reductions and simplifications is toroidal topology, as expressed by Eq. (2.25), and magnetic shear.

Equations (5.10) and (5.11) obviously can be combined to provide uncoupled, fourth-order equations for φ and ψ [71]. The following artifice allows one integration, and thus yields a second order equation for

$$E \equiv \varphi' \ ,$$

measuring the radial electric field [72]. Noticing that

$$x\,\psi'' = (x\,\psi'-\psi)' = [x^2(\psi/x)']' \ ,$$

we integrate Eq. (5.10) to obtain

$$-\omega E + k_\parallel' \, x^2(\psi/x)' = C \ , \tag{5.12}$$

where C is constant. We next divide Eq. (5.11) by x and differentiate the result. Then simple manipulation using Eq. (5.12) provides the boundary-layer equation

$$E[1-(k_\parallel' x/\omega)^2] - i(x^2/\omega)(\eta E'/x^2)' = -C/\omega \ . \tag{5.13}$$

We note that our derivation of Eq. (5.13) remains valid when the resistivity varies with x.

Next consider the asymptotic form of E for $|x| \to \infty$ (i.e., for $|r-r_s| \gg w$). The boundary-layer solution must become smooth in this limit; since

$$\eta \ll 1 \ ,$$

we can neglect the resistive term to obtain

$$E \to \frac{\omega C}{(k_\parallel' x)^2} \quad , \quad |x| \to \infty \ . \tag{5.14}$$

Since Eq. (5.14) cannot be integrated through the origin, we must allow for different integration constants, φ_+ and φ_-, on either side:

$$\varphi \to \varphi_{\pm} - \frac{\omega C}{(k_{\parallel}')^2 x} \quad , \quad x \to \pm \infty \ . \tag{5.15}$$

We substitute this result into the asymptotic form of Eq. (5.11),

$$-\omega\psi + k_{\parallel}' \, x \, \varphi \to 0 \ ,$$

to obtain the current-free flux

$$\psi \to A_0 + A_{\pm} x \quad , \quad x \to \pm \infty \ , \tag{5.16}$$

where $A_0 = -C/k_{\parallel}'$ and $A_{\pm} = (k_{\parallel}'/\omega)\varphi_{\pm}$.

Hence the layer solution is characterized by three integration constants. A fourth constant does not occur because of the implicit requirement that the current density,

$$J = \psi'' = \frac{\omega}{k_{\parallel}' x} E' \tag{5.17}$$

must be finite at x=0:

$$E'(x=0) = 0 \ . \tag{5.18}$$

The constants A_+ and A_- determine the total current flowing through the layer:

$$\int dx\, J = A_+ - A_- \,. \tag{5.19}$$

Here and below we use the notation

$$\int dx \equiv \int_{-\infty}^{\infty} dx \,. \tag{5.20}$$

The normalized, integrated sheet current is conventionally denoted by

$$\Delta' = (A_+ - A_-)/A_0 \,. \tag{5.21}$$

It must chosen to match appropriate asymptotic forms of the solutions, for $x<0$ and $x>0$, to the exterior problem. Presuming the latter has been solved, we can consider Δ' to be fixed, and Eqs. (5.17) and (5.21) provide a constraint on $E(x)$,

$$A_0\Delta' = \frac{\omega}{k_\parallel'} \int dx\, E'/x \,. \tag{5.22}$$

Equation (5.22) allows us to express Eq. (5.13) as an integrodifferential equation [73]

$$E\left[1 - \left(\frac{k_\parallel' x}{\omega}\right)^2\right] - i\,\frac{x^2}{\omega}\left(\frac{\eta E'}{x^2}\right)' = \frac{1}{\Delta'}\int \frac{dx E'}{x} \tag{5.23}$$

which is to be solved with the simple boundary condition

$$E \to 0 \,, \quad |x| \to \infty \tag{5.24}$$

as in Eq. (5.14).

An alternative form of Eq. (5.23) is more complicated, but especially useful in certain applications. It is expressed in terms of the parallel electric field, $\mathscr{E}$, which is related to E by [recall Eq. (4.160)]

$$(\omega^2-k_\parallel^2)E = ik_\parallel^2(\mathscr{E}/k_\parallel)' + \omega k_\parallel' A_0$$

as follows from Eqs. (5.10), (5.11) and (5.16). The derivation of a second order equation for $\mathscr{E}$ is similar to that of Eq. (5.23) [74]. We give only the result:

$$\left[\frac{x^2(\mathscr{E}/x)'}{k_\parallel^2-\omega^2}\right]' - \frac{i\mathscr{E}x}{\omega\eta} = \frac{-4\omega^2(k_\parallel')^4}{(\Delta' + \frac{i\pi k_\parallel'}{\omega})} \frac{x}{(k_\parallel^2-\omega^2)^2} \int dx \frac{\mathscr{E}}{(k_\parallel^2-\omega^2)^2} \qquad (5.25)$$

where $k_\parallel = k_\parallel' x$ as usual. The application of Eq. (5.25) is considered in Sec. D.

3. Eigenmode classification

An important feature of Eq. (5.23) is the symmetry of its integrodifferential operator under $x \to -x$. Hence eigenmode solutions can be chosen to have definite parity: $E = E_+(x)$ or $E_-(x)$, where

$$E_\sigma(-x) = \sigma E_\sigma(x) \ , \ \sigma = \pm 1 \ .$$

We call the solutions $E_+(E_-)$ even (odd). Notice that ψ and J must have the same parity as E, while φ has the opposite parity.

Recalling that "strong" magnetic reconnection requires $\psi(x=0) \neq 0$, we see that topology change is primarily associated with even eigenmodes. We therefore call them "tearing" modes, using the terminology of Furth, Killeen and Rosenbluth (FKR) [75], who first analyzed reconnection is a confined plasma context. The odd eigenmodes are called "twisting" modes [76]; they exemplify a class of instabilities which display boundary-layer behavior while still satisfying the Newcomb condition [since $\psi_-(0)$ must vanish]. Drift waves, in particular, belong to this class.

A distinct eigenmode classification involves the size of Δ'. The case

$$\Delta' \sim 1 \quad (\Delta' w \ll 1) \tag{5.26}$$

is called "small Δ'", while

$$\Delta' \gg 1 \quad (\Delta' w \gtrsim 1) \tag{5.27}$$

refers to "large Δ'". Since Δ' measures the slope of $\psi(x)$, we see that ψ is nearly constant (despite its large curvature, ψ'') when $\Delta' w$ is small. In studying the small Δ' case, FKR simplified Eq. (5.10) by replacing ψ, on the left-hand side, by A_0 ("constant-ψ approximation").

Large Δ' is associated either with steep slopes or with negligibly small A_0. In general, one specializes the field equations to the large-Δ' case by means of the limits

$$A_0 \to 0 \quad , \text{ or } \quad \Delta' \to \infty \; . \tag{5.28}$$

In Subsection 5, we will find that large-Δ' describes, in particular, tearing eigenmodes with poloidal mode number m=1.

4. Dispersion Relations

We are finally prepared to compute the eigenvalues, $\omega(k_\parallel', \Delta', \eta)$, of Eq. (5.23). The large-Δ' case is simplest. Using Eq. (5.28) to neglect the right-hand side of Eq. (5.23), we find that its solutions can be written in terms of confluent hypergeometric functions, M [77], as follows:

$$E_{+(n)} = \exp(-\alpha x^2/2) M\left(-n, -\frac{1}{2}, \alpha x^2\right) ,$$

$$E_{-(n)} = \exp(-\alpha x^2/2) x^3 M\left(-n, \frac{5}{2}, \alpha x^2\right) ,$$

where n=0,1,2,..., and

$$\alpha^2 = i(k_\parallel')^2/(\omega\eta) .$$

The dispersion relations are

$$\omega^2 = (4n-1)\frac{(k_\parallel')^2}{\alpha}$$

for E_+, and

$$\omega^2 = (4n+5)\frac{(k_\parallel')^2}{\alpha}$$

for E_-. Equation (5.24) requires that

$$\mathrm{Re}(\alpha) > 0 \ ,$$

which importantly restricts the solutions. In fact one finds that only one unstable mode is permitted: the n=0 tearing mode,

$$E = E_{+(0)} = \exp(-\alpha x^2/2) \ . \tag{5.29}$$

Its growth rate, $\gamma = -i\omega$, is given by

$$\gamma = (k_\parallel')^{2/3} \ \eta^{1/3} \tag{5.30}$$

and

$$\alpha = k_\parallel'(\gamma\eta)^{-1/2} = (k_\parallel'/\eta)^{2/3} \ .$$

These results are easily checked by direct substitution.

Equation (5.29) displays a boundary-layer localization of the radial electric field which is typical of tearing instability. (Recall that ψ and φ are not localized, but instead connect to the exterior kink structure.) The boundary-layer width is evidently given by $w = \alpha^{-1/2}$ or

$$w = (\eta/k_\parallel')^{1/3} \ . \tag{5.31}$$

Since $\eta \lesssim 10^{-8}$ in typical experiments, Eq. (5.8) is easily satisfied.

Notice also that $\varphi(x)$ is an error function whose asymptotic form,

$$\varphi = \text{const.} + O(e^{-x^2}) \ , \ |x| \to \infty \ ,$$

is consistent with Eq. (5.15), since $C \propto A_0 = 0$. This justifies our neglect of the right-hand side of Eq. (5.23).

In the case of small Δ', the integral term in Eq. (5.23) is important and simple, exact solutions are not available. The small-Δ' eigenvalues are most efficiently derived by variational methods. Thus Eq. (5.23) is rewritten as

$$E\left[1 + \left(\frac{\gamma}{k_\parallel' x}\right)^2\right] - \frac{\gamma}{(k_\parallel')^2}\left(\frac{\eta E'}{x^2}\right)' - \left(\frac{\gamma}{k_\parallel' x}\right)^2 \frac{1}{\Delta'} \int \frac{dx E}{x^2} = 0 \ ,$$

or $\mathscr{L}E=0$, where the linear operator $\mathscr{L}$ can be seen to be self-adjoint:

$$\int dx \ f \ \mathscr{L} g \ = \ \int dx \ g \ \mathscr{L} f \ ,$$

for any suitably localized functions f and g. Self-adjointness allows one to construct a quadratic function $S[f,f]$ which is variational, in the sense that

$$\delta S = 0$$

at f=E. By using a trial function, $f(x;\alpha_1,\alpha_2,\ldots)$, where the α_i are variational parameters, one can compute $S(\alpha_i)$, extremize with respect to the α_i, and thus obtain a variationally accurate dispersion relation.

The accuracy of the variational approach is well documented [73,74]. It has the important virtue of remaining tractable when the resistivity becomes a function of x, as in Eq. (4.101). Alternative variational prescriptions, which can be more convenient in certain circumstances, are expressed in terms of the parallel electric field [74], or the parallel current density [78], instead of E.

Here we review neither the variational procedure nor other analytical methods, such as those based on the constant-ψ approximation. Instead we estimate the eigenvalues of Eq. (5.23) by means of dimensional arguments. While missing quantitative details, such estimates have the advantage of being both brief and physically instructive.

Thus, returning to Eq. (5.23), we first identify three relevant scale lengths: the radial width, w, of the (localized) radial electric field; the shear-Alfvén width, x_A, at which γ is locally equal to the shear-Alfvén frequency,

$$x_A \equiv \gamma / k_\parallel' \ ; \tag{5.32}$$

and the resistive skin-depth, x_R, given by the normalized classical formula,

$$x_R^2 \equiv \eta / \gamma \ . \tag{5.33}$$

Hence Eq. (5.23) is rewritten as

$$[1 + (x_A/x)^2]E - x_R^2 x_A^2 (E'/x^2)'$$

$$= -(\Delta')^{-1}(x_A/x)^2 \int dx\, E'/x \ . \qquad (5.34)$$

Consider first the resistive term,

$$x_R^2 x_A^2 (E'/x^2)' \sim (x_R x_A/w^2)^2 \, E \ ,$$

according to the estimate,

$$E' \sim E/w \ .$$

If $(x_R x_A/w^2) \gg 1$, this term can be balanced only by the Δ'-term on the right-hand side, in which case the common factor of x_A^2 can be eliminated. Thus the Alfvén speed disappears from the linear problem, leaving only slow resistive diffusion. On the other hand, when $(x_R x_A/w^2) \ll 1$, Eq. (5.34) can be seen to describe ideal Alfvénic motion, with unresolved singularity at x=0.

We conclude that the boundary-layer width is generally characterized by

$$w \sim (x_R x_A)^{1/2} \ , \qquad (5.35)$$

i.e., it is the geometric mean of x_R and x_A. This ordering holds quite generally (when η = constant) and reflects the compromise between Alfvénic oscillation and resistive diffusion which characterizes boundary-layer evolution [75,79]. In particular, Eq. (5.35) is

consistent with our previous, exact results for the large-Δ' mode, Eqs. (5.30) and (5.31).

Consider next the ratio

$$x_R/x_A = k_\parallel' \eta^{1/2}/\gamma^{3/2} .$$

For the large-Δ' case, Eq. (5.30) shows that $x_R/x_A = 1$; more general models reveal a variety of modes for which

$$|x_R/x_A| \sim 1 \quad , \quad w \sim x_R \sim x_A . \tag{5.36}$$

Equation (5.36), which implies $\gamma \propto \eta^{1/3}$, characterizes any disturbance for which $\ell n\psi$ (rather than only J) varies sharply within the layer:

$$\psi'' \sim \psi/w^2 . \tag{5.37}$$

The other important case,

$$|x_R/x_A| \gg 1 , \tag{5.38}$$

can be seen to correspond to small-Δ' modes, as follows. We know that the right-hand side of Eq. (5.34) is comparable to the left-hand side for small Δ', and we have just shown that the left-hand side is estimated by E. Hence a straightforward estimate of

$$(\Delta')^{-1}(x_A/x)^2 \int dx E'/x \sim (\Delta')^{-1}(x_A/w)^2 E/w$$

yields the relation

$$\Delta' w \sim (x_A/w)^2 \sim x_A/x_R \ . \tag{5.39}$$

Here the second form follows from Eq. (5.35) and obviously verifies Eq. (5.38): the resistive layer is much wider than the Alfvén layer for small Δ'.

An analogous argument can be applied to the coupled equations, Eqs. (5.10) and (5.11). One then finds that small-Δ' corresponds to the ordering

$$\psi'' \sim \Delta' \psi / w \ , \tag{5.40}$$

which is to be compared to Eq. (5.37). The constant-ψ approximation is evidently based upon the ordering

$$\psi' \sim \Delta' \psi << \psi / w \ .$$

Here we emphasize the necessary connection between Eqs. (5.38) and (5.40).

To find the dispersion relation for the small-Δ' case, we first note that

$$-x_R^2 x_A^2 (E'/x^2)' \sim \eta \gamma E (k_\parallel')^{-2} \ w^{-4} \ ,$$

including the correct <u>sign</u> (for tearing parity). The point is that proper localization requires $E'' \propto -E$ near x=0. Since, on the other hand, the right-hand side of Eq. (5.34) has the sign of $\Delta' E$, we see

that $\mathrm{sgn}(\gamma) = \mathrm{sgn}(\Delta')$ and conclude that current-driven tearing modes are unstable only if

$$\Delta' > 0 \ . \tag{5.41}$$

In fact, as Furth has shown explicitly [80], Δ' measures the free energy which kink activity has made available in the exterior ($|x| \gg w$) region.

The form of the growth rate follows from Eqs. (5.35) and (5.39):

$$\Delta'(x_R x_A)^{1/2} \simeq x_A/x_R \ ,$$

which implies

$$\gamma \simeq \eta^{3/5} \ (k_\parallel')^{2/5} \ (\Delta')^{4/5} \ . \tag{5.42}$$

The quantitative version of this result, the "classical" tearing mode growth-rate, was first obtained by FKR; it differs from Eq. (5.42) by a factor of approximately 1.7.

5. Current gradient

Our analysis of the tearing layer interior has omitted the kink term, $k_\perp J_0' \psi$, in Eq. (5.3). Such omission is not obviously justified, in general, and our main purpose here is to consider current-gradient effects on the interior more carefully. However, we begin by considering the neighboring equilibrium equations which describe the kinked region, exterior to the layer.

The exterior region is primarily distinguished by its relatively slow field variation:

$$\nabla_\perp^2 \sim 1 \quad , \quad |x| >> w \ .$$

This ordering implies that, in the exterior,

$$\psi \simeq k_\parallel \varphi/\omega \ , \tag{5.43}$$

or $E_\parallel \simeq 0$, in view of Eq. (5.4) and the fact that $\eta << 1$. Because vanishing $E_\parallel$ characterizes ideal MHD, the exterior region is sometimes called the "ideal" region. However, two comments are in order. First, when long mean-free-path effects on the electron response are included, as in Chapter IV, one finds that the parallel resistivity may not be small enough to justify Eq. (5.43). This issue is discussed further in Section D. Second, the pertinent exterior equation, Eq. (5.5), is independent of the size of η or $E_\parallel$: it only requires $\omega << k_\parallel(r)v_A$ - a rather weak constraint since $k_\parallel$ is relatively large outside the layer.

In other words, it is the absence of a boundary layer, rather than the absence of dissipation, which properly characterizes the ideal kink. Equation (5.5) is more robust than Eq. (5.43).

We next consider salient properties of the ideal kink. Equations (5.6) and (5.7) specify two distinct ways in which boundary-layer formation can be avoided. The first way, $J_0'(r_s) = 0$, is most easily achieved when the singular surface lies in a vacuum region, separating the plasma boundary from a conducting liner. The corresponding perturbations involve helical deformation of the plasma boundary [15], without constraint on $\psi(r_s)$. Called "free-boundary" or "external" kink

modes, their evolution is fairly well understood, even nonlinearly [33]. However, external modes are rarely amenable to any local analysis.

In the absence of a vacuum region (that is, when the plasma boundary coincides with a conducting wall), Eq. (5.6) is unlikely to pertain, so that the relevant, "internal" kink-modes are constrained by Eq. (5.7). In this case it is instructive to write

$$\psi(r) = rk_{\parallel}\xi(r) \tag{5.44}$$

where $\xi \propto k_{\perp}\varphi$ measures the radial plasma displacement, and must therefore be everywhere finite. To express Eq. (5.5) concisely in terms of ξ, we note that

$$J_0 = \frac{1}{r}\frac{\partial}{\partial r}\, r\, \frac{\partial \psi_0}{\partial r} \ .$$

Hence, in view of Eqs. (4.151) and (4.152),

$$k_{\perp}J_0' = -\frac{1}{r}\frac{\partial}{\partial r}\left[\frac{1}{r}\frac{\partial}{\partial r}\,(r^2k_{\parallel})\right] \ . \tag{5.45}$$

After some manipulation, Eqs. (5.44) and (5.45) allow us to express Eq. (5.5) as

$$(r^3k_{\parallel}^2\xi')' + k_{\parallel}^2 r(1-m^2)\xi = 0 \ . \tag{5.46}$$

The key feature here is the $(1-m^2)$ factor, showing that internal modes with unit poloidal mode number have special stability properties [81].

Let us multiply Eq. (5.46) by ξ and integrate over r. After partial integration, we find that

$$\int_0^1 dr\ r^3 k_\parallel^2 (\xi')^2 = \int_0^1 dr\ r\ k_\parallel^2 (1-m^2)\xi^2 \ . \tag{5.47}$$

Since, by Eq. (5.46), ξ can be presumed real, the left-hand side of Eq. (5.47) is necessarily positive, while the right-hand side is negative unless m=1: Eq. (5.46) has acceptable solutions only for m=1. Recalling that marginal stability depends upon the existence of neighboring equilibria, we conclude that internal kink modes with m>1 are stable in reduced MHD.

Equation (5.46) also shows that the marginally stable m=1 internal kink is characterized by a constant radial displacement, $\xi' = 0$, on both sides of the rational surface. Since $\xi(1)$ must vanish for internal modes, we can construct a non-vanishing ξ only by allowing for discontinuity at $r=r_s$. The structure of this discontinuity can be resolved, within the context of ideal theory, by including inertia in Eq. (5.46) [81]. The resulting "inertial layer" has width x_A; dissipation is not involved since Eq. (5.7) is satisfied.

Since the minimum q-value is only slightly less than one in a tokamak, $m=1 \Longrightarrow n=1$ and the relevant singular surface corresponds to q=1, near the magnetic axis. Hence one expects m=1 kink activity to be concentrated in a small radial domain, enclosing the magnetic axis, where $q \lesssim 1$. Indeed, such activity is almost universally observed in tokamak experiments; it significantly limits confinement in the central region. However, the observed oscillations seem very likely to involve

dissipative boundary layers: m=1 tearing instability, rather than the ideal kink.

The m=1 case remains distinctive in the dissipative case. Consider the near-axis region where $x<0$ but $|x| >> w$. There, ξ is approximately constant and Eq. (5.44) holds, so that

$$\psi \simeq (\text{const.})x \tag{5.48}$$

Comparing Eqs. (5.16) and (5.48), we see that A_0 vanishes for m=1 perturbations. Thus, as we noted previously, m=1 tearing modes must have large Δ'.

We next consider the role of current gradients in the analysis of small-Δ' tearing modes. There are three regions of interest. In the far exterior region, $|x| >> w$, the global structure of J_0' determines the value of Δ'; we don't attempt to calculate Δ' here, but remark that m^2 terms are strongly stabilizing, as in Eq. (5.46), so that Δ' is usually negative for m larger than two or three. Proceeding to smaller values of $|x|$, we next come to the "matching region", described by the small-$|x|$ limit of Eq. (5.5):

$$k_\parallel' x\psi'' + k_\perp J_0'\psi \simeq 0 \ . \tag{5.49}$$

Finally, the description of the layer interior ($|x| \lesssim w$) differs from Eq. (5.49) only in that inertia must be retained:

$$-\omega\varphi'' + k_\parallel' x\psi'' + k_\perp J_0'\psi \simeq 0 \ . \tag{5.50}$$

Consider first Eq. (5.49). Its solution can be written as

$$\psi = A_0 + A_{\pm}x - \frac{k_\perp J_0'}{k_\parallel'} A_0 \, x\ell n|x| + O(x^2) \ .$$

The logarithmic term appearing here is characteristic of current-driven modes. It corrects Eq. (5.16), but not very seriously, because $x\ell n|x| \sim x$ for any physically relevant range of x.

The modified interior equation, Eq. (5.50), is more interesting. Of course it corrects Eq. (5.10). To estimate the importance of the new term, we compare it to the line-bending term:

$$k_\perp J_0'\psi/(k_\parallel' x\psi'') \sim k_\perp J_0'/(k_\parallel'\Delta') \sim (\Delta')^{-1} \ . \qquad (5.51)$$

Evidently, current gradients are not negligible inside the layer for small Δ'.

Let us combine Eq. (5.50) with the usual closure relation, Eq. (5.11), and attempt to solve the coupled system. Notice that the J_0'-term breaks the reflection symmetry of Eqs. (5.10) and (5.11): it couples the odd and even modes. Partly for this reason, our previous reduction to a single second order equation is no longer rigorously applicable. However, Eq. (5.51) allows limited use of the constant-ψ approximation: we replace the last term of Eq. (5.50) by $k_\perp J_0' A_0$. Then straightforward generalization of our previous treatment yields the eigenmode equation

$$E[1 - (\frac{k_\parallel' x}{\omega})^2] - \frac{ix^2}{\omega}\left(\frac{\eta E'}{x^2}\right)'$$

$$= -\frac{C}{\omega} + \frac{k_\perp' J_0' A_0 k_\parallel'}{\omega}\left(x + \frac{2i\eta}{\omega x}\right) . \qquad (5.52)$$

Similarly, we can compute

$$A_0\Delta' = \int dx \frac{\omega}{k_\parallel' x}\left(E' + \frac{k_\perp J_0' A_0}{\omega}\right) . \qquad (5.53)$$

Equation (5.52) shows that J_0' drives an odd contribution, $E_-(x)$, to E. This odd piece removes the singularity in the integrand of Eq. (5.53),

$$E_-'(0) = -k_\perp J_0' A_0/\omega ,$$

without affecting the value of Δ'. Thus the tearing mode dispersion relation can depend only upon E_+, which is unaffected by J_0'. We conclude that the current-gradient or kink-term, while not necessarily small, is safely neglected in the interior analysis of a tearing layer [56].

C. Boundary layers with pressure

1. Introduction

We have seen that at low beta the shear-Alfvén law describes a balance between line-bending and gradients in the

equilibrium current. Rational surface singularity (q=m/n) corresponds to vanishing of the line-bending term and leads to boundary-layer structures, inside of which plasma inertia becomes important. Because q is a flux function, the boundary layer adheres to a well defined flux surface and the radial mode structure is of dominant importance. In other words, the strictly radial dependence of q implies a predominantly radial dependence of all the perturbed fields.

The situation at higher beta, when the interchange term becomes comparable to line bending, can be quite different. The point is that neither $\underset{\sim}{\kappa}$ nor (in general) the perturbed pressure are flux functions; hence the shear-Alfvén dynamics need not be dominated even approximately by radial variation. Partly for this reason, the analysis of pressure-driven modes is relatively complicated, and the resulting dispersion relations are typically very sensitive to magnetic field geometry.

Another reason for the relative complexity of pressure-driven modes is obvious: they require at least one additional coupled equation, to determine the evolution of pressure perturbations.

In this section we consider the simplest variety of pressure-driven modes: the boundary-layer modes, for which the perturbed field structure remains approximately one-dimensional. Thus we consider pressure-modified tearing instability, as well as radially localized interchange modes. It will be seen that even in the boundary-layer case, the inherent multi-dimensionality of the interchange term entails relatively elaborate manipulation. In fact, the main burden of pressure-driven mode analysis is the extraction of

coupled ordinary differential equations from the original partial-differential-equation system.

We note in passing that the extraction procedure can be obviated by replacing the curvature force by an artificial, constant gravitational force. Such "g-models" can give rapid qualitative insight into interchange effects. However, because they involve uncontrolled approximation, they are not reviewed here.

Pressure-driven modes which are not radially localized (such as ballooning modes) must be analyzed using the more general scale-separation arguments of Chapter VI.

2. Linearization

In order to include compressibility, this section uses the four-field model, rather than reduced MHD. Our analysis is simplified by the neglect of FLR terms (δ=0) and by equating the two species temperatures. Then Eqs. (4.143)-(4.146) become

$$\dot{U} + [\varphi,U] + \nabla_{\parallel}J + 2[h,p_e] = 0 \tag{5.54}$$

$$\dot{\psi} + \nabla_{\parallel}\varphi = \eta J \tag{5.55}$$

$$\dot{v} + [\varphi,v] + \nabla_{\parallel}p_e = 0 \tag{5.56}$$

$$\dot{p}_e + [\varphi,p_e] = \beta\left(2[h,\varphi] - \nabla_{\parallel}v + \eta\nabla_{\perp}^2 p_e\right) . \tag{5.57}$$

When δ=0, the four-field equilibrium coincides with that of reduced MHD. We recall from Eq. (4.148) that pressure distorts the flux surfaces, with respect to concentric circular geometry. Hence flux coordinates, (r_f,ϑ_f,ζ), become appropriate. Here, r_f is a normalized radius which labels equilibrium surfaces:

$$r_f = r_f(\psi_0)$$

while ϑ_f is chosen such that

$$q(r_f) = \underset{\sim}{B}\cdot\nabla z/\underset{\sim}{B}\cdot\nabla\vartheta_f \ .$$

(We have noted that the reduced coordinate z coincides with the symmetry angle ζ.) Linear theory is often simplified by replacing z by the approximate field line label

$$u \equiv z - q_s\vartheta_f$$

where

$$q_s = m/n$$

is the rational safety factor of the relevant mode-rational surface. This section uses the coordinates (r_f,ϑ_f,u) exclusively; the f-subscripts are hereafter suppressed.

Recall that the bracket in Eqs. (5.54)-(5.57) is defined by

$$[F,G] = \nabla z\cdot\nabla F\times\nabla G \ .$$

We introduce the Jacobian

$$\nabla z\cdot\nabla r\times\nabla\vartheta = \nabla u\cdot\nabla r\times\nabla\vartheta \equiv 1/\sqrt{g}$$

in order to write

$$[F,G] = [F,G]_* + \frac{q_s}{\sqrt{g}}\left(F_u G_r - F_r G_u\right) \tag{5.58}$$

where

$$[F,G]_* \equiv \frac{1}{\sqrt{g}}\left(F_r G_\vartheta - F_\vartheta G_r\right)$$

and the subscripts indicate partial differentiation.

In order to linearize the bracket, we note that the equilibrium quantities can depend only on r and ϑ, by axisymmetry. (Even in asymmetric geometry, the same assumption is conventional, as an approximation based on scale-length separation.) Thus the variable u is cyclic and we have

$$f = \hat{f}(r,\vartheta)\exp(-inu) \ . \tag{5.59}$$

The perpendicular wave vector is defined in analogy to Eq. (4.153):

$$k_\perp \equiv m/\sqrt{g}$$

whence

$$f_u = -inf = -i\left(\sqrt{g}/q_s\right)k_\perp f \ .$$

Then, if $G_0(r,\vartheta)$ is any equilibrium quantity, we have

$$[G_0,f] = [G_0,f]_* + ik_\perp G_{0r} f \ .$$

The linearized parallel gradient operator is slightly more complicated, due to the contribution from the equilibrium flux, ψ_0. We use the simplified notation,

$$\psi \to \psi_0+\psi$$

so that, below, ψ refers to the linear perturbation of the total flux. The same convention will be used for the other field variables: $p_e \to p_0+p$, etc. The normalized parallel wave vector,

$$k_\parallel = \left(\frac{1}{q} - \frac{1}{q_s}\right) \sqrt{g}\, k_\perp = m/q-n$$

generalizes Eq. (4.152) and yields the linear expression

$$\nabla_\parallel (f_0+f) = ik_\parallel f + \frac{1}{q} f_\vartheta - [\psi, f_0]_* + ik_\perp f_{0r}\psi \ . \qquad (5.60)$$

It is important to notice that the Jacobian is a flux function in reduced geometry:

$$\sqrt{g} = \sqrt{g}\ (r) \ .$$

This follows from the relation

$$1/q = -\psi_{0r}/\sqrt{g} \qquad (5.61)$$

and the fact that q and ψ_0 depend only on r.

We use Eqs. (5.58)-(5.61) to write the linearized equations as follows:

$$-i\omega U+ik_{\parallel}J+J_{\vartheta}/q - [\psi,J_0]_*+ik_{\perp}J_{0r}\psi + 2[h,p]_* + 2ik_{\perp}h_r p = 0 \tag{5.62}$$

$$-i\omega\psi+ik_{\parallel}\varphi + \varphi_{\vartheta}/q = \eta J \tag{5.63}$$

$$-i\omega v+ik_{\parallel}p+p_{\vartheta}/q - [\psi,p_0]_*+ik_{\perp}p_0'\psi = 0 \tag{5.64}$$

$$-i\omega p+[\varphi,p_0]_*-ik_{\perp}p_0'\varphi = \beta\left(2[h,\varphi]_*+2ik_{\perp}h_r\varphi\right.$$

$$\left.-ik_{\parallel}v-v_{\vartheta}/q+\eta\nabla_{\perp}^2 p\right) . \tag{5.65}$$

Note also, from Eq. (2.76), that

$$\begin{pmatrix} U \\ J \end{pmatrix} = \frac{1}{\sqrt{g}}\frac{\partial}{\partial\xi^{\mu}}\sqrt{g}\,\nabla\xi^{\mu}\cdot\nabla\begin{pmatrix}\varphi\\ \psi\end{pmatrix} \tag{5.66}$$

with $(\xi^1,\xi^2) = (r,\vartheta)$.

3. Boundary layer ordering

Equations (5.62)-(5.66) are more complicated than their low-beta counterparts essentially because they lack poloidal symmetry: the curvature function h (and therefore J_0) varies with ϑ. Thus, for each fixed helical harmonic n, the linear eigenmodes will involve a number of coupled poloidal harmonics. In the notation of Eq. (5.59), we can write

$$\hat{f}(r,\vartheta) = \sum_{m'} f_{m'}(r)\exp(im'\vartheta) . \tag{5.67}$$

For prescribed $\psi_0(r)$, one could compute $h(r,\vartheta)$, thus making explicit

all the poloidal couplings in Eqs. (5.62)-(5.66), and then solve the resulting system for each $f_{m'}$. Such a brute-force procedure would have general validity, but would be extremely complicated. For the boundary-layer modes of present interest, it would be difficult to carry out even numerically, because of the disparate scale lengths involved.

We therefore consider an alternative approach [82], which grossly simplifies Eqs. (5.62)-(5.66) by exploiting the disparity in scale-lengths. This approach applies only to modes having distinct boundary layers and in fact concentrates its attention on the boundary-layer interior. It is based on the assumption that the radial scale-length of the perturbation is shorter than any other length in the system: the "boundary-layer ordering",

$$w \ll 1 \quad , \quad k_\perp \sim 1 \ . \tag{5.68}$$

Application of the boundary-layer ordering does not require <u>a priori</u> knowledge of ψ_0 or $h(r,\vartheta)$, and does not use Eq. (5.67) for f. We write instead

$$\hat{f} = \bar{f}(r) + \tilde{f}(r,\vartheta) \ .$$

where

$$\bar{f} = \langle \hat{f} \rangle$$

with

$$\langle A \rangle = \oint \frac{d\vartheta}{2\pi} A = \bar{A} \ .$$

Of course $\bar{f}$ coincides with the $m'=0$ term in Eq. (5.67); it describes that component of f which depends on ϑ only through u and which is therefore resonant at the rational surface, $q=q_s$. The purpose of the boundary-layer ordering is to reduce Eqs. (5.62)-(5.66) to a closed set of four coupled ordinary differential equations for the resonant field components, $\bar{\psi}$, $\bar{\varphi}$, $\bar{p}$ and $\bar{v}$. Solution of this coupled system remains a formidable task, and in fact usually requires additional approximation. But at least the problem has been reduced to one-dimensional form.

Equation (5.68) alone does not define a boundary-layer ordering; one must also order the various parameters and fields with respect to w. There is more than one internally consistent way to choose such ancillary orderings; different choices affect intermediate steps in the calculation but yield equivalent results. A relatively simple choice [83] is defined by Eqs. (5.68), together with

$$\omega \sim w \quad , \quad \eta \sim w^3 \tag{5.69}$$

$$k_{\|} \sim w \quad , \quad \beta \sim 1$$

$$\partial f/\partial r \sim f/w \tag{5.70}$$

$$\varphi \sim \psi \sim w \ ; \ p \sim v \sim 1 \ ; \ J \sim U \sim w^{-1} \ .$$

In Eq. (5.70), f represents a field perturbation; for equilibrium quantities we have instead

$$\partial f_0/\partial r \sim f_0 \ .$$

Inspection shows these assumptions to be consistent with Eqs. (5.62)–(5.66). Notice that Eqs. (5.69) imply $\omega \sim \eta^{1/3}$ and therefore correspond to the large–Δ' case of Eq. (5.37); this is convenient for technical reasons and, as shall be seen, does not prevent treatment of small–Δ' modes.

4. Derivation of layer equations

We begin our derivation of simplified equations for the layer interior by computing the ϑ–averages (at fixed r and u) of Eqs. (5.62)–(5.66). Using the identities

$$\bar{f}_\vartheta = 0 = \overline{[\bar{g}, f]_*}$$

together with the boundary–layer ordering, we find that

$$\omega\bar{U} - k_\parallel \bar{J} + i\overline{[\tilde{J}_0, \psi]_*} + 2i\overline{[\tilde{h}, p]_*} - 2k_\perp \overline{h_r p} = O(w) \qquad (5.71)$$

$$\omega\bar{\psi} - k_\parallel \bar{\varphi} = i\eta\bar{J} \qquad (5.72)$$

$$\omega\bar{v} - k_\parallel \bar{p} - k_\perp p_0' \bar{\psi} = 0 \qquad (5.73)$$

$$\omega\bar{p} + k_\perp p_0' \bar{\varphi} = \beta\{2i\overline{[\tilde{h}, \varphi]_*} - 2k_\perp \overline{h_r \varphi} + k_\parallel \bar{v} + i\eta\overline{\nabla_\perp^2 p}\} \ . \qquad (5.74)$$

Our objective is to eliminate the non–resonant field perturbations, $\tilde{f}$, from Eqs. (5.71)–(5.74). Notice that these appear both explicitly and implicitly, through Eq. (5.66). For example, from Eq. (5.70),

$$J = |\nabla r|^2 \psi_{rr} + O(1) \qquad (5.75)$$

where the first term on the right-hand side is $O(w^{-1})$. Since ∇r depends on ϑ,

$$\bar{J} = \overline{|\nabla r|^2}\ \overline{\psi_{rr}} + \langle|\nabla r|^2\tilde{\psi}_{rr}\rangle \ .$$

We next calculate the non-resonant fields by considering the lowest order terms in Eqs. (5.62)-(5.66). These are easily seen to imply

$$\frac{1}{q}\,\tilde{J}_\vartheta - \frac{1}{\sqrt{g}}\,\tilde{h}_\vartheta p_r = O(1)$$

$$\tilde{\varphi}_\vartheta = O(w^2),\ \tilde{p}_\vartheta = O(w)$$

$$-\frac{2}{\sqrt{g}}\,\tilde{h}_\vartheta \varphi_r - \frac{1}{q}\,\tilde{v}_\vartheta = O(w)$$

whence

$$\tilde{J} = \frac{2q}{\sqrt{g}}\,\bar{p}_r\tilde{h} + O(1) \qquad (5.76)$$

$$\tilde{\varphi} = O(w^2),\ \tilde{p} = O(w) \qquad (5.77)$$

$$\tilde{v} = \frac{-2q}{\sqrt{g}}\,\bar{\varphi}_r\tilde{h} + O(w) \ . \qquad (5.78)$$

As an example of the application of these formulae, we return to Eq. (5.75), which implies

$$\bar{\psi}_{rr} = \bar{J}\langle|\nabla r|^{-2}\rangle + \langle\tilde{J}|\nabla r|^{-2}\rangle$$

or, in view of Eq. (5.76),

$$\bar{J} = \langle |\nabla r|^{-2} \rangle^{-1} [\bar{\psi}_{rr} - \frac{2q}{\sqrt{g}} \langle \frac{\tilde{h}}{|\nabla r|^2} \rangle \bar{p}_r] \quad . \tag{5.79}$$

Thus, even for δ=0, the perturbed radial pressure gradient enters the reduced Ohm's law, Eq. (5.72), essentially through the perturbed return current; compare Eqs. (5.76) and (4.148).

The relation between U and φ is much simpler, because of Eq. (5.77). One finds

$$\bar{U} = \overline{|\nabla r|^2}\, \bar{\varphi}_{rr} + O(1) \quad .$$

The other $\tilde{f}$-contributions in Eqs. (5.71)-(5.74) can be eliminated, in favor of $\bar{f}$, in a similar manner. We consider in detail only the most complicated step, involving the two bracket terms in Eq. (5.71). Denoting these terms by

$$X = \langle [\tilde{J}_0, \psi]_* \rangle + 2 \langle [\tilde{h}, p]_* \rangle$$

we have, after partial integration,

$$\sqrt{g}\, X = 2 \langle h (\frac{q}{\sqrt{g}}\, p_0' \tilde{\psi}_{r\vartheta} + \tilde{p}_{r\vartheta}) \rangle \quad .$$

To evaluate the average, we use the O(w) form of Eq. (5.64) to deduce that

$$\tilde{p}_\vartheta + \frac{qp_0'}{\sqrt{g}}\tilde{\psi}_\vartheta = i\omega q\tilde{v} - iqk_\perp p_0'\tilde{\psi} + O(w^2)$$

and therefore that

$$\sqrt{g}\ X = 2iq\ \langle\tilde{h}(\omega\tilde{v}_r - k_\perp p_0'\tilde{\psi}_r)\rangle\ .$$

Here the term involving ψ can be found from Eq. (5.75), with the result,

$$\langle\tilde{h}\tilde{\psi}_r\rangle = \langle|\nabla r|^{-2}\rangle^{-1}\langle\tilde{h}|\nabla r|^{-2}\rangle\ \bar{\psi}_r + \frac{2q}{\sqrt{g}}\bar{p}[\langle\tilde{h}^2|\nabla r|^{-2}\rangle - \langle|\nabla r|^{-2}\rangle^{-1}\ \langle\tilde{h}|\nabla r|^{-2}\rangle^2]$$

while the v_r-term can be computed from Eq. (5.78). Thus one finds

$$\sqrt{g}\ X = \frac{-4iq^2}{\sqrt{g}}[\omega\bar{\varphi}_{rr}\langle\tilde{h}^2\rangle + k_\perp p_0'\bar{p}(\langle\frac{\tilde{h}^2}{|\nabla r|^2}\rangle - \langle|\nabla r|^{-2}\rangle^{-1}\ \langle\frac{\tilde{h}}{|\nabla r|^2}\rangle^2)]$$

$$- \frac{2ik_\perp qp_0'}{\langle|\nabla r|^{-2}\rangle}\langle\frac{\tilde{h}}{|\nabla r|^2}\rangle\ \bar{\psi}_r$$

and Eq. (5.71) becomes

$$\omega M\bar{\varphi}_{rr} - k_\parallel\bar{\psi}_{rr} - H(k_\parallel\bar{p}_r + k_\perp p_0'\bar{\psi}_r) + 2k_\perp K\bar{p} = 0 \qquad (5.80)$$

where

$$M = \langle|\nabla r|^{-2}\rangle\langle|\nabla r|^{2}\rangle \left(1 + \frac{4q^2}{g}\frac{\langle\tilde{h}^2\rangle}{\langle|\nabla r|^{2}\rangle}\right) ,$$

$$H = -\frac{2q}{\sqrt{g}}\langle\tilde{h}|\nabla r|^{-2}\rangle$$

$$K = \langle|\nabla r|^{-2}\rangle\left[\frac{2q^2}{g}p_0'\left(\langle\tilde{h}^2|\nabla r|^{-2}\rangle - \langle|\nabla r|^{-2}\rangle^{-1}\langle|\nabla r|^{-2}\tilde{h}\rangle^{2}\right) - \bar{h}_r\right] . \quad (5.81)$$

The quantity K measures the averaged curvature; its last term represents the vacuum curvature,

$$\underset{\sim}{\kappa}_v = -\nabla h$$

while the remaining terms give diamagnetic corrections.

The other averaged equations are much easier to simplify and we present only the results. One finds that Eqs. (5.72)-(5.74) become, for small w,

$$\omega\bar{\psi} - k_{\parallel}\bar{\varphi} = \frac{i\eta}{\langle|\nabla r|^{-2}\rangle}\left(\bar{\psi}_{rr} + H\bar{p}_r\right) \quad (5.82)$$

$$\omega\bar{v} - k_{\parallel}\bar{p} - k_{\perp}p_0'\bar{\psi} = 0 \quad (5.83)$$

$$\omega\bar{p} + k_{\perp}p_0'\bar{\varphi} = \beta\left(-2k_{\perp}\bar{h}_r\bar{\varphi} + k_{\parallel}\bar{v} + i\eta\langle|\nabla r|^{2}\rangle\bar{p}_{rr}\right) . \quad (5.84)$$

Equations (5.80)-(5.84) provide a closed set for the four averaged, or resonant, fields.

5. Discussion

Equations (5.80)–(5.84) differ from the low-beta eigenmode equations, Eqs. (5.3) and (5.4), because they include various effects of pressure and toroidal curvature. The salient difference is the appearance in Eq. (5.80) of the interchange term, proportional to K. Notice that the kink term is absent, due to our use of the large-Δ' ordering. The quantity H, which reflects variation of B on the magnetic surface, changes the form of both the shear-Alfvén law and the Ohm's law, Eq. (5.82). Finally compressibility affects the evolution of pressure, requiring an additional equation for v, and various coefficients, such as that of the inertial term in Eq. (5.58), are modified by curvature. Here, before attempting to solve Eqs. (5.80)–(5.84), we comment on the significance of the functions H and K.

Consider first the ideal modes without compressibility. When η and β vanish, Eqs. (5,82) and (5.84) can be combined to yield

$$k_{\|}\bar{p} = -k_{\perp}p_0'\,\bar{\psi} \tag{5.85}$$

which is the linearized expression of $\underset{\sim}{B}\cdot\nabla p = 0$. The point is that both ψ and p are advected by the same $\underset{\sim}{E}\times\underset{\sim}{B}$ flow, so the pressure remains a flux function in the perturbed state. Recalling that ideal stability depends upon the existence of neighboring equilibria, we neglect inertia ($\omega\to 0$) in Eq. (5.80), and eliminate p by means of Eq. (5.85). The result can be expressed as

$$-k_{\|}\bar{\psi}_{rr} + k_{\perp}p_0'[Hk_{\|}(1/k_{\|})_r - 2k_{\perp}K/k_{\|}]\bar{\psi} = 0$$

or, after using Eq. (5.9) for $k_{\|}$, as

$$(k_{\|}')^2 x^2\bar{\psi}'' + k_{\perp}p_0'(Hk_{\|}'+2k_{\perp}K)\bar{\psi} = 0 \qquad (5.86)$$

where the primes indicate derivatives with respect to radius (or x) and all equilibrium quantities are to be evaluated at r_s.

Equation (5.86), describing localized, ideal interchange modes, is the analogue of the kink-mode neighboring equilibrium relation, Eq. (5.5). We have simply replaced the kink driving term by the interchange term. Note that the interchange version is simpler because it is local and therefore depends on radius, through x, in a simple and explicit way. [Recall that Eq. (5.5) cannot be solved without global knowledge of the equilibrium current profile.] Of course both equations are subject to the Newcomb condition,

$$\psi(r_s) = 0 \ . \qquad (5.87)$$

in order to avoid singularity in the perturbed current.

Because Eq. (5,86) is equidimensional, its solution is easily written down:

$$\bar{\psi} = c_+x^{\alpha_+} + c_-x^{\alpha_-}$$

where the $c_{\pm}$ are constants,

$$\alpha_{\pm} = \frac{1}{2} \pm \frac{1}{2}\sqrt{1-4\Delta_I} \qquad (5.88)$$

and

$$\Delta_I = \frac{2k_\perp^2 p_0'}{(k_\parallel')^2} K_I$$

with

$$K_I = K + \frac{k_\parallel'}{2k_\perp} H$$

When $\alpha_\pm$ is complex, this solution oscillates and can be localized by choosing it to vanish for all x beyond its first zero. For real $\alpha_\pm$, however, it can be seen that any solution satisfying Eq. (5.87) must grow algebraically with x: a localized solution does not exist. The stability condition is therefore $\mathrm{Im}(\alpha_\pm) = 0$, or

$$\Delta_I - \frac{1}{4} < 0 \ . \qquad (5.89)$$

In this condition, the 1/4 can be traced back to the line-bending term in Eq. (5.86). It therefore is said to reflect shear-stabilization of the ideal interchange. This stabilizing mechanism was first noted, in cylindrical geometry, by Suydam [84].

The unreduced version of Eq. (5.89) is derived in Chapter VI. Called the Mercier condition [8.85], it can be expressed as

$$D_I - \frac{1}{4} < 0$$

where the quantity D_I differs from Δ_I essentially by including higher

aspect-ratio order terms in the averaged curvature. Under the high-beta assumption, Eq. (4.119), the higher order terms yield relatively small corrections to Δ_I. At low beta, however, these corrections can be of critical importance. For example, in the Shafranov equilibrium (recall Sec. D of Chapter II) $\bar{h}_r (<<h_r)$ becomes $O(\varepsilon^2)$ and therefore comparable to terms, such as the contribution to K from poloidal curvature, which Eqs. (4.24) and (5.81) omit. Thus Δ_I is not a reliable stability parameter in the low-beta case.

The quantity H enters ideal theory only through K_I. More generally, Eqs. (5.80)-(5.84) show that H is significant by itself [82]; in fact, it severely complicates solution of the resistive, compressible equations [83]. Fortunately, the most important effect of H on resistive instability is easily described, at least in typical parameter regimes. One finds that the measure of magnetic curvature appropriate to the resistive case is not K_I, but rather

$$K_R \equiv K + \frac{1}{2} p_0' H^2 \ .$$

Notice here that the H^2 term cancels a term in Eq. (5.81), leaving the modified average curvature,

$$K_R = \langle |\nabla r|^{-2} \rangle \left[\frac{2q^2}{g} p_0' \langle \tilde{h}^2 |\nabla r|^{-2} \rangle - \bar{h}_r \right] \ . \qquad (5.90)$$

We will comment presently on the origin of the quantity K_R.

6. Subsidiary ordering

We consider next the solution to Eqs. (5.80)-(5.84). Appropriate rescaling allows one to replace most of the coefficients in these equations by unity. However, since the rescaled equations are not perspicuous, we simply suppress factors of M and $|\nabla r|$. We also denote $-\bar{h}_r$ by K_v, since it measures the vacuum curvature, and restrict our attention, initially, to the H=0 case. Thus we consider the eigenmode equations (overbars are suppressed),

$$ix_A\varphi'' - x\psi'' + \frac{2k_\perp}{k_\parallel'} Kp = 0 \tag{5.91}$$

$$ix_A\psi - x\varphi = ix_R^2\, x_A\psi'' \tag{5.92}$$

$$ix_A v - xp = \frac{k_\perp p_0'}{k_\parallel'}\,\psi \tag{5.93}$$

$$ix_A p + \frac{k_\perp p_0'}{k_\parallel'}\,\varphi = \beta\left(\frac{2k_\perp}{k_\parallel'} K_v\,\varphi + xv + ix_R^2\, x_A p''\right) . \tag{5.94}$$

Here x_R and x_A are the resistive and Alfvén lengths defined by Eqs. (5.32) and (5.33) respectively.

Consider first Eq. (5.94). It is convenient to express the left-hand side as

$$ix_A p + \frac{k_\perp p_0'}{k_\parallel'}\,\varphi = \frac{k_\perp p_0'}{k_\parallel'}\,(\varphi - p_*)$$

where

$$p_* = - \frac{ik_\parallel' x_A}{k_\perp p_0'} p \ .$$

Thus $p_*=\varphi$ in the incompressible case. On the right-hand side of Eq. (5.94), we use Eq. (5.93) to eliminate v, and find that the expression in brackets is proportional to

$$\mathscr{L}_R p_*' + i \frac{x}{x_A} \psi - \frac{2K_v}{p_0'} \varphi$$

where the operator

$$\mathscr{L}_R \equiv x_R^2 \nabla_\perp^2 - x^2/x_A^2$$

is characteristic of resistive modes. We noted in Sec. B that the layer width scales as $w = (x_R x_A)^{1/2}$; hence the two terms in $\mathscr{L}_R$ are comparable, and

$$\mathscr{L}_R \sim x_R/x_A \ . \tag{5.95}$$

With regard to the shear-Alfvén law, Eq. (5.91), it is convenient to eliminate ψ'' by means of Eq. (5.92). Then, after straightforward manipulation, we obtain the following system:

$$\mathscr{L}_R \psi = i \frac{x}{x_A} \varphi + \left(1 - \frac{x^2}{x_A^2}\right) \psi \tag{5.96}$$

$$\mathscr{L}_R\varphi = -i\,\frac{x}{x_A}\,\psi - \frac{x_R^2}{x_A^2}\,Dp_* \tag{5.97}$$

$$\mathscr{L}_R p_* = -i\,\frac{x}{x_A}\,\psi + \frac{2K_v}{p_0'}\,\varphi + \frac{1}{\beta}\,(p_*-\varphi) \tag{5.98}$$

where

$$D = \frac{2k_\perp^2 p_0' K}{(k_\parallel')^2} \tag{5.99}$$

is the relevant measure of curvature.

Equations (5.96)–(5.98) define a sixth order system. It can be solved numerically (even with $H\neq 0$) [86], but analytical progress requires further approximation. Thus one takes advantage of the fact that the two equilibrium parameters, β and D, are both smaller than unity under experimental conditions of interest. The remaining important parameter, x_A/x_R, occurred also in the low-beta theory of Sec. B. It depends on the linear growth rate but is extremely small except in the case of large-Δ' modes. Since Eq. (5.97) shows that large-Δ' modes are hardly affected by D, we assume here that

$$x_A/x_R \ll 1 \tag{5.100}$$

and thus avoid repeating the discussion of Sec. B. Then, in order to study competition between curvature effects and the resistive diffusion contained in $\mathscr{L}_R$, we allow

$$D \sim x_A/x_R \tag{5.101}$$

which implies $\left(\frac{x_R}{x_A}\right)^2 D \sim \mathscr{L}_R$, in view of Eq. (5.95).

The remaining ordering issue concerns β, or compressibility. The two limiting cases,

$$\beta x_R/x_A << 1$$

and

$$\beta x_R/x_A >> 1 \tag{5.102}$$

can be seen, from Eq. (5.98), to correspond to incompressible and compressible perturbations respectively. Because $p_*=\varphi$ in the incompressible case, neglecting β yields a fourth order, rather than sixth order, system. In this sense, compressibility is a singular perturbation, which can be expected to have striking effects even when it is small. We adopt the compressible ordering here, assuming $\beta\sim1$, both because Eq. (5.102) is more consistent with modern toroidal experiments, and because it yields more interesting results.

We remark that the "maximal" β-ordering, $\beta x_R/x_A\sim1$, has also been studied [87]. It yields results more complicated than, but qualitatively similar to, Eq. (5.102).

Equations (5.100)-(5.102) define what has been called the "subsidiary ordering" [83].

7. Dispersion relation

Systematic application of the subsidiary ordering yields a sequence of coupled equations, which must be solved order by order. A dispersion relation is obtained by matching the ordered layer solutions to those which describe the exterior region. Our procedure will be less rigorously convincing, but much shorter and perhaps more instructive. After commenting upon special features of the matching problem in the interchange case, we will solve Eqs. (5.96)–(5.98) by means of the scaling arguments introduced in Sec. B.

The exterior region is defined by $|x| \gg x_A$, x_R and w, and by $\nabla_\perp^2 \sim 1$, whence $\mathscr{L}_R \sim -x^2/x_A^2$. Then Eqs. (5.96) and (5.98) combine to show that $\psi = -i \frac{x}{x_A} \varphi$ and $p_* = \varphi$ outside the layer. Notice that we did <u>not</u> use incompressibility to obtain these results. The neighboring equilibrium equation is obtained by first dividing Eq. (5.97) by x_R^2, then eliminating $\psi + i(x/x_A)\varphi$ by means of the Ohm's law, and finally neglecting inertia. The result is

$$x^2\psi'' + D\psi = 0 \ ,$$

analogous to Eq. (5.86). The exterior solution is therefore a linear combination of two algebraic terms, with powers given by the two roots of Eq. (5.88). For D=0, these solutions naturally reduce to Eq. (5.16) of the low-beta case; for $D \neq 0$, however, it can be seen that one of the terms is singular, having an infinite derivative in the $x \to 0$ limit. It is this singularity which primarily distinguishes exterior solutions in the interchange case.

The singularity explains why the formal large-Δ' ordering represented by Eq. (5.69) is most appropriate for high-beta boundary layers: the interchange term forces ψ' to become large for small x. Evidently, the singularity requires a generalized definition of Δ', since the asymptotic slopes are no longer well defined. Thus Δ' is redefined in terms of the difference between ratios of the coefficients of the two algebraic terms, evaluated on either side of the boundary layer [83]. We emphasize that the physical interpretation of Δ' is not changed: it still measures the total current flowing through the boundary layer, as in Eq. (5.22). Moreover, since the subsidiary ordering requires D to be small, the redefinition of Δ' only mildly affects the mathematics.

With these remarks in mind, we turn to the dimensional "solution" of the interior system. After integrating Eq. (5.96) across the layer, we obtain

$$x_R^2 \psi_0 \Delta' = \int dx \left(\psi + \frac{ix}{x_A} \varphi \right) . \tag{5.103}$$

Next Eqs. (5.97) and (5.98) are used to determine φ. To lowest order in x_A/x_R, Eq. (5.98) is

$$\mathscr{L}_R p_* = -i \frac{x}{x_A} \psi \tag{5.104}$$

since, in particular, the K_v term can be seen to be $O(x_A^2/x_R^2)$ and negligible. We determine the scaling of φ by using Eq. (5.95) to invert both Eq. (5.97) and Eq. (5.104). One finds that

$$\varphi \sim -i \frac{x}{x_R} \left(1 - \frac{x_R}{x_A} D\right)\psi \ . \qquad (5.105)$$

Of course scaling arguments cannot fix the signs in Eq. (5.105). But the sign of the first term on the right-hand side is known from the D=0 theory, and that of the second is fixed because it involves two consecutive inversions of $\mathscr{L}_R$.

We substitute Eq. (5.105) into Eq. (5.103) and integrate. The integral yields an additional factor of $w \simeq (x_R x_A)^{1/2}$, so we have

$$x_R^2 \Delta' \cong (x_R x_A)^{1/2}\left(1 - \frac{x_R}{x_A} D\right) \ .$$

This approximate dispersion relation agrees with the rigorous version [83], apart from differences in numerical constants. The more perspicuous form,

$$\Delta' w = \frac{x_A}{x_R} - D \qquad (5.106)$$

verifies the consistency of the small-Δ' and subsidiary orderings.

Thus the final result — after use of the boundary-layer ordering, after decoupling the non-resonant field components, and after application of the subsidiary ordering — is to reproduce the familiar small-Δ' dispersion relation, Eq. (5.42), with one additional term. Of course the additional term summarizes interchange effects: the coupling of magnetic curvature with plasma pressure gradients. The

quantity D is positive when the averaged curvature is unfavorable (destabilizing) and negative for favorable curvature. Because prevalent experimental devices, including tokamaks, have $D<0$, Eq. (5.106) most commonly describes the stabilizing influence of curvature on tearing modes. For those devices, such as the reversed field pinch, in which $D>0$, Eq. (5.106) predicts a new instability, the resistive interchange. Both cases are considered in more detail after we comment on the form of D.

The proportionality between D and K shown in Eq. (5.99), is not reliable, even in the context of reduced theory, because H was neglected. As indicated earlier a more accurate version, which includes the most pertinent effects of H, would have K replaced by K_R (it would also include factors of $|\nabla r|$ which we have suppressed). Although the detailed theory with finite H is very complicated, it is not hard to see how K_R enters the result. Consider the averaged Ohm's law, Eq. (5.82). It is evident that the right-hand side includes an overall factor of x_R/x_A compared to the left. Hence the subsidiary ordering implies, in lowest order,

$$\bar{\psi}_{rr} + H\bar{p}_r \simeq 0 \ .$$

After integration this result is substituted into the shear-Alfvén law, Eq. (5.80). Upon noting some cancellations one sees that the coefficient of p becomes proportional to K_R.

We now return to Eq. (5.106), which can be written more explicitly as

$$\Delta' = \left(\frac{\gamma^5}{k_\parallel'^2 \eta^3}\right)^{1/4} - D\left(\frac{k_\parallel'^2}{\eta\gamma}\right)^{1/4} . \qquad (5.107)$$

Identification of the unstable roots of Eq. (5.107) would be trivial if all the roots were known to be real, and it's only mildly complicated by the occurrence of complex roots. By means of either routine examination, or a Nyquist procedure [83], one reaches the following conclusions.

When D>0, Eq. (5.107) has a single unstable root, corresponding to the resistive interchange. Its simplest version occurs in the limit of vanishing Δ', or very small η. Then Eq. (5.106) becomes

$$x_A/x_R \simeq D$$

which implies

$$\gamma \simeq (k_\parallel' D)^{2/3} \eta^{1/3} . \qquad (5.108)$$

The resistive interchange is driven by unfavorable curvature. It differs from the ideal interchange by the replacement of K by K_R and also by the absence of the shear-stabilizing term, 1/4, which appears in Eq. (5.89). (Note, however, that while the stability boundary of the resistive interchange is unaffected by shear, the growth rate diminishes with increasing shear.) It differs from the tearing mode in its scaling and in not requiring $\Delta'>0$ for instability. In fact, as Eq. (5.108) shows, the resistive interchange remains unstable when Δ'

vanishes: while necessarily localized, it does not require the formation of a current layer.

When D<0, Eq. (5.107) displays a striking feature: the right-hand side is bounded away from zero for all (positive) values of γ. It follows that γ can become complex ("overstability" [88]) and, more importantly, that no unstable roots can occur unless Δ' exceeds a certain critical value. Thus, in the presence of favorable curvature and finite pressure, the tearing mode stability condition becomes

$$\Delta' > \Delta_c \tag{5.109}$$

instead of Eq. (5.41).

An estimate of Δ_c can be obtained from Eq. (5.107), by minimizing the right-hand side with respect to γ. One finds that

$$\Delta_c \sim \left(|k_\parallel'|/\eta\right)^{1/3}|D|^{5/6} . \tag{5.110}$$

Since Δ_c turns out to be of significant size (it can be larger than ten) in typical tokamak experiments [89], tearing mode theories which omit the physics of Δ_c, such as the low-beta theory of Sec. B, can be seriously misleading.

The complex, unstable roots of Eq. (5.107) are said to correspond to the "modified" tearing mode [83]. The existence of Δ_c was first noticed in [87]. It is significant that the early investigations of tearing [75,90] included curvature (at least in a gravitational model) and pressure, yet still predicted instability for all positive values of Δ'. This circumstance can be understood by noticing, from Eqs. (5.103)-(5.106), that Δ_c requires more than favorable

curvature: compressibility is also an essential ingredient [83,87]. What matters is the evolution of pressure within the layer. When pressure is incompressibily advected (as FKR, in particular, assume) then D simply modifies the tearing mode growth rate without affecting the stability boundary. But in compressible theory, the pressure perturbation is determined by competition between resistive diffusive and parallel sound wave propagation, as in Eq. (5.104). The resulting sixth order system is more sensitive to positive D, and completely stabilized for sufficiently small Δ'.

It should be remarked that Δ_c is not an artifact of toroidicity; it pertains to any compressible model with favorable curvature. On the other hand, the precise value of D and therefore Δ_c depend quite sensitively on details of the equilibrium geometry.

Finally, we point out that critical values of Δ', as in Eq. (5.109), can arise in contexts besides the fluid-interchange case considered here [56,91]. In particular, the small radial flow associated with <u>equilibrium</u> resistive diffusion has a stabilizing influence, expressed qualitatively by Eq. (5.109). However the corresponding Δ_c is relatively small [91].

D. Current-channel boundary layers

1. Introduction

The results of the previous two sections assume the plasma resistivity to be spatially constant. In fact the plasma response to $E_\parallel$ depends on $k_\parallel$, and therefore on radial position. In other words, as was emphasized in Chapter IV, one should replace the classical conductivity, σ_s, by a more uniformly accurate response function, σ_*.

Because σ_* becomes small for appreciable $k_\parallel$, such replacement can significantly affect boundary-layer structure. In certain parameter regimes it will concentrate the perturbed current in an inner layer ("current channel") which is narrow compared to the classical layer width w. We review the modified layer theory in this section.

Spatial variation of σ_* matters in so far as the collisional mean-free-path, λ_{mfp}, exceeds a parallel wavelength: $k_\parallel \lambda_{mfp} > 1$. Thus we are concerned with the extension of boundary-layer theory to regimes of longer mean-free-path, or smaller collisionality. Such extension is complicated by various effects mentioned in Chapter IV (trapped particles, temperature gradients, etc.) and in fact remains incompletely understood. For this reason and for reasons of brevity we consider only the simplest aspects of long mean-free-path boundary layers.

It should be noted that even σ_s depends on position because it depends on temperature. The x-dependence of σ_s arising through temperature perturbation yields a distinct instability, the rippling mode [75], which is not reviewed here, but which might be important in strongly collision-dominated regions of the toroidal discharge [92].

2. Scale lengths

The long mean-free-path case is distinguished by involving an additional scale length, w_*, which measures the width of the generalized conductivity. An estimate of w_* is provided by Eq. (4.112) or Eq. (4.170):

$$w_* \simeq |\omega(\omega+i\nu)|^{1/2}/|k_\parallel' v_{the}|. \qquad (5.111)$$

We wish to compare w_* with the classical layer width, w. But first the definition of the latter must be generalized, because our previous formula, $w = (x_A x_R)^{1/2}$, becomes ambiguous when η depends on position.

A generalized definition of w, which is independent of the closure relations, is obtained from the shear-Alfvén law. Recalling that Eq. (5.3) must reduce to the neighboring equilibrium equation, Eq. (5.5), for $x >> w$, we see that w measures, in general, that distance from the rational surface at which plasma inertia becomes comparable to line bending. Thus, for the case of small-Δ' modes, Eqs. (5.3) and (5.40) give

$$x_A \varphi / w^2 \sim \Delta' \psi \ .$$

To estimate φ we assume that, at least when $x \gtrsim w$, the electrostatic and electromagnetic contributions to $E_\parallel$ are comparable:

$$(w/x_A)\varphi \sim \psi \ . \tag{5.112}$$

Then we have $x_A^2 \sim \Delta' w^3$ or

$$w = x_A^{2/3} \ (\Delta')^{-1/3} \ . \tag{5.113}$$

We can confirm this formula by noting that in combination with Eq. (5.39) it reproduces the standard small-Δ' dispersion relation. It is also applicable to large-Δ' modes, since Eq. (5.27) allows us to replace Δ' by w^{-1}, and thus reproduce Eq. (5.31) in the large-Δ' case.

In dimensional (unnormalized) form, Eq. (5.113) becomes

$$w = (\Delta')^{-1/3} \, |\omega/k_\parallel' v_A|^{2/3} \, .$$

Therefore, from Eq. (5.111),

$$\frac{w}{w_*} = \frac{v_e}{v_A} \left(\frac{k_\parallel' v_A}{|\omega| \Delta'}\right)^{1/3} \left|\frac{\omega}{\omega + i\nu}\right|^{1/2} \, . \tag{5.114}$$

When this ratio is small, spatial variation of σ_* occurs in the exterior region where dissipation is irrelevant; our previous results are obviously valid in this case. But when w/w_* is large, the boundary-layer structure is more complicated — a current channel of width w_* is imbedded within the layer — and short mean-free-path theory is no longer reliable.

Evidently an explicit formula for w/w_* requires knowledge of the mode frequency: it can only be evaluated a posteriori. However, the most important cases are covered by the following three examples.

(i) In the classical small-Δ' case, $\omega = i\gamma$ is given by Eq. (5.42). In dimensional form, from Eqs. (4.9), (4.33) and (4.34)

$$|\omega| = (\Delta' a)^{4/5} (k_\parallel' a^2)^{2/5} \tau_s^{-3/5} \tau_A^{-2/5} \, .$$

Using also the relation,

$$v_e/v_A = (m_i \beta_e / m_e)^{1/2}$$

we find that

$$w/w_* = (m_i\beta_e/m_e)^{1/2}\,\frac{(k_\parallel' a^2)^{1/5}}{(\Delta' a)^{3/5}}\,\left|\frac{\omega}{\omega+i\nu}\right|^{1/2}\,\left(\frac{\tau_s}{\tau_A}\right)^{1/5} .$$

Here the last two factors are the most important. While $\tau_s/\tau_A \sim 10^8$, ν usually exceeds ω, near the q=2 surface, by at least an order of magnitude. A fair conclusion is that the classical value of w/w_* is device-specific: while large in typical reactor designs, it can be comparable to or smaller than one in some present-day experiments.

(ii) For large-Δ' modes, such as the m=1 tearing mode, we use Eq. (5.31) to find that

$$w/w_* = (v_e/v_A)\,|\omega/(\omega+i\nu)|^{1/2} .$$

Again, $v_e/v_A \simeq 1$, under typical conditions, so current channel behavior depends mostly on ω/ν. Note that the m=1 mode usually resides in the central, hottest region of the discharge, where ν is relatively small.

(iii) When $\omega \simeq \omega_*$, the small-Δ' formula yields

$$\frac{w}{w_*} = \left(\frac{a}{\rho_e}\right)^{1/3}\left(\frac{v_e^2}{v_A^2}\,\frac{L_n}{L_s\Delta' a}\right)^{1/3}\,\left|\frac{\omega}{\omega+i\nu}\right|^{1/2} . \qquad (5.115)$$

Because of the smallness of ρ_e, the electron gyroradius, this quantity will be large under most experimental conditions of interest.

The general conclusion to be drawn from these examples is that current channel formation will be prevalent when $\nu \lesssim \omega$, and not uncommon otherwise [58].

Two equally important comparisons involve the ion gyroradius. Of course classical theories assume the ions to be magnetized, i.e., that ρ_i is smaller than any scale length of interest. [Equation (4.127), in particular, depends on magnetized ions.] In fact one finds that

$$\rho_i \ll w \tag{5.116}$$

so that ions are magnetized in the tearing layer. With regard to the current channel, we assume $\omega \sim \omega_*$ in order to estimate

$$\rho_i/w_* \sim |\omega/(\omega+i\nu)|^{1/2}(\rho_i a/\rho_e L_s) .$$

The second factor in this expression is roughly two or three under typical conditions; hence ions are magnetized in the current channel only when $\nu \gg \omega$ [58].

The presence of unmagnetized ions might be expected to complicate analysis of the current channel. However, Eq. (5.112) shows that

$$\psi+i(x/x_A)\varphi = \psi + O(w_*/w) \tag{5.117}$$

when $x \lesssim w_*$. For small-Δ' modes, it follows that electrostatic fields can be neglected inside the channel, making the ion dynamics irrelevant. This simplification is made explicit in the following two subsections, which consider respectively collisionless and collisional current channels, in the small-Δ' case.

3. Collisionless current channel

With the neglect of the electrostatic contribution to $E_\parallel$ (for $x \lesssim w_* \ll w$), the generalized Ohm's law,

$$J_\parallel = \sigma_* E_\parallel$$

becomes

$$-\frac{c}{4\pi} A_\parallel'' = (i\omega/c)\sigma_* A_\parallel \quad . \tag{5.118}$$

In the case of small-Δ', we can easily integrate Eq. (5.118), across the layer. The integral of the right-hand side is controlled by σ_*, and evidently measured by

$$(i\omega/c)A_\parallel \int \sigma_* \, dx \sim (i\omega/c)A_\parallel \, \sigma_{*o} w_*$$

where σ_{*o} is defined by Eq. (4.106). Since the integral of the left-hand side is $-\Delta' A_\parallel$, we obtain the dispersion relation

$$i\Delta' \simeq 4\pi \, \sigma_{*o} w_* \, \omega/c^2 \quad . \tag{5.119}$$

Before making Eq. (5.119) more explicit, we comment on its significance. Recall that boundary-layer theory begins by considering a neighboring equilibrium equation, such as Eq. (5.5), which pertains for sufficiently large $k_\parallel$, but which is singular at x=0. The singularity is resolved by including, in regions of smaller $k_\parallel$, corrections to Eq. (5.5) which involve additional field variables and therefore require additional equations, such as Ohm's law, for closure.

From this "canonical" point of view, Eq. (5.118) appears paradoxical: involving only $A_{\parallel}(\propto\psi)$, it can hardly be a closure relation. How are Eqs. (5.118) and (5.5) related?

To answer this question we recall that the current channel case involves two nested layers. The outer layer, which has width w and is appropriately considered the "tearing layer", cannot be described in terms of $A_{\parallel}$ alone. In fact, because of Eq. (5.116), the electrostatic potential enters the description of the tearing layer, through ion inertia, in precisely the usual manner. Of course, the tearing layer analysis is modified by the presence of the inner layer, or current channel. Thus, one should strictly solve a double layer problem, first matching the exterior solution to that of the tearing layer, and then matching the tearing layer solution to that of the current channel [49,56]. Such an elaborate solution would show explicitly how electrostatic terms become first crucial (for $w \gtrsim |x| > w_*$) and then negligible (for $|x| \lesssim w_*$). It would also involve two distinct versions of Δ', corresponding to the two nested layers.

If the Δ' appearing in Eq. (5.119) is identified with that of the inner layer, then the result is clearly correct, but incomplete and not directly comparable to other tearing mode dispersion relations. On the other hand, if Δ' is given the usual interpretation, then Eq. (5.119) will remain correct if virtually all the perturbed current is concentrated in the channel, so that both measures of Δ' coincide. Because σ_* has a significant tail, the question of current concentration is not trivial; it is found that Eq. (5.119), with the usual interpretation of Δ', is often [49], but not always [56], valid.

We now return to Eq. (5.118) to derive a more rigorous version of the dispersion relation. Considering the collisionless case, we neglect ν in Eq. (4.101), which can then be written as [55]

$$\sigma_* = - \frac{ine^2}{2T_e} \frac{(\omega-\omega_{e*})}{k_\parallel^2} \frac{dZ}{dz}$$

or, in view of Eq. (4.82),

$$\sigma_* = - \frac{ine^2}{2T_e} \frac{(\omega-\omega_{e*})}{|k_\parallel'|\omega} v_{the} \frac{dZ}{dx} .$$

Hence we have

$$\Delta' = - \frac{4\pi\, ne^2}{c^2\, T_e} \frac{(\omega-\omega_{e*})}{|k_\parallel'|} v_{the} \int_0^\infty dx \frac{dZ}{dz}$$

which yields the dispersion relation [58,93]

$$\omega=\omega_{e*}+i \frac{c^2 k_\perp v_{the}\Delta'}{2\sqrt{\pi}\, \omega_p^2 L_s} \equiv \omega_{e*}+i\gamma_0 . \qquad (5.120)$$

Equation (5.120) is said to describe the collisionless tearing mode. We have seen that it is an artifact of simple "resistive" diffusion, with σ replaced by σ_*. Because of the concentration of current discussed previously, the dispersion relation does not involve the Alfvén speed. For the same reason, and also because we neglected

the ion acoustic corrections to σ_*, it does not involve ion dynamics (we remark that ion corrections have been shown to have a stabilizing influence [59]).

It is sometimes suggested that collisionless tearing depends upon Landau damping, to provide the dissipation which ordinarily comes from collisions. In fact Landau damping has no qualitative effect on Eq. (5.120). One way to confirm this statement is to repeat the calculation with σ_* replaced by σ_{4*}, from Eq. (4.170). Recall that the latter function results from a strict fluid model, without wave-particle resonance. Yet it is easily seen to give the same dispersion relation, apart from a minor difference in the numerical coefficient. As was emphasized in Chapter IV, it is the gross spatial structure of the conductivity which matters, not Landau resonance.

4. Collision-dominated current channel

We have already remarked that the tearing mode frequency and growth rate are often small compared to the local ($r=r_s$) collision frequency. This by no means rules out channel formation, especially since, commonly, the mode frequency is estimated by ω_* and Eq. (5.115) becomes pertinent. Thus the limiting case

$$w_* \ll w \quad , \quad \omega \ll \nu \tag{5.121}$$

is of particular experimental importance [58].

We use Eq. (5.119) to obtain an approximate dispersion relation for the collision-dominated current channel. Since now

$$\sigma_{*o} \simeq \frac{e^2 n(\omega-\omega_{e*})}{m_e \nu}$$

we find that

$$\Delta' = \frac{\omega_p^2}{c^2} \frac{(\omega-\omega_{e*})}{|k_\parallel' v_{the}|} \left(\frac{\omega}{i\nu}\right)^{1/2} \tag{5.122}$$

in view of Eq. (5.111). There are two limits of interest. When $\omega >> \omega_*$, Eq. (5.122) implies

$$\mathrm{Im}(\omega) = \gamma \simeq \gamma_0^{2/3} \nu^{1/3} \tag{5.123}$$

where γ_0 is the collisionless growth rate of Eq. (5.120). Under typical experimental conditions, it is somewhat hard to reconcile Eq. (5.123) with $w/w_* >> 1$. The more realistic case has

$$\omega \sim \omega_*$$

with $\gamma << \omega_*$. Then Eq. (5.122) yields $\omega \simeq \omega_{*e} + i\gamma$, with

$$\gamma \simeq \gamma_0 (\nu/\omega_*)^{1/2} .$$

The exact versions of these results were first presented by Drake and Lee [58], who named the corresponding eigenmode "semi-collisional". The point of this nomenclature is that while $\nu >> \omega$, the existence of a current channel depends on long mean-free-path physics. Similarly, Eq. (5.121) is said to refer to the semi-collisional regime.

It is noteworthy that the exact semi-collisional dispersion relation differs from Eq. (5.122) not only with regard to the numerical constants. The rigorous version also contains terms proportional to ∇T_e which we neglected (in Chapter IV) and which significantly enhance the growth rate. A related ∇T_e-destabilization also occurs at short mean-free-path [53].

We do not attempt to review the complicated effects of temperature gradients here, but one feature of the $\nabla T \neq 0$ case requires comment. While Eq. (5.122) can be derived from σ_{4*} and therefore from simple fluid theory, the temperature-gradient terms require a significantly more careful analysis. In treating the ∇T-terms, one must take into account their distinctive energy dependence [recall Eq. (4.71)], and also, in general, the interaction of this energy dependence with that of the Coulomb cross-section [53,94]. Recent investigations of such effects, using either a kinetic [56] or generalized fluid formulation [57], have found that temperature gradients become stabilizing for sufficiently large plasma beta.

5. Large-Δ' current channel

The large-Δ' case is rather different. First of all, its dispersion relation cannot be obtained directly from Eq. (5.119), which depends upon a constant-ψ approximation. Second, the sharp variation of φ in the large-Δ' tearing layer yields electrostatic fields sufficiently strong to cast doubt on such simplifications as Eq. (5.117). For these reasons, a dimensional argument for the large-Δ' current channel dispersion relation which is both simple and physical has not been found. Large-Δ' current channels are most

coveniently studied using Eq. (5.25), the eigenmode equation written in terms of $E_\parallel$. After replacing η^{-1} by σ_* in that relation, and including the ion diamagnetic correction, as in Eq. (4.159), we obtain

$$\left[\frac{x^2(E_\parallel/x)'}{x^2+x_{A*}^2}\right]' + \frac{4\pi i\omega x}{c^2 x_{A*}^2}\,\sigma_* E_\parallel = \frac{4x_{A*}^2}{(\Delta' + \frac{i\pi}{x_{A*}})}\,\frac{x}{(x^2+x_{A*}^2)^2}\int \frac{dx E_\parallel}{(x^2+x_{A*}^2)^2} \qquad (5.124)$$

where, in unnormalized notation,

$$x_{A*}^2 \equiv -\omega(\omega-\omega_{i*})/(k_\parallel' v_A)^2 \ .$$

In the current channel case, Eq. (5.124) is more useful than Eq. (5.23) because of scale-length differences between $E_\parallel$ and E. As can be seen from Eq. (5.110), $E' \propto xJ_\parallel \propto x\sigma_* E_\parallel$. Hence E necessarily involves the short width, w_*, while $E_\parallel$ can be presumed nearly constant in the current channel. The "constant-$E_\parallel$" approximation turns out to be very powerful, especially in combination with the variational methods outlined in Sec. B [74]. Unlike the constant-ψ approximation, it yields dispersion relations which are applicable to both large-Δ' and small-Δ' modes.

In the absence of collisions, one finds from Eq. (5.124) that (for $\omega_{i*} = 0$)

$$\omega(\omega-\omega_{e*}) \cong -\frac{\sqrt{\pi}}{2}\,(k_\parallel' v_{the})^2\,\left(\frac{c}{\omega_p}\right)^2\,\frac{v_A}{v_{the}} \ . \qquad (5.125)$$

This result is related to the small-Δ' version in a simple and

instructive way. Recalling Eqs. (5.27) and (5.36), we replace Δ' in Eq. (5.120) by $w^{-1} \simeq x_A^{-1}$. The result is Eq. (5.125), giving an indication of how v_A enters the current channel dynamics.

Generalizations of Eq. (5.125), which include, for example, collisions and temperature gradients, can be found in the literature [74,95]. A weakness of these results is their assumption that the ions are magnetized. We have already noted that the ion gyroradius can easily exceed the current channel width.

Such results as Eqs. (5.120), (5.122) and (5.125) — the simplest examples of current-channel dispersion relations — demonstrate that long mean-free-path effects can dramatically alter tearing stability issues. It should also be clear that a number of questions remain to be answered. One obvious issue concerns the interaction between long mean-free-path effects, such as current channels, and the effects of toroidicity, such as the interchange term.

Finally, we point out that the preceding discussion has neither assumed nor needed information concerning the asymptotic behavior of $E_\parallel$ for large x. [In particular, the tearing layer width of Eq. (5.113) is not necessarily the width of $E_\parallel$.] The ratio $|E_\parallel(x\to\infty)/E_\parallel(x=0)|$, which is assumed to vanish in classical theory, can be estimated using the generalized Ohm's law. It is convenient to use reduced, normalized fields:

$$E_\parallel(0) \to \mathscr{E}(0) = -i\omega\psi(0)$$

from Eq. (4.160). For the large-x limit we have Eq. (4.161),

$$\mathscr{E}(\infty) = J(\infty)/\sigma_4(\infty) \ .$$

Let us consider a low-m tearing mode (e.g., m=2), for which the perturbation scale-lengths are O(1) in the exterior region. Then we have $J(\infty) \sim \psi(\infty) \sim \psi(0)$. For σ_4 we use Eq. (4.169), noting that $|x| >> x_i \implies \beta k_\parallel^2(1+\Delta_i) \simeq -\omega^2$. This yields the ratio,

$$|\mathscr{E}(\infty)/\mathscr{E}(0)| \sim |(2\delta^2\omega+i\eta)/\omega| \ .$$

Of course an equivalent result can be obtained from the kinetic version σ_*; cf. Eq. (4.114).

Recall here that $\eta = \omega_p^{-2}\nu$ corresponds to ordinary resistive diffusion and is always very small compared to the mode frequency. Hence the asymptotic $E_\parallel$ is indeed negligible when δ=0. But for finite $\delta\left(= \frac{1}{2}\frac{c}{\omega_{pi}a}\right.$, as noted in Chapter IV$\left.\right)$,

$$|\mathscr{E}(\infty)/\mathscr{E}(0)| \sim \delta^2$$

is finite and potentially important. It is therefore fortunate that such current channel results as Eqs. (5.120), (5.122), and (5.125), along with the exterior description, Eq. (5.5), are insensitive to the asymptotic form of $E_\parallel$.

E. Nonlinear boundary layer: island evolution

1. Introduction

It was pointed out in Chapter III that nonlinear terms in the shear-Alfvén law, rather than inertia, can act to remove the rational surface singularity. The important nonlinearity involves

magnetic perturbation, which acts by changing the local flux surface topology: closed field lines "inflate" to form helically twisted magnetic islands. We noted that while such island structures are present even in the linear, small-amplitude regime, they can affect boundary-layer dynamics only after the island width, W [cf. Eq. (3.55)], has grown large enough to occupy a significant fraction of the linear boundary layer:

$$W \sim w \ . \tag{5.126}$$

Similarly current-channel behavior will be determined by island evolution when $W \sim w_*$.

Since $W \sim \psi^{1/2}$ grows exponentially in the linear phase, it can be expected to reach the nonlinear threshold promptly. Hence strictly linear behavior is typically unobservable. Furthermore, even equilibrium rational surfaces will frequently support islands, due, for example, to small misalignments in external coils. Because w is very small, such equilibrium islands can often satisfy Eq. (5.126) and thereby invalidate linear theory [96]. Thus the issue of nonlinear island evolution has particular realism and importance.

Present understanding of nonlinear tearing dynamics in the coherent (non-turbulent) case is based mainly on a famous paper by Rutherford [97]. This section is primarily a review of the Rutherford theory.

2. Shear-Alfvén law

We begin by considering the nonlinear shear-Alfvén law, Eq. (4.35). For simplicity we assume $\beta \propto \varepsilon^2$, in order to neglect the interchange term. More importantly, we assume the nonlinear dynamics to be so slow that inertia is also negligible — an assumption which will be verified a posteriori. Thus island evolution is constrained by the relation,

$$\nabla_{\|} J = 0 \ . \tag{5.127}$$

This of course is the nonlinear version of Eq. (5.5), the neighboring equilibrium equation. But Eq. (5.127) has an entirely different significance. In particular, rather than describing some "exterior" region, it is presumed to hold arbitrarily close to the equilibrium rational surface. It is not singular at the rational surface because it involves the nonlinear parallel gradient. Schematically,

$$\nabla_{\|} J_1 = \underset{\sim}{B}_0 \cdot \nabla J_1 + \underset{\sim}{B}_1 \cdot \nabla J_1 \ . \tag{5.128}$$

For a perturbation with helicity m/n, the first term on the right-hand side of Eq. (5.128) vanishes at $q=q_s=m/n$. In linear theory, this term alone acts on the perturbation, giving the linear singularity. Its nonlinear resolution evidently results from the second term, which therefore plays a role similar to that of inertia in the linear case. Of course the width W measures that region — the "reconnection region" — in which the second term in Eq. (5.128) is comparable to the first.

We may recall from Chapter II that Eq. (5.127) is solved by any function J which is constant on flux surfaces — in this case, on the perturbed (island) flux surfaces. In other words, when island evolution is sufficiently slow, the current-density distribution relaxes to become a flux label of the reconnected field.

3. Helical symmetry

In order to make further analytical progress we assume the nonlinear field configuration to be helically symmetric, depending on ϑ and z only through the helical angle $u=z-q_s\vartheta$. Within the low-beta model, which omits curvature effects from the start, this is not a strong assumption. However, it localizes reconnection to the vicinity of a single rational surface, where $q\approx q_s$. Also, since symmetry rules out magnetic stochasticity, we now restrict our attention to <u>coherent</u> island evolution.

A general flux label can be defined by [recall Eq. (2.5)]

$$\nabla_{\|}\psi_* = 0 \ .$$

Spatial symmetry allows exact integration of this magnetic differential equation. For axial symmetry ($\partial/\partial z=0$), a solution is given by $\psi_*=\psi$, the poloidal flux. The corresponding solution for the case of helical symmetry ($\partial/\partial z = -q_s^{-1}\partial/\partial\vartheta$) is given by the "helical flux"

$$\psi_*(r,u) = \psi(r,u) + r^2/2q_s \ , \qquad (5.129)$$

as can be verified using Eq. (4.39). Of course r and ϑ are the cylindrical variables introduced at the end of Chapter IV.

Knowing the flux function for the perturbed magnetic field, we can express the solution to Eq. (5.127) as

$$J(r,u) = J(\psi_*) \ . \tag{5.130}$$

4. Ohm's law

The significance of Eq. (5.130) can be seen from Ohm's law, Eq. (4.36). Notice that a flux surface average (with respect to the perturbed surfaces) will eliminate the electrostatic term,

$$\langle \nabla_\parallel \varphi \rangle_{\psi_*} = 0 \ ,$$

in view of Eq. (2.36). But, because the average is performed at fixed ψ_*, it will not affect the current: $\langle J \rangle_{\psi_*} = J$. Hence we have

$$\langle \frac{\partial \psi}{\partial t} \rangle_{\psi_*} = \eta J \ , \tag{5.131}$$

a diffusion equation for ψ, without electrostatic coupling.

Equation (5.131) resembles the current channel relation, Eq. (5.118), in which electrostatic effects also decoupled, and it is amenable to the same sort of dimensional solution. (Of course, the physics underlying the two diffusion equations is very different.) Let us therefore integrate Eq. (5.131) over a radial domain which much exceeds w or W, but within which ψ is nearly constant; such a domain exists when

$$\Delta' W,\ \Delta' w \ll 1 \ .$$

(Here it may be helpful to recall, from Chapter III, that radial variation of ψ is not necessary for island formation.) The integral of the right-hand side is clearly approximated by $\eta\psi\Delta'$; for the left-hand side, we shall show that

$$\int dx \left\langle \frac{\partial \psi}{\partial t} \right\rangle_{\psi_*} \simeq \frac{\partial \psi}{\partial t} W \ . \tag{5.132}$$

Hence, since $W \propto \psi^{1/2}$, nonlinear island evolution is governed by the simple equation,

$$\frac{\partial W}{\partial t} \simeq \eta\Delta' \ . \tag{5.133}$$

The time scale in Eq. (5.133) is easily seen to be consistent with our neglect of inertia in the shear Alfvén law, at least when φ is estimated by Eq. (5.112).

The main point of Eq. (5.133) is that the exponential growth of the linear phase is nonlinearly replaced by a much slower evolution, on the resistive time scale, of the island width: $W \sim \Delta'\eta t$. (The latter can eventually saturate when distortion of the global current profile changes Δ'.) Island growth consistent with Eq. (5.133) is routinely observed in tokamak simulations; the "Rutherford regime" seems consistent with experimental observation as well. Most theories of tokamak disruption make crucial use of Eq. (5.133) [98].

There remains the verification of Eq. (5.132). Consider first the general, helically symmetric flux perturbation: for $q_s = m/n$, toroidal periodicity requires

$$\psi(r,u,t) = \sum_{\ell} \psi_{\ell}(r,t)\cos(\ell nu+u_{\ell}) \ , \tag{5.134}$$

where ψ_{ℓ} is the amplitude of the ℓ-th harmonic and the u_{ℓ} can be chosen to vanish. Since each harmonic corresponds to a distinct Δ',

$$\psi_{\ell}\Delta'_{\ell} = \int dx \ J_{\ell}(\psi_*) \ , \tag{5.135}$$

and since the island geometry necessarily couples many harmonics, Eq. (5.133) appears grossly oversimplified.

What saves the problem from becoming hopelessly complicated is the fact that, under realistic conditions, the Δ'_{ℓ} are negative for $\ell>1$: only the fundamental is linearly unstable. It is then consistent to assume that the $\ell>1$ contributions to Eq. (5.134) are relatively small. The dominant weight of ψ_1 yields a tractable island structure — in fact, the very structure which was studied at the end of Chapter III.

We next combine Eqs. (5.130) and (5.134) with the $\ell=1$ version of Eq. (5.135) in order to write, after appropriate change of integration variable,

$$\psi_1(r_s,t)\Delta'_1 = \frac{1}{\pi\eta}\int_0^{\infty} d\psi_* \oint du \ \frac{\cos nu}{|d\psi_*/dx|} \left\langle \frac{\partial\psi}{\partial t} \right\rangle_{\psi_*} \ ,$$

where

$$\psi \simeq \psi_0(r) + \psi_1(r,t)\cos nu \ .$$

We next use Eq. (2.38) to express the flux-surface average as

$$\langle A \rangle_{\psi_*} = \frac{\oint du A |\nabla\psi_*|^{-1}}{\oint du |\nabla\psi_*|^{-1}} \ ,$$

where $\nabla\psi_* \simeq d\psi_*/dx$. Thus we have

$$\psi_1 \Delta_1' = \frac{1}{\pi\eta} \frac{\partial\psi_1}{\partial t} \int_0^\infty d\psi_* \langle \cos nu \rangle_{\psi_*}^2 \oint du |d\psi_*/dx|^{-1} \ . \qquad (5.136)$$

Since Eq. (3.50) implies that

$$|d\psi_*/dx| = \frac{(2r_s q')^{1/2}}{q_s} \left[\psi_* - \psi_*(r_s,u)\right]^{1/2} \ ,$$

the right-hand side of Eq. (5.136) can be expressed in terms of elliptic integrals [22] and evaluated [97]. The result confirms Eq. (5.132).

The crucial feature of Eq. (5.136) is the $\langle \cos nu \rangle^2$ factor. Note that when x much exceeds W, the flux surfaces of ψ_* nearly coincide with those of ψ, as in Eq. (3.47). Hence the average of cosnu nearly vanishes for $x >> W$. For smaller x, that is, within or close to the island separatrix, averaging at fixed ψ_* involves a limited range of u, in which cosnu is predominantly positive. Thus, because of both Eq. (5.130) and the reconnected topology, the relevant Fourier

component of the current is localized to the island region, as expressed by the W in Eq. (5.132).

5. Generalizations

The importance of the Rutherford theory has encouraged numerous generalizations, only a few of which can be mentioned here.

At longer mean-free-path, island growth within a current channel becomes relevant. In the absence of collisions, one finds that island growth terminates, $\partial W/\partial t = 0$, near the obvious threshold, $W=w_*$. More realistically, the evolution becomes semi-collisional as saturation is approached, and the ultimate behavior is not unlike Eq. (5.133) [99]. The relation between collisionless and collisional (as well as linear and nonlinear) regimes has also been investigated [22].

Nonlinear evolution of large-Δ' tearing modes has been studied. The most striking difference is observed numerically: one finds that exponential growth of the perturbation continues, at close to the linear growth rate, far into the nonlinear regime [100].

Corrections to the nonlinear shear-Alfvén law have been considered, for example in [101]. The correction terms allow J to vary somewhat over a flux surface; surprisingly, the ultimate effect on island growth is mild. Inclusion of the interchange term, at finite beta, leads to an analysis very similar to the linear one outlined in Sec. C. The nonlinear manifestation of favorable curvature is similar to Eq. (5.109); however, for island widths exceeding a certain size curvature becomes unimportant and Eq. (5.133) approximately pertains [102].

VI. Pressure Driven Modes: The Eikonal Theory

A. Introduction

In this chapter we consider perturbations driven by the interaction of field curvature with fluid pressure gradients, that is, by the interchange term in the shear-Alfvén law. Such modes can be destabilized by the Rayleigh-Taylor mechanism [103], since an effective gravitational force results from the non-inertial motion of the fluid along curved field lines ($\underset{\sim}{g} \simeq -\underset{\sim}{\kappa} v_{th}^2$). If the pressure gradient is such that a denser fluid is supported by a lighter fluid ($\underset{\sim}{g}\cdot\nabla p < 0$), then fluted motion ($k_\parallel = 0$) develops, ultimately relaxing the pressure gradient. As in the fluid case, larger perpendicular wavenumbers are typically the most rapidly growing.

This simple picture must be qualified in several important ways. In a system with magnetic shear, a mode with definite helicity,

$$\varphi \sim \varphi_{mn}(V)\ \exp[i(n\zeta - m\vartheta)]$$

can have $k_\parallel = 0$ only at a rational surface. Off such surfaces, finite-$k_\parallel$ implies that the field lines are bent, giving rise to a stabilizing force from field-line tension. [The line-bending force is explicit in, for example, Eq. (3.22).] Such restoring forces are evidently minimized by peturbations which rotate in the sheared field, keeping $k_\parallel$ small, and thus making the helicity a function of V:

$$\varphi \sim \varphi_n(V)\ \exp[in(\zeta - q(V)\vartheta)]\ . \qquad (6.1)$$

The resulting stability criterion is the same as the shear-free case ($\underset{\sim}{g}\cdot\nabla p > 0$), although the growth rate is reduced by rotational kinetic

energy requirements. Because the growth is largest when $k_\perp \sim n/R$ is large, the fluid moves vertically in narrow slices, and because these slices twist with the field as the fluid rises in the effective gravity, these modes have been called "twisted slicing modes" [104].

It must be noted, however, that Eq. (6.1) is not generally consistent with ϑ-periodicity (i.e., single valuedness) of the peturbations. A technique for constructing periodic twisted slices in the presence of magnetic shear, based on ideas of Taylor [105], was discovered almost simultaneously by several authors [106,107,108]. This technique, which has become known as the "ballooning representation," is reviewed in the following section.

The basic idea is that the "slices" correspond to a coupled set of modes with various helicities, each centered on its own rational surface. In the large $k_\perp$ limit the distance between rational surfaces, Eq. (3.57), becomes small, and the various modes strongly overlap. Furthermore, in this limit, conditions are nearly the same on each of the closely spaced rational surfaces, and growth rates and mode amplitudes will be slowly varying functions of radius. Thus to lowest order (the local approximation), the perturbation is a superposition of identical single helicity modes. The local theory reduces to the solution of the so-called "ballooning equation" which describes the Fourier transform of the radial envelope of each mode.

Another important modification of the simple Rayleigh-Taylor picture is that in a toroidal device the curvature is not constant on magnetic surfaces. In fact $\underset{\sim}{\kappa}\cdot\nabla P$ typically changes sign with the local poloidal current. Therefore unstable modes tend to localize in regions

of unfavorable curvature. The up-welling of lower density fluid in such regions has led to the term "ballooning".

Modes which only weakly balloon have well-defined helicity and therefore tend to be localized to the neighborhood of a rational surface, where the right-hand side of Eq. (6.1) is nearly periodic. The radially localized limit is said to describe interchange modes; it is analyzed by methods very similar to the tearing layer theory of Chapter V. The reduced interchange stability criterion, or Mercier condition, was discussed in Chapter V [recall Eq. (5.89)]. Its exact version is derived in Subsection C.2.

Perturbations which are slightly less localized in radius are amenable to a multiple spatial-scale analysis, in which the parallel mode width is assumed to exceed the scale for variation of $\underset{\sim}{\kappa}$. Considering this case in Subsection C.4, we find unstable modes, even when the Mercier criterion predicts stability.

In the strongly ballooning case, modes are poloidally localized to the region of unfavorable curvature, but have considerable radial extent. This case must be treated using the full apparatus of the ballooning representation. It naturally breaks into two parts, local and global theories, which are considered in Secs. C and B respectively. Local theory consists of the solution of ballooning equation describing the structure of the mode, on a given magnetic surface. Once the local theory is solved on each surface, a global eigenmode can be constructed by combining local modes with the same eigenfrequency. This treatment, which is WKB theory in the ballooning representation, leads to a quantization condition for the frequencies of global modes [109-112].

Further modifications to the Rayleigh–Taylor picture arise when the effects of compressibility are considered. As we have seen in Chapters IV and V, parallel compressibility couples sound waves to the shear–Alfvén mode and thus reduces the coupling between pressure and fluid displacement. In classical Rayleigh–Taylor theory, it is well known that stability criteria are sensitive to whether the fluid is assumed to evolve adiabatically or isothermally. We will see that the ballooning stability boundary is unaffected by compressibility; however, the growth rates are significantly changed. For the analysis of the compressible case in Sec. D, we use the four–field model. Resistive ballooning modes and the effects of diamagnetic drifts are also treated with this model.

B. The Ballooning Representation

1. Local Theory

The analytical treatment of pressure driven instabilities appears to be tractable only when the scale length of perturbations is much smaller than that of the equilibrium. Since flute–like modes with $k_\perp a \gg 1$ are often the most unstable perturbations, this limit is also a fruitful one. The natural technique for problems with disparate length scales is the eikonal or WKB analysis, where the functions of interest are represented as

$$\phi(\underset{\sim}{x}) = \varphi(\underset{\sim}{x}) \exp\left(\frac{i}{\varepsilon} S(\underset{\sim}{x})\right) \tag{6.2}$$

with $\nabla S(\underset{\sim}{x}) \sim \nabla\varphi \sim O(1)$. In our case the eikonal, $S(\underset{\sim}{x})$, represents the rapid perpendicular motion while the envelope, φ, determines the

parallel structural; recall Eq. (3.5). The small parameter ε represents, as usual, the scale separation.

Since by assumption the eikonal represents only the perpendicular mode structure, we insist that

$$\underset{\sim}{B}\cdot\nabla S(\underset{\sim}{x}) = 0 \quad . \tag{6.3}$$

This leads to the natural definition of the perpendicular wavenumber as

$$\underset{\sim}{k}_{\perp}(\underset{\sim}{x}) = \nabla S(\underset{\sim}{x}) \quad . \tag{6.4}$$

In terms of the notation of Eq. (3.1) we have $k_{\perp}/\varepsilon \sim m/r \sim nq/r$ so that the limit $\varepsilon \to 0$ corresponds to $n \to \infty$.

In this section it is convenient to use the flux coordinates (q,ϑ,ζ) where the flux label is taken to be $q(V)$. Field line coordinates, (q,η,α), which will also be used are related to Hamada coordinates through

$$\begin{aligned} \eta &= \vartheta \\ \alpha &= \zeta - q(V)\vartheta \end{aligned} \tag{6.5}$$

whence $\underset{\sim}{B}\cdot\nabla$ becomes $\chi'\frac{\partial}{\partial\eta}$. It is clear that (q,α) labels a field line and that η represents the parallel coordinate. When no confusion can arise functions will be referred to in both coordinate systems by the same label: $f(q,\vartheta,\zeta) = f(q,\eta,\alpha)$.

As we have seen in IIID.1, the general solution to the magnetic differential equation (6.3) is an arbitrary function $S(q,\alpha)$. This function, however, may not represent a physical perturbation since it

cannot be periodic except on rational surfaces. To demonstrate this, define the poloidal and toroidal symmetry operators, P and T, by

$$Pf(q,\vartheta,\zeta) = f(q,\vartheta+2\pi,\zeta) = f(q,\eta+2\pi,\alpha-2\pi q) \tag{6.6a}$$

$$Tf(q,\vartheta,\zeta) = f(q,\vartheta,\zeta+2\pi) = f(q,\eta,\alpha+2\pi) \ . \tag{6.6b}$$

Clearly any physical function must satisfy Pf=Tf=f. Applying the symmetry operations to Φ in Eq. (6.2) yields

$$S(q,\alpha-2\pi q) = S(q,\alpha) + 2\pi m\varepsilon \tag{6.7a}$$

$$S(q,\alpha+2\pi) = S(q,\alpha) - 2\pi n\varepsilon \tag{6.7b}$$

where m,n are arbitrary integers representing toroidal and poloidal mode numbers. Toroidal periodicity, Eq. (6.7b), implies that S can be expanded in a Fourier series as

$$S(q,\alpha) = -\alpha n\varepsilon + \sum_{\ell} S_{\ell}(q)\ e^{i\ell\alpha}$$

where the first term represents the aperiodic part. Applying Eq. (6.7a) to this form yields

$$0 = 2\pi\varepsilon(n-mq) + \sum_{\ell} S_{\ell}(q)\ [1-e^{-2\pi i\ell q}]\ e^{i\ell\alpha} \ .$$

Hence nq(V) must be integral and S_{ℓ} must vanish unless ℓq is an integer. Thus the eikonal form, Eq. (6.2), satisfies the periodicity requirements only on rational surfaces.

The ballooning representation is a modification of Eq. (6.2) that yields a periodic solution. The first step is counter-intuitive [105,111]: we drop the poloidal periodicity requirement of the eikonal and envelope. Instead we will look for solutions S and φ defined on the range $-\infty<\eta<\infty$, which is called the "covering space." As we have seen, an $S(q,\alpha)$ which is toroidally periodic necessarily oscillates in ϑ with period $2\pi/q$. The envelope, on the other hand, will turn out to decay as $|\eta|\to\infty$, and usually be square integrable. The second step is to observe that WKB problems typically have more than one branch in their solution. If we label the branches by the index j, then the general solution on the covering space may be written

$$\Phi(\underset{\sim}{x}) = \sum_j a^j \varphi^j(\underset{\sim}{x}) \exp\left(\frac{i}{\varepsilon} S^j(\underset{\sim}{x})\right) \tag{6.8}$$

where the a^j are arbitrary coefficients. Finally, we will see that the requirement that $\Phi(\underset{\sim}{x})$ be periodic can be satisfied by appropriate choice of the coefficients a^j in the small ε limit, even though each branch solution is not poloidally periodic. Our presentation of the ballooning analysis follows closely the discussion of Dewar and Glasser [112] and Lee and Van Dam [106,109].

The eikonal ansätz will be used to solve a system of equations which can be represented schematically as

$$L(\nabla_\perp, \nabla_\parallel, \underset{\sim}{x}, \lambda)\ \Phi = 0 \tag{6.9}$$

where L is a linear operator obtained by expanding about equilibrium and λ is the eigenvalue, which is typically a function of the frequency

(in MHD, for example $\lambda = -\omega^2$). The field ϕ may consist of several components in which case L is an array. We will assume that each component of L is at most second order in $\nabla_\perp$. Substitution of Eq. (6.8) into Eq. (6.9) yields

$$L\left(\frac{i}{\varepsilon}\,\underset{\sim}{k}_\perp+\nabla_\perp,\nabla_\parallel,\underset{\sim}{x},\lambda\right)a\varphi = 0 \tag{6.10}$$

for each branch of the solution. Expansion of L under the assumption that its first argument occurs at most quadratically gives

$$La\varphi = -\frac{a}{\varepsilon^2}\,L_o(\underset{\sim}{k}_\perp,\nabla_\parallel,\underset{\sim}{x},\lambda)\varphi + O(\frac{1}{\varepsilon})$$

therefore the lowest order equation for the envelope is an <u>ordinary</u> differential equation in the parallel direction. It is commonly referred to as the ballooning equation, and may be written in a more perspicuous form in field line coordinates:

$$L_o\varphi = \mathscr{L}\left(\frac{\partial}{\partial\eta},\eta|q,\alpha,\underset{\sim}{k}_\perp,\lambda\right)\,\varphi(\underset{\sim}{x}) = 0 \tag{6.11}$$

showing the explicit dependence on η and parametric dependencies on the field line labels, (q,α), and on $k_\perp$ and λ. Solutions of this equation on the covering space must fall to zero as $|\eta|\to\infty$; this requirement yields a well defined eigenvalue problem.

It is interesting to note that the ballooning equation on the covering space is identical to the equation that would be obtained by naively using the eikonal as in Eq. (6.2). The insight is to allow

consideration of solutions which are not poloidally periodic [105]. Of course it is still necessary to show that a periodic function Φ can be constructed by a linear combination of solutions of Eq. (6.11).

A particular solution of Eq. (6.11), $\hat{\varphi}$, depends only parametrically on the field line labels and $\underset{\sim}{k}_\perp$:

$$\varphi(q,\vartheta,\zeta) = \hat{\varphi}(\eta|q,\alpha,\underset{\sim}{k}_\perp) \tag{6.12}$$

$$\lambda = \Lambda(q,\alpha,\underset{\sim}{k}_\perp) \ . \tag{6.13}$$

The dispersion relation (6.13) describes the <u>local</u> eigenvalue on the field line (q,α) and is the goal of most practical ballooning calculations. Typically, one varies the arguments of the dispersion relation to find the most unstable modes [111]. While this gives an estimate of the growth rate of a global eigenmode Φ, periodicity requirements restrict the allowed values of λ; therefore, as we will see in the next subsection, the actual growth rate is smaller.

Inversion of Eq. (6.13) yields the solution for $\underset{\sim}{k}_\perp(q,\alpha,\lambda)$ which in general has more than one branch. It is convenient to represent these solutions in terms of the covariant components of Eq. (6.4):

$$\underset{\sim}{k}_\perp = k_\alpha \nabla\alpha + k_q \nabla q \quad = k_\alpha(\nabla\alpha + \vartheta_k \nabla q) \ . \tag{6.14}$$

Here k_α and k_q are manifestly functions of q and α, given by the partial derivatives of S, and $\vartheta_k \equiv k_q/k_\alpha$. Alternatively, $k_\perp$ can be written in the coordinates (q,ϑ,ζ) as

$$\underset{\sim}{k}_\perp = (k_q - \vartheta k_\alpha)\nabla q + k_\alpha(\nabla\zeta - q\nabla\vartheta) \quad = \quad k_\alpha[(\vartheta_k - \vartheta)\nabla q + \nabla\zeta - q\nabla\vartheta] \tag{6.15}$$

showing that $\vartheta_k(q,\alpha)$ occurs in conjunction with ϑ. That $\underset{\sim}{k}_\perp$ explicitly depends on ϑ in an aperiodic way is a manifestation of the fact that S is not periodic and therefore only well defined on the covering space.

The covariant representation for $\underset{\sim}{k}_\perp$ displays a symmetry property of the ballooning equation, which implies that there is an infinity of branch solutions [109,112]. It is precisely this symmetry which will allow the construction of a periodic ϕ, in Eq. (6.8), from a sum of aperiodic functions. The symmetry follows from two observations: first, the expansion of L to obtain L_o naturally results in a homogeneous function of $\underset{\sim}{k}_\perp$. Thus the factor k_α is common to all the terms in L_o and may be eliminated (here we have noted that $\nabla_\parallel$ commutes with k_α). Second, since the explicit spatial dependence of L_o arises from the physical spatial variation of the equilibrium, the entire aperiodic variation of L_o resides in the $\vartheta_k - \vartheta$ factor in Eq. (6.15). Therefore the operator L_o is invariant when <u>both</u> ϑ <u>and</u> ϑ_k are increased by 2π. This implies that given one solution to Eq. (6.10), there is another solution, a translation of the first, with the same eigenvalue; that is,

$$\Lambda(q,\alpha,\vartheta_k) = \Lambda(q,\alpha-2\pi q,\vartheta_k+2\pi) \ . \tag{6.16}$$

We see that the parameter ϑ_k has the properties of an angle, which explains the notation.

It follows from Eq. (6.16) that each eigenvalue, λ, must correspond to an infinity of roots, differing only by translation. It is convenient to label these with the branch index j:

$$\vartheta_k^j(q,\alpha,\lambda) = \hat{\vartheta}_k(q,\alpha - 2\pi qj,\lambda) - 2\pi j \tag{6.17}$$

where $\hat{\vartheta}_k$ is a particular root of Eq. (6.13). Similarly the related branches of the envelope function are given in terms of a particular solution as

$$\varphi^j(q,\vartheta,\zeta) = \hat{\varphi}(\eta|q,\alpha,\vartheta_k^j) \tag{6.18}$$

(up to a constant which we equate to one). Using the symmetry of L_o it is easy to see that

$$\varphi^j(q,\vartheta,\zeta) = \varphi^{j-1}(q,\vartheta+2\pi,\zeta) \ . \tag{6.19}$$

It is only with this infinite set of branches that a periodic solution can be constructed, from the aperiodic eikonal, upon substitution into Eq. (6.8). Note that all the branches in the sum have the same eigenvalue; hence the solution Φ is a true normal mode (not the so called quasi-mode [104]). Equations (6.17) and (6.19) imply that applying the poloidal symmetry operator is equivalent to shifting the index j by one:

$$\begin{aligned} P\varphi^j &= \varphi^{j+1}(q,\vartheta,\zeta) \\ P\vartheta_k^j &= \vartheta_k^{j+1}(q,\alpha) + 2\pi \ . \end{aligned} \tag{6.20}$$

Periodicity then requires that $Pa^j = a^{j+1}$ and that the eikonal satisfy

$$PS^j(q,\alpha) = S^{j+1}(q,\alpha) + 2\pi m\varepsilon \tag{6.21}$$

[instead of Eq. (6.7a)]. The eikonal is obtained by solving Eq. (6.4) using the known $\underset{\sim}{k}_\perp$. This equation is equivalent to $\underset{\sim}{k}_\perp \times \nabla S = 0$, or

$$\frac{\partial S}{\partial q} - \vartheta_k \frac{\partial S}{\partial \alpha} = 0 \quad . \tag{6.22}$$

To show that this partial differential equation has solutions which obey Eq. (6.21), we operate on it with P. After noting that P does not commute with the q derivative

$$P \frac{\partial}{\partial q} - \frac{\partial}{\partial q} P = 2\pi P \frac{\partial}{\partial \alpha}$$

we obtain

$$\frac{\partial}{\partial q} PS - (P\vartheta_k - 2\pi) \frac{\partial}{\partial \alpha} PS = 0 \quad . \tag{6.23}$$

However, this is just Eq. (6.22), with ϑ_k^j replaced by ϑ_k^{j+1}. Therefore, we have shown that if S^j satisfies Eq. (6.22) then PS^j satisfies the same equation as S^{j+1}. The solution obeying (6.21) can be obtained by suitable choice of a multiplicative constant.

This formalism suffices for the local theory of ballooning. We have shown that a periodic eigenfunction of the form Eq. (6.8) can be found. The amplitude φ obeys the ballooning equation, which also determines the local eigenvalue via Eq. (6.13). The ballooning equation only determines the parallel structure of the mode. A complete global eigenfunction is obtained by continuing the ε expansion to next order.

2. Global Theory

In this subsection and the next, we sketch the global ballooning formalism. While this formalism has both mathematical and physical interest, applications of it are rare in the literature and not reviewed here. Thus the detailed developments of Subsections 2 and 3 are not crucial for understanding the remainder of Chapter VI.

The quantization conditions for the mode given by Eq. (6.8) are obtained following the usual prescriptions of WKB theory. First the equations for the mode amplitude are derived by continuing the expansion of Eq. (6.10) to $O(1/\varepsilon)$. Assume the single branch solution takes the form:

$$\Phi = \left(a\varphi_o + \varepsilon\varphi_1\right) \exp\left(\frac{i}{\varepsilon} S\right) .$$

The parallel structure of the envelope, φ_o, is determined by the $O(\varepsilon^{-2})$ terms which yield the ballooning equation (6.11). The global structure of the envelope is contained in the amplitude $a(q,\alpha)$ now allowed to depend on the field line labels. It is determined from the $O(1/\varepsilon)$ equations

$$L_1 a\varphi_o + L_o\varphi_1 = 0 \qquad (6.24)$$

where L_1 is obtained by straightforward expansion of Eq. (6.10) Typically the operator L_o is self-adjoint with respect to an inner product, $< >$:

$$<fL_o g> = <gL_o f> .$$

The solubility condition for Eq. (6.24) is then given by

$$\langle \varphi_o L_1 a \varphi_o \rangle = 0 \tag{6.25}$$

which constrains the radial structure of the mode. This is the "transport" equation for the wave amplitude [113].

Equation (6.25) and the whole WKB ordering are valid only away from the turning points, where branches of ϑ_k coalesce, i.e.,

$$\frac{\partial}{\partial \vartheta_k} \Lambda(q,\alpha,\vartheta_k) = 0 \ . \tag{6.26}$$

At a turning point there is a square root singularity in ϑ_k and consequently two choices for the branch. For a given value of λ the turning point condition Eq. (6.26) describes a curve in (q,α) space. Near the turning points a new expansion in powers of $\varepsilon^{1/3}$ yields an Airy equation which gives a connection formula for propagating through the turning points [109,112]. This formula is identical to the usual one [114] in the theory of second order equations.

Far from the turning points the eikonal is obtained by solving (6.22) by the method of characteristics. Let $S(q,\alpha) = S(q,\alpha(q))$ where $\alpha(q)$ is determined by

$$\frac{d\alpha}{dq} = - \vartheta_k(q,\alpha,\lambda) \ . \tag{6.27}$$

This is essentially the equation for the trajectory of a wavepacket in (q,α) space. Since it is a first order differential equation it is easily solved in general. The equation for the eikonal is now dS/dq =

0, so that S is constant along the ray trajectories. At turning points, on the other hand, the connection formula implies that S/ε jumps by the value $\pm\pi/2$.

The quantization condition arises from demanding that the eikonal satisfy both the toroidal periodicity requirement, Eq. (6.7b), as well as single-valuedness in q. Recall that when α increases by 2π, S/ε must change by $-2\pi n$. Single-valuedness is imposed by requiring that when a ray returns to the same value of q (including turning points), the total phase change is $2\pi N$, for some integer ("radial quantum number") N. The two requirements are not trivially satisfied and they lead to consideration of the existence of periodic orbits in maps of the circle [112]. In this review we restrict the discussion to the axisymmetric case where the quantization is easy.

3. Ballooning in Axisymmetric Systems

For the axisymmetric case, the ballooning equation (6.11), and hence the eigenvalue, Eq. (6.13), are independent of α. This implies that Eq. (6.27) for $\alpha(q)$ can be integrated explicitly:

$$\alpha(q) = \alpha_o - \int dq \vartheta_k(q,\lambda)$$

where α_o is a constant. The eikonal can depend on α and q only through α_o, and must satisfy Eq. (6.7b). Hence

$$S(q,\alpha) = -n\varepsilon\alpha_o = -n\varepsilon\left(\alpha + \int dq\ \vartheta_k\right) . \qquad (6.28)$$

This representation is of a familiar form, with the variables (q,ϑ_k) being a canonically conjugate pair. The ballooning representation in

the axisymmetric case resembles a Fourier transform: corresponding to the radial variable, q, is an effective radial wavenumber, ϑ_k.

We can combine Eqs. (6.8) and (6.17)-(6.19), to write the general form for the solution

$$\Phi(\underset{\sim}{x}) = a(q)\sum_j \hat{\varphi}(\eta+2\pi j\,|\,q,\hat{\vartheta}_k)\ \exp[-in(\alpha + \int dq\hat{\vartheta}_k - 2\pi qj)] \qquad (6.29)$$

where the sum extends over a related set of branches. Note that a can depend only on q in the axisymmetric case; it is determined by Eq. (6.25). The representation Eq. (6.29) is commonly referred to as the ballooning representation. It clearly satisfies the poloidal periodicity requirement by virtue of the fact that shifting ϑ by 2π is equivalent to shifting the branch label by one.

The relationship between Fourier modes, rational surfaces, and the ballooning representation can be determined by computing the (m,n)-Fourier component of Eq. (6.29). Using Eq. (2.28) and shifting the integration variable by $2\pi j$ we obtain

$$\Phi_{mn}(q) = \frac{1}{2\pi}\int_{-\infty}^{\infty} d\eta\ \hat{\varphi}(\eta)\ \exp[i(nq-m)\eta]\ a(q)\ \exp(-in\int dq\hat{\vartheta}_k)\ .$$

There are two Fourier conjugate relationships displayed here. Firstly, η is conjugate to the radial variable nq-m, providing the local mode structure. Secondly, ϑ_k is conjugate to nq, providing [with a(q)] the global structure. A shift in ϑ_k by 2π can be considered as a change in nq-m by 1, which is equivalent to moving to the next rational surface. We see that the translation symmetry (in ϑ_k) of L_o is related to the fact that, on a sufficiently small scale, the plasma appears radially

homogeneous. When φ is broad in η, each Fourier mode is localized near its rational surface and so for one n only a few m's are important. This is the case of flute or interchange modes. When φ is narrow we have the case of strong ballooning, where each Fourier mode extends across many rational surfaces. A strongly ballooning mode has no definite helicity at each value of q. The amplitude function a and ϑ_k determine the weight assigned each of the definite helicities. From the transport equation we know that a(q) is nearly localized within the turning points.

The quantization condition for the modes is given by demanding that S be single valued with respect to q:

$$n\oint dq\ \hat{\vartheta}_k(q,\lambda) = 2\pi(N + \mu) \qquad N=0,1,2,\ldots \tag{6.30}$$

where N is the radial quantum number and μ the Maslov index [114]. The Maslov index depends on the topology of the constant Λ curves in the (q,ϑ_k) plane. For a closed curve, μ=1/2, and the integral represents the area enclosed. When the contour is not closed then ϑ_k must increase by 2π in one cycle according to Eq. (6.16). The integral then represents the area of this cycle and the Maslov index is 0.

There is a degeneracy in the quantization condition for ballooning modes. For example, modes with quantum numbers (n,N) and $(3n,3N+2\mu),(5n,5N+4\mu)$ etc. have the same eigenvalue. This degeneracy can be expected to be important when any perturbations are added to the system. For example a small amount of α dependence in the equilibrium breaks the degeneracy causing an unstable continuum to form [112].

Similarly, a nonlinear theory of ballooning should treat this degeneracy carefully.

The dispersion relation, (6.30), is a generalized form for the so-called 1/n corrections to the local ballooning dispersion relation. When n>>N a simple expression for these corrections can be obtained. Recall that the local theory takes the solution to be the maximum of the function Λ in the (q,ϑ_k) plane. Expanding near this maximum and keeping the quadratic terms allows the integral Eq. (6.30) to be done and yields the dispersion relation [111]

$$\lambda = \lambda_{max} - \left[\frac{\partial^2\Lambda}{\partial q^2}\,\frac{\partial^2\Lambda}{\partial \vartheta_k{}^2}\right]^{1/2}\frac{(2N+1)}{2n} \quad . \tag{6.31}$$

This formula is valid only when the contours of Λ are nearly elliptical. More generally the full integral, Eq. (6.30), must be used. It is of interest in this context that the WKB quantization formula often provides results that are accurate for quite moderate values of the quantum numbers.

In the limit of Eq. (6.31), the radial mode width, which is given by the extent of the constant λ contour in q, scales as $n^{-1/2}$. Similarly the eigenmode is a superposition of modes with ϑ_k ranging over a width $n^{-1/2}$. This scaling, which was the basis of early theories of global ballooning [111], only holds when the contours are nearly elliptical.

C. Local Theory of Ideal, Incompressible, MHD Ballooning

1. The Ballooning Equation

In this section we obtain the explicit ballooning equation, as well as approximations to the local dispersion relation, for pressure driven modes in general geometry. As we have seen in Sec. IIID, the flute-like ordering with $k_\perp a \gg 1$ leads naturally to the flute-reduced shear-Alfvén law, Eq. (3.41). The same procedure can be applied to closure relations to obtain a flute-reduced model. It is similar to the four-field model of Sec. IVC except that the approximation depends on large n, rather than large aspect ratio. To simplify the resulting dispersion relation, we restrict the analysis of this section to the incompressible MHD case.

The needed closure relations from MHD are equations (4.30) and (4.31) in the limits $\eta_\parallel = 0$ and $\nabla\cdot\underset{\sim}{V} = 0$. Applying the orderings of Sec. IIID, we let $\underset{\sim}{E} = \varepsilon\underset{\sim}{E}_1$ and define the potentials

$$\phi = \varepsilon^2\varphi$$

$$\underset{\sim}{A} = \underset{\sim}{A}_o + \varepsilon^2(\underset{\sim}{B}_o\psi + \underset{\sim}{A}_{2\perp})$$

where the perturbing potentials are assumed to be $O(\varepsilon^2)$ to make the perturbing electromagnetic fields $O(\varepsilon)$, and the parallel vector potential is written in accord with Eq. (3.28). Using these equations we immediately obtain the $O(\varepsilon)$ velocity in terms of the electrostatic $\underset{\sim}{E}\times\underset{\sim}{B}$ drift,

$$\underset{\sim}{V}_1 = \frac{c}{B_o^2}\nabla_f\varphi\times\underset{\sim}{B}_o + V_\parallel\frac{\underset{\sim}{B}_o}{B_o^2},$$

and consequently obtain the expressions for the parallel vorticity, Eq. (3.38), and for the convective derivative:

$$U = c\nabla_f^2\varphi$$

$$\frac{d}{dt} = \frac{\partial}{\partial t} + [\varphi, \quad] \tag{6.32}$$

where the bracket is the generalized one defined in Eq. (3.31). Finally the orderings can be used to reduce the parallel Ohm's law and pressure convection equation to

$$\frac{B_o^2}{c}\frac{\partial\psi}{\partial t} + \underset{\sim}{B}_o\cdot\nabla_s\varphi - [\psi,\varphi] = 0$$

$$\frac{B_o^2}{c}\frac{\partial P_1}{\partial t} + [\varphi,P_1] = -\underset{\sim}{B}_o\times\nabla_f\varphi\cdot\nabla_s P_o \tag{6.33}$$

The set of equations (3.41) and (6.33) form a closed set describing flute-like modes in the scale-separation limit.

Because flute-reduction has elminated the slow spatial scale, the linearized set of equations, correspond to the operator L_o in Eq. (6.11). These are obtained simply by neglecting the bracket terms. After linearization we easily obtain a closed equation for φ by taking the time derivative of the shear-Alfvén law:

$$\left(\frac{\chi'}{B_o}\right)^2 \frac{\partial^2}{\partial\tau^2}\nabla_f^2\varphi = \underset{\sim}{B}_o\cdot\nabla_s \frac{\nabla_f^2}{B_o^2}\underset{\sim}{B}_o\cdot\nabla_s\varphi + \frac{8\pi}{B_o^4}\underset{\sim}{B}_o\times\underset{\sim}{\kappa}_o\cdot\nabla_f[\underset{\sim}{B}_o\times\nabla_s P_o\cdot\nabla_f]\varphi \ . \tag{6.34}$$

Here we have normalized time, $\tau = t/\tau_A$ with the Alfv́en scale

$$\tau_A^2 \equiv \frac{4\pi m_i n}{\chi'^2} \simeq \left(\frac{aq}{\varepsilon v_A}\right)^2 .$$

It is easy to estimate the local dispersion relation for Eq. (6.34). Let the gradients be represented by parallel and perpendicular wavenumbers, and take $\kappa \sim 1/L_c$, where L_c is the curvature radius, and $\nabla P_o \sim P_o/L_n$ to obtain

$$\omega^2 \simeq v_A^2\left(k_\parallel^2 - \frac{\beta_o}{L_n L_c}\right) . \tag{6.35}$$

The sign of the line bending term is positive, showing its stabilizing effect. To obtain the negative, "unfavorable" sign of the interchange term we assumed

$$\underset{\sim}{\kappa}\cdot\nabla P_o > 0 \tag{6.36}$$

which is the Rayleigh–Taylor instability criterion for $k_\parallel = 0$. More generally Eq. (6.35) implies there is a critical value of β below which modes are stable. With $k_\parallel \sim (qR)^{-1}$, $L_n \sim a$, and $L_c \sim R$, this is

$$\beta_{crit} \sim \frac{\varepsilon}{q^2} \tag{6.37}$$

for an inverse aspect ratio $\varepsilon = a/R$. Above critical β the growth rate is

$$\gamma = \frac{\varepsilon v_A}{aq}\left(\frac{\beta}{\beta_{crit}} - 1\right)^{1/2} .$$

There are two aspects of Eq. (6.34) which modify the dispersion relation from the simple form of Eq. (6.35). The first is that, in the presence of magnetic shear, $k_\parallel$ is not a constant. Thus the ballooning representation must be used. We will see that this leads to a change in the effective connection length, $k_\parallel^{-1}$. The second is that in toroidal geometry the curvature varies along the field line, being unfavorable on the outside of the torus ($\vartheta=0$) and favorable on the inside ($\vartheta=\pi$). Unstable modes will tend to be localized in the regions of bad curvature, just the behavior which gives rise to the term "ballooning."

To treat these effects we use the ballooning representation of Eq. (6.8). The form of the interchange term depends on the representation of the curvature, Eq. (3.42), in terms of normal and geodesic components. In particular,

$$\underset{\sim}{B}_o\times\underset{\sim}{\kappa}_o\cdot\nabla_f \rightarrow i\underset{\sim}{B}_o\times\underset{\sim}{\kappa}_o\cdot\underset{\sim}{k}_\perp = -i\frac{B_o^2 k_\alpha}{\chi'}\left[\kappa_n + (\vartheta-\vartheta_k)q'\kappa_g\right] \qquad (6.38)$$

where the definition of $\underset{\sim}{k}_\perp$ in Eq. (6.16) has been used, and primes indicate derivatives with respect to V. Furthermore, noting that $\nabla_s P_o = P_o'\nabla V$, we obtain

$$\underset{\sim}{B}_o\times\nabla_s P_o\cdot\nabla_f \rightarrow -iP_o'\frac{B_o^2 k_\alpha}{\chi'} .$$

Therefore Eq. (6.34) becomes

$$-\omega^2 F^2 \varphi = \frac{\partial}{\partial \eta} F^2 \frac{\partial}{\partial \eta} \varphi + \tilde{\beta}[\kappa_n + (\eta - \vartheta_k) q' \kappa_g]\varphi \qquad (6.39)$$

in field line coordinates, Eq. (6.5). The normalized pressure gradient, $\tilde{\beta}$, and the normalized perpendicular wavenumber, F, are defined as

$$\tilde{\beta} \equiv 8\pi P_o'/\chi'^2 \sim \frac{\beta q^2}{\varepsilon L_n} ;$$

$$F \equiv \frac{k_\perp \chi'}{k_\alpha B_o} = \frac{\chi'}{B_o} |\nabla\alpha + \vartheta_k \nabla q| \ . \qquad (6.40)$$

Equation (6.39) is the ideal, incompressible MHD ballooning equation.

The equilibrium enters Eq. (6.39) explicitly through the functions B_o, κ_n, and κ_g. For a non-axisymmetric equilibrium these functions depend periodically on both ϑ and ζ. On a given field line (that is at fixed α) they are quasi-periodic functions of η, e.g.

$$f(q,\vartheta,\zeta) = f(q,\eta,\alpha+q\eta) \ . \qquad (6.41)$$

Of course when the equilibrium is axisymmetric these functions are simply periodic. The equilibrium also influences the ballooning equation implicitly through the metric elements in $k_\perp^2$.

A useful form for the perpendicular wavenumber can be obtained by noting that Eq. (6.14) implies

$$k_\perp^2 = \frac{B^2 k_\alpha^2 + (k^\chi)^2}{\chi'^2 |\nabla V|^2}$$

where

$$k^\chi = \underset{\sim}{k}_\perp \cdot \nabla\chi = k_\alpha \chi' [q' \nabla V \cdot \nabla V (\vartheta_k - \vartheta) + \nabla V \cdot \nabla \zeta - q \nabla V \cdot \nabla \vartheta] \tag{6.42}$$

is a contravariant component of $\underset{\sim}{k}_\perp$. This component of the perpendicular wavenumber is related to the local shear [19] which is defined by

$$S_* \equiv - \frac{\underset{\sim}{B} \times \nabla\chi}{|\nabla\chi|^2} \cdot \nabla \times \frac{\underset{\sim}{B} \times \nabla\chi}{|\nabla\chi|^2} \, . \tag{6.43}$$

Note that S_* represents the degree to which the vector perpendicular to $\underset{\sim}{B}$ and $\nabla\chi$ rotates. As we will see, $S_* \sim q'$ to lowest order. After some manipulation, S_* can be expressed as

$$S_* = - \underset{\sim}{B} \cdot \nabla \frac{\nabla\chi \cdot \nabla\alpha}{|\nabla\chi|^2} = - \underset{\sim}{B} \cdot \nabla \frac{k^\chi}{k_\alpha |\nabla\chi|^2} \tag{6.44}$$

and upon integration we obtain

$$k^\chi = - k_\alpha \chi' |\nabla V|^2 \int d\eta \; S_* \, .$$

Here the constant of integration has been chosen to be $\vartheta_k(q,\alpha)$.

The ballooning equation can be rewritten in a form which explicitly depends on the local shear parameter. Using the above definitions, F becomes

$$F^2 = \frac{1}{|\nabla V|^2}\left[1 + \left(\frac{\chi'|\nabla V|^2}{B_o}\int d\eta S_*\right)^2\right] . \tag{6.45}$$

The ballooning equation (6.39) is now

$$-\omega^2 F^2 \varphi = \frac{\partial}{\partial \eta} F^2 \frac{\partial}{\partial \eta}\varphi + \tilde{\beta}(\kappa^n + \kappa_g \int d\eta S_*)\varphi . \tag{6.46}$$

Here we have used Eq. (6.44) to re-express the curvature terms and defined

$$\kappa^n = \frac{\underset{\sim}{\kappa}\cdot\nabla V}{|\nabla V|^2} \tag{6.47}$$

which is proportional to the contravariant component in the V direction.

We conclude this section by expressing the curvature components in terms of $\underset{\sim}{B}$ and P. The geodesic curvature, defined in (3.42), can be obtained from

$$\kappa_g = -\frac{\chi'}{B^2}\underset{\sim}{B}\times\nabla V\cdot\underset{\sim}{\kappa} . \tag{6.48}$$

Using Eq. (2.1), we can express Eq. (6.48) in terms of the equilibrium perpendicular current:

$$\kappa_g = -\frac{\chi'}{cP'}\,\underset{\sim}{J}_\perp\cdot\underset{\sim}{\kappa}\ .$$

The definition of $\underset{\sim}{\kappa}$, (3.15), and Eq. (2.90) give

$$\kappa_g = \frac{\chi'}{2cP'}\,\nabla\cdot\underset{\sim}{J}_\perp = -\frac{\chi'}{2cP'}\,\underset{\sim}{B}\cdot\nabla\left(\frac{J_\parallel}{B}\right)\ . \tag{6.49}$$

The importance of Eq. (6.49) is to show that the flux surface average of the geodesic curvature is zero [recall Eq. (2.36)]:

$$\langle\kappa_g\rangle = 0 \tag{6.50}$$

a relation which we will use repeatedly below. The geodesic curvature can also be written in terms of covariant components of B:

$$\kappa_g = \frac{\chi'}{2}\left(B_\zeta\frac{\partial}{\partial\vartheta} - B_\vartheta\frac{\partial}{\partial\zeta}\right)B^{-2}\ . \tag{6.51}$$

The normal curvature is defined by

$$\kappa_n = \nabla\vartheta\times\nabla\zeta\cdot\underset{\sim}{\kappa}\ . \tag{6.52}$$

In view of Eq. (2.90), this becomes

$$\kappa_n = \frac{4\pi}{B^2}\left(P + \frac{B^2}{8\pi}\right)' + \frac{B_V}{2}\,B\cdot\nabla B^{-2}\ . \tag{6.53}$$

The normal curvature typically has a non-zero field line average.

Finally, the contravariant component is related to the normal and geodesic curvatures through

$$\kappa^n = \kappa_n + \kappa_g \frac{\nabla V \cdot (\nabla \zeta - q \nabla \vartheta)}{|\nabla V|^2} . \tag{6.54}$$

2. Asymptotic Analysis: The Mercier Criterion

The ballooning equation, Eq. (6.39), is to be solved on the covering space, $-\infty<\eta<\infty$, for a square integrable function $\varphi(\eta|q,\alpha)$. It has the form of a Sturm-Liouville eigenvalue problem [115] where the eigenvalue is ω^2. Thus the ballooning operator, L_o, is self-adjoint and its eigenvalues are real. Therefore, as is characteristic of ideal MHD, modes are either stable or purely growing. To elucidate the asymptotic behavior of φ, we next analyze the large $|\eta|$ limit. Treatment of the asymptotic behavior in the marginally stable case will lead to a necessary condition for stability, the Mercier criterion. Before prceeding to its derivation we discuss asymptotics in the general case.

As $\eta \to \infty$ the perpendicular wavenumber becomes arbitrarily large

$$F(\eta) \to \eta \frac{\chi' |\nabla q|}{B_o} + O(1) = G(\eta)\eta + O(1)$$

where $G(\eta)$ is defined to be the oscillatory coefficient of the secularity. The ballooning equation reduces to

$$\frac{\partial}{\partial \eta} G^2 \frac{\partial}{\partial \eta} \varphi = -\omega^2 G^2 \varphi + O(\eta^{-1}) \tag{6.55}$$

so that the secular variation drops out and the equation now has quasi-periodic coefficients [recall Eq. (6.41)].

In the axisymmetric case G is a simply-periodic function of η. The Floquet theory of equations with periodic coefficients [115] implies that the solutions have the form

$$\varphi(\eta) = e^{\lambda_i \eta}\, p^{(i)}(\eta) + O(\eta^{-1}), \quad i=1,2 \tag{6.56}$$

where $p(\eta)$ is periodic and λ is the characteristic exponent. Since the coefficients in Eq. (6.55) are real we know that if λ is a characteristic exponent then so is its complex conjugate. If, furthermore, the equilibrium is "up-down symmetric" ($G(-\eta) = G(\eta)$) it is easy to see that when λ is a characteristic exponent then so is $-\lambda$. Thus for this case the exponents are either purely real or purely imaginary (plus $2j\pi i$ for any j).

The asymptotic expansion for φ can be continued in the form

$$\varphi = \eta^{\nu} e^{\lambda\eta}\, (\varphi_o + \eta^{-1}\varphi_1 + \ldots) \tag{6.57}$$

where the φ_i are assumed to be periodic functions of η and the exponent ν is determined by higher orders in the expansion (we obtain an analagous result below in the marginal case). When the characteristic exponents, λ, are real only one of the two solutions is acceptable. Requiring φ to asymptote to the decaying solution at both $\pm\infty$ leads to a well defined eigenvalue problem with discrete eigenvalues.

However when λ is purely imaginary then both solutions have an oscillatory limit. In analogy with the Schrödinger equation, these values of λ lead to a continuous spectrum of ω^2. Since any value of ω

which leads to imaginary exponents provides an acceptable "unbound state" and λ depends continuously on ω, these values of ω form a continuum.

The problem of determining the characteristic exponents is in general very difficult. A simple solution is obtained in the marginal case, $\omega^2=0$, for then $\lambda=0$ and p=1 solves Eq. (6.55). Thus we expect that marginal stability is a boundary between a stable continuum and a discrete set of unstable modes. To show this we can solve Eq. (6.55) in the neighborhood of $\omega^2=0$ by a multiple scale expansion (like that in Subsec. 4) where the slow scale represents the characteristic exponent λ. This expansion gives

$$\lambda = i\omega\langle G^2\rangle\langle 1/G^2\rangle + O(\omega^3)$$

$$p = 1 + i\omega\langle G^2\rangle\int d\eta(1/G^2-\langle 1/G^2\rangle) + O(\omega^2) \quad .$$

Here $\langle\rangle$ is a flux surface average. This gives the promised result to first order in ω. Note that $\lambda\neq i\omega$ in systems with non-uniform shear.

A more general result concerning λ is obtained by transforming Eq. (6.65) to Hill's equation by letting $\varphi = \phi/G$. If the potential in this equation is always positive, e.g.

$$\omega^2 < -\left|\frac{G''}{G}\right| \simeq -\varepsilon$$

the characteristic exponents are real; thus stongly unstable modes are discrete. It is not obvious, and probably not true, that all damped modes form continua. For example, recall that the Mathieu equation has bands of real λ for arbitrarily large ω^2.

For the non-axisymmetric case, determination of the precise asymptotic behavior of the mode function has not been accomplished [112], although for the case of a discrete spectrum, a general theorem implies that the eigenvalues depend analytically on the size of the departures from axisymmetry.

When ω=0, the marginal case, the asymptotic behavior is not governed by the inertia term in the shear-Alfvén law, and a new expansion should be carried out. Because of the Sturm-Liouville form of Eq. (6.46) the asymptotic behavior of the marginal case leads to a stability criterion. This is due to the Sturm comparison theorem which implies the eigenvalues can be put in one-to-one correspondence with the number of zero crossings of the eigenfunction, the smallest eigenvalue corresponding to none. Since the eigenvalue is ω^2, the larger the growth rate the slower the oscillations. Furthermore, one can compare any two solutions, not necessarily eigenfunctions, and find the same result.

It follows that a necessary and sufficient condition for stability is that the marginal solution have no zero crossings. A simpler condition, which is only necesssary, is obtained from the asymptotic behavior of the marginal solution: for there to be no unstable modes the marginal solution necessarily cannot oscillate at large η (see Newcomb [18] for an alternative formulation and [88] for a discussion of exchange of stability). The explicit form of this criterion was obtained first by Mercier [85], and later in Hamada coordinates by Greene and Johnson [8]. Of course, even if the Mercier criterion is satisfied, stability is not assured, because oscillations could still occur at finite values of η.

We derive the Mercier criterion in general geometry by substituting Eq. (6.57) into the ballooning equation (6.39). To $O(\eta^{\nu+2})$ we obtain Eq. (6.55) with $\omega=0$, implying $\lambda=0$. Integrating once we obtain

$$\frac{\partial \varphi_0}{\partial \eta} = \frac{A}{G^2} \tag{6.58}$$

where A is a constant. The fact that the flux surface average annihilates the parallel gradient $\partial/\partial\eta$ [recall Eq. (2.36)] leads to the solubility condition

$$\left\langle \frac{A}{G^2} \right\rangle = 0 \tag{6.59}$$

which is satisfied if A is zero. Therefore φ_0 is a constant which can be taken to be unity without loss of generality. The order $\eta^{\nu+1}$ equation is

$$\frac{\partial}{\partial \eta} G^2 \left(\frac{\partial \varphi_1}{\partial \eta} + \nu \right) + \tilde{\beta} q' \kappa_g = 0 \ .$$

This equation is solvable for a quasi-periodic φ_1 if and only if the flux surface average of κ_g is zero. This has been verified already as Eq. (6.50). Define the function h by [recall Eq. (4.24)]

$$\kappa_g = \frac{\partial}{\partial \eta} h \tag{6.60}$$

The solution for φ_1 is

$$\frac{\partial \varphi_1}{\partial \eta} = -\nu - \frac{1}{G^2}\left(\tilde{\beta} q' h - C\right) . \tag{6.61}$$

The constant C is determined by the solubility condition for Eq. (6.61), which gives

$$\frac{\partial \varphi_1}{\partial \eta} = -\frac{\tilde{\beta} q'}{G^2}\left[h - \frac{\langle h/G^2\rangle}{\langle 1/G^2\rangle}\right] - \nu\left[1 - \frac{1/G^2}{\langle 1/G^2\rangle}\right] . \tag{6.62}$$

Note that since we have found $\varphi_0=1$, it is the η dependence of φ_1 which represents ballooning. The two terms above show that this is due to the surface dependence of the geodesic curvature and the non-uniformity of the shear.

The Mercier criterion is finally obtained from the next order equation, which involves the line bending operator on φ_2. The solubility condition for this equation is

$$(\nu+1) < G^2\left(\frac{\partial \varphi_1}{\partial \eta} + \nu\right)> + \tilde{\beta}\left(\langle \kappa_n\rangle + q'\langle \kappa_g \varphi_1\rangle\right) = 0 \quad .$$

Using Eq. (6.62) for φ_1 gives the equation

$$\nu(\nu+1) + D_I = 0 \ ,$$

$$D_I = \tilde{\beta}\left\langle\frac{1}{G^2}\right\rangle\left[\langle \kappa_n\rangle + \tilde{\beta} q'^2\left(\left\langle\frac{h^2}{G^2}\right\rangle - \frac{\langle h/G^2\rangle^2}{\langle 1/G^2\rangle}\right) - q'\left(\langle h\rangle - \frac{\langle h/G^2\rangle}{\langle 1/G^2\rangle}\right)\right] \tag{6.63}$$

which determines the exponent ν.

When $D < 1/4$ we have $\nu<0$ and therefore $\varphi\sim\eta^{\nu}$ falls off as $\eta\to\infty$. A square integrable asymptotic form is attainable by choosing the smaller exponent which is $\nu<-1/2$. However when $D > 1/4$ the exponent is complex and

$$\varphi \sim \eta^{-1/2}\cos[(D_I-1/4)^{1/2}\log\eta]$$

which oscillates as $\eta\to\infty$. The Sturm comparison theorem then implies that there is an unstable eigenvalue with a square integrable φ.

The necessary condition for stability, $1/4 - D_I>0$ can be written

$$\frac{q'^2}{4} - \tilde{\beta}\left[\left\langle\frac{B^2}{|\nabla\chi|^2}\right\rangle\langle\kappa_n\rangle + \left\langle\left(\tilde{\beta}\frac{hB^2}{|\nabla\chi|^2} - q'\right)\left(h\left\langle\frac{B^2}{|\nabla\chi|^2}\right\rangle - \left\langle\frac{hB^2}{|\nabla\chi|^2}\right\rangle\right)\right\rangle\right] > 0 \ . \quad (6.64)$$

The first term can be interpreted as the stabilizing effect of shear—it is analogous to the $k_{\|}^2$ term in the local dispersion relation (6.35) and reflects the fact that $k_{\|}$ can not be identically zero in a sheared field. The second term, involving $\langle\kappa_n\rangle$, shows the stabilizing effect of the average normal curvature, if $\langle\kappa_n\rangle P_o'<0$; otherwise it leads to a critical value of β like that in Eq. (6.37). The last terms in the Mercier criterion represent the effect of geodesic curvature which, though it has zero average, is important at large η due to shear. These terms can have either sign.

Recall from Eq. (6.29) that modes with large extent in η are narrow in q (at least in axisymmetric systems). Thus Mercier unstable modes are surface localized and can be recognized as interchange modes.

These were treated in Sec. VC.4, where we obtained a reduced version of this criterion, Eq. (5.89).

We have also seen from Eq. (6.62) that, in the interchange limit, the ballooning effect (represented by φ_1) is weak. Thus it is not surprising that the present analysis gives a result similar to the one obtained for surface localized modes. It is remarkable, however, that the present result, which is valid only in the limit $n\to\infty$, reproduces the low-n Mercier criterion exactly. It is also significant that the present analysis, which does not use an aspect ratio expansion, is nonetheless somewhat simpler than that of Chapter V. This circumstance shows the power of the ballooning formalism.

After some algebra, the Mercier criterion can be written in terms of parallel current and other natural equilibrium quantities [8,85]. In a low β expansion [116,117] the geodesic curvature terms cancel and only an averaged normal curvature remains. It is proportional to $(1-q^2)$ (see the next subsection).

It is clear that the Mercier criterion is necessary but not sufficient for stability. It is relevant for modes which are relatively constant for moderate η and only begin to oscillate at large η. A mode with oscillations only at finite η would not be determined unstable by the Mercier criterion. The treatment of modes for which the ballooning terms dominate and hence are not surface-localized must go beyond the Mercier criterion.

3. Model Ballooning Equation

Solution of the general ballooning equation is quite difficult analytically because of its awkward dependence on the explicit form of the equilibrium. The point is that no characterization of flux surfaces in terms of a parameter like the Δ' of boundary layer modes is available. The basic technique in the literature for attacking this problem (aside from the most obvious one: a computer program) is to expand about a known, simple case. In this way Greene and Chance [118] discuss the first order effects of variations in the shear and pressure on a given solution. A variation on this is to use a near-axis expansion of the equilbrium, taking into account that the shear and aspect ratio are always small near the magnetic axis of a tokamak [119-123].

Here we introduce a model equation which has many of the features of the more rigorous expansions (except quantitative validity) with the advantage that analytical calcuations are not so burdensome. This widely used model [106,108,124,125] uses Shafranov geometry (Sec. IID). Its disadvantage is that Shafranov geometry is obtained in a low β expansion, while the modes we consider are typically unstable only in the high β limit [e.g. Eq. (2.133) and Eq. (6.37)].

To obtain the model equation we will need expressions for F^2, and for the curvature components. The local shear in an axisymmetric system can be written using Eq. (6.44) as

$$S_* = \frac{dq}{dV} + q \frac{\partial \nabla V \cdot \nabla \vartheta}{\partial \vartheta \nabla V \cdot \nabla V} . \qquad (6.65)$$

When the flux surfaces are circles, the non-orthogonality of the metric is due to the Shafranov shift, Eq. (2.108):

$$S_* = \frac{dq}{dV} + q\frac{dR_c}{dV}\frac{\cos\vartheta}{r} + O(\varepsilon^2) \quad . \tag{6.66}$$

Equation (2.126) expresses the shift in terms of the hoop force and plasma pressure. Assuming that the pressure is large, so that the hoop force is negligible, the shift can be obtained from

$$P - \bar{P} \sim r\frac{dP}{dr} \quad .$$

Corrections to and the appropriateness of this model are discussed in [126]. Substitution into Eq. (2.126) gives

$$\frac{dR_c}{dV} = \frac{\tilde{\beta}}{R} \tag{6.67}$$

where $|\nabla V| \simeq rR$.

The geodesic curvature can be obtained from Eq. (6.51) using Eq. (2.116) and $B_T \simeq Rq\chi'$:

$$\kappa_g = -\frac{r}{Rq}\sin\vartheta + O(\varepsilon^2) \quad . \tag{6.68}$$

The normal curvature and, to the same order, κ^n are obtained from Eq. (6.53). Here we only compute the lowest order oscillatory contribution, which is due to the term B'/B. We obtain

$$\kappa^n = -\frac{1}{R|\nabla V|}\cos\vartheta + \langle\kappa^n\rangle + O(\varepsilon^2) \quad . \tag{6.69}$$

Calculation of the average normal curvature is a more subtle affair. In the zero β limit it is possible to show that [39,83,89,119,127]

$$\langle\kappa^n\rangle \simeq \frac{r}{R_o^2\langle|\nabla V|\rangle}\left(1 - \frac{1}{q^2}\right) \quad . \tag{6.70}$$

In this expression the factor $1/R_o|\nabla V|$ is just the covariant component of the curvature of a circle of radius R_o. The remaining factor is due to poloidal curvature and the Shafranov shift. Note that when $q>1$ the average curvature is favorable in the sense of (6.36). Of course in the high β case the average curvature could be expected to differ substantially from (6.70). Corrections to (6.70) can be calculated in an expansion about the magnetic axis [121].

Putting these expressions into the ballooning equation, (6.46), results in the model system

$$-\omega^2 f^2\varphi = \frac{\partial}{\partial\eta} f^2 \frac{\partial}{\partial\eta}\varphi + \rho\left(\bar{\kappa} + \cos\eta + (s\eta - \rho\sin\eta)\sin\eta\right)\varphi \tag{6.71}$$

where ρ and $\bar{\kappa}$ are dimensionless measures of the pressure gradient and average curvature, respectively:

$$\rho = -r\tilde{\beta} \simeq \left|\frac{r}{L_n}\frac{\beta q^2}{\varepsilon}\right|$$

$$\bar{\kappa} = -\frac{\langle|\nabla V|^2\rangle}{r}\langle\kappa^n\rangle \tag{6.72}$$

and f is the normalized version of F,

$$f^2 = 1 + [s(\eta-\vartheta_k) - \rho\sin\eta]^2 \tag{6.73}$$

where s is a dimensionless measure of the shear

$$s = q' \frac{\chi'<|\nabla V|^2>}{B_o} \simeq \frac{d\ell nq}{d\ell nr} \quad . \tag{6.74}$$

Neglected in this model are higher harmonics in η which arise from non-circularity of the flux surfaces. Solutions to Eq. (6.71) are studied in the following subsections.

The Mercier criterion, (6.63), can be written using the model expressions in the dimensionless form

$$\nu(\nu+1)s^2 + \rho\overline{\kappa} = 0 \quad .$$

The geodesic curvature terms have canceled completely and instability occurs if

$$\rho\overline{\kappa} > s^2/4 \quad . \tag{6.75}$$

4. Weak Ballooning

When the mode extent is large compared to 2π a multiple scale analysis can be applied to solve the ballooning equation [121-125]. In this technique weak ballooning effects are represented by slow modulation of the mode along the field line, and a first correction to

the Mercier criterion is obtained. The most important result of this analysis is the discovery of a second region of stability at large pressure gradient.

The primary analytical tool used is a subsidiary ordering on the length scale represented by the shear. We anticipate that the mode width is $\eta \sim 1/s$ which implies that weak shear gives a large mode width. For a tokamak the shear is always weak near the axis where q has a minumum:

$$s \simeq \frac{r^2}{q}\frac{d^2q}{dr^2} \sim \delta^2 .$$

Here a small parameter $\delta = r/a$ represents the near-axis expansion.

Due to the oscillatory curvature terms the mode will have rapid oscillations on the scale $\eta \sim 2\pi$. In order that the modulation influence stability of the mode, ω^2 must be comparable to the slow-scale line bending term in Eq. (6.71): $\omega \sim \delta^2$. For pressure terms to be important we expect $\beta \sim \beta_{crit}$, which implies the dimensionless pressure parameter is of the order $\rho \sim \delta$.

So that the weak ballooning effects are not dominated by strong interchange effects, we demand that the Mercier criterion be marginally satisfied. Eq. (6.75) implies that the curvature $\bar{\kappa}$ is $O(\delta^3)$ which, by the (6.70), implies $q=1 + O(\delta^2)$. Therefore marginal stability to interchange modes near the axis of a (low β) tokamak occurs at the so called Kruskal-Shafranov limit, $q(0) = 1$. Note that q is indeed close to one near the magnetic axis of a tokamak. We will not explicitly use Eq. (6.70) but only insist that $\bar{\kappa}$ be of the correct order.

To implement the ordering we allow variation in φ on two length scales: $\eta\sim 1$ and $\eta\sim 1/s$. The slow variable is naturally given by

$$z=s(\eta-\vartheta_k) \quad . \tag{6.76}$$

This is the scale which enters into the aperiodic terms in the ballooning equation. To allow a dependence on both the z and η variables, the η derivatives must be expanded as

$$\frac{\partial}{\partial\eta} \to \frac{\partial}{\partial\eta} + s\,\frac{\partial}{\partial z}$$

showing that the slow derivatives enter at order δ^2.

Expand the mode function in powers of δ,

$$\varphi(\eta) = \varphi_0(z,\eta) + \varphi_1(z,\eta) + \ldots \tag{6.77}$$

where φ_i is assumed to be $O(\delta^i)$. Substituting the expansions in the model ballooning equation (6.71) provides relations to determine the φ_i. Integrating the order δ^0 equation yields

$$\frac{\partial}{\partial\eta}\,\varphi_0 = \frac{A(z)}{1+z^2} \tag{6.78}$$

where A is independent of η. We demand there be no secular terms in η: all the slow scale behavior is to be absorbed into the z dependence. This implies the solubility condition

$$\left\langle \frac{A}{1+z^2} \right\rangle = 0$$

where the average is taken holding z fixed. Thus A=0. Integrating (6.78) once more gives $\varphi_o = \varphi_o(z)$, an arbitrary function of z. φ_o represents the envelope function and its z dependence will be fixed by a solubility condition at fourth order.

The $O(\varepsilon)$ equation is

$$\frac{\partial}{\partial\eta}(1+z^2)\frac{\partial}{\partial\eta}\varphi_1 + \rho(\cos\eta + z\sin\eta)\varphi_o = 0 \ .$$

The solubility condition for this equation is satisfied since $\langle\sin\eta\rangle = \langle\cos\eta\rangle = 0$. Integrating twice yields

$$\varphi_1 = \frac{\cos\eta + z\sin\eta}{1+z^2}\varphi_o + C(z) \qquad (6.79)$$

where C is an undetermined function of z at this order.

The second order solubility condition is satisfied if the the Mercier criterion is marginal to $O(\delta^2)$, which is equivalent to $\bar{\kappa} = o(\delta^2)$. The solution for φ_2 is

$$\varphi_2 = \frac{\rho^2}{4}\frac{(1-2z^2)\cos 2\eta + 3z\sin 2\eta}{(1+z^2)^2} + \rho\frac{\cos\eta + z\sin\eta}{1+z^2}C(z) + D(z)$$

where D(z) represents the averaged part of φ_2. It is the harmonic coupling of the $e^{2i\eta}$ terms with $e^{i\eta}$ terms which will give an average ballooning effect and cause modulation of the envelope.

The third order solubility equation is trivially satisfied. The solubility condition at fourth order yields a non-trivial equation:

$$-\omega^2(1+z^2)\varphi_o = 2\rho s \frac{\partial}{\partial z} z\langle\cos\eta\varphi_1\rangle + s^2 \frac{\partial}{\partial z}(1+z^2)\frac{\partial}{\partial z}\varphi_o + \rho\bar{\kappa}\varphi_o$$

$$- \rho^2\langle\sin^2\eta\varphi_2\rangle + \rho\langle(\cos\eta + z\sin\eta)\varphi_3\rangle \ .$$

To obtain the equation for φ_o it is evidently necessary to solve only for the terms of φ_3 behaving as $\cos\eta$ and $\sin\eta$ (there are 3η terms which do not enter the solubility condition). After considerable algebra we obtain

$$-\omega^2(1+z^2)\varphi_o = s^2 \frac{\partial}{\partial z}(1+z^2)\frac{\partial}{\partial z}\varphi_o + \left[\rho\bar{\kappa} + \frac{\rho^2(2s - 3\rho^2/8)}{(1+z^2)^2}\right]\varphi_o \qquad (6.79)$$

which is the goal of the analysis. Versions of this averaged, or "distilled" ballooning equation have been obtained in many papers [121-124,126]. Though the details of Eq. (6.79) depend on the specfics of the model, its qualitative behavior is similar to that obtained in more realistic equilibria [118,121,129].

The average curvature term $\rho\bar{\kappa}$ is the fourth order term of the Mercier criterion and thus represents interchange effects. The last term in Eq. (6.79) describes the ballooning effects. The destabilizing term proportional to $s\rho^2$ arises from the interaction of the line bending with geodesic curvature. The stabilizing term results from the average of the rapid curvature oscillations. Note that as $z\to\infty$ the ballooning term vanishes and the Mercier analysis is recovered. Modes with structure at finite z are influenced by the ballooning term.

Equation (6.79) can be rewritten as a Schrödinger equation by letting

$$\varphi_o = (1+z^2)^{-1/2}\ \phi(z)$$

whence

$$\omega^2\phi = -s^2\ \frac{\partial^2}{\partial z^2}\ \phi + V(z)\phi$$

where the potential is

$$V(z) = \frac{1}{1+z^2}\left[\ -\rho\overline{\kappa} + \frac{s^2}{1+z^2} + \frac{\rho^2(3\rho^2/8 - 2s)}{(1+z^2)^2}\right] . \qquad (6.80)$$

It is clear that if $\rho\overline{\kappa} > 0$ then the potential is negative at sufficiently large z, which leads to interchange instability. A simple sufficient condition for stability is that $V(z) > 0$ for all z. This gives the stability criteria

$$\rho\overline{\kappa} < 0$$

$$s^2 + |\rho\overline{\kappa}| + \rho^2\ \left(\frac{3\rho^2}{8} - 2s\right) > 0 . \qquad (6.81)$$

The first relation implies interchange stability and the second ballooning stability.

Equation (6.81) shows that ballooning modes are stable for sufficiently small pressure (ρ) and again for sufficiently large pressure. Rewriting (6.81) as

$$(s-\rho^2)^2 + |\rho\bar{\kappa}| - \frac{5\rho^4}{8} > 0$$

we obtain the two stability boundaries

$$s = \rho^2 \pm \left[\frac{5\rho^4}{8} - |\rho\bar{\kappa}|\right]^{1/2} . \qquad (6.82)$$

Instability occurs between these curves. Equation (6.82) implies there is a minimum ρ, $(8\bar{\kappa}/5)^{1/3}$, below which no instability is possible for any value of s. For larger values of the pressure parameter the two stability curves are approximately parabolas. These curves agree well with those obtained numerically for the model ballooning equation [130,131] as shown in Fig. 2. As the shear gets larger the negative-sign solution breaks towards smaller pressure, opening a larger window of instability.

The fact that ballooning modes are stabilized at sufficiently large pressure gradients is confirmed by many calculations with realistic equilibria [118,121,129]. This second stability regime makes feasible the operation of tokamaks in an economically favorable regime of high β.

5. Strong Ballooning

In the strong ballooning limit the mode is localized to a narrow range of η, typically near the outside of torus where the curvature is unfavorable. For this case the ballooning representation, Eq. (6.29), shows that the mode is spread over a large range in radius and hence contains many helicities. To treat this case we expand the ballooning equation for small mode width. We will see that this approximation is valid in the regime $s \sim \rho \gg 1$.

It is convenient to use the transformation

$$\varphi = \phi/f$$

to turn the ballooning equation (6.71) into a Schrödinger equation

$$\omega^2 \phi = -\frac{d^2\phi}{d\eta^2} + V(\eta)\phi$$

$$V(\eta) = \frac{(s-\rho\cos\eta)^2}{f^4} - \frac{\rho}{f^2}(\varkappa + \cos\eta) \quad . \tag{6.83}$$

This potential is shown in Fig. 3. For the case $s \sim O(1)$, Fig. 3b, the mode is clearly localized near $\eta=0$.

For simplicity we concentrate on the case $\vartheta_k = 0$. Usually this leads to the smallest minimum of V, and hence the most unstable mode (we remark on an important exception below). Of course to obtain the global quantization condition, it would be necessary to determine the dependence of ω^2 on ϑ_k.

When the mode is localized near η=0, the potential can be expanded up to $O(\eta^2)$ so that Eq. (6.83) becomes Weber's equation:

$$V(\eta) = a + b^2\eta^2$$

$$a = -\rho(\bar{\kappa}+1) + (s-\rho)^2$$

$$b^2 = \rho\left[s-\rho + \frac{1}{2} + (s-\rho)^2(\bar{\kappa}+1)\right] - 2(s-\rho)^4 \ .$$

The solutions to this equation are

$$\phi = e^{-b\eta^2/2}\, H_j(\sqrt{b}\ \eta)$$

$$\omega^2 = a + (2j+1)b \ , \qquad j=0,1,2,\ldots$$

where H_j is the Hermite polynomial. Since b must be positive it is clear that the lowest mode (j=0) is most unstable. Localization of the mode implies b is large; when $s\sim\rho$ this requires large ρ. The only consistent ordering is $(s-\rho) \sim \sqrt{\rho}$ which implies that the mode is always unstable:

$$\omega^2 = -\ c^2 + c(s-\rho) - (s-\rho)^2$$

$$c = \left[\rho(\bar{\kappa}+1) - 2(s-\rho)^2\right]^{1/2} \ .$$

The localization approximation is invalid if $b^2 < 0$; this determines the two curves

$$s = \rho \pm \left[\frac{\rho(\bar{\kappa}+1)}{2}\right]^{1/2} \qquad (6.84)$$

outside of which the potential develops a local maximum at $\eta=0$. The upper shear boundary lies quite close to the numerically determined "first stability" boundary as shown in Fig. 2. Stability in this case is due to the positive shear-induced potential overwhelming the local well due to the curvature term, $\bar{\kappa}+1$. The lower sign of Eq. (6.84) does not agree well with the "second stability" boundary in Fig. 2. This is due to quartic terms in the potential; the local maximum at $\eta=0$ only causes a small dimple (Fig. 4). Since the minimum of V now occurs at $\eta\neq0$ it is reasonable that the most unstable modes have $\vartheta_k\neq0$ as well [118]. Keeping ϑ_k leads to an increase in the size of the unstable region over that predicted by Eq. (6.84). This effect could be analyzed by an expansion about the minumum of V, but the algebra involved is prodigious.

In general, the instability we have found at $s\sim\rho$ is replaced by one near points of vanishing local shear, S_* [118]. Near such points the stabilizing effect of the line bending term is minimized, and if the local curvature is unfavorable, an instability can result.

D. Non-Ideal Effects

1. Four-Field Ballooning Equations

In this section the four-field model is used to treat the effects of compressibility, resistivity, and kinetic effects (finite δ) on ballooning modes. Rather than ambitiously including all of these terms in a single dispersion relation we treat them one by one, only commenting occasionally on the interaction between them.

The first step is to linearize the four-field equations and write them in the ballooning representation. We adopt the reduced flux coordinates discussed in Sec. VC.2., using the field line variables $(r,\vartheta,\alpha = z-q\vartheta)$. In this section the variable α replaces the variable $u = z-q_s\vartheta$ used in Chapter V, and for notational reasons ϑ is used for the field line coordinate η. Note that the use of α will,to some extent, actually simplify the resulting expressions; however, it also necessitates use of the ballooning representation and consequently the covering space.

The equilibrium of the four field model is given in Eqs. (4.128)-(4.129). The eikonal form, Eq. (6.2), with the axisymmetric eikonal, Eq. (6.28), is used for perturbed quantities:

$$\varphi \to \varphi(\vartheta)\ \exp\left[-in(\alpha + \int dq\vartheta_k)\right] .$$

Naturally the full eigenmode is the shifted sum of the all branches corresponding to the same eigenvalue, as in Eq. (6.29).

Linearizing the nonlinear parallel gradient, Eq. (4.147) yields

$$\nabla_\parallel f = \frac{\partial f}{\partial z} - [\psi_o, f] - [\psi, f_o] \to \frac{1}{q}\frac{\partial f}{\partial \vartheta} + [f_o, \psi] .$$

Here the definition of q, Eq. (5.61), was used, and in the last expression the perturbed quantities are represented by their envelope functions. Another quantity needed for the linearization is the bracket of a perturbed quantity with a flux function, for example:

$$[\psi, p_o] = \left(\hat{z}\cdot\nabla\alpha\times\nabla r\ \frac{\partial\psi}{\partial\alpha} + \hat{z}\cdot\nabla\vartheta\times\nabla r\ \frac{\partial\psi}{\partial\vartheta}\right)p_o' \to \frac{p_o'}{\psi_o'}\left(in\psi + \frac{1}{q}\frac{\partial}{\partial\vartheta}\psi\right)$$

where we follow the convention of indicating derivatives with respect to the flux coordinate, r, with a prime. The last term, which represents the parallel derivative of the envelope, can be neglected in the ballooning limit, $n \gg 1$. Similarly the bracket with the curvature scalar $h(r,\vartheta)$ can be expanded as

$$[h, p_e] \to -\frac{in}{\psi_o'}\left(h_r - s\frac{h_\vartheta}{\sqrt{g}}\,(\vartheta-\vartheta_k)\right)p_e \ . \tag{6.85}$$

The shear parameter is defined by analogy with Eq. (6.74) as

$$s = \frac{\sqrt{g}}{q}\frac{dq}{dr} \ .$$

Finally the diamagnetic terms on the right hand side of Eq. (4.143) reduce to

$$\delta\,\frac{T_i}{T_e}\,[U, p_o] \to in\delta\,\frac{T_i p_o'}{T_e \psi_o'}\,U \equiv -i\omega_{*i}U$$

where derivatives of equilibrium quantities are assumed to be relatively small, as usual. The diamagnetic frequency is defined in accord with Eq. (4.157). Using this notation and setting $T_i = T_e$, we can express Eqs. (4.143)-(4.146) as

$$-i(\omega-\omega_{*i})k_\perp^2\varphi + \frac{1}{q}\frac{\partial}{\partial\vartheta}k_\perp^2\psi - 2[h,p_e] = 0 \tag{6.86}$$

$$\left[-i\omega(1+4k_\perp^2\delta^2\frac{m_e}{m_i}) + i\omega_{*e} + \eta k_\perp^2\right]\psi + \frac{1}{q}\frac{\partial}{\partial\vartheta}(\varphi-\delta p_e) = 0 \tag{6.87}$$

$$-i\omega v + [\varphi,v_o] + \frac{1}{q}\frac{\partial}{\partial\vartheta}p_e - in\frac{p_o'}{\psi_o'}\psi = 0 \tag{6.88}$$

$$(-i\omega + \beta\eta k_\perp^2)p_e + in\frac{p_o'}{\psi_o'}\varphi = \beta\{2[h,\varphi-\delta p_e] - \frac{1}{q}\frac{\partial}{\partial\vartheta}(v + 2\delta J) +$$

$$[\psi, v_o + 2\delta J_o]\} \ . \tag{6.89}$$

The kink term does not appear in Eq. (6.86) since it is negligible in the ballooning limit.

The limit $\beta=\delta=\eta = 0$ is reduced MHD. We recover the reduced version of the ideal ballooning equation of the last section:

$$-\omega^2k_\perp^2\varphi = \frac{\partial}{\partial\vartheta}\frac{k_\perp^2}{q^2}\frac{\partial}{\partial\vartheta}\varphi - 2n^2\frac{p_o'}{\psi_o'^2}\left[h_r - s\frac{h_\vartheta}{\sqrt{g}}(\vartheta-\vartheta_k)\right]\varphi \ . \tag{6.90}$$

There are two differences between the reduced ballooning equation and Eq. (6.39). First the relatively unimportant factor of B_o is missing from the line bending term of Eq. (6.90). It is clear that this is an $O(\varepsilon)$ corrrection. Possibly the more serious defect of Eq. (6.90) is that the curvature is replaced by $-\nabla h$ [e.g. Eq. (4.24)]. It is clear that $-h_r$ represents the normal curvature and $h_\vartheta/\sqrt{g}$ represents the geodesic curvature. While the exact curvature of Eqs. (6.51) and Eq. (6.53) cannot be written as the gradient of a scalar, the high β,

large aspect ratio limit of these expressions can. Finally we note that the factor of q^2 in Eq. (6.90) is due to a different normalization of time as compared with Eq. (6.39) [compare Eqs. (6.34) and (3.37)].

The simplest model for h is the shifted circle equilibrium for which $\sqrt{g} \simeq r$ and

$$h_r \simeq -R_c' - \cos\vartheta$$

$$\frac{h_\vartheta}{\sqrt{g}} \simeq -\sin\vartheta \ . \tag{6.91}$$

It is clear that these expressions give a similar model to that of Sec. VIC.3. with $-R_c'$ representing $\langle\kappa_n\rangle$. Of course, this is not a consistent solution of the reduced equilbrium equation (4.45). We will not use this approximation in this section.

2. Resistive Ballooning

Following the procedure of treating complications to ideal, incompressible MHD ballooning one at a time, we set $\delta=\beta = 0$ in this section and consider the effects of finite resistivity. When $\beta=0$ the parallel velocity equation can be neglected and the pressure perturbation is simply advected by the incompressible flow. Equations (6.86), (6.87) and (6.89) can be combined to give

$$\frac{F^2}{\vartheta_A^2 s^2}\varphi = \frac{\partial}{\partial\vartheta}\frac{F^2}{1+F^2/\vartheta_R^2}\frac{\partial}{\partial\vartheta}\varphi - 2p_o'q^2\left[h_r - \frac{s}{\sqrt{g}}h_\vartheta(\vartheta-\vartheta_k)\right]\varphi \tag{6.92}$$

where we have defined

$$\vartheta_R^2 = \frac{\chi}{\eta}\left(\frac{\sqrt{g}}{nq}\right)^2$$

$$\vartheta_A^2 = (\gamma qs)^{-2}$$

$$F = \frac{\sqrt{g}}{nq} k_\perp = \left| \frac{\sqrt{g}}{q} (\nabla z + q\nabla\vartheta) + (\vartheta_k - \vartheta) s\nabla r \right| . \qquad (6.93)$$

Note that the factor $nq/\sqrt{g}$ approximately represents the magnitude of $k_\perp$ at $\vartheta=0$.

The primary effect of resistivity in Eq. (6.92) is a significant reduction of the stabilizing line-bending term for $\vartheta \sim \vartheta_R s$. Thus the shear, which is important in the localization of the ideal mode, is defeated by the resistivity at large ϑ: η permits unstable modes to be extended in ϑ by allowing the perturbed field lines to slip relative to the flow.

The resistive ballooning equation has three basic scales: that of the curvature oscillation, $\vartheta \sim 1$; the scale at which inertia becomes important, $\vartheta \sim \vartheta_A$; and finally the resistive scale, ϑ_R. The resistive scale, always important at large enough ϑ, forces the mode to have an asymptotic form,

$$\varphi \sim \exp\left(-\frac{\vartheta^2}{2w^2}\right) , \qquad (6.94)$$

which is unlike the ideal one, Eq. (6.57). Here the mode width is

$$w = (\vartheta_A \vartheta_R)^{1/2} = \left[(nqq')^2 \eta\gamma\right]^{-1/4} \qquad (6.95)$$

showing that unstable modes are localized by resistivity. This equation is equivalent to (5.35) for the resistive tearing mode, except that our definitions of ϑ_R and ϑ_A are inverse to those of the corresponding tearing scales. This is due to the Fourier transform relationship between ϑ and radial variable implicit in the ballooning represention; recall Eq. (6.29).

There are two distinct unstable resistive modes [132], distinguished by different orderings of the three scales. We take $\vartheta_A >> 1$, considering modes that grow on a time scale slower than the ideal one. The fast mode is determined by $\vartheta_R << 1 << \vartheta_A$ implying that resistive destabilization is important for all ϑ. For the slow mode, $\vartheta_R \sim \vartheta_A >> 1$ so that the mode is ideally driven at $\vartheta \sim 1$, the resistivity only acting at large ϑ to localize the mode.

To treat resistive modes analytically, it is convenient to introduce a subsidiary ordering of the mode width. Taking $w >> 1$ permits a multiple scale analysis, analagous to that in Subsection C.4; in this limit the curvature oscillates rapidly compared to the scale over which the mode is localized. Introducing a small parameter δ, we suppose that

$$w \sim \delta^{-1} \quad . \tag{6.96}$$

The slow scale modulation is represented by a variable $z = \delta\vartheta$, and following our previous analysis we let

$$\varphi(\vartheta) = \varphi_0(\vartheta, z) + \delta\varphi_1(\vartheta, z) + \ \ldots \quad .$$

In order that the mode be unstable, but not overwhelmingly so, the

geodesic driving term is assumed one order smaller than the fast-scale line-bending term yielding

$$p_o' \simeq \delta v_R^2 \ . \tag{6.97}$$

We begin with the fast mode for which the resistive scale is small. Taking

$$v_R^2 \sim \delta \tag{6.98}$$

together with Eqs. (6.96)-(6.97) implies $v_A^2 \sim \delta^{-5}$ and $p_o' \sim \delta^3$. Substitution of these orderings into the resistive ballooning equation and expansion to second order gives a solubility condition for φ_2 which determines the slow-scale dependence of φ_o:

$$v_R^2 \varphi_o'' - 2p_o' q^2 \langle h_r \rangle \varphi_o - z^2 \frac{\hat{M}}{v_A^2 \langle |\nabla r|^{-2} \rangle} \varphi_o = 0 \tag{6.99}$$

where we define

$$\hat{M} = \langle |\nabla r|^2 \rangle \langle |\nabla r|^{-2} \rangle \left[1 - (2p_o' q^2 s)^2 \frac{v_A^2}{g v_R^2} \frac{\langle \tilde{h}^2 \rangle}{\langle |\nabla r|^2 \rangle} \right] . \tag{6.100}$$

The condition for instability is that the average curvature be unfavorable:

$$p_o' \langle h_r \rangle < 0 \ .$$

This is clearly less stringent then the Mercier criterion, Eq. (5.89), which includes the shear stabilization term. There is an infinite sequence of unstable modes [recall Eq. (6.33) et seq.] with the j=0 mode most unstable. Its dispersion relation is

$$\gamma^3 = \frac{n^2\eta}{g}\,\frac{(2p_o'q^2)^2}{s^2\langle|\nabla r|^2\rangle}\left(\langle h_r\rangle^2 + \frac{s^2\langle\tilde{h}^2\rangle}{g}\right) \tag{6.101}$$

showing the characteristic behavior [133]

$$\gamma^3 \sim \eta(p_o')^2 \ . \tag{6.102}$$

This mode is essentially driven by the RMS geodesic curvature. Our expansions are valid when

$$\frac{\vartheta_R}{\vartheta_A} \sim 2p_o'q^2 << 1 \ ;$$

that is, providing one is below the ideal critical β. When the mode is very extended in ϑ, and hence localized in radius, it is similar to the resistive interchange, Eq. (5.108). As β increases toward β_{crit} the mode becomes more localized in ϑ, and though it is still unstable [125], the multiple scale approximation breaks down. In this case the mode exists for average favorable curvature as well.

The above treatment is easily generalized to unreduced MHD and general geometry [132,134]; the corresponding dispersion relation is nearly identical. A further generalization to the compressible case also gives an unstable fast resistive mode [125,132]. It is

perpendicular compressibility which is important in this case. It is interesting that the $\beta \to 0$ limit of the compressible equations does not reproduce Eq. (6.99). The difference is accounted for by replacing $\hat{M}$ by M, given in Eq. (5.80). Thus the growth rate is significantly different, even in the small β limit.

The slow resistive mode is obtained by assuming [124,132,134]

$$\vartheta_R \sim \vartheta_A \sim w \sim \delta^{-1} \quad . \tag{6.103}$$

In this case the pressure can be of order of the ideal critical value: $p_o' \sim 1$. As we suggested above, the slow mode can be treated by a boundary layer analysis very similar to that used for tearing instabilities. There are two distinct layers, ideal and resistive, occurring at $\vartheta \sim 1$ and $\vartheta \sim \vartheta_R$ respectively. Since ϑ_R is large the resistive layer occurs at large ϑ; thus this analysis is an inverted tearing theory.

When $\vartheta \sim 1$ the resistive ballooning equation reduces to the ideal, marginal equation in lowest order:

$$\frac{\partial}{\partial \vartheta} F^2 \frac{\partial}{\partial \vartheta} \varphi - 2p_o' q^2 [h_r - \frac{s}{\sqrt{g}} h_\vartheta (\vartheta - \vartheta_k)] \varphi = O(\delta) \quad . \tag{6.104}$$

This equation can be solved numerically, or by the techniques discussed in Sec. C. However when $\vartheta \sim \vartheta_R$, which implies $z \sim 1$, the effects of resistivity and inertia become important. The matching between the ideal and resistive solutions is accomplished in an intermediate region, $\vartheta \sim \delta^{-1/2}$, say. In this region the form of the ideal solution is obtained by the Mercier analysis:

$$\varphi \to A\vartheta^{\nu} + B\vartheta^{-\nu-1} \tag{6.105}$$

where the exponents ν are given by Eq. (6.63) or in the reduced case by the negative of Eq. (5.88). We proceed next to solve for the mode function with $z\sim1$ by multiple scale analysis. Once this solution is obtained, it will be matched to Eq. (6.105) in the range $z \sim \delta^{1/2}$.

The multiple scale analysis is entirely analagous to the fast mode case, and at second order gives:

$$\frac{\partial}{\partial z}\frac{z^2}{1+\Lambda z^2}\frac{\partial}{\partial z}\varphi_o + (D_R + \gamma^2 q^2 \hat{M}z^2)\,\varphi_o +$$

$$\frac{\hat{H}-\hat{H}^2}{1+\Lambda z^2}\varphi_o - \frac{2\Lambda z^2\hat{H}}{(1+\Lambda z^2)^2}\varphi_o = 0 \tag{6.106}$$

where $D_R = D_I + \hat{H}^2 - \hat{H}$, and $\hat{H}$ are related to quantities in Eqs. (5.81) and (5.90):

$$D_R = \frac{2p_o' q^2}{s^2} K_R$$

$$\hat{H} = \frac{p_o' q}{s} H$$

and

$$\Lambda = \frac{s^2}{\vartheta_R^2 \langle |\nabla r|^{-2} \rangle} \,. \tag{6.108}$$

It is easy to see that when $z \ll 1$ the solution to Eq. (6.106) obeys Eq. (6.105). When $z \gg 1$ the asymptotic limit takes the form of Eq. (6.94), with

$$w^4 = v_R^2 v_A^2 \frac{\langle |\nabla r|^{-2} \rangle}{s^2 \hat{M}} .$$

The physical solution of course obeys $w^2 > 0$. Equation (6.106) can be solved exactly in terms of Kummer functions. Imposing the boundary condition at small z, Eq. (6.105), gives the eigenvalue. Since Eq. (6.106) is symmetric under reflection in z there are both even and odd solutions. If $\hat{M}$ is positive the most unstable mode is the lowest even one.

An estimate for the eigenvalue is easily obtained by methods similar those we used in Chapter V. For simplicity we neglect the factors of $\hat{H}$ in Eq. (6.106). Integrating Eq. (6.106) from $-\infty$ to ∞, and noting the singular behavior near z=0 gives:

$$\frac{[z^2 \varphi_o']_{z=0}}{\varphi_o} + D_R w - \gamma^2 q^2 \hat{M} w^3 = 0 \qquad (6.109)$$

where the first term is the jump in $z^2 \varphi_o^2$ across z=0, which is evaluated from the ideal marginal solution, Eq. (6.105). In the spirit of our derivation, this coefficient is -B/A which we define as the ballooning equivalent of $-\Delta'$.

The resulting dispersion relation has the same form as Eq. (5.107). In particular, when D_R is negligible

$$\gamma \sim (n^2\eta)^{3/5}\Delta'^{4/5} \quad . \tag{6.110}$$

While this dispersion relation looks very similar to the simple resistive tearing mode, we should emphasize that the calulation of Δ' is very different in the two cases. In particular the ballooning Δ' involves only the form of the equilibrium on a single flux surface. In the small shear limit one can show that Δ' is positive in the ideally stable regions; for example, below the first stability boundary $\Delta' \propto (p_o')^2 s$ [124].

The generalization of the slow resistive mode to the compressive case [132] shows that the low β limit of this mode is singular. As we found for the fast mode, the equation obtained has the same form as Eq. (6.106), but $\hat{M}$ is replaced by M. This mode has apparently not been treated properly in the finite β case (important perpendicular compressibility terms were neglected in [125]). One major difficulty in this case is that the solution in the ideal region is no longer given by the incompressible marginal ballooning equation [96] (see, for example Eqs. (73) and (85) of [132]).

3. Finite Larmor Radius Effects

The finite Larmor radius parameter, δ, can be included in the analysis with no essential complication. The ballooning equation obtained for this case is

$$-\omega(\omega-\omega_{*i})q^2F^2\varphi = \frac{\partial}{\partial\vartheta}\frac{F^2}{1+F^2/\vartheta_*^2}\frac{\partial}{\partial\vartheta}\varphi - 2p_o'q^2[h_r - \frac{s}{\sqrt{g}}h_\vartheta(\vartheta-\vartheta_k)]\varphi \qquad (6.111)$$

where the collisionless scale parameter is

$$\vartheta_*^2 = \left(1 - \frac{\omega_{*e}}{\omega}\right)\frac{m_i}{m_e}\left(\frac{\psi_o'}{2n\delta}\right)^2 . \qquad (6.112)$$

There are two distinct effects contained in Eq. (6.111). The first is the modification of the inertia from the diamagetic drift [135]. This can be easily treated since (setting ϑ_* to ∞) the form of the equation is identical to the ideal case. The resulting dispersion relation is

$$\omega(\omega-\omega_{*i}) = -\gamma_{MHD}^2$$

where, following Eq. (6.35), the ideal growth rate can be estimated as

$$\gamma_{MHD}^2 \sim 2|p_o'| - 1/q^2 . \qquad (6.113)$$

The effect of the drift term is to increase the critical β to

$$-|p_o'| = \frac{1}{2q^2} + \frac{\omega^2_{*i}}{8} .$$

Using the definition of ω_{*i} and assuming $n\delta<1$ we find

$$|p_o'| = \frac{1}{2q^2}\left(1 + \frac{n^2\delta^2}{16g}\right) .$$

More generally it is easily seen that an unstable mode can exist only when $n\delta z < 2g$. Thus the effect of ω_{*i} is to provide an effective cut-off in n beyond which ballooning modes are stable.

The effect of the electron inertia term, ϑ_*, is very similar to the resistivity. Collisionless modes have been treated by [136], and other kinetic effects on ballooning modes have been studied in [137-140].

4. Compressibility

To study the effect of compressibility set $\delta=\eta=0$ in Eqs. (6.86)-(6.89). Define the field

$$\upsilon = \frac{\omega\psi_o'}{n} p_e - p_o'\varphi \qquad (6.114)$$

which is proportional to the parallel velocity. In general υ represents the departure from pure convection of the pressure. The four-field ballooning equations can be reduced to two coupled second order equations for the fields φ and υ:

$$q^2\omega^2F^2\varphi + \frac{\partial}{\partial\vartheta} F^2 \frac{\partial}{\partial\vartheta}\varphi - 2q^2[h_r - \frac{s}{\sqrt{g}} h_\vartheta(\vartheta-\vartheta_k)](p_o'\varphi + v) = 0 \qquad (6.115)$$

$$(\beta\frac{\partial^2}{\partial\vartheta^2} + \omega^2q^2)v = 2\beta\omega^2q^2[h_r - \frac{s}{\sqrt{g}} h_\vartheta(\vartheta-\vartheta_k)]\varphi \ . \qquad (6.116)$$

Equation (6.115) represents the standard ideal ballooning equation with a single additional term coupling φ to the compressibility through the curvature. The left-hand side of Eq. (6.116) allows for the propagation of sound waves along the field lines with the speed $v_s^2 = \beta/q^2$ [recall the definition of β, Eq. (4.141)]. The first term arises from the parallel compressibility, $\nabla_\parallel v$. The right hand side of Eq. (6.116) arises from the perpendicular compressibility term, reflecting the fact that $\nabla\cdot v_\perp$ is non-zero through the variation of $\underset{\sim}{B}$ on a flux surface. Compressibility introduces a final scale into the ballooning equations:

$$\vartheta_s = \frac{\sqrt{\beta}}{\gamma q} \ .$$

It is commonly known that in MHD the marginal stability point is unaffected by compressibility. Equations (6.115)-(6.116) indeed exhibit this behavior, since the coupling term in Eq. (6.116) is proportional to ω^2. Away from marginal stability, a simple estimate of the form of the dispersion relation is obtained by the local dispersion relation. By Eq. (6.91) we can estimate the curvature terms by unity (choosing the unfavorable sign) and similarly F^2 is of order unity for moderate ϑ; thus,

$$\omega^2 q^2 - k_\parallel^2 - 2q^2 p_o' = 4\beta q^2 \frac{\omega^2}{\omega^2 - v_s^2 k_\parallel^2} . \tag{6.117}$$

When ω is small compared to the sound frequency $v_s k_\parallel$, this reduces to

$$\gamma^2 \simeq \frac{\gamma_{MHD}^2}{1 + 4q^2/k_\parallel^2} . \tag{6.118}$$

Note that even though the parameter β cancels from the equation, the growth rate is not equal to the incompressible limit. This is the same phenomena on which we remarked in Subsection 2. Physically the reduction in growth rate comes from the increased fluid inertia contributed by the parallel flow [128]. For modes which grow rapidly relative to $k_\parallel v_s$, the dispersion relation (6.117) becomes

$$\gamma^2 \simeq \gamma_{MHD}^2 - 4\beta \tag{6.119}$$

again showing a decrease in the growth rate. This decrease is a true compressible effect due to free energy being used to compress the fluid.

A more rigorous theory of the effects of compressibility can be carried out by the near-axis expansion method of Subsection C.4. It is not difficult to see [128] that the result of this expansion is equivalent to the growth rate reduction given in Eq. (6.118) (an averaging of the squared curvature changes the $4q^2$ to $2q^2$, e.g. the factor M of Eq. (5.80)). Additional compressible corrections arise only upon continuing the expansion to $O(\delta^6)$.

When s~1, compressibility is more significant than the local dispersion relation predicts [96]. It is easy to see that the parallel compressibility must be important near marginal stability. If it is neglected, Eq. (6.116) can be combined with (6.115) to give a significant, positive-definite contribution to ω^2, as estimated in Eq. (6.119). However, we know that the compressible equations have the same marginal point as the incompressible ones. Therefore, near marginality parallel compressibility must cancel the stabilizing contribution of perpendicular compressibility. To treat this, a more careful treatment of Eq. (6.116) must be given.

Equation (6.116) can be solved with a Green function to obtain

$$v = \gamma q\sqrt{\beta} \int_{-\infty}^{\infty} d\vartheta' \exp[-|\vartheta-\vartheta'|/\vartheta_s] \left[h_r - \frac{s}{\sqrt{g}} h_\vartheta(\vartheta'-\vartheta_k] \varphi(\vartheta') \right. . \qquad (6.120)$$

Note that v is proportional to the square root of β, confirming that the limit $\beta \to 0$ is singular. For small enough frequency, ϑ_s will always be larger than the scale of φ. For example at the marginal point, φ decays on the scale O(1), Eq. (6.57). Using use this equation for φ and Eq. (6.91) for the curvature gives

$$v \sim \gamma qs\sqrt{\beta} .$$

Comparing terms in Eq. (6.115) shows that the compressibility always dominates the inertia when γ is small enough:

$$\gamma \leqslant qs\sqrt{\beta}$$

that is, when the sound scale, ϑ_s, is larger than $1/sq^2$. This estimate yields the approximate growth rate,

$$\gamma \sim \frac{1}{qs\sqrt{\beta}} \gamma_{MHD}^2 ,$$

which no longer scales as the square root of the critical pressure gradient. Further analysis can be done by computer solution of the integral equation obtained by substituting Eq. (6.120) into (6.115).

Acknowledgments

We are grateful to many colleagues at the Institute for Fusion Studies and elsewhere for helpful advice and instruction. We especially wish to thank Ahmet Aydemir, John Cary, Pat Diamond, Michael Kotschenreuther, and James Van Dam for beneficial discussions. This work was supported by the U. S. Department of Energy contract no. DE-FG05-80ET-53088.

Figure Captions

1) Magnetic surfaces in Shafranov geometry.

2) Stability boundaries for the model equation, (6.71); $\bar{\kappa} = \vartheta_k = 0$. Instability occurs between the solid curves which were obtained numerically. The dashed curves, representing the weak shear case are given by Eq. (6.82). The dash-dot curves are the approximate strong shear limit of Eq. (6.84).

3) Ballooning Potential, $V(\eta)$, from Eq. (6.83) for $\bar{\kappa} = \vartheta_k = 0$.
   a) The weak shear case, s=0.1, ρ=0.3. Note the scale disparity leading to Eq. (6.76).
   b) Strong shear case, s=1.0, ρ=0.8, near the first stability boundary.

4) Ballooning potential near the second stability boundary. Parameters are s=1.0, ρ=2.2, $\bar{\kappa} = \vartheta_k = 0$.

References

1. Edward Teller, in: Fusion, edited by Edward Teller (Academic, New York, 1981), Vol. 1, 1; M. N. Rosenbluth and P. H. Rutherford, in: ibid., 32.

2. A. Lieberman and M. Lichtenburg, Regular and Stochastic Motion (Springer-Verlag, New York,1983) Applied Mathematical Sciences Series Vol. 38, 41.

3. M. D. Kruskal and R. M. Kulsrud, Phys. Fluids 1 (1958) 265.

4. H. Grad, Phys. Fluids 10 (1967) 137.

5. V. D. Shafranov, in: Reviews of Plasma Physics, edited by M. A. Leontovich (Consultants Bureau, New York, 1966) Vol. 2, 103.

6. W. A. Newcomb, Phys. Fluids 2 (1959) 362.

7. S. Hamada, Nucl. Fusion 2 (1962) 23.

8. J. M. Greene and J. L. Johnson, Phys. Fluids 5 (1962) 510.

9. See, for example, S. Weinberg, Gravitation and Cosmology (John Wiley and Sons, New York, 1972) 91.

10. See, for example, J. D. Hanson and J. R. Cary, Phys. Fluids 27 (1984) 767.

11. H. Grad and H. Rubin, in: Proceedings of Second International Conference on the Peaceful Uses of Atomic Energy (United Nations, Geneva,1958) Vol. 31, 190.

12. V. D. Shafranov, Sov. Phys.-JETP 8 (1958) 545.

13. D. Pfirsch and A. Schluter, Max-Planck-Institut Report MPI/PA/7/62 (1962; unpublished). See also J. M. Greene and J. L. Johnson, Phys. Fluids 4 (1961) 875.

14. R. Galvao, "Magnetohydrodynamical Theory of High-beta Diffuse Plasmas" to be published in Radiation in Plasmas, Vol. II, edited by B. McNamara.

15. J. P. Freidberg, Rev. Mod Phys. 54 (1982) 801.

16. W. B. Thompson, An Introduction to Plasma Physics (Addison-Wesley, Reading, 1962) 70.

17. G. L. Chew, M. L. Goldberger, and F. E. Low, Proc. R. Soc. Lond. 236A 1956) 112.

18. W. A. Newcomb, Ann. Phys. 10 (1960) 232.

19. J. M. Greene and J. L. Johnson, Plasma Phys. 10 (1968) 729.

20. A. A. Ware, Culham Laboratory Report CLM-M53 (1965; unpublished).

21. J. R. Cary and R. G. Littlejohn, Ann. Phys. 151 (1983) 1.

22. K. Swartz and R. D. Hazeltine, to be published in Phys. Fluids.

23. J. D. Callen, Phys. Rev. Lett. 39 (1977) 1540.

24. A. B. Chirikov, Phys. Rep. 52 (1979) 263; cf. also G. H. Walker and J. Ford, Phys. Rev. 188 (1969) 416.

25. M. N. Rosenbluth, R. Z. Sagdeev, J. B. Taylor and G. M. Zaslavski, Nucl. Fusion 6 (1966) 297.

26. T. H. Stix, Phys. Rev. Lett. 30 (1973) 833; Phys. Rev. Lett. 36 (1976) 521.

27. A. B. Rechester and M. N. Rosenbluth, Phys. Rev. Lett. 40 (1978) 38.

28. S. P. Hirshman and K. Molvig, Phys. Rev. Lett. 42 (1979) 648.

29. B. V. Waddell, B. Carreras. H. R. Hicks, J. A. Holmes, and D. K. Lee, Phys. Rev. Lett. 20 (1978) 1386.

30. R. B. White, D. A. Monticello, M. N. Rosenbluth, and B. V. Waddell, in: Proceedings of the Sixth Conference on Plasma Physics and Controlled Nuclear Fusion Research, Berchtesgaden (International Atomic Energy Agency, Vienna, 1976), Vol. I, 569.

31. B. Carreras, B. V. Waddell, and H. R. Hicks, Nucl. Fusion 19 (1979) 1423.

32. B. B. Kadomtsev and O. P. Pogutse, Sov. Phys.-JETP 38 (1974) 283.

33. M. N. Rosenbluth, D. A. Monticello, H. R. Strauss, and R. B. White, Phys. Fluids 19 (1976) 198.

34. H. R. Strauss, Phys. Fluids 19 (1976) 134.

35. H. R. Strauss, Phys. Fluids 20 (1977) 1354.

36. J. Boussinesq, Theorie Analytique de la Chaleur (Gathier-Villars, Paris, 1903), Vol. 2; E. A. Spiegiel and G. Veronis, Astrophys. J. 131 (1960) 442.

37. P. J. Morrison and R. D. Hazeltine, Phys. Fluids 27 (1984) 886.

38. R. Schmalz, Phys. Lett. 82 (1981) 14.

39. H. R. Strauss, Nucl. Fusion 23 (1983) 649.

40. L. Spitzer, Jr. and R. Härm, Phys. Rev. 89 (1953) 977.

41. A. Hasegawa and M. Wakatani, Phys. Fluids 26 (1983) 1770.

42. R. D. Hazeltine, Phys. Fluids 26 (1983) 3242.

43. J. F. Drake and T. M. Antonsen, Jr., Phys. Fluids 27 (1984) 898.

44. D. Biskamp, Nucl. Fusion 19 (1979) 777.

45. P. H. Rutherford and E. A. Frieman, Phys. Fluids 11 (1968) 569.

46. R. D. Hazeltine, Plasma Phys. 15 (1973) 77.

47. P. J. Catto, W. M. Tang, and D. E. Baldwin, Plasma Phys. 23 (1983) 639.

48. P. J. Catto and M. N. Rosenbluth, Phys. Fluids 24 (1981) 24 3.

49. L. Chen, P. H. Rutherford, and W. M. Tang, Phys. Rev. Lett. 39 (1977) 460.

50. B. Coppi, Riv. Nuovo Cimento 1 (1969) 3.

51. B. B. Kadomtsev and O. P. Pogutse, Nucl. Fusion 11 (1971) 67.

52. P. L. Bhatnagar, E. P. Gross, and M. Krook, Phys. Rev. 94 (1954) 511.

53. R. D. Hazeltine, D. Dobrott, and T. S. Wang, Phys. Fluids 18 (1975) 1778.

54. F. L. Hinton and R. D. Hazeltine, Rev. Mod. Phys. 48 (1976) 239.

55. B. D. Fried and S. D. Conte, The Plasma Dispersion Function (Academic, New York, 1961).

56. B. Coppi, J. Mark, L. Sugiyama, and G. Bertin, Phys. Rev Lett. 42 (1979) 1058; Ann. Phy. 119 (1979) 370.

57. J. F. Drake, T. M. Antonsen, Jr., A. B. Hassam, and N. T. Gladd, Phys.Fluids 26 (1983) 2509.

58. J. F. Drake and Y. C. Lee, Phys. Fluids 20 (1977) 1341.

59. M. N. Bussac, D. Edery, R. Pellat, and J. L. Soule, Phys Rev. Lett. 40 (1978) 1500.

60. P. L. Pritchett, Y. C. Lee, and J .F. Drake, Phys. Fluids 23 (1980) 1368; S. M. Mahajan and R. D. Hazeltine, Nucl. Fusion 22 (1982) 1191.

61. P. J. Catto, A. M. El Nadi, C. S. Liu, and M. N. Rosenbluth, Nucl. Fusion 14 (1974) 1054.

62. R. D. Hazeltine, M. Kotschenreuther and P. J. Morrison, in preparation.

63. A. N. Kaufman, Phys. Fluids 3 (1960) 610.

64. T. E. Stringer, Princeton Plasma Physics Laboratory Report MATT-320 (1965; unpublished).

65. F. L. Hinton and C. W. Horton, Phys. Fluids 14 (1971) 116.

66. M. N. Rosenbluth and A. Simon, Phys. Fluids 8 (1965) 1300.

67. X. S. Lee, Doctoral Dissertation, The University of Texas (1980; unpublished) 24.

68. S. I. Braginskii, in: Reviews of Plasma Physics, edited by M. A. Leontovich (Consultants Bureau, New York, 1965) Vol. 1, 205.

69. A. B. Mikhailovskii, Sov. Phys.-JETP 25 (1967) 623.

70. P. H. Rutherford and H. P. Furth, Princeton Plasma Physics Laboratory Report MATT-872 (1971; unpublished).

71. H. V. Wong, University of Texas at Austin Fusion Research Center Report FRCR No. 113 (1976).

72. B. Coppi, R. Galvao, R. Pellat, M. N. Rosenbluth, and P. H. Rutherford, Sov. J. Plasma Phys. 2 (1977) 533.

73. R. D. Hazeltine and D. W. Ross, Phys. Phys. 21 (1978) 1140.

74. S. M. Mahajan, R. D. Hazeltine, H. R. Strauss, and D. W. Ross, Phys. Fluids 22 (1979) 2147.

75. H. P. Furth, J. Killeen, and M. N. Rosenbluth, Phys. Fluids 6 (1963) 459.

76. H. R. Strauss, R. D. Hazeltine, S. M. Mahajan, and D. W. Ross, Phys. Fluids 22 (1979) 889.

77. L. J. Slater, in Handbook of Mathematical Functions, edited by M. Abramovitz and I. A. Stegun (Dover, New York, 1970) 504.

78. S. M. Mahajan, Phys. Fluids 26 (1983) 139.

79. R. D. Hazeltine, U. S. Department of Energy Report HCP/74478-01 (1978; unpublished).

80. H. P. Furth, in Propagation and Instabilities in Plasmas, edited by W. I. Futterman (Stanford University Press, Stanford, 1963) 87.

81. M. N. Rosenbluth, R. Y. Dagazian, and P. H. Rutherford, Phys. Fluids 16 (1973) 1894.

82. J. L Johnson and J. M. Greene, Plasma Phys. 9 (1967) 611.

83. A. H. Glasser, J. M. Greene, and J. L. Johnson, Phys. Fluids 18 (1975) 875.

84. B. R. Suydam, Proc. U.N. Intern. Conf. Peaceful Uses At. Energy, 2nd, Geneva (Columbia University Press, New York, 1959) Vol. 31, 85.

85. C. Mercier, Nuclear Fusion Suppl. Pt. 2 (1962) 801.

86. A. H. Glasser, S. C. Jardin, and G. Tesauro, Phys. Fluids 27 (1984) 1225.

87. B. Coppi, J. M. Greene. and J. L. Johnson, Nucl. Fusion 6 (1966) 101.

88. S. Chandrasekhar, Hydrodynamic and Hydromagnetic Stability (Oxford Univ. Press, London, 1961), p. 3.

89. A. H. Glasser, J. M. Greene, and J. L. Johnson, Phys. Fluids 19 (1976) 567.

90. J. L. Johnson, J. M. Greene, and B. Coppi, Phys. Fluids 6 (1963) 1169.

91. D. Dobrott, S. C. Prager, and J. B. Taylor, Phys. Fluids 20 (1977) 2179.

92. B. A. Carreras, P. W. Gaffney, H. R. Hicks and J. D. Callen, Phys. Fluids 25 (1982) 1231.

93. G. Laval, R. Pellat, and M. Vuillemin, in Plasma Physics and Controlled Fusion Research (International Atomic Energy Agency, Vienna, 1965), Vol. II, 259.

94. A. B. Hassam, Phys. Fluids 23 (1980) 38.

95. J. F. Drake, Phys. Fluids 21 (1978) 1777.

96. M. Kotschenreuther, private communication.

97. P. H. Rutherford, Phys. Fluids 16 (1973) 1903.

98. See, for example, B. A. Carreras, H. R. Hicks, J. A. Holmes, and B. V. Waddell, Phys. Fluids 23 (1980) 1811.

99. J. F. Drake and Y. C. Lee, Phys. Rev. Lett. 39 (1977) 453.

100. B. V. Waddell, M. N. Rosenbluth, D. A. Monticello, and R. B. White, Nucl. Fusion 16 (1976) 528.

101. D. Edery, M. Frey, J. P. Somon, M. Tagger, J. L. Soule, R. Pellat, and M. N. Bussac, Phys. Fluids 26 (1983) 1165.

102. M. Kotschenreuther, R. D. Hazeltine and P. J. Morrison, to be published in Phys. Fluids.

103. S. Chandrasekhar, op. cit., 428.

104. K. V. Roberts and J. B. Taylor, Phys. Fluids 8 (1965) 315.

105. J. B. Taylor, in: Proceedings of the Sixth Conference on Plasma Physics and Controlled Nuclear Fusion Research, Berchtesgaden (International Atomic Energy Agency, Vienna, 1976), Vol. II, 323.

106. Y.C. Lee and J. Van Dam , in: Proceedings of the Finite Beta Workshop (Varenna Summer School of Plasma Physics Sept. 1977), B. Coppi and W. Sadowski (eds.), (USDOE OFE Conf-7709167,1979), 93.

107. A.H. Glasser , in: Ibid., 55.

108. J. W. Connor, R. J. Hastie, and J. B. Taylor, Phys. Rev. Lett. 40 (1978) 396.

109. J. Van Dam, Kinetic Theory of Ballooning Instabilities, Ph.D. Thesis, Univ. of California, Los Angeles, 1979.

110. R. L. Dewar, J. Manickam, R. C. Grimm, and M. S. Chance, Nucl. Fusion 21 (1981) 493.

111. J. W. Connor, R. J. Hastie and J. B. Taylor, Proc. R. Soc. Lond. A. 365, (1979) 1.

112. R. L. Dewar and A. H. Glasser, Phys. Fluids 26 (1983) 3038.

113. G. M. Whitham, Linear and Nonlinear Waves, (John Wiley and Sons, New York, 1972).

114. J. Heading, An Intoduction to Phase-Integral Methods (Methuen, London, 1962) 57.

115. E. L. Ince, Ordinary Differential Equations, (Dover, New York,1956) 223.

116. V. D. Shafranov and E. I. Yurchenko, in: Plasma Physics and Controlled Nuclear Fusion Research, Madison (International Atomic Energy Agency, Vienna, 1971), Vol. II, 519.

117. A. A. Ware and F. A. Haas, Phys. Fluids 9 (1966) 956.

118. J. M. Greene and M. S. Chance, Nucl. Fusion 21 (1981) 453.

119. V. D. Shafranov and E. I. Yurchenko, Sov. Phys. JETP 26 (1968) 682.

120. A. B. Mikhailovskii, Nucl. Fusion 14 (1974) 483.

121. D. Lortz, and J. Nuhrenberg, Nucl. Fusion 19 (1979) 1207.

122. B. Coppi, A. Ferreira and J. J. Ramos, Phys. Rev. Lett. 44 (1980) 990.

123. A. B. Mikhailovskii and E. I. Yurchenko, Plas. Phys. 24 (1982) 977.

124. H. R. Strauss, Phys. Fluids 24 (1981) 2004.

125. T. C. Hender, B. A. Carreras, W. A. Cooper, J. A. Holmes, P. H. Diamond, and P. L. Similon, Phys. Fluids 24 (1984) 1439.

126. B. Coppi, A. Ferreira, J. W.-K. Mark, and J. J. Ramos, Nucl. Fusion 19 (1979) 715.

127. C. Mercier and H. Luc, Lectures in Plasma Physics: the Magnetohydrodynamic Approach to the Problem of Plasma Confinement in Closed Magnetic Configurations (Commission of the European Communities, Luxembourg, 1974), 94.

128. T. M. Antonsen, Jr., A. Ferreira and J. J. Ramos, Plas. Phys. 24 (1982) 197.

129. H. R. Strauss, W. Park, D. A. Monticello, R. B.White, S. C. Jardin, M.S. Chance, A. M. M. Todd, A. H. Glasser, Nucl. Fusion 20 (1980) 638.

130. A. Sykes, M. F. Turner, P. J. Fielding, F. A. Haas, in: Plasma Physics and Controlled Nuclear Fusion Research, Innsbruck (International Atomic Energy Agency, Vienna, 1978), Vol. I 625.

131. O. P. Pogutse and E. I. Yurchenko, Sov. J. Plas. Phys. 5 (1979) 441.

132. D. Correa-Restrepo, Z. Naturforsch. 37a (1982) 848.

133. V. M. Gribkov, D. K. Morozov, O. P. Pogutse, E. I. Yurchenko, Plasma Physics and Controlled Nuclear Fusion Research, Brussels (I.A.E.A., Vienna, 1981), Vol. I, 571; B. A. Carreras, P. H. Diamond, M. Murakami, J. L.Dunlap, J. D. Bell, H. R. Hicks, J. A. Holmes, E.A . Lazarus, V. K. Pare, P. Similon, C. E. Thomas, R. M. Wieland, Phys. Rev. Lett. 50 (1983) 503.

134. M. S. Chance, P. L. Dewar, E. A. Frieman, A. H. Glasser, J. M. Greene, R.C. Grimm, S.C. Jardin, J. L. Johnson, J. Manickam, M. Okabayashi, A. M. M. Todd, in: Proceedings of the Sixth Conference on Plasma Physics and Controlled Nuclear Fusion Research, Innsbruck (International Atomic Energy Agency, Vienna, 1978), Vol I 677.

135. W. M. Tang, J. W. Connor and R. B. White, Nucl. Fusion 21 (1981) 891; W. M. Tang, R. L. Dewar, and J. Manickam, Princeton Plasma Physics Lab Report, PPPL-1895 (1982) (unpublished).

136. C. Z. Cheng, Phys. Fluids 25 (1982) 1020; C. Z. Cheng, Nucl. Fusion 22 1982) 773.

137. W. M. Tang, J. W. Connor, R. J. Hastie, Nucl. Fusion 20 (1980) 1439; K. T. Tsang, Phys. Fluids 24 (1981) 2017.

138. F. Pegoraro and T. J. Schep, Phys. Fluids 24, (1981) 479.

139. P. H. Diamond, P. L. Similon, T. C. Hender, and B. A. Carreras, Institute for Fusion Studies Report, IFSR #113 (1983) (unpublished).

140. J. W. Connor, L. Chen, and M. S. Chance, Princeton Plasma Physics Lab Report, PPPL-1957 (1983) (unpublished).

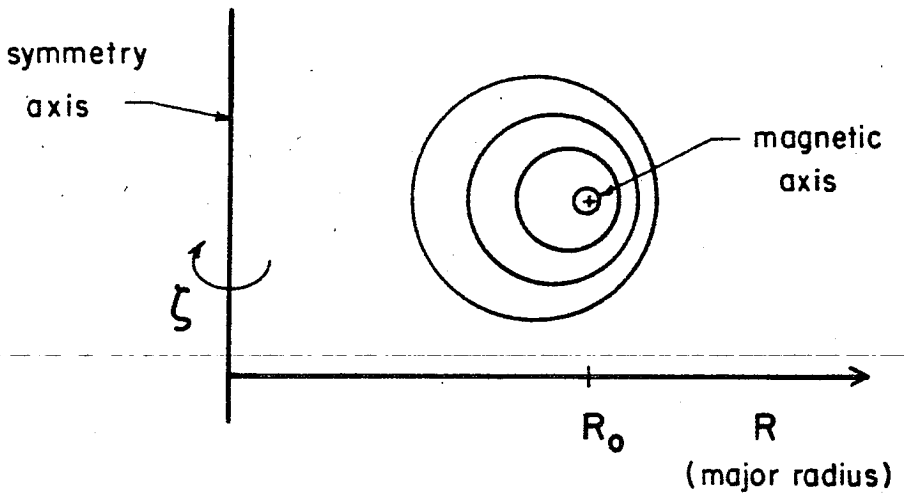

Fig. 1

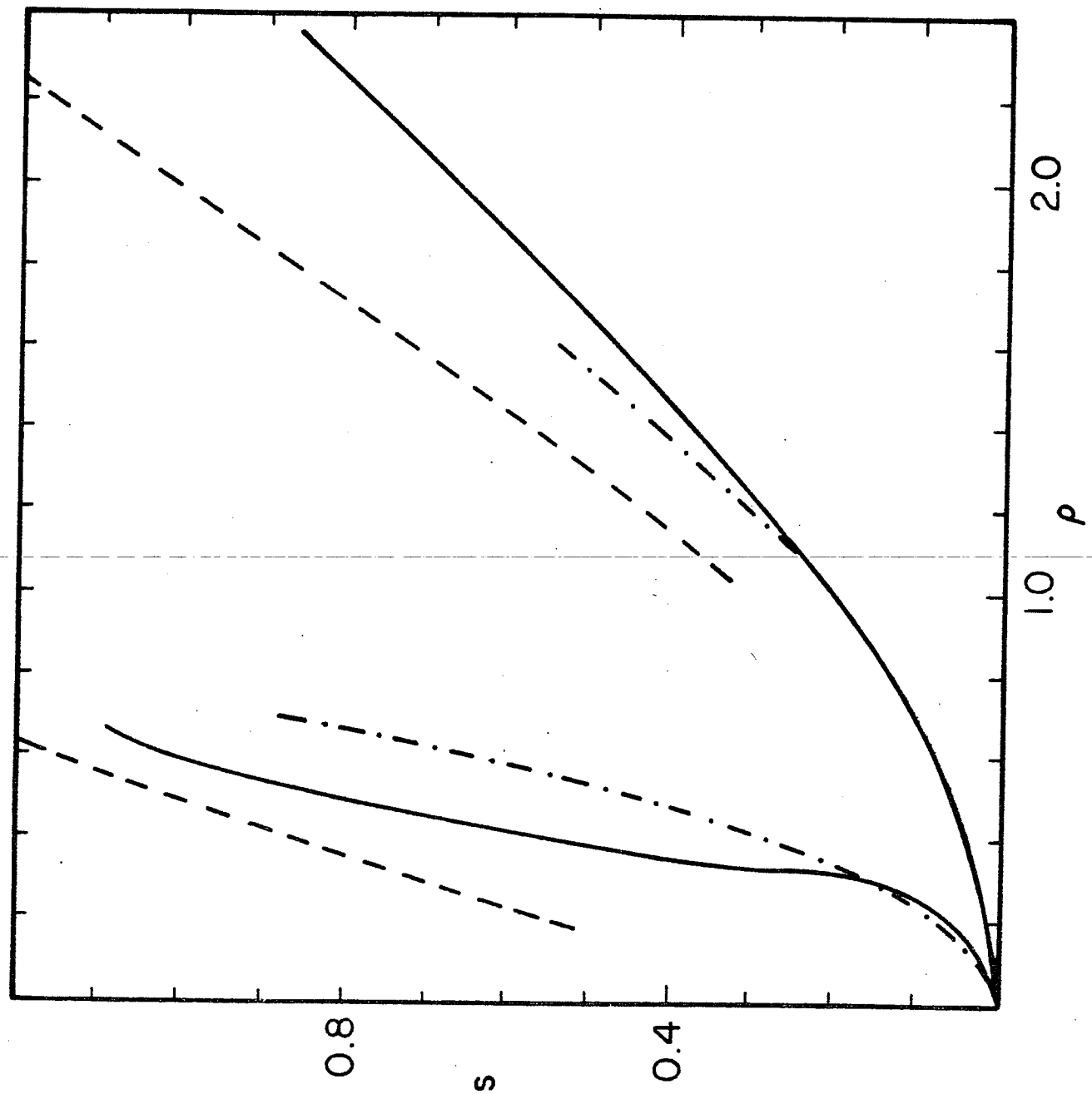

Fig. 2

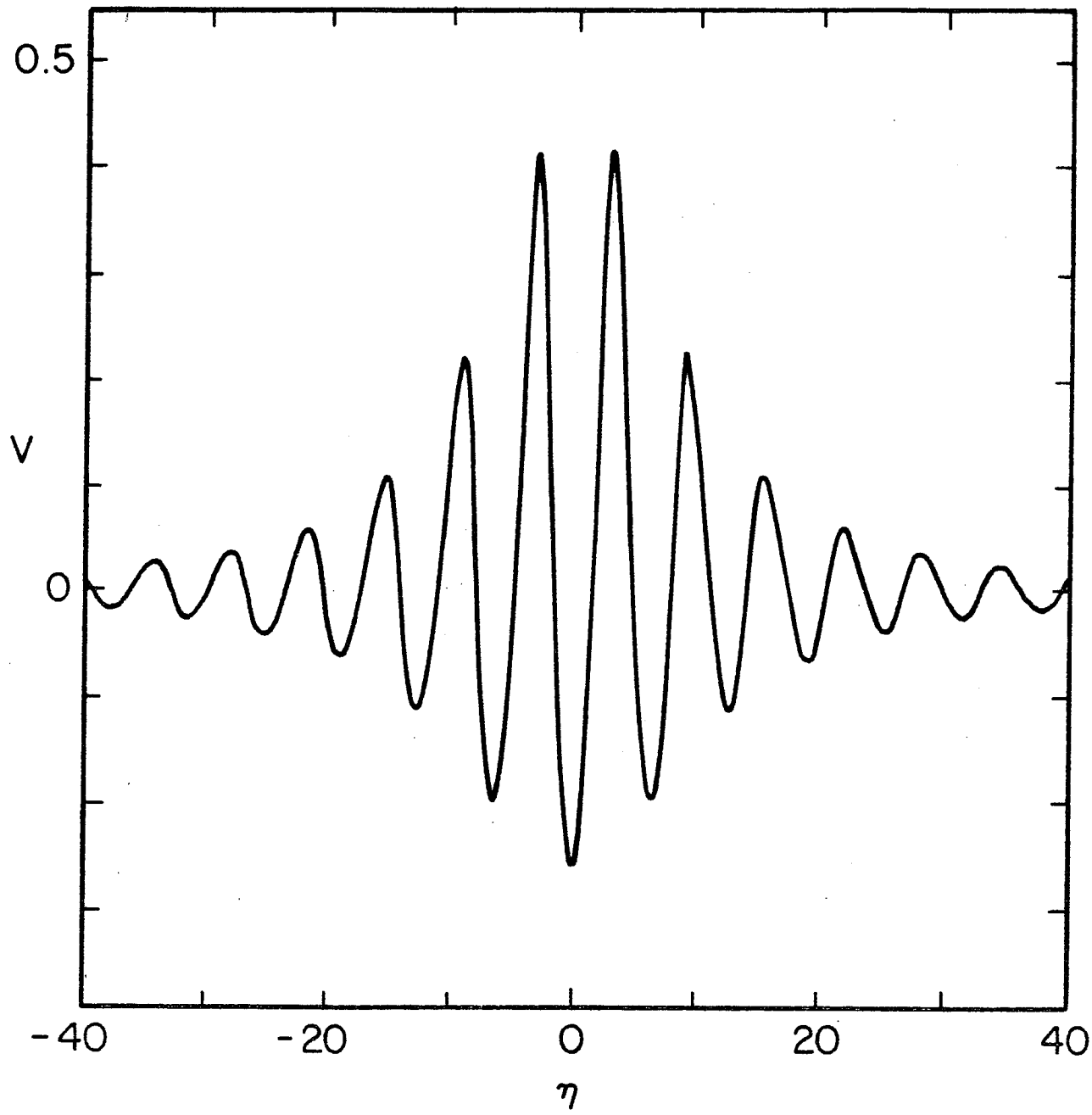

Fig. 3a

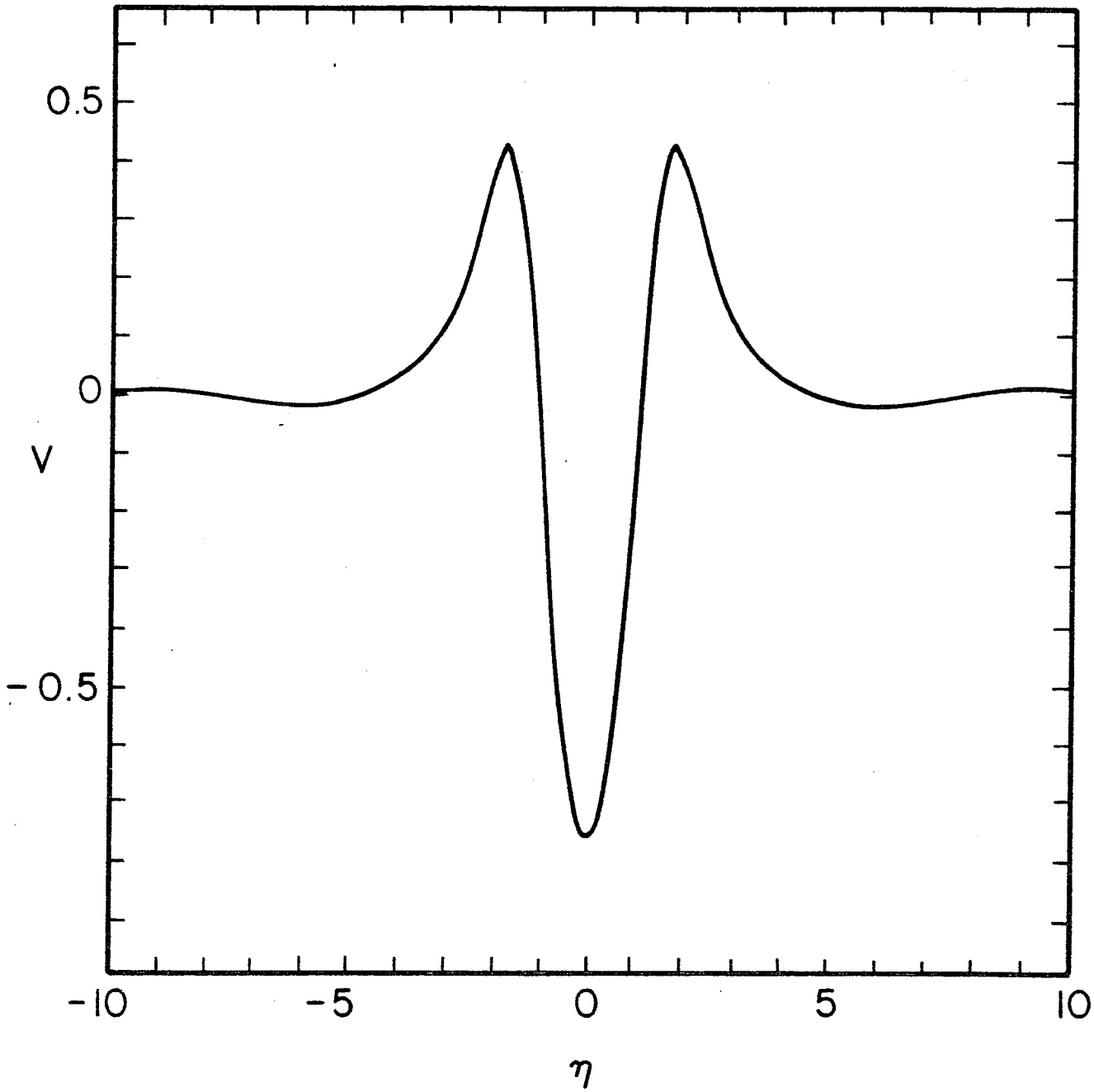

Fig. 3b

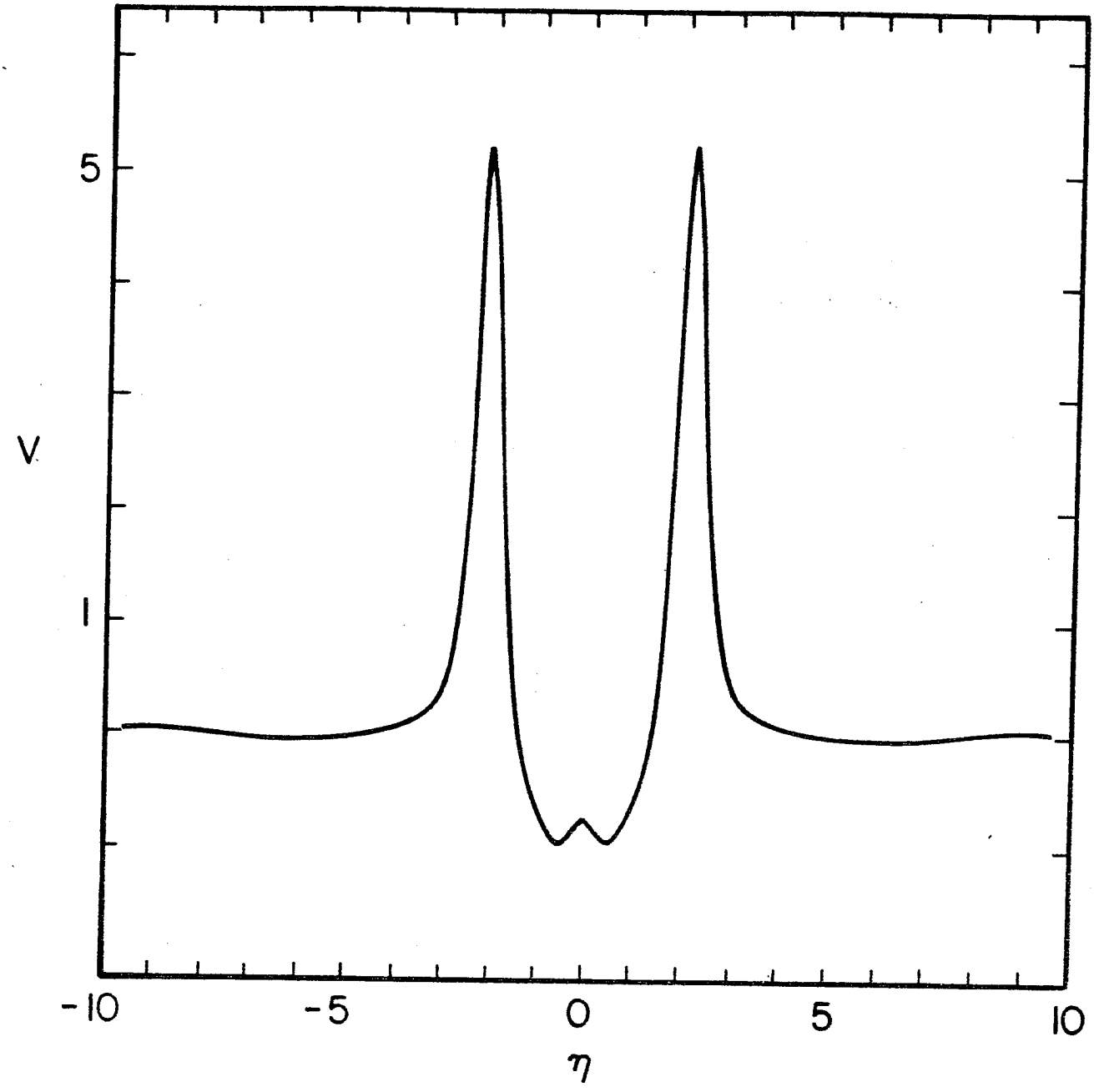

Fig. 4